ANALYSIS OF HYDROLOGICAL PROCESSES IN UNSTABLE CLAYEY SLOPES

Analysis of hydrological processes in unstable clayey slopes

Analyse van hydrologische processen in onstabiele kleihellingen

(met een samenvatting in het Nederlands)

PROEFSCHRIFT

ter verkrijging van de graad van doctor aan de Universiteit Utrecht op gezag van de Rector Magnificus, Prof. Dr. W.H. Gispen, ingevolge het besluit van het College voor Promoties in het openbaar te verdedigen op 1 oktober 2001 des middags te 14.30 uur

door

THOMAS ADRIANUS BOGAARD

geboren op 13 november 1968 te Bussum

Promoter	Prof. Dr. J.D. Nieuwenhuis Faculteit Ruimtelijke Wetenschappen
Co-promoters	Dr. Th.W.J. Van Asch Dr. M.R. Hendriks Faculteit Ruimtelijke Wetenschappen

Dit onderzoek werd mede mogelijk gemaakt met financiële steun van de Europese Commissie, DG XII Environment Programme, Climatology and Natural Hazard Unit, in het kader van het contract EV5V-CT93-0295.

Nederlandse Geografische Studies 287

Analysis of hydrological processes in unstable clayey slopes

Thom Bogaard

Utrecht 2001

Koninklijk Nederlands Aardrijkskundig Genootschap/
Faculteit Ruimtelijke Wetenschappen, Universiteit Utrecht

This research was (in part) supported by the Commission of the European Communities, DG XII Environment Programme, Climatology and Natural Hazards Unit, in the framework of the contract EV5V-CT93-0295.

This publication also serves as the thesis submitted for the title of Doctor, which was defended in public 1 October 2001 at the Utrecht University.

Promoter	Prof. Dr. J.D. Nieuwenhuis Faculteit Ruimtelijke Wetenschappen
Co-promoters	Dr. Th.W.J. Van Asch Dr. M.R. Hendriks Faculteit Ruimtelijke Wetenschappen

Examination committee:

Prof. Dr. M.G. Anderson	University of Bristol
Prof. Dr. S.M. de Jong	Utrecht University / Wageningen Research Centre
Prof. H.H.G Savenije	Technical University Delft / IHE Delft
Dr. C.J. Ritsema	Alterra green world research
Dr. H.R.G.K. Hack	ITC, Delft

ISBN 90-6809-321-5

Published by Labor b.v. – Utrecht.

Aan de naamlozen die ons opleiden en zo een onzichtbaar doch onmisbaar deel aan onze kennisopbouw bijgedragen

CONTENTS

List of figures 11

List of tables 15

Dankwoord 17

PART I GENERAL INTRODUCTION

1 Introduction 21
1.1 Problem definition 21
1.2 The Hycosi project 21
1.3 Objectives of the thesis 22
1.4 Thesis outline 22

2 Hydrology and mass movement processes: a review 25
2.1 Introduction 25
2.2 Effective stress, shear stress and shear strength 25
2.3 Landslide causes and triggering 27
2.4 Hydrogeology in mountainous areas 31
2.5 The unsaturated zone: concepts of flow in partially saturated porous media 32
2.6 Unsaturated and saturated zone modelling approaches for landslide research 35
2.7 Summary and conclusions 36

PART II GEOCHEMICAL STUDY

3 Testing the potential of geochemical techniques in identifying hydrological systems within landslides in partly weathered marls 37
3.1 Introduction 37
3.2 Physiography of the test locations 38
3.3 Previous research 41
3.4 Field methods 42
3.5 Description of the laboratory techniques 43
3.6 Results 44
3.7 Discussion 51
3.8 Conclusions / Further outlook 53

PART III PHYSICAL AND HYDROLOGICAL ANALYSIS

4 Physical and hydrological characteristics of the Beline study site 55
4.1 Topographical information of the Beline slope 55
4.2 Previous research at the Beline slope 58
4.3 Regional and local geology 60
4.4 Geophysical surveys at the Beline slope 63
4.5 Geomorphology of the region and the Beline site 65
4.6 Regional hydrological setting of the study area 66
4.7 Determination of the soil water hydraulic parameters of the Beline slope 68

5 Collection, evaluation and correlation of hydrological time series 73
5.1 Introduction 73
5.2 Meteorological data 73
5.3 Hydrological data 80
5.4 Statistical relationships between meteorological and hydrological time series 88
5.5 Conceptual model of the hydrological processes at the Beline slope 94
5.6 Conclusions 98

6 Hydrological modelling of the unsaturated zone 101
6.1 Introduction 101
6.2 Empirical models for water transfer through the unsaturated zone 101
6.3 Physically-based unsaturated zone modelling 106
6.3.1 Aim and parameterisation of the Beline unsaturated zone model 106
6.3.2 Inverse modelling 108
6.3.3 Direct modelling 116
6.3.4 The effect of changes in input variables on ground water recharge 119
6.3.5 Discussion and conclusions of the deterministic unsaturated zone model 121
6.4 Discussion and conclusions of the unsaturated zone modelling 122

7 The effect of ground water recharge on the hydrological modelling of the saturated zone of the Beline slope 125
7.1 Introduction 125
7.2 The Beline saturated zone model 125
7.2.1 Model description and parameterisation 125
7.2.2 Model calibration and validation 128
7.2.3 Precipitation as recharge series 134
7.3 State-dependent recharge 135
7.4 A scenario study on the impact of environmental change on the ground water level 140
7.5 Summary and discussion 142

PART IV GEOTECHNICAL ANALYSIS

8 Slope stability analysis in relation to ground water level fluctuations 145
8.1 Introduction 145
8.2 Subsurface schematisation and field deformation measurements 145
8.3 Laboratory measurements of geotechnical soil parameters 146
8.4 Static stability model 150
8.5 Displacement model 156

PART V SUMMARY

9 Summary 165

Samenvatting 173

References 181

Curriculum Vitae 189

Publications 191

FIGURES

2.1	Principle of effective stress for static conditions	26
2.2	Schematic representation of mechanisms initiating landslides	30
3.1	Geomorphological map of the Boulc-Mondorès landslide	38
3.2	Interpreted geological cross-section	39
3.3	Topographical setting Alvera landslide	40
3.4	Comparison NH_4Ac and NaCl laboratory analyses of cation exchange capacity and cation composition for the Boulc-Mondoès and the Alvera landslide samples	45
3.5	Geochemical profile of core A from Boulc-Mondorès	47
3.6	Geochemical profile of core B from Boulc-Mondorès	48
3.7	Geochemical profile of core I2 from Alvera	49
3.8	CEC values and carbonate content with depth for all three cores	50
3.9	Profile of cation fraction possession from cores A and B of the Boulc-Mondorès landslide: $Mg^{2+}+Ca^{2+}$ vs. Na^{+}	53
4.1	Location of the study area	55
4.2	Topographical map of Salins-les-Bains and surroundings	56
4.3	Detailed topographical map with land registration information of the Beline slope	57
4.4	Landslide delimitation and instrumentation set-up in 1988	58
4.5	Detailed lithological profile through the MES landslide area	59
4.6	Maximum and minimum observed groundwater levels in the research area of Lainé between 1988 and 1989	60
4.7	Regional geological map	61
4.8	Field survey locations, borehole locations and drilling depth	62
4.9	Two transect of geophysical results of VES and of refraction seismic	64
4.10	The geomorphological map of the Beline slope	66
4.11	Overview of regional hydrology and hydrochemistry around the Clucy plateau	67
4.12	Dry bulk density as a function of depth	68
4.13	Soil water retention curves and the fit of the hydraulic function	69
4.14	Frequency distribution of saturated permeability values at the Beline site	71
5.1	Locations of precipitation gauges between Salins-les-Bains and Nans-sous-ste-Anne	74
5.2	Overview of operation periods of the precipitation measurements in the Salins-les-Bains region	74
5.3	Cumulative precipitation at Clucy limestone plateau in summer 1996	77
5.4	Comparison of 14 days running total precipitation measurements of Arbois, Beline and Clucy stations in 1996-1997	78
5.5	Precipitation excess calculated at Arbois météo station in 1996-1997	79
5.6	Overview of operation periods of the ground water level measurements at the Beline site, Salins-les-Bains	81
5.7	Coarse ground water level data measured at the Beline slope in 1996-1997	82
5.8	Autocorrelation function for ground water level fluctuations	83
5.9	Overview of operation periods of the soil moisture and temperature measurements at the Beline site, Salins-les-Bains	85
5.10	Results soil moisture measurements with Humilog system in 1996-1997	87
5.11	Cross association results of hum085 soil moisture fluctuation	90
5.12	Cross association results of D2 ground water level fluctuation	91

5.13 Cross correlation results of hum085 soil moisture fluctuations 92
5.14 Cross correlation results of D2 ground water level fluctuations 93
5.15 Relationship between precipitation and soil moisture content 94
5.16 Relationship between soil moisture content and ground water level 95
5.17 Summary of hydrological system within the Beline slope 96
5.18 Zero flux plane explanation for hydrological system at the Beline slope 97

6.1 Time series of the observed and predicted ground water level for monitoring station D2 using empirical models 103
6.2 The equivalent soil moisture profiles that are used as the initial soil moisture content for the unsaturated zone model 108
6.3 Results of the sensitivity analyses of the inverse model on initial parameter setting 110
6.4 Sensitivity of increased porosity on the parameter optimisation 112
6.5 Example of the unsaturated zone bottom flux as function of the porosity for ground water time series D1 113
6.6 Results of the parameter optimisation using hydrological (HY) and calendar (CA) year of data combined with constant ground water levels at -3, -4, -5 or -6 m 113
6.7 Measured and modelled soil moisture (30 and 80 cm depth) 117
6.8 Model results of the bottom flux of the Beline model as a function of the ground water level 118
6.9 Relative effect of input changes on the change in ground water recharge 120
6.10 Relative effect of the combination of input changes on the change in ground water recharge 121

7.1 Overview of the observation sites and a 2D ground water model cross-section at the Beline slope, Salins-les-Bains, France 126
7.2 Geometry of the 2D Beline ground water model and the initial, horizontal, ground water setting 127
7.3 Modelled and measured steady-state ground water level at the Beline slope 129
7.4 Results of modelled ground water level fluctuation in observation points D1, D2 and D3 using hypothetically fluctuating long and short term recharge series 131
7.5 Results of the ground water modelling at the Beline slope for 1996 and 1997 for two recharge time series 132
7.6 Comparison of modelled and measured ground water level at D1 with the recharge time series 133
7.7 Ground water level modelling results using a fraction of the daily precipitation data as recharge series (SP) for observation sites D1 and D2 134
7.8 Ground water model results using the state-dependent ground water recharge time series (SR) for observation sites D1 and D2 137
7.9 Overview of cumulative precipitation and recharge in relation to the relative bottom flux of the unsaturated zone model 138
7.10 Ground water model results using state-dependent recharge time series (SR) and its extended version (SER, with f_{dir}=0.10) for observation sites D1 and D2 139
7.11 Ground water fluctuations as response to different input change scenarios for observation point D1 using the state-dependent recharge function 141
7.12 Comparison of scenario results using the recharge input series of the unsaturated zone model and of the state-dependent recharge model 142

8.1 The total cumulative displacement recorded with the inclinometer at the Beline slope (January 1996 - December 1997) 146
8.2 Schematic representation of the viscosity apparatus 148
8.3 Example of the determination of viscosity from a laboratory test 149
8.4 Relationships of the yield strength and dynamic viscosity with the normal stress in the soil, as determined with the laboratory viscosity tests 149
8.5 Relationship between the Factor of Safety (FS) and ratio pore pressure/soil depth (m) with the depth of the slipsurface (z), cohesion (c') and the angle of internal friction (φ') 153
8.6 Location of the slipsurface of a rotational slide using the Bishop's method of slices at the Beline slope 154
8.7 Effects of the depth of the slipsurface and the strength parameters (cohesion and angle of internal friction) on dFS/dh 155
8.8 Coordinate system for the creep description 157
8.9 Results of the Yen creep model with different combinations of creep zone thickness and viscosity values 159
8.10 Changes in monthly displacement as a function of an increase of the maximum ground water level (March 1997) for example models 1, 2 and 3 160
8.11 Changes in ground water level as a result of changes in potential evapotranspiration 161
8.12 Effects of changes in potential evapotranspiration on the displacement velocity of the Beline slope 162

TABLES

2.1	List of examples of mass movement causes	28
2.2	Classification of mechanisms initiating landslides	29
3.1	Distribution of particle size and clay types of the Albian-Aptian marls	41
3.2	Relative difference between the analyses of duplicate samples	44
4.1	Typical values of compressional wave velocity (V_p)	64
5.1	Specifications of precipitation measurements in Salins-les-Bains region	75
5.2	Precipitation characteristics at three rain gauges in Salins-les-Bains region	76
5.3a	Rainfall intensity characteristics of the Clucy rain gauge	76
5.3b	Rainfall intensity characteristics of the Arbois rain gauge in 1996	76
5.4	Linear correlations (r) between the rain gauges of Arbois, Beline and Clucy	78
5.5	Precipitation excess calculated for the Arbois Météo station	80
5.6	Basic information of the coarse ground water level data	80
5.7	Highest and lowest ground water level measurements	81
5.8	Basic information of the Humilog soil moisture data collection at the Beline slope	84
5.9	Summary of the soil moisture measurements at the Beline slope, Salins-les-Bains	86
5.10	Overview of the cross-association and cross-correlation calculations analyses	89
5.11	Results of the cross-correlation between soil moisture content changes and effective precipitation	92
6.1	List of the empirical ground water level models	102
6.2	Overview of the fit parameters for the different empirical models	104
6.3	Results of the goodness of fit calculations for the empirical modelling	105
6.4	Parametrisation for the Beline inverse unsaturated zone model	108
6.5	Results of the inverse modelling	109
6.6	Indicative correlogram of parameters used in the inversed model	111
6.7	Results of the inverse unsaturated zone modelling with $n_1 = 1.2$ and $n_2 = 1.5$	115
6.8	Validation results of the Beline unsaturated zone model	118
6.9	Scenario definitions for the Beline unsaturated zone modelling	120
7.1	Initial values of the hydrological parameters of the Beline ground water model	128
7.2	List of the stress periods with hypothetical recharge values to test the Beline ground water model on its capability to model ground water level fluctuations	130
7.3	Final hydrological parameter setting of the 2D Beline ground water model after calibration	131
7.4	The RMSE values and the range of ground water level fluctuations, both measured and modelled for the calibration and validation of the Beline ground water model	133
8.1	Results of the strength tests at the Beline slope	147
8.2	The initial parameter setting for the 2D Beline stability analysis	151
8.3	Parameterisation of the Yen creep model	158
8.4	Relationship of the thickness and depth of the slipsurface with the calibrated dynamic viscosity	159

DANKWOORD

Het schrijven van een proefschrift gaat door voor een individuele aangelegenheid, eenzaam zeggen sommigen. Maar het is - net als bij een individuele sport als atletiek - onmogelijk alleen uit te voeren. De eindprestatie is ontsprongen uit een bouwwerk dat is neergezet door begeleiders, collega's, vrienden en familie. Dit is de gelegenheid om een aantal van hen te bedanken.

Allereerst wil ik mijn promotor, prof.Dr. Jan Nieuwenhuis, bedanken voor zijn begeleiding in het Hycosi project en daarna bij dit proefschrift. Je scherpe analyses heb ik zeer waardevol gevonden. De dagelijkse begeleiding kwam van co-promotor Dr. Theo van Asch ("Een intelligent persoon zorgt voor orde, een genie beheerst de chaos."). Je overmaat aan enthousiasme en vakinhoudelijk steun hebben mij enorm gemotiveerd. Ook je veldbezoeken waren altijd een bron van nieuwe inzichten. Ik hoop nog lang van je te mogen blijven leren. De structuur in het proefschrift is zeer wel toevertrouwd geweest aan didactisch hydroloog Dr. Martin Hendriks. Martin, als co-promotor heb je een wezenlijke bijdrage aan dit proefschrift geleverd door alle ruwe teksten en fragmenten van ruwe teksten zeer grondig te herschrijven. Zonder jouw bijdrage was er geen leesbaar proefschrift verschenen. Ook dank ik je voor het vertrouwen dat je in mijn functioneren hebt gesteld.

A special thanks I want to give to my french colleagues and friends of the Service Risques naturels et Géodynamique récente, BRGM, Marseille, especially Ir. Eric Leroi, Ir. Olivier Monge and Ir. Daniel Chassagneux. Together we worked very hard on the Hycosi project. The discussions on hydrology and landslides were very inspiring for me. The hospitality and support, also in the period after the official project, are greatly acknowledged. The introductions in the French culture and that of the French Antilles ('the petit Ponche') have positively influenced my life.

Door de jaren heen heb ik meerdere kamergenoten versleten. De inhoudelijke discussies hebben mij, denk ik, het meest gevormd en hebben een zeer grote invloed op dit proefschrift gehad. Trans 2, kamer 310 was een sportzaal, een broeinest voor verhitte discussies, een rustpunt met koffie, een ontmoetingsruimte voor gezelligheid en een ideale plek voor het ontwikkelen en uitvoeren van nieuwe ideeën. Henk, Jelle en @lfred, dankzij jullie heb ik me in Utrecht meteen thuis gevoeld. Verhuisd naar 130 aan het eind van de Jan Zonneveld*vleugel* hebben ook Rens en Karin voor een onvergetelijke sfeer en ondersteuning gezorgd. Rens, aan jou ben ik heel veel dank verschuldigd. Jouw antwoorden op mijn geotechnische en statistische vragen waren onmisbaar. Maar ook onze discussies over wetenschap dwalen nog wel eens door mijn hoofd.

Veel werk dat ten grondslag ligt aan dit proefschrift is voorbereid of (mede) uitgevoerd door het elektronisch, hydrologisch, mechanisch en geotechnisch lab. Dank aan Theo Tiemissen ("Als ik niet in het dankwoord sta, kom ik niet!"), Bas van Dam en Marcel van Maarseveen voor jullie hulp op electronische vlak: altijd bereid tijd te maken en mee te denken. Veel dank ben ik ook verschuldigd aan Kees Klawer, Marieke van Duin en Ton van Warmenhoven voor het analyseren van honderden water- en grondmonsters. Kees, je hebt op jouw 'eigen wijze' een belangrijke bijdrage geleverd bij het meedenken over de geochemie en bij de veldwerk voorbereidingen. Jaap Barneveld, jou wil ik bedanken voor de vele kwaliteitsoplossingen die je uit je apparatuur liet draaien. Een speciaal woord van dank aan de eenzame strijder van het geotechnische lab, 'tandarts' Wim Haak. Alles draaiende houden, tegen de stroom in. Wim, hardstikke bedankt voor het vele werk dat je verzet hebt en de gezellige sfeer die ik gevoeld heb in het geotechnische lab.

Edzer Pebesma en Gualbert Oude-Essing, jullie hulp en correcties op statistisch en modelleer gebied heb ik zeer op prijs gesteld. Hans-Peter Broers, jouw enthousiasme en vasthoudendheid inspireren nog steeds. De geochemen Pieter-Jan van Helvoort, Job Spijker en Pauline van Gaans wil ik bedanken voor de aanwijzingen en discussie op hun vakgebied.

Aan dit onderzoek hebben ook vele doctoraal studenten meegewerkt. Vincent de Graaf, Marco Boekelo, Kirsten Hennrich en Jane Wisemann vele hoogtemeters overwonnen en het hydrologisch onderzoek op de Boulc-Mondorès aardverschuiving mede opgezet. Het regionale karst onderzoek is fantastisch uitgevoerd door Arjen Roelandse, Kirsty Blatter, Hans Leushuis, Ingrid Kroon en Ronald Hemel. Als laatsten hebben Erik van der Zee en Bart van den Eijnden een grondig onderzoek uitgevoerd op de Beline helling. Jullie hulp en inzet heb ik zeer gewaardeerd.

Ton Markus ("Hoe doe je dat nou?" –"Ja joh, dat is mijn vak!") en Rob Kromwijk van Kartlab hebben zorg gedragen voor alle figuren. Jongens, vakwerk!

De (ex-)collega's van de Jan Zonneveld*vleugel* hebben gezorgd en zorgen nog steeds voor een zeer collegiale en prettige sfeer. Tijdens de koffie, Bata44race, lunchlezing, Educatorium diner of squash competitie. Met name wil ik noemen Nathalie, Birgitta, Simone, Anja, Oscar, Aart, Rudi, Derrek, Kor, Raymond, Annika, Sandra, Sandra en Irene. Heleen Hayes, Celia Nijenhuis, Annina Andriessen en Irene Esser stonden immer klaar om mij te helpen met allerhande taken. Bedankt!

Buiten het werk heb ik gedurende de lange periode veel steun en begrip ontmoet van mijn vrienden: Noel, Judith, Roel, Margreet, Leontine, Jaap, Marlies, Guus en Wolfgang. Bedankt voor de etentjes en het aanhoren van werk gerelateerde pijntjes. Het wordt tijd weer wat attentie terug te geven. Wolfgang, het gezamenlijke klimmen en de vele discussies over het leven, fotografie of huisinrichting hebben me meermalen de relativiteit van een proefschrift doen inzien!

Ook de familie heeft behoorlijk bij gedragen aan het ondersteunen van het bouwwerk. Te vaak heb ik geschitterd door afwezigheid. Maar jullie geloof in mij, de steun en de afleiding waren onmisbaar. Pa, ma, Bob, Denise, Hans, Emmy, Leen, Lies, Sander, Jos, Floor en Siem, ik zal het niet licht vergeten.

De grootste steun die ik bij dit project heb mogen genieten komt van jou, Suus. Vier jaar zou het duren, het werden er door alle ontwikkelingen ruim zeven. Menig keer heb je vrije dagen opgenomen om met veldwerk te helpen, menig treinreis heb je besteed aan mijn teksten en continu heb je geluisterd. Je hebt me gesteund door me tegen mezelf te beschermen, door me ruimte te geven, door me op te jutten, maar vooral door er altijd te zijn.

1 INTRODUCTION

1.1 Problem definition

Society all over the world demands an increasingly level of protection against natural risks. The view that natural incidents - whether catastrophic or not - are returning and inevitable is no longer accepted. At the same time increasing spatial demands by society lead to infrastructural building activities at less favourable locations such as river beds and slopes. A large number of these sites would never have been considered, taking only natural and environmental conditions into account.

Increasing knowledge of processes inducing hazards is required to cope with growing risk for society. What processes control slope stability? Slope stability is determined by processes, which are the research fields of the disciplines meteorology, biology, pedology, hydrology and geology. Its analysis combines both earth and civil engineering sciences. Landslides are located in undulating or mountainous terrains, where, due to the inherent spatial variability and the difficult access of many sites, the collection of representative experimental data poses an additional problem. In 1988 a special congress of the International Association of Hydrological Sciences (IAHS) was organized on the subject of hydrology of mountainous areas. For this occasion, Klemes (1990) wrote that "hydrologists are still being trained mostly as engineering technologists rather than as earth scientists", and that the latter was needed for developing more knowledge concerning "the processes that shape the hydrological cycle" in mountainous areas. These statements certainly hold true for slope stability research. It is the complexity of factors determining slope stability that forces us to study the hydrological and geotechnical processes of the slope in detail.

In slope stability research a ground water level increase is often the critical factor. High ground water levels and hence high pore water pressures reduce the internal strength (shear resistance) of slopes. It is recognised for quite some time that fast infiltration of precipitation towards the (perched) ground water table can induce rapid pore pressure increase and thus instability of shallow soil masses. However, instability of larger soil masses by a deep-seated failure plane is affected on a longer time scale by slow but distinct ground water table rise, which may take place a significant time after the occurrence of rainfall. For long-term risk assessment in case of changes in land use or climate, it is desirable to gain insight in the hydrological processes within a slope susceptible to landsliding.

1.2 Hycosi project

The research outlined in this thesis originates from the HYCOSI project, which stands for Impact of HYdrometeorological Changes On Slope Instability. This project was financed by the European Commission under the "Environment Research Programme - 1991/1994", with the support of the French Ministry of Environment (DGAD/SRAE). The project was carried out jointly by four French and Dutch organizations: BRGM (coordinator), Utrecht University, Delft Geotechnics, and Iris Instruments. The aim of the

research is to improve knowledge of water circulation and concentration in the ground, from site scale to basin scale, in order to understand the impact of hydrometeorological changes on slope stability. This also involves analysing and improving the design and installation of monitoring networks as well as methods of interpreting the results and assessing the effectiveness of classical slope reinforcement structures. The final part of the project considered the development of management systems for information exchange using proven electronic highways such as Hypertext and Internet. The research is based on a conceptual and experimental approach applied to three study sites in France: Harmalières (Trièves) in the Isère, Boulc-en-Diois in the Drôme and Salins-les-Bains in the Jura. The research project is documented in a final report (Leroi, 1997).

The emphasis on monitoring and ground water circulation analysis has resulted in an interesting database of precipitation, soil moisture and ground water time series for a natural slope affected by mass movement, called the Beline site (Salins-les-Bains, Jura). This database formed the starting point of this thesis: an analysis of the hydrological system of a slope consisting of clay and marls. Furthermore, attention has been paid to test the potential of geochemical methods for the refinement of on-site hydrological knowledge.

1.3 Objectives of the thesis

The objective of this thesis is to analyse and quantify the hydrological processes that play a role in landslides within clayey slopes. The following questions are addressed:

- What can hydro- and geochemistry add to our knowledge of a hydrological system in a clayey slope?
- What processes dominate the ground water recharge in unstable clayey slopes and how can the ground water recharge be quantified?
- What is the consequence of changes in land use or climate for unstable clayey slopes?

1.4 Thesis outline

This thesis is composed of five parts with in total nine chapters. The first two chapters (part I) comprise the general introduction. Chapter 2 presents the theoretical background of slope stability and examines the landslide triggering mechanisms and proposes some adjustments. Also, this chapter renders a literature review on hydrology in mountainous areas with respect to slope stability and discusses the flow concepts of water in the unsaturated zone. At the end of this chapter, an inventory is made of the model concepts that are generally used in landslide research.

The study of the potential use of hydro- and geochemistry in refining the hydrological knowledge of a site is described in the second part (chapter 3). What is the potential of cation exchange capacity analysis to complement standard geohydrological research in a clay and marls unstable terrain? Also, it was tested whether the proposed techniques are applicable to (weathered) marls, in which landslides often develop.

The third part of this thesis focuses on the hydrological analyses of the Beline study area at Salins-les-Bains. Chapter 4 gives a basic overview of the physiography of the

Beline research area and its surroundings. It also describes the field surveys, field instruments and laboratory analyses. Chapter 5 evaluates the meteorological and hydrological time series. Statistical relationships between the time series are used to explore the time series and this results in a conceptual model of the hydrological processes at the Beline site.

Hydrological modelling of the unsaturated zone is dealt with in chapter 6, the saturated zone in chapter 7. Both empirical and physically-based deterministic models are used to quantify the ground water recharge in chapter 6. The models are calibrated and validated in order to test their applicability for predictions. After this the effects of changes in land use or in climate on the ground water recharge are calculated. In chapter 7 the effect of ground water recharge on the ground water system is modelled. Also, a state-dependent ground water recharge model is defined using precipitation and a measure for the soil moisture content in the unsaturated zone that incorporates preferential flow. This state-dependent ground water recharge model is compared with the ground water recharge data stemming from the unsaturated zone modelling.

Chapter 8 (part IV) describes the investigation on the slope stability at the Beline slope. The effects of ground water level fluctuations on slope displacement and on changes in the ground water level are studied.

Finally part V (chapter 9) presents a summary and conclusions. Both a conceptual description of the hydrological processes in a clayey slope and some recommendations for future research are presented.

It must be realised that an “extensive” database on natural phenomena is small compared with localised databases prepared for infrastructural works and that the available data only limitedly render the size and complexity of mountainous slopes. The interpretation tools, robust, quasi-linear and a limited number of parameters, have been elected accordingly.

2 HYDROLOGY AND MASS MOVEMENT PROCESSES: A REVIEW

2.1 Introduction

As most persons will know intuitively, water plays a major role in mass movement. Most information on mass movements is sent into the world by media after spectacular and often tragic disasters. But also smaller mass movements, with higher temporal frequency, are a constant threat to the mountainous society and can result in loss of life, property and infrastructure. Most of the hazards are triggered by extreme precipitation, but other landslide triggers are e.g. seismic activity, volcanic outburst or human activity.

Precipitation in mountainous regions (snow and rain) is the result of large-scale weather patterns (frontal precipitation) as well as local effects (orographic and convectional rainfall). In its downslope transport, the precipitation can flow quickly (superficially or via the subsurface) towards the drainage network of streams and rivers. In contrast, precipitation can also infiltrate into the soil and percolate more slowly through the unsaturated zone to the saturated zone. Precipitation can also be stored temporarily as snow or be delayed in lakes. The speed of the transport depends strongly on the hydrological characteristics of the soil and intensity and duration of the precipitation.

This chapter describe the role of water in landslide research. The influence of water on the stability of a slope can be described with the 'principle of effective stress' (§2.2). The hydrological triggering mechanisms of landslides are described in §2.3, followed by the role of hydrogeology and deeper ground water flow (§2.4) and a description of the hydrological processes within the unsaturated zone (§2.5). Paragraph 2.6 is used for describing the hydrological models in landslide research. The chapter finishes with a summary (§2.7).

2.2 Effective stress, shear stress and shear strength

In a fully saturated soil, the following stresses are mutually related according to Terzaghi (1923 on cit. Craig, 1992): the total normal stress, the pore water pressure and the effective normal stress. Total normal stress (σ in [kN/m^2]) is the total force per unit area normal to an arbitrary surface within the soil. The pore water pressure (u in [kN/m^2]) is the force that water develops in the voids. The effective normal stress (σ' in [kN/m^2]) is the stress that is transmitted through the soil skeleton only. In formula the relationship is:

$$\sigma = \sigma' + u \tag{1.1}$$

The total normal stress is based on the total weight per unit area including water in the voids. For a wet soil the weight per unit area is equal to the height of the dry soil times the soil unit weight and added to this the height of the saturated soil times the saturated soil unit weight. In formula:

$$\sigma=(z-z_w)\gamma_d+z_w\gamma_s \tag{1.2}$$

γ_d = Dry soil unit weight in [kN/m^3]
γ_s = Saturated soil unit weight [kN/m^3]
γ_w = Unit weight of water [kN/m^3]
z = Soil height above reference level [m]
z_w = Water height above reference level [m]

The pore water pressure equals under hydrostatic conditions the water height times the unit weight of water. In formula:

$$u=z_w\gamma_w \tag{1.3}$$

The principle of effective stress is illustrated with an example in figure 2.1.

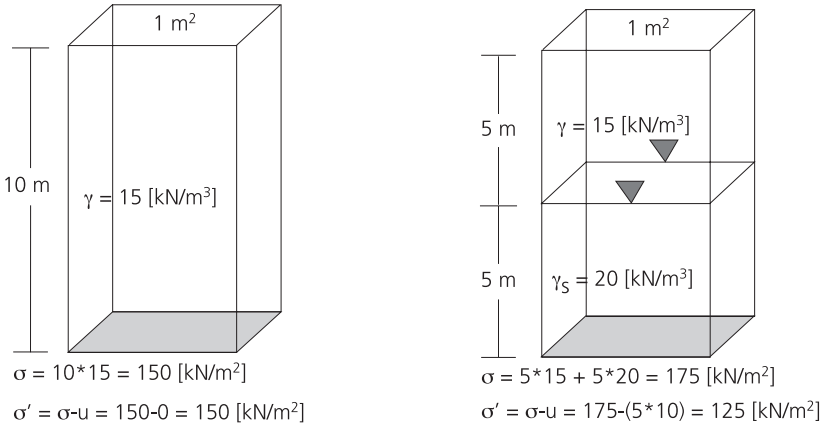

Figure 2.1 Principle of effective stress for static conditions.

The lower effective normal stress in figure 2.1b compared to the normal stress, results from the buoyant force of water on soil particles (Archimedes' principle). The total normal stress can also be influenced by additional pressure, the so-called 'overburden pressure'. An overburden pressure is e.g. the weight of trees on a slope, a landfill area or a building.

In a soil body resistance to failure exists, i.e. the soil has a shear strength. The shear strength is made up of friction and cohesion. Frictional resistance depends on the effective normal stress in the soil, whereas cohesion does not and has a constant value. The mobilised shear strength (τ) of a soil is given by the Mohr-Coulomb theory (eq.1.4), which is a linear equation approaching the curved failure envelope.

$$\tau = c + \sigma \cdot \tan(\varphi) \tag{1.4}$$

c = cohesion [kPa]
ϕ = angle of internal friction [°]

Cohesion and angle of internal friction are material properties, which can be measured in laboratory experiments. In terms of effective stress the Mohr-Coulomb model can be described as follows:

$$\tau = c' + \sigma' \cdot \tan(\varphi) \tag{1.5}$$

On a (partly) saturated soil body the following forces are working: gravity, mobilised friction, buoyancy and seepage forces. These forces make equilibrium. Instability occurs when the gravity-induced shear stress surpasses the maximum mobilised shear strength in a mass body.

The amount of increase of pore water pressure that is necessary to initiate slope movement depends on the depth of the slip plane. In case of a shallow slip plane only a limited amount of water is sufficient for slope movement initiation. In case of deeper located slip planes (a deep-seated mass movement) a larger increase in pore water pressure is needed and thus more infiltrated rain. It is this interaction between hydrology and development of slope instability that will be addressed in this chapter.

2.3 Landslide causes and triggering

Mass movement research has given a lot of attention to the causes of landsliding. Why and when does a stable slope loose its stability? This has led to field and laboratory investigations concerning the factors contributing to slope instability. Table 2.1 gives a list of those causes as compiled from literature.

Table 2.1 has its major subdivision in slope movement causes, which reduce the friction force (internal causes) or increase the gravity force (external causes) as also used by e.g. Chandler (1986) and Gostelow (1996). The reduction of the effective shear strength can be caused by an increase of pore water pressure or a decrease of material strength properties (e.g. weathering of the rock). The increase of gravitational shear stresses can be caused by an undercutting of the slope (e.g. riverbank erosion or human activity).

Table 2.1 List of examples of mass movement causes compiled from Varnes (1978), Crozier (1984), Hutchinson (1988), Cruden and Varnes (1996) and Wieczorek (1996).

Internal	
Changes in water regime	Precipitation → pore pressure increase (incl. decrease in suction head)
	Water leakage from utilities
	Change in reservoir water level
	Increase of snow melt
Weathering, erosion and progressive failure	Reduction of cohesion
	Thawing
	Freeze/Thaw cycle
	Shrink/swell cycle
	Clay mineral change (CEC-composition change)
	Seepage erosion
External	
Geometry changes	Slope erosion, riverbank erosion, wave erosion, glacial and stream incision
	Excavation, mining
Vibrations	Earthquake and other tectonic activity
	Artificial and other natural vibrations (explosions, thunder, volcanic eruptions)
	Point impulse (rock fall)
Surcharges	Vegetation growth
	Increasing weight because of wetting
	Accumulation of sediment
	Landfill
	Building

The difference between a cause and a trigger is that a cause can develop during a long time period while a trigger develops very rapidly. Wieczorek (1996) defines triggering as an "external stimulus (..) that causes a near-immediate response in the form of a landslide by rapidly increasing the stresses or by reducing the strength of slope materials.". He also states that: "The requisite short time frame of cause and effect is the critical element in the identification of a landslide trigger". The difference between triggering and slope instability causes is the time domain. Varnes (1978) quotes Sowers and Sowers (1970): "In most cases a number of causes exist simultaneously and so attempting to decide which one finally produced failure is not only difficult but also incorrect. Often the final factor is nothing more than a trigger that sets in motion an earth mass that was already on the verge of failure. Calling the final factor the cause is like calling the match that lit the fuse that detonated the dynamite that destroyed the building the cause of the disaster."

In case of a short monitoring period of a mass movement, one does not take into account the long-term changes or processes that may have occurred. Why does a slope remain stable for decades and then suddenly looses its stability during a quite normal rain event with a recurrence interval of e.g. 10 years? In other words: what is the cause and what is the trigger?

If the time stretch in which a cause develops, is added, a landslide-cause matrix can be constructed (table 2.2).

Table 2.2 Classification of mechanisms initiating landslides with in italic some examples.

Process \ **Time scale**		Short time scale	Long time scale
Shear strength decrease [Internal]	Increase of pore water pressure	Instantaneous hydrological factors or hydrological triggers *Infiltration & percolation*	Long-term hydrological factors *Regional ground water flow, Change in land use or climate*
	Decrease of material strength	Instantaneous strength factors or strength triggers *Artificial freezing-thawing, chemical treatment*	Long-term strength factors *Weathering and dissolution Increase strength by roots grow*
Shear stress increase [External]		Instantaneous gravitational factors or gravitational triggers *Earthquake, excavation*	Long-term gravitational factors *Erosion or Accumulation*

The names for the different cells in table 2.2 are combinations of time and process. The internal cause (reduction of shear strength) is divided into 'hydrological' (=increase in pore water pressure) and 'strength' (=reduction of material strength properties). The external cause is called 'gravitational'.

Let's consider a slope with an annual average ground water level of 6 m below surface and a normal seasonal variation of 3 m (figures 2.2). Let's also assume that a ground water level of -2 m is necessary for failure to occur. Moreover, consider no change in soil characteristics and an average ground water level with a 'normal distribution' of short-term fluctuations. Mass movements can then be triggered by an extreme rainfall event for a short period resulting in a larger ground water level fluctuation (Instantaneous hydrological cause or hydrological trigger – figure 2.2a).

In figure 2.2b the short-term fluctuation is within normal limits but the average ground water level is rising. This could be the result of e.g. land use change in a certain area, or a slowly occurring climatic change. But it can also be due to external factors such as the closing of drinking water wells, the closing of an open pit mine or the filling of a reservoir lake. In this example the cause for the landslide to occur is the ground water level rise, but the trigger was a 'normal' rain event. A third option is that a slowly lowering critical ground water level (figure 2.2c) causes slope instability. This may be due to slow physical and chemical reactions changing the material characteristics. This is a long-term strength cause for landsliding. The instantaneous strength cause (figure 2.2d) can be the result of very vigorous physical or chemical processes. Figures 2.2e and 2.2f schematise the triggering due to a shear stress increase. The former shows that in time a gradual lower ground water level can cause failure (decreasing safety factor in time). This may be due to erosion at the toe of a slope (Long-term gravitational cause). The latter gives an impression of an instantaneous gravitational cause e.g. caused by an earthquake or caused by riverbank erosion due to a high discharge period.

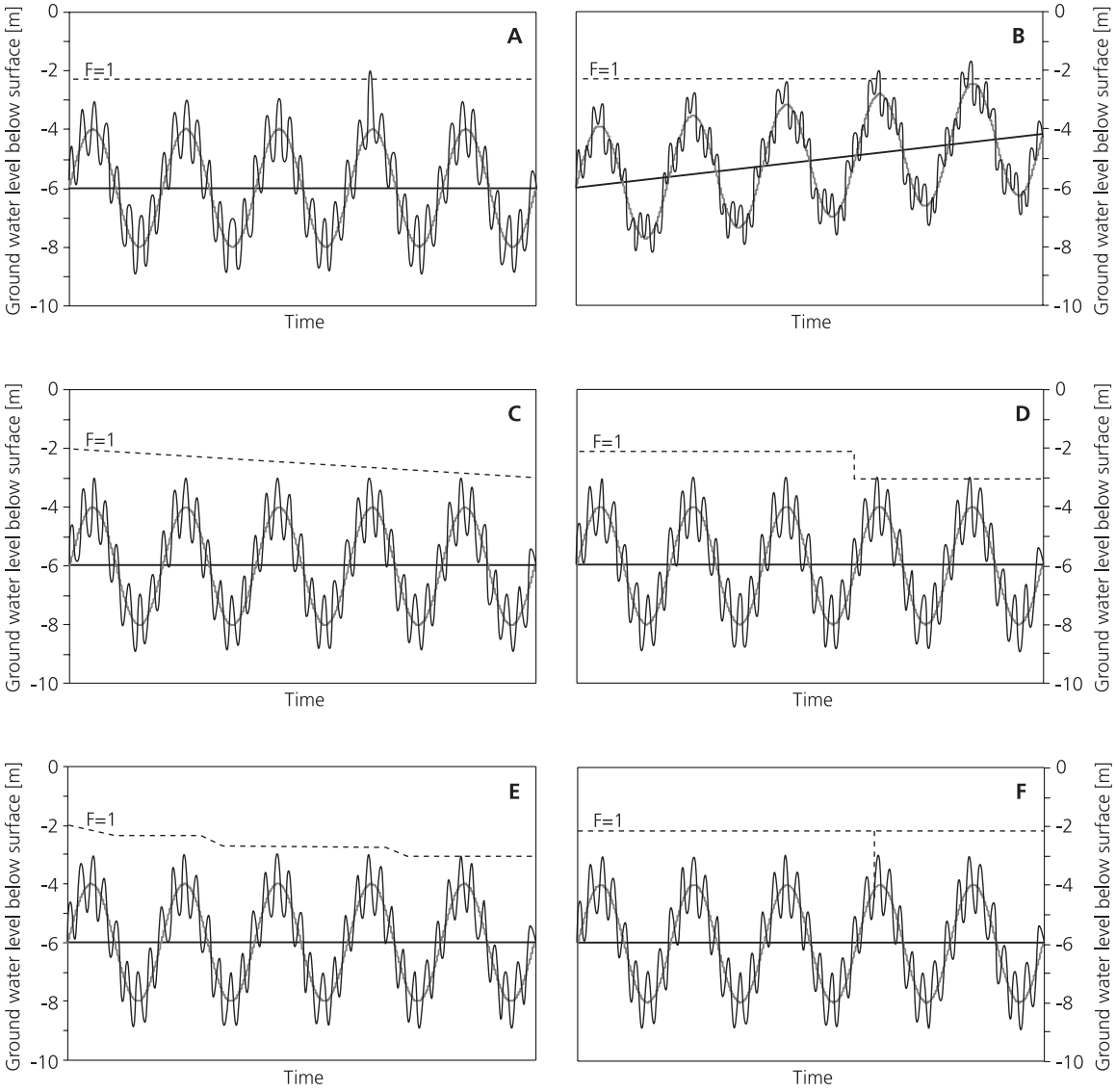

Figure 2.2 Schematic representation of mechanisms initiating landslides (see also table 2.2).

A triggering classification such as described above helps in improving our insight in the processes that act in mass movements. Indirectly it is also a plea for long monitoring records, which may improve our understanding of the processes operating in potentially unstable areas.

The temporal aspect of the development of a hydrological trigger is a function of the travel time of recharge towards the ground water level and thus of the distance between the surface and the ground water level and the permeability of the material. The amplitude of the reaction is a function of the amount of recharge and the extension and context of the hydrological system.

2.4 Hydrogeology in mountainous areas

The influence of ground water on slope stability has been recognised already at the beginning of the 20th century and can be found in every soil mechanics textbook. As the role of the hydrology in slope stability is most important, a short review is given of hydrogeological research in relation with slope stability.

In 1963 Tóth published his article in which he showed, using numerical simulations of a 2D, steady-state ground water flow model, that the ground water system generally follows the topography in a catchment. He described local, intermediate and regional ground water systems in a small drainage basin and the alternation of recharge and discharge areas. The local areas were characterised by quick response (and short travel time) of ground water and regional ground water systems reacted with large time delay and attenuation. He also concluded: "the higher the topographic relief, the greater is the importance of the local systems". In their article, Freeze and Witherspoon (1967) showed that recharge areas were invariably larger than discharge areas and described the development of local ground water systems to develop in hummocky terrain.

The latter article also showed with a 3D, steady-state, heterogeneous and anisotropic ground water model, the influence of subsurface permeability variations on the ground water flow pattern. The influence of temporal variations in recharge and discharge on the ground water system was shown by Freeze in 1969 and 1971. Rulon et al. (1985) showed with both a numerical model and a physical model, the development of (multiple) perched water tables and unsaturated wedges in horizontal layered slopes and pointed out the importance of the permeability ratio between layers. Foster and Smith (1988a,b) modelled ground water flow with a fluctuating water table coupled with heat transport under mountainous terrain and studied the controlling factors. They concluded that the bulk permeability had the largest influence on both water and heat flux. Also the quantity of the infiltration flux and the slope profile had a significant influence on both the water- and heat flux. Hodge and Freeze (1977) coupled a hydrogeological ground water model and a slope stability model and showed the influence of the saturated permeability distribution within a slope on its stability. The results showed that a positive pore pressure can develop in a heterogeneous stratigraphy and that this can result in slope instability.

Iverson and Reid (1992) and Reid and Iverson (1992) included seepage forces in their calculation of potential slope failure to elucidate the physics of the influence of ground water flow on the effective stress pattern in slopes. Their results showed that shear stresses are influenced by ground water flow. Thus ground water flow increases the slope failure potential and its effect is highest for seepage areas. These researchers also showed a large influence of the saturated permeability distribution within slopes on slope stability. They calculated that heterogeneity of saturated permeability of 3-4 orders between two layers had the largest effect on the ground water flow and seepage force and thus on slope failure potential.

Above discussed results are all mainly based on computational evidence, and less on field evidence. The field normally tends to behave more complex. Wilson and Dietrich (1987) showed the importance of bedrock flow and concluded: "that the hydrological response of one small unchannelized basin is to a large extent controlled by the ground water circulation patterns in the bedrock, and that these patterns result from large-scale topographic controls and heterogeneities in bedrock permeability". Johnson and Sitar

(1990) inspected the slopes where debris flows started and described “that scars with exposed bedrock continue to emit significant amounts of water from the bedrock for days or weeks following failure”. Ewert (1990) gives numerous examples of ground water flow problems in engineering practice. He states: “I have got the impression that we still lack basic information which would enable us to better predict the behaviour of rock masses in view of their ground water flow". Every investigation site will need to cope with this kind of local circumstances. Some of the underlying processes, however, are identified in hillslope hydrology.

Especially streamflow response for flood prevention and landdegradation (e.g. surface erosion) following rainfall events made researchers identify the hydrological processes on hillslopes. The theory of contributing areas (source areas) is probably the most well known (e.g. Hewlett and Hibbert, 1967, Kirkby, 1978, Dunne, 1983, Ward, 1984). This model describes the hydrological response on rainfall for a uniform slope and how a saturated zone develops at the base of the slope and progresses upward. This leads to pore water pressure increase and possible slope failures at the lowest part of the slope.

The above-described mechanisms of the development of contributing areas development does not explain the observations of saturated source areas and mass movements higher on the slope. Not only can existing ground water bodies be enlarged, also can perched ground water bodies develop in unsaturated soils. Especially in hillslope environments the processes of infiltration and unsaturated lateral flow in relation to the development of saturated overland flow areas has had a lot of attention.

2.5 The unsaturated zone: concepts of flow in partially saturated porous media

One of the first concepts was the concept of "piston flow" in which infiltrating, new water replaces older water in the pores that are still bound to the soil particles. This concept was partly based on the evidence of experiments with tritium tracers (e.g. Horton and Hawkins, 1965; Zimmerman et al, 1966).

The concept of piston flow was based on the premise of a continuous pore network. However, in part by landslide research, field evidence disproved this fundamental assumption as during the late 70s and early 80s the existence of pipes and root channels and their large permeability under storm conditions were reported. In 1982 Beven and Germann published a review paper on macropores. They gave definitions for macropores and listed the processes that created them. The most important implication of macropores is the absence of a continuum for the soil water, and thus a so-called ‘double porosity’ exists. In the matrix negative pore pressure or suction applies, while in the larger macropores atmospheric pressure prevails.

The preferential flow paths in the double-porosity system increase the block permeability and the infiltration rate under near-saturated conditions, but also may restrict infiltration under drier conditions or facilitate the subsequent drainage of a soil. In landslides, the influence of macropores, which to a large extent consist of fissures, is complicated further by the continuous opening and closing of the apertures by the reworking of the sliding material. As an addition to the concept of preferential flow in double-porosity networks, recent experiments also inferred preferential flow paths (or ‘fingers’) as a consequence of wetting front instability in a continuous porous network.

Possible causes for wetting front instability are (De Rooij, 2000): increasing saturated permeability with depth, water repellency, redistribution of infiltration after the end of a rain shower, air entrapment and non-ponding rainfall. Ritsema and Dekker (1994) and Dekker and Ritsema (1996) showed that in apparently homogeneous but water repellent soils (both sand and clay) in the Netherlands, preferential flow paths develop under homogeneous infiltration. Once established, the process of preferential flow will strengthen itself since along the path water repellency decreases and the material remains moister and, as a consequence, the unsaturated permeability will increase (hysterese). Ritsema and Dekker (2000) showed with both laboratory tests and numerical modelling that, once established, preferential flow paths recur at the same location due to the hysterese in soil moisture behaviour of the repellent soil. Flury et al. (1994) conducted dye-tracer infiltration tests on 14 soils and concluded that: "The occurrence of preferential flow is the rule rather than the exception". On the basis of the amassed evidence, small-scale preferential flow is the apparent way to transfer water through the unsaturated zone, even in continuous porous media. With respect to the persistence of preferential flow paths the question remains whether the flow disperses deeper in the soil, where the short-term meteorological influence is less felt, or extends as a discrete process as deep as the capillary fringe. Ritsema (1998) showed that the fingers disperse with increasing soil moisture content and thus with depth.

Hillslope infiltration and lateral subsurface unsaturated flow

The unsaturated zone on slopes shows some additional problems compared to the situation on horizontal planes. This can be referred to as the two-dimensional character of the unsaturated water flow. Hillslope infiltration and downslope unsaturated flow has undergone considerable attention in the last decades. Does a slope augment infiltration rates compared to horizontal surface infiltration? How does infiltrated rainfall move within the hillslope unsaturated zone, and does unsaturated downslope flow exist and what is its magnitude?

Several authors described the infiltration process in hillslopes on both a theoretical basis (e.g. Zaslavsky and Sinai 1981a-b-c-d-e, Philip 1991a-b-c, Wallach and Zaslavsky 1991) and on the basis of (experimental) observations (e.g. McCord and Stephens 1987, Miyazaki 1988). Most authors explained the downslope water movement with anisotropy, but Philip (1991) concluded on the basis of quasi-analytical analysis of infiltration that downslope unsaturated water flow also existed in homogeneous, isotropic soils.

A word about the definition of downslope water movement is necessary here. Philip (1991, 1992) defines downslope water flow as the water flows downslope of the orthogonal. Jackson (1992a-b) replies that for hillslope hydrologists downslope flow exists if water flows downstream of the vertical because only in that situation can water flow downstream towards an exfiltration point without first recharging the ground water. Infiltration of water with a flow vector between the orthogonal and the vertical has unquestionably a downslope component but will end in the ground water system before exfiltrating. It is felt that the definition of Jackson is more appropriate for hillslope hydrological use.

Infiltration has an upslope component at the wetting front because the soil suction equipotential lines are parallel to the surface and thus the soil suction gradient is perpendicular to the soil surface. If time passes the upslope component will move deeper

as the wetting front comes deeper. At the same time the upslope component will decrease as normally the soil suction gradient decreases with depth. At the surface, saturation or near saturation develops and the total potential gradient will become vertical and thus the infiltration vector will rotate towards the vertical (called downslope by Philip 1991). The first period of rain infiltration is called capillary or suction controlled and when time progresses the infiltration process becomes gravitational controlled. Philip (1991) clearly showed that, as long as the rainfall continues no downslope flow - downstream of the vertical - can develop in a homogeneous isotropic soil. In case of lateral downslope flow during rainfall, anisotropy must be present within the soil.

McCord et al (1991) and Jackson (1992) asked themselves how lateral unsaturated subsurface flow could exist in an apparently homogeneous soil. McCord et al (1991) modelled the field experiment of McCord and Stephens (1987) using state-dependent anisotropy. With constant anisotropy, determined under saturated and unsaturated conditions, the experimental results could not be modelled. Defining a 'state-dependent' anisotropy they succeeded in modelling the experimental results of a tracer test in a homogeneous sand dune of McCord and Stephens (1987). The variable, state-dependent anisotropy in unsaturated soils is an effective, large-scale (macroscopic) flow property, which results from media textural heterogeneities at a smaller scale (McCord et al. 1991). Jackson (1992) explained lateral downslope unsaturated flow by assuming a no-flow boundary (no evaporation) after rainfall ceases. The equipotential lines will curve upwards in the direction of the surface and an unsaturated downslope flow will develop. Jackson showed, that lateral downslope flow in a homogeneous isotropic soil is a drainage phenomenon.

Most authors that use numerical modelling techniques showed that the magnitude of the lateral subsurface downslope flow is small compared to the vertical infiltration flux in homogeneous, isotropic soils (Zaslavsky and Sinai 1981d, Philip 1991, Jackson 1992). Philip (1991) calculated that the difference between infiltration on a horizontal surface and a sloped surface is negligible for slope angles up to 30°. In the following analysis using his quasi-analytical solution for hillslope infiltration and lateral downslope unsaturated flow, Philip (1991b-c) showed that the influence of divergence and convergence and of concave and convex terrain has only theoretical influence on the infiltration magnitude in homogeneous isotropic soils.

According to Philip's theoretical model, the lateral downslope flow component in isotropic conditions must be multiplied by the (slope parallel) anisotropy factor, to obtain the lateral downslope flow component in condition of slope parallel anisotropy.

Conclusions

The articles of Ritsema and Dekker (1994) and Dekker and Ritsema (1996) and the ones by McCord and Stephens (1987) and McCord et al. (1991) enforce each other. The former authors write: "The presence of the fingers induce a system of anisotropy in the actual unsaturated hydraulic conductivity. Hysteresis tends to magnify this phenomenon as it is one of the major causes for the long-term persistence of fingers.". The latter authors talk about "state-dependent anisotropy" for which they found strong indications. It is clear that both groups have found the same process only in different situations: a process of preferential matrix flow through apparently homogeneous soils, which is initiated by initial water repellence and persists because of state-dependent anisotropy.

From the foregoing discussion it can also be concluded that 2D effects of unsaturated flow on slopes exist but are limited to the case that the anisotropy factor within a layer and heterogeneity differences are large. Lateral (re-)distribution of water via surface runoff and flow through the litter layer can in different situations be significant. So generally spoken it seems reasonable to presume that one-dimensional vertical unsaturated flow prevails in many slopes.

2.6 Unsaturated and saturated zone modelling approaches for landslide research

Mathematical modelling of the hydrological behaviour in the subsurface serves several goals. It is a tool to calculate water flow and to predict future hydrological behaviour after changes in e.g. land use. It can also be a tool to obtain insight in situations were it is impossible to gather field data. Furthermore, it serves to help the researcher to organise his/her data and to get insight in a specific problem.

The physically based ground water models that are used in mass movement research are mainly based on laminar Darcian flow equations. Double porosity models with turbulent flow through fractures and fissures are not found frequently. Generally, existing numerical ground water models like Modflow (McDonald and Harbaugh, 1988) are used. In these cases the ground water level fluctuations are described in a fully physical-deterministic manner with a finite element or finite difference scheme. The most important drawback is the data demand for such models. Input parameters like saturated permeability are hard to obtain and are known to be spatially very variable. The structure of a finite difference model combines well with geographical databases (GIS). This also facilitates the output of the hydrological models.

Most landslide research uses simple ground water models like the 1D ‘tank’ model (reservoir model) (e.g. Angeli et al. 1998, Van Asch et al. 1996). Tanks with one or more outlets or separate tanks are used to describe relevant hydrological processes. By arranging tanks parallel or serial, all hydrological processes within the slope can be modelled (Okunishi and Okimura, 1987). Most important disadvantage is the lack of physical laws making these ‘tank’ models site specific. The model parameters are obtained by fitting and cannot be obtained otherwise. For this fitting, long, continuous, measurement series are needed. Such models are only applicable if the natural situation does not change with time.

The behaviour of the unsaturated zone obtained a lot of attention because most landslides are triggered by precipitation. A clear knowledge of the transfer of precipitation through the unsaturated zone is therefore of utmost importance. But because of the complex, non-linear behaviour of the unsaturated zone, many simplifications are used. The unsaturated zone models range from black-box (statistical) models to physical deterministic models. The black-box models provide a relationship between precipitation and mass movement. Empirical and distributed empirical models provide the relation between precipitation and ground water level fluctuations. The fully physical-deterministic unsaturated-saturated zone models solve the Richards’ equation numerically (see Feddes et al, 1988 for a review). Well-known computer codes are Unsat (Neuman, 1973 used by Rulon, et al, 1985), Swatre (with crop influence) (Belmans et al, 1983) and SWMS-2D with solute transport (Simunek et al, 1994) and its successor Hydrus

(Simunek et al., 1998). In the latter category the most important and influencing difference is the choice of the unsaturated permeability model (e.g. van Genuchten (1980), Brooks and Corey (1964) or other relationships, see Kutilek and Nielsen (1994) for a review).

Other attempts are made to model the unsaturated zone behaviour with alternative models like the diffusion model (Iverson and Major, 1987, Reid, 1994). Also stochastic approaches are being introduced (e.g. Bierkens, 1998). The latter category has clear advantages in quantifying the uncertainty of model results. As a last category can be mentioned the fully physical-deterministic 3D unsaturated-saturated, heterogeneous, anisotropic catchment model SHE (Bathurst and O'Connel, 1992). It is the well-known attempt to model all hydrological surface and subsurface processes within one model. A last category is the combined hydrological-stability models, for example CHASM (Anderson et al, 1988, Wilkinson et al, 2000). CHASM is a 2D model that combines unsaturated and saturated zone modelling with a static analysis of the slope stability.

2.7 Summary

In mass movement research (ground) water plays an important role in both the saturated and unsaturated zones. The influence of pore water is incorporated in the effective stress model for strength calculations of the soil. The transport of water in the unsaturated zone is generally one-dimensional. Only in case of a slope parallel heterogeneity or anisotropy, lateral flow will occur.

Slope stability research combines well-known difficulties of infiltrating rainfall (interception, surface storage, surface runoff, preferential flow, subsurface flow, perched water tables, etc) with the problems associated with the saturated zone with highly variable subsurface and water table configuration and often very limited 'ground truth'. Although several observations of bedrock ground water contribution exist, the vast majority of the landslide investigations do not take this into account. Almost no work exists in which the origin of the ground water is traced.

Many different hydrological models exist of which some are linked to stability models. This is to facilitate scenario calculations for slope stability. Some are built within a GIS environment and some use GIS for pre- and post-processing. None of the hydrological models, the slope stability models or a combination has become a generally accepted standard.

3 TESTING THE POTENTIAL OF GEOCHEMICAL TECHNIQUES IN IDENTIFYING HYDROLOGICAL SYSTEMS WITHIN LANDSLIDES IN PARTLY WEATHERED MARLS

with: J.T. Buma and C.J.M. Klawer

3.1 Introduction

In the study of hydrological processes in landslides, little attention is paid to techniques to determine the origin of ground water and flowing system within landslides. Knowledge of the ground water system in landslide areas is important when (cumulative) precipitation is related to mass movement via pore water pressure increase. Often a black box modelling approach is adopted to relate mass movement to precipitation. However, without knowledge of the hydrological system it can be difficult to set up a model concept for predicting changes in landslide activity due to stabilising measures, land use or climate change. To predict slope movement as a reaction to precipitation it is important to know the extent of the area feeding the landslide with ground water and to have knowledge of the internal flow system.

For this purpose hydrochemical research can be useful. Appelo and Postma (1993) write: "Ground water chemistry also has a potential use for tracing the origins and history of water. Water composition changes through reactions with the environment, and water quality may yield information about the environment through which the water circulated."

In addition to hydrochemical methods, geochemical techniques can be of value, since ground water chemistry and soil geochemistry interact. The high vertical resolution that can be obtained by geochemical analyses of soil profiles may not only reveal the broad (hydro)geological structure of a landslide, but may also provide indications for zones that are important for slope movement, such as slip surfaces or preferential flow tracks.

Furthermore, changes in exchanger composition of subsurface materials due to interactions with ground water can induce changes in soil shear strength, and thus form another subject of geochemical investigations on landslides. The relation between catastrophic quick clay landslides and freshening of pore water in Norwegian and Canadian marine clays was already recognized by e.g. Bjerrum (1954) and Hutchinson (1961) and still receives a lot of attention (see Senneset, 1996). The type and concentration of salts in pore water exert a significant influence on residual shear strength of e.g. flysch clay (Michaelides, 1995) and several clay types from Italian slopes (Di Maio, 1996). This relates to local clay mineralogy.

This chapter objectives are twofold: first to test the potential of cation exchange capacity (CEC) analysis for refinement of the knowledge of the hydrological system in landslide areas, secondly to examine two laboratory CEC analysis techniques for their applicability to partly weathered marls. In other words, what additional information can be gained by CEC analysis in respect to the hydrological system of a landslide area and are these tests feasible for marls.

In a joint research of the EU-funded HYCOSI (Leroi, 1997) and NEWTECH (Corominas et al, 1998) projects, CEC analyses were executed on samples of 3 cored

drillings, 2 from the Boulc-Mondorès landslide complex in France and 1 from the Alvera landslide in Italy. Cation exchange capacity and exchanger composition were measured with two different laboratory techniques. The results were then compared with the geological descriptions of the drillings.

3.2 Physiography of the test locations

Boulc-Mondorès

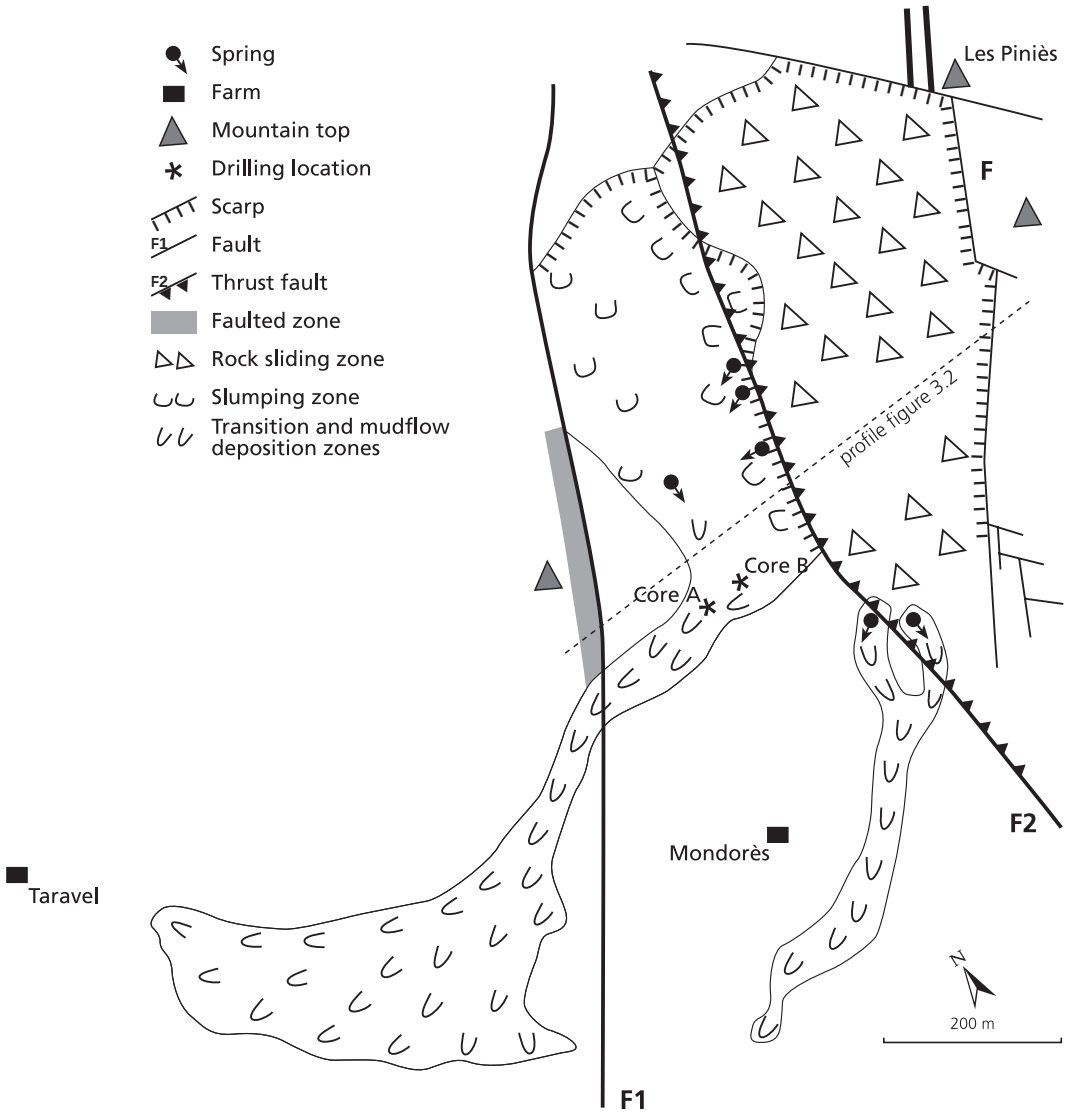

Figure 3.1 Geomorphological map of the Boulc-Mondorès landslide (adapted from Bogaard et al., 2000).

The Boulc-Mondorès landslide complex (figure 3.1) was one of the study sites of the HYCOSI-project, which studies the effects of hydrometeorological changes on slope stability (Leroi, 1997). It is situated in the department Drôme in the French pré-Alps. The area consists of Mesozoic limestone and marls and has a polyphasic structural history from Trias to Tertiary (Bogaard et al, 2000). The main geological structure is a N-S running graben crossing the landslide. In the graben depositions from lower Cretaceous are found, east of the graben a sequence from upper Jurassic and west of the graben an anticlinal from upper Jurassic is located (figure 3.2).

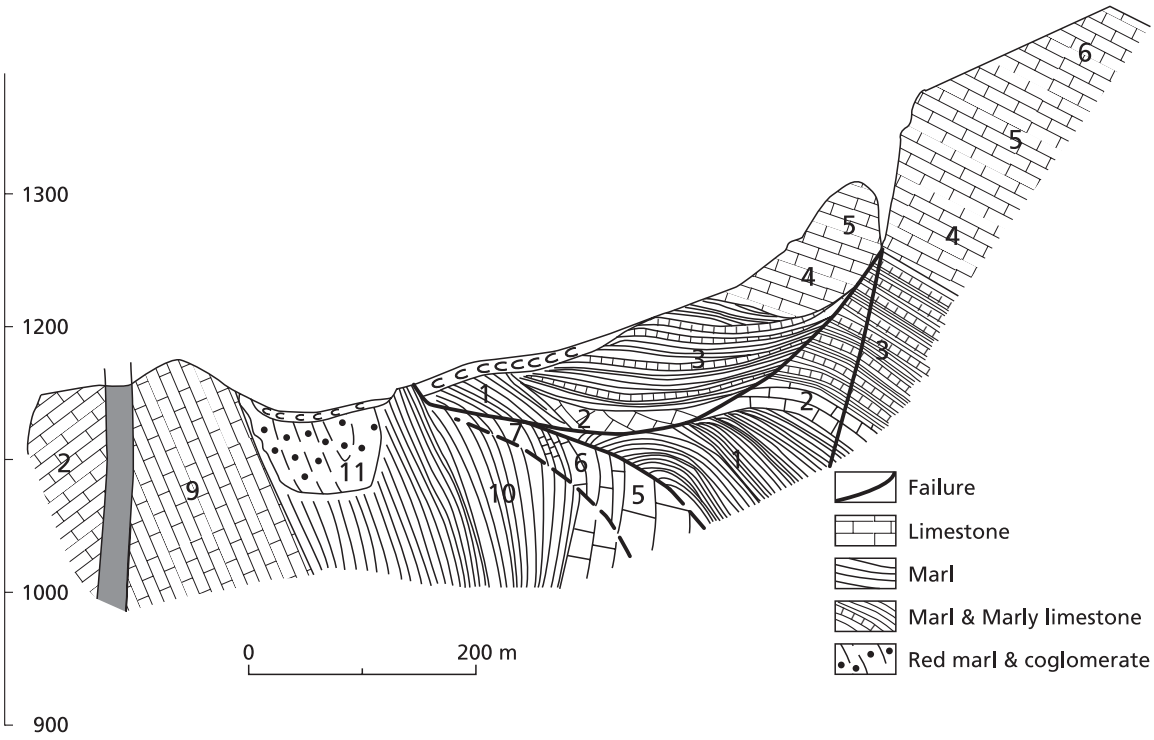

Figure 3.2 Interpreted geological cross-section (for location see figure 3.1). 1, Callovo-Oxfordian; 2, Sequanian; 3, Lower Kimmeridgian; 4, Upper Kimmeridgian; 5, Tithonian; 6, Berrasian; 7, Valanginian; 8, Barremo-Bedoulian; Albian-Aptian; 11, Oligocene (adapted from Bogaard et al., 2000).

The landslide can be divided into four geomorphological units (Bogaard et al, 2000): a rock sliding zone with slowly sinking huge limestone blocks ('Calcaires Tithonique') accompanied by secondary rock falls; a slumping zone with arcuated headscarps in mainly blue marls (Albian-Aptian), sliding and flowing in direction of a narrow opening towards the transition zone; a transition zone in which mudflows are channelled; and a mud flow deposition zone (figure 3.1). The slumping zone approximately coincides with the 'Terres Rouges' graben.

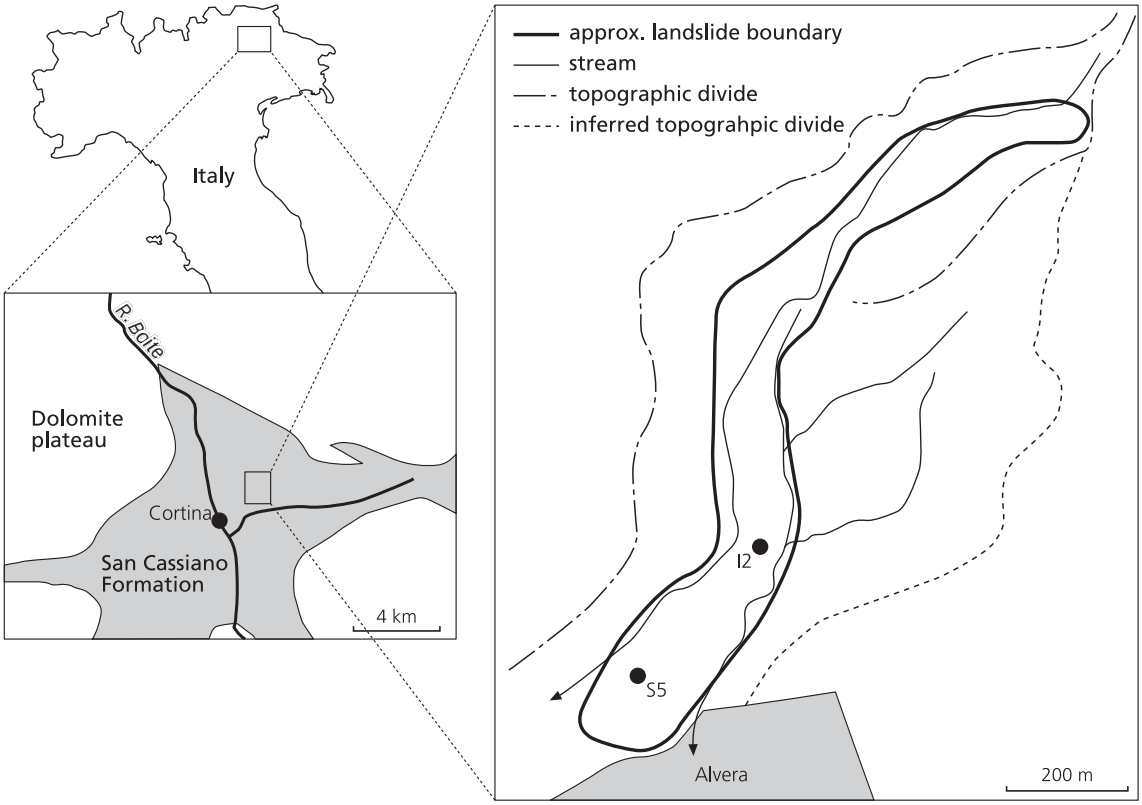

Figure 3.3 Topographical setting Alvera landslide.

The Alvera landslide was a study site in the NEWTECH-project (Corominas et al, 1998), which studies new methods for landslide monitoring and modelling. It is situated near Cortina d'Ampezzo, Eastern Dolomites in Italy (figure 3.3). It is described in detail by Angeli et al. (1992), Deganutti & Gasparetto (1992), Gasparetto et al. (1994) and Angeli et al. (1999).

The landscape of the Dolomites is dominated by very steep dolomitic plateaux (Dolomia Principale) with at their base gentler slopes, developed in the less resistant San Cassiano Formation. The Alvera landslide developed on such a gentle slope consists of weathering products of the San Cassiano Formation: overconsolidated marine clays with calcareous, dolomitic and loamy fragments. However, due to its long history of mass movement the landslide body has a complex structure. It consists of badly sorted fragments of the original rock set, with thin layers of calcareous and organic material. The landslide is 1700 m long, 80 m wide and the average inclination is 7.3°. Measurements show movement totalling about 40 cm in 5 years (Gasparetto et al., 1996). The landslide is probably a reactivation of a much larger prehistoric landslide.

3.3 Previous research

Boulc-Mondorès

Phan (1992) analysed samples from the Boulc-Mondorès landslide on a.o. calcium content, percentage material < 74 μm, < 2 μm and determined the various clay types and their concentration in the Albian/Aptian blue marls. Both disturbed (weathered) surface material and relatively undisturbed (less weathered) material from the Albian-Aptian marls were analysed. The analyses are summarised in table 3.1:

Table 3.1 Distribution of particle size and clay types of the Albian-Aptian marls (from Phan, 1992).

Particle size distribution		Clay mineralogy		
<74 μm [%]	<2 μm [%]	Illite [%]	Kaolinite [%]	Montmorillonite [%]
96	10	25	15	60

The Aptian marls are composed of limestone, silicates and (mainly montmorillonitic) clays. Electron-microscope photographs showed abundant micro-caves of ± 2 μm in the Aptian marls and the complete absence of larger minerals (Phan, 1992). It also showed a mixture of coccoliths (calcareous planktonic organisms with <1 % $MgCO_3$, Morse and Mackenzie, 1990), coccospheres (composed of several attached coccoliths), occasional carbonate deposition and clay. The important fine fraction with the nanofossils causes a system that is totally disorganised in structure, facilitating water circulation. Phan (1992) concluded that the Boulc-Mondorès landslide is the result of hydration-dehydration of clay and dissolution of limestone coccoliths. If CEC is assumed to be related only to the clay fraction (10 %), this corresponds to a CEC of 7-13 meq/100g (CEC for montmorillonite is 70-130 meq/100g).

Hydrochemical samples were obtained at the Boulc-Mondorès landslide to investigate the hydrogeological system of the most active part of the landslide area: the slumping zone (Bogaard and van Asch, 1996; Bogaard et al, 2000). The samples were taken from thirteen shallow piezometers that were placed in phreatic ground water at 1.5-2.5 m depth with a filter length of 40 cm, located in the slumping, transition and mud flow deposition zones (figure 3.1). Two different water types were distinguished: low ion concentration water of around 6 meq/l in the red Oligocene marls (western part of the slumping zone, see figure 3.1-3.2) and high ion concentration water of around 20 meq/l exfiltrating the Albian blue marls (eastern part of slumping zone, see figures 3.1-3.2) (Bogaard and van Asch, 1996). Both discharge in the direction of the transition zone. The red Oligocene molasse are underlain by Albian-Aptian blue marls (figure 3.2). The water chemistry indicates that the ground water has not been in contact with the underlying deposits. The superficial hydrological system of the landslide was described by Bogaard et al. (2000) as a shallow, perched ground water table fed by precipitation. Of the deeper ground water system it was suggested that it could be fed by the perched ground water system, from the scree slope in the rock sliding zone or even by karstic supply from the eastern limestone mountains.

Gasparetto et al. (1994) and Angeli et al. (1999) examined lithological profiles from Alvera, and found that the landslide body consists almost entirely of remoulded clay with occasional calcite, dolomite and calcarenite fragments. Vertical differentiation is made up by organic layers separating zones with different degrees of consolidation. This feature indicates buried vegetation related to landslide events (Gasparetto et al., 1994). On the basis of these observations alone, no active slide surfaces could be inferred. Inclinometric measurements and from excavations revealed movement taking place mainly in zones of several mm thickness at depths ranging between 2.5-5 m and 20-25 m depth across the landslide (Deganutti and Gasparetto, 1992; Angeli et al., 1999).

The samples for geochemical analysis were taken from borehole I2 (figure 3.3). The lithological record of this borehole displays the characteristics outlined above. A thin peat layer was found at 24.3 m, which supported the inclinometric observations of a slide surface between 20 and 25 m (Angeli, et al, 1999). A clay content of 71 % and a Skempton activity index of 0.72 were found for a sample from borehole S5 (see figure 3.3) at 5 m depth. The activity index value is intermediate to values reported by Grimm (1962) for illite and montmorrilonite (0.3-0.6 and >1.2 respectively). X-ray diffraction on samples from borehole I2 at depths of 7.2, 16.5, 22.5 and 24.3 m revealed spectra that are characteristic for montmorillonitic clays (Angeli et al., 1999).

Some hydrochemical data were obtained by sampling water from streams and piezometers. Unfortunately, many of the piezometers have filters of several meters length. This induces mixing of different water qualities and thus interpretation of the measurements is difficult. The only significant trend that can be observed, is a change of $CaHCO_3$-water to $NaHCO_3$-water with increasing depth. However, the nature and depth of the transition between these water 'types' could not be inferred.

The hydrological system of Alvera is given by Angeli et al. (1998). They describe an upper zone ('root zone') of 0.5 to 2 m thickness with abundant superficial cracks, which facilitates infiltration as well as discharge. Underneath the root zone they define a clay layer of unknown thickness with some dead-end cracks facilitating deeper infiltration.

3.4 Description of drilling method and cores

Both in Boulc-Mondorès and in Alvera, a rotation, double envelop, 115 mm diameter drilling technique was applied, with a cable sampler to facilitate sampling. In both cases, local surface water was used as drilling fluid. Penetration of drilling fluid into the soil core is assumed negligible.

In Boulc-Mondorès, two cored drillings were placed (figure 3.1) at the margin of the slumping and transition zones, the most active part of the landslide area where the ground water system was thought to converge into the transition zone (Chassagneux and Leroi, 1995). Core A is a 'cored drilling': all material is lifted undisturbed and stored in wooden 'core boxes'. Core B is 'destructive': the cores were taken more rapidly and stored in 2 m long PVC tubes, slightly disturbing the sample. In both cases the total core length was saved, 21 m of core A and 25 m of core B. The upper 5-6 m were lost during drilling because the incoherent material was flushed with drilling fluid. Plasticity of material, progress of drilling and occurrences of waterbearing layers were described during

drilling. In a later stage the cores were described hydrogeologically (lamination, fractures, fissures and secondary calcite precipitation) and subsamples were taken. 20 Samples of 5-10 cm were taken from the undisturbed core A and 12 from the disturbed core B. The core descriptions give information about disturbance of the material during drilling, which may occur when the core cylinder is full, or when less coherent material is encountered resulting in twisting of the sample.

The drillings were located in the Albian-Aptian blue marls. The first drilling (core A) has three main units: until 4.5 m remoulded unconsolidated sediment of recent mass movements, followed by Albian-Aptian marls down to 19.5 m where the Barrémo-Bédoulian limestone (see figure 3.2) was encountered. Core B consist of two units, first until a depth of 6.5 m remoulded unconsolidated sediment of recent mass movements, followed by Albian-Aptian blue marls until the voluntary stop of the drilling at 25 m where the Barrémo-Bédoulian limestone was not yet encountered (see also figure 3.5).

In Alvera, the CEC measurements were carried out on 8 subsamples from borehole I2 (figure 3.3). The drilling had a total length of 24 m, but so far CEC measurements have been carried out to a maximum depth of 16.5 m only. The drilled core was stored in a moist state in sealed plastic bags, so some chemical alteration prior to analysis may not be excluded.

3.5 Description of laboratory analyses

A brief description of the laboratory techniques for determination of exchanger composition and cation exchange capacity (CEC) is given. Furthermore, unmarked double samples (duplicates) were included from each core to test the reproducibility of the analyses of both techniques (part of the second objective). Lastly, carbonate determinations were performed to adjust CEC determinations for carbonate content.

The samples were air dried, crushed manually with a mortar and sieved repeatedly with a 300 µm sieve, until all material had passed the sieve. Exchanger composition and CEC were analysed with a 'displacement after washing technique' (Thomas, 1982) using two different salt solutions: Ammonium Acetate and Sodium Chloride.

In the Ammonium Acetate (NH_4Ac) technique, the cations at the adsorption complex are displaced with 1M NH_4Ac. The concentration of the cations in the fluid is analysed using ICP-AES. The CEC is determined by flushing the sample with 1M Sodium Acetate (NaAc), resulting in only exchangeable Na^+, the called 'index cation'. The sample is washed with 96 % ethanol, removing excess Na^+. The sample is again flushed with NH_4Ac extracting all Na^+ from the adsorption complex. Subsequently, the Na^+ is measured by flame photometry. The total Na^+ concentration equals the CEC.

The Sodium Chloride (NaCl) technique follows the same principle. The sample is flushed with 1M NaCl solution and the concentration of the Ca^{2+}, Mg^{2+} and K^+ from the adsorption complex is measured using ICP-AES (Na^+ cannot be determined). Determination of the CEC was performed by washing the soil with 70 % ethanol to replace the porefluid. The Na^+ sample was then flushed with 1M $MgCl_2$ solution. Seasand, with a known CEC, was added to the sample (ratio seasand-sample is 1:1) to bring the sample into suspension. The Na^+ concentration in the extract is then determined by flame photometry.

Both described techniques have Na^+ as 'index cation', but different displacement solutions (NH_4Ac and $MgCl_2$). The main drawback of the NH_4Ac technique is that NH_4Ac (carried out at pH=7) dissolves calcite and gypsum. This can result in an overestimation of the Ca^{2+} concentration, impeding a check of the analyses by comparing the CEC to the sum of the analysed exchanger cations. Results obtained with the NaCl technique (carried out at pH=8.2) are used to compare CEC, K^+ and Mg^{2+} determinations and to improve measurement of Ca^{2+}.

The Scheibler test (NEN5757, 1991) was used to determine the carbonate content in the sample. If a sample has relatively high $CaCO_3$ concentration, this decreases the CEC (less exchanger per 100g dry soil). It furthermore can point out differences in lithology within one drilling, e.g. secondary calcite deposition.

3.6 Results

Evaluation and comparison of the two laboratory methods

The results for the duplicates are given in table 3.2. The relative difference is 3 to 6 % except for the calcium determination. Generally, the results of the duplicates show that the analyses were performed accurately and that the applied techniques give consistent results. Table 3.2, however, also shows that the laboratory analyses with NaCl are slightly better reproducible than the analyses using the NH_4Ac method.

The two techniques gave identical results for CEC (figure 3.4a) except for sample I2.1 (resp. 35 and 75 meq/100g). The latter was interpreted as an unexplained laboratory error and consequently removed from the data set. The CEC values of the Boulc samples range from 15 to 35 % and are in some cases a higher than would be expected on the basis of Phan's results (§ 3.3). Probably the clay content of the blue marls is higher. The amounts of exchangeable magnesium (Mg^{2+}, figure 3.4b) determined by the two techniques are in good agreement with each other for all Boulc samples, and at low values for the Alvera samples. At higher values the NH_4Ac technique gives higher values for the Alvera samples than the NaCl technique.

Table 3.2 Relative difference between the analyses of duplicate samples. In the last column the average of the 5 duplicate samples is given.

Method	Element	A.7 %	A.16 %	B.5 %	B.8 %	S1.1 %	Average %
NH_4Ac	Ca	16	25	9	6	3	12
NaCl	Ca	12	1	19	20	3	11
NH_4Ac	K	6	12	2	4	5	6
NaCl	K	1	1	3	2	8	3
NH_4Ac	Mg	0	10	1	1	9	4
NaCl	Mg	3	1	3	2	7	3
NH_4Ac	Na	3	9	2	8	9	6
NaCl	CEC	2	1	2	3	6	3
NH_4Ac	CEC	1	1	4	6	5	4

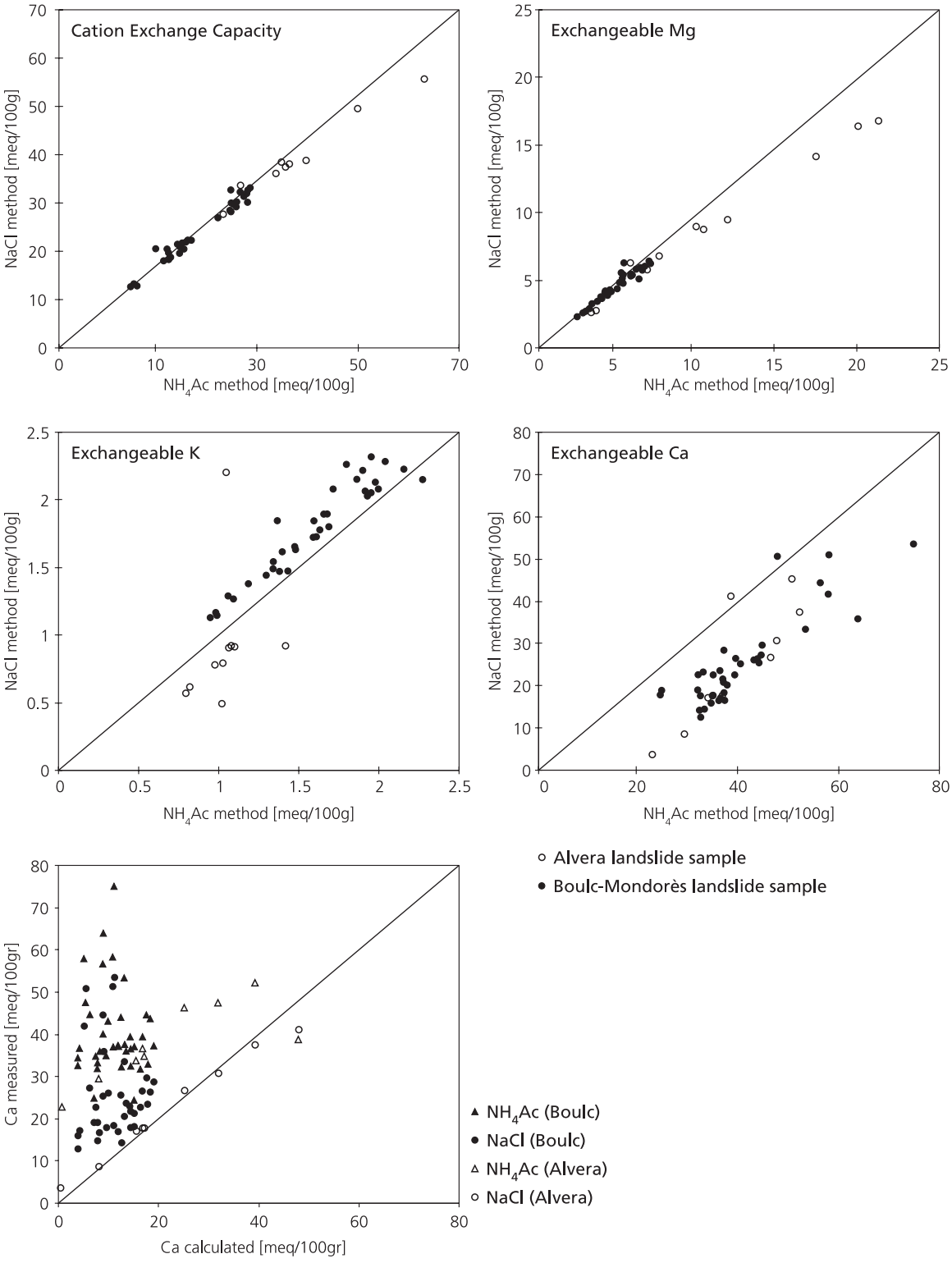

Figure 3.4 Comparison NH_4Ac and NaCl laboratory analyses of cation exchange capacity and cation composition for the Boulc-Mondorès (black dots) and the Alvera (open dots) landslide samples.

The amounts of exchangeable potassium (K^+, figure 3.4c) show that the NH_4Ac technique tends to analyse more K^+ than the NaCl technique for the Alvera samples, but for the samples from Boulc the opposite is true. Exchangeable Na^+ could only be determined with the NH_4Ac-technique. Although the Na^+ results could not be validated, it is assumed that these values are accurate due to the conservative nature of Na^+.

Figure 3.4d shows the results of the concentration exchangeable Ca^{2+} determined with both methods. The NH_4Ac method seems to result in 15-25 meq/100g higher fraction than using the NaCl technique. Both techniques, however, result in Ca^{2+} concentrations that are higher than the CEC, which is impossible. The amount of exchangeable calcium determined by both techniques was therefore compared with the values that would be expected if the amounts of exchangeable Mg^{2+}, K^+ and Na^+ are subtracted from the CEC (figure 3.4e). Mg^{2+}, K^+ and CEC are taken from the NaCl results and Na^+ from the NH_4Ac method. This result shows that also the NaCl method seems to overestimate the Ca^{2+} concentration for a large number of samples. Only the Alvera samples in combination with the NaCl technique resulted in a corresponding Ca^{2+}. The overestimation of exchangeable Ca^{2+} by both techniques is more severe in the marls from the Boulc-Mondorès site than in the more clayey site of Alvera. Stronger overestimation of exchangeable Ca^{2+} by NH_4Ac may be related to the slightly acid character of the displacement fluid. The problem of determining exchangeable Ca^{2+} when calcite or gypsum is available in the soil is also described by Thomas (1982).

In case of determination of CEC and exchangeable cations in marly sediments, the NaCl-technique appears to be more suitable then the NH_4Ac method. The determination of exchangeable Ca^{2+} remains difficult. Furthermore, exchangeable Na^+ cannot be determined with this method and has to be measured using another laboratory method. It was therefore decided to use values of CEC, Mg^{2+} and K^+ obtained with the NaCl method. The Na^+ fraction comes from the NH_4Ac method. Lastly, the Ca^{2+} was calculated as the difference of the CEC and the sum of the analysed cations (Mg^{2+}, K^+ and Na^+).

Results of the CEC and exchanger cation measurements I: Boulc-Mondorès

In figure 3.5 the CEC and the exchanger cations of core A are given together with a schematic geological column. The CEC profile corresponds well with the description of the drilling. A low CEC (20 meq/100g) is found in the marls directly underneath the remoulded deposition at 5 m depth, in the two disturbed zones at 9.5 and 10.5 m depth and at the transition of the marls formation towards the limestone formation at 19 m. Below the disturbed zone of 9.5 m depth also a calcite vein was observed. No difference in CEC was found above and below the observed fracture at 16.5 m depth with secondary calcite deposition at the fracture surface.

The exchanger cations are expressed as a fraction of the total CEC and plotted against depth. It shows a stable K^+ fraction with depth, a slowly decreasing Mg^{2+} fraction, a quickly decreasing Ca^{2+} fraction and a quickly increasing Na^+ fraction with depth. Obviously, between 19 and 19.5 m depth the Ca^{2+} fraction increases again while the sodium fraction decreases.

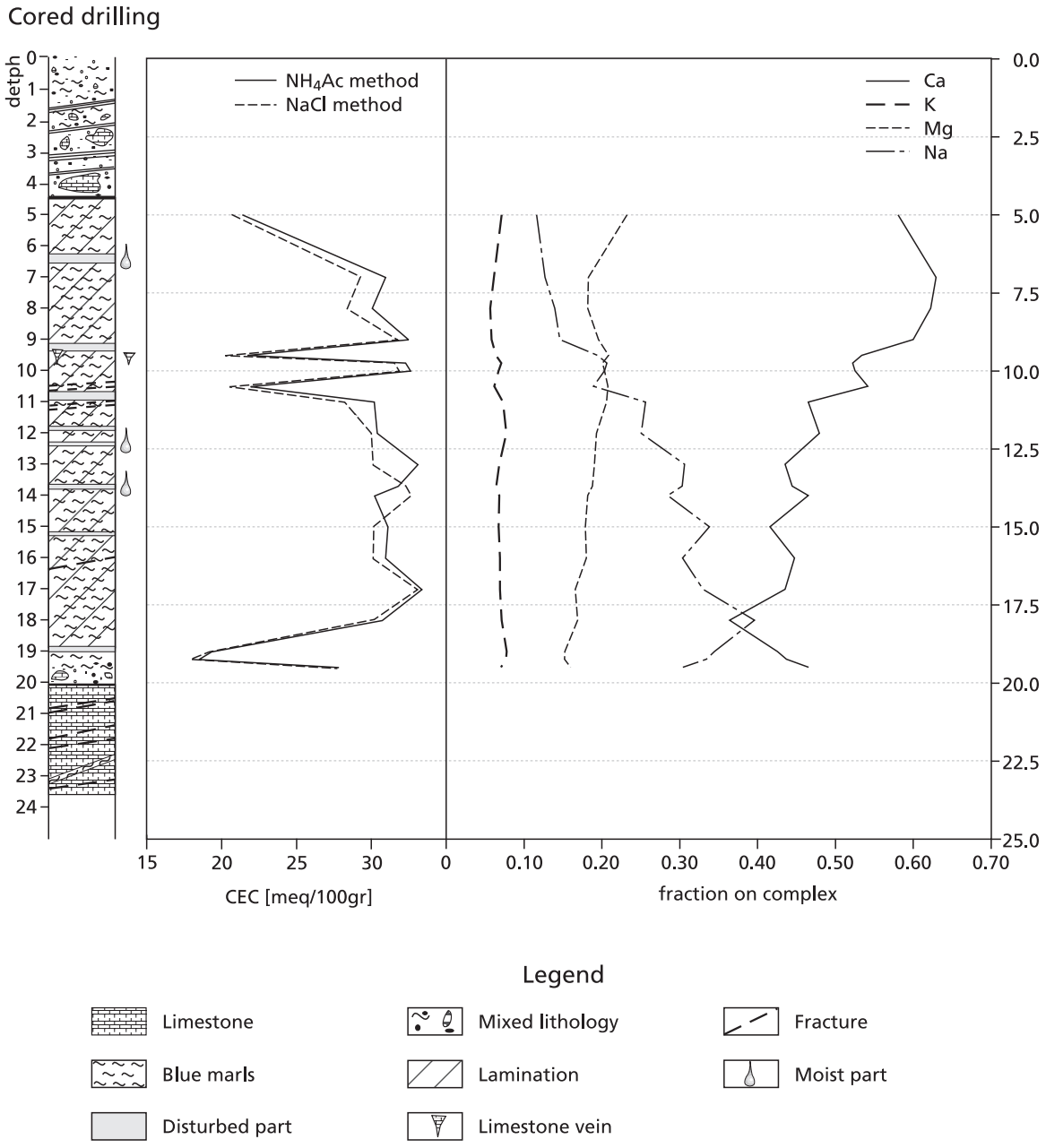

Figure 3.5 Geochemical profile of core A from Boulc-Mondorès.

For core B, the CEC is lower than for core A (figure 3.6). Values are around 20 meq/100g with a clear minimum of 13 meq/100g between 17-20 m. The exchanger cations expressed as fractions of the CEC give a constant potassium fraction and slowly decreasing magnesium fraction with depth except for 16.5 m below surface. The sodium fraction increases rapidly down to 12 m, gradually increases until 21 m depth and decreases afterwards. The calcium fraction decreases until 16.5 m, remains constant until 21 m and increases afterwards.

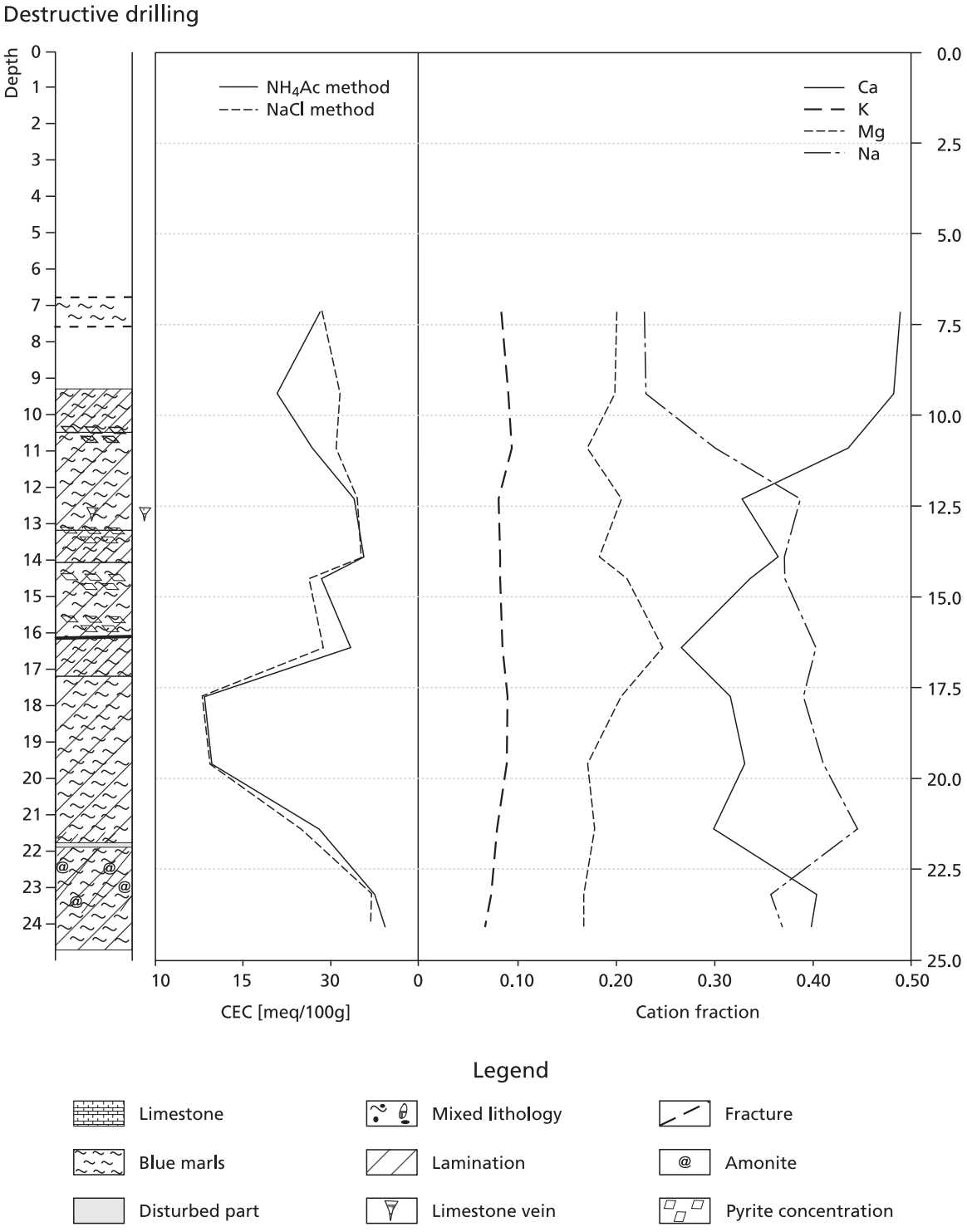

Figure 3.6 Geochemical profile of core B from Boulc-Mondorès.

Results of the CEC and exchanger cation measurements II: Alvera

The CEC profile does not reveal any distinct intervals (figure 3.7). The CEC appears to be slightly higher in the upper 5 m and then diminishes with depth. No samples between 7.2 and 16.5 m depth could be obtained to support this observation. The analysis of exchanger cation fractions with depth shows two distinct intervals with a transition between 4 and 5.5 m depth (figure 3.7): above this transition, Ca^{2+} is the dominant cation, while below it Ca^{2+} and Mg^{2+} dominate. Another feature is the gradual increase in exchanger Na^{+} below this transition.

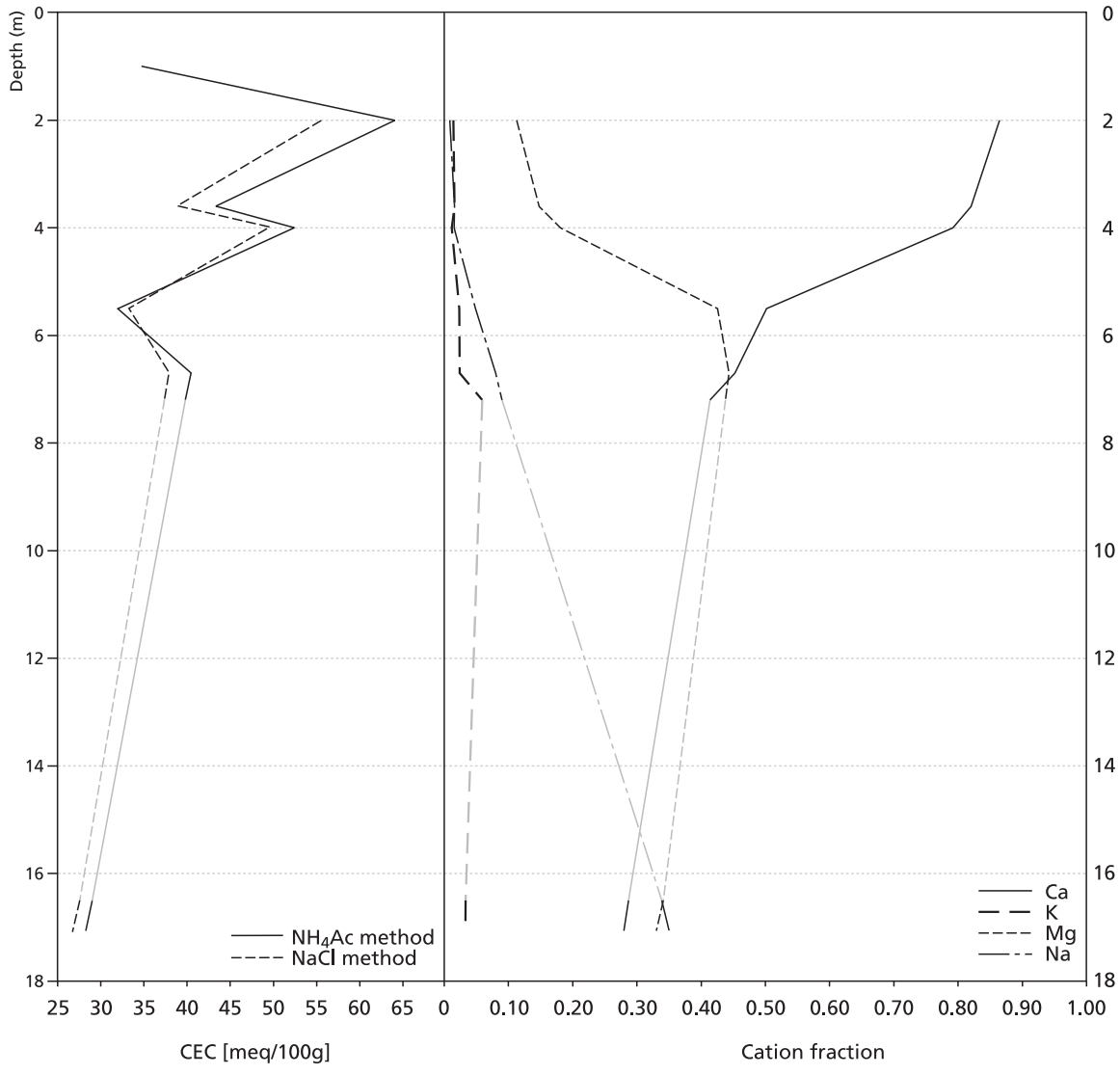

Figure 3.7 Geochemical profile of core I2 from Alvera.

Results of the Scheibler carbonate test

The carbonate concentrations in the Boulc-Mondorès cores vary between 1 % and 15 % (average 5.7 %) for core A and in core B between 0 % and 28 % (average 7 %). The carbonate concentration in the Alvera samples range from 0 % to 18 % (average 9 %). The Scheibler carbonate tests show strong variations with depth that correlate with the variations in CEC (figure 3.8). In the Boulc cores the negative correlation between $CaCO_3$ concentration and CEC values of a sample is very pronounced. In the Alvera core the CEC and $CaCO_3$ are positively correlated.

The CEC values as determined and described earlier should be corrected for the carbonate fraction in the samples. Carbonate does not contribute to the CEC of a sample. High percentage of carbonate would automatically result in a lower CEC. The carbonate fraction in a sample could explain the CEC variations in the core samples. The carbonate content is deducted from the dry weight of soil. Figure 3.8 also shows the corrected CEC values. Only the very low CEC value in core B of Boulc-Mondorès between 17.5 and 20 m depth becomes less pronounced. Generally, the carbonate correction does not alter the CEC patterns with depth.

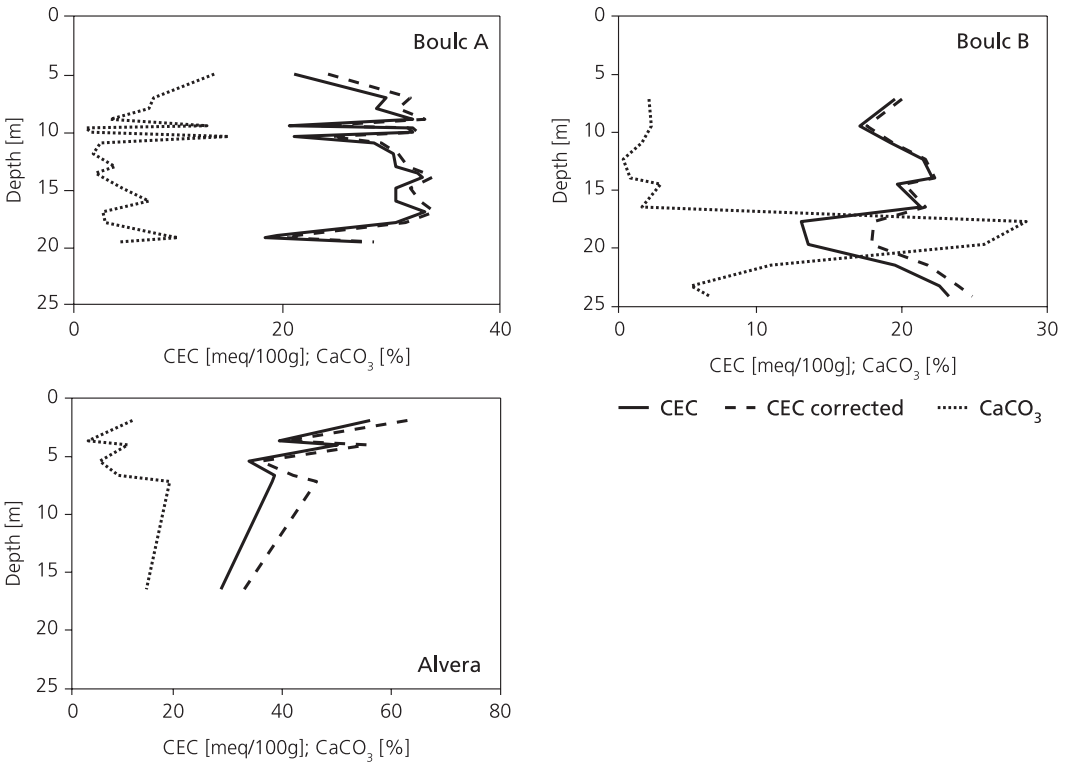

Figure 3.8 CEC values and carbonate content with depth for all three cores.

3.7 Discussion

This discussion will first deal with the presented laboratory methods and then the measurement results will be discussed (CEC, $CaCO_3$, cation fraction) for each core. Here, the measurements are evaluated and explained and placed into their local context.

The two laboratory techniques show that reliable geochemical results can be obtained not only for clays, but for marls as well. The tests showed to be reproducible and consistent. Where soluble minerals like calcite are known or expected to be present in the sample, the use of NaCl as displacement fluid is preferred over the slightly acid NH_4Ac. The omission of sodium as exchanger cation when using the NaCl method can be prevented by applying other salt solutions like $SrCl_2$.

Of the Boulc-Mondorès drillings, core A was an undisturbed drilling for sampling and geological description purposes. Core B was a so-called 'destructive' drilling, i.e. it was not meant for sampling. It used the same drilling technique but was executed faster. Therefore, core A shows more detailed information. The lower CEC values for core B are most probably caused by the way in which this core was stored: in a moist state and in PVC tubes. The core is probably influenced by weathering due to exposure to oxygen in the PVC tubes. On the other hand it shows that in the case of possible oxidation of soil samples, geotechnical tests should be carried out as soon as possible after sampling to exclude a change in chemistry and mineralogy that may have a large influence on shear strength.

In Boulc-Mondorès core A, distinct geological and geochemical differentiations were observed. However, before attempting to link these with e.g. landslide phenomena, it needs to be examined whether the geochemical differences can be related to artificial drilling disturbances. Drilling fluid and deposition of drilling mud could be an explanation for the geochemical variation. Disturbance and twisting of the sample is either the consequence of a weaker layer, which has less coherence than the undisturbed marls, or the result of drilling with a completely full core length inhibiting further drilling progress. Figure 3.5 shows that all combinations between the occurrence and absence of a drilling disturbance with both high and low CEC exist. On the basis of these observations, it can be assumed that a drilling disturbance in itself does not affect the CEC values.

If the CEC variations are not artificial, the question arises what has caused these variations? The differences in CEC values could be the result of differences in material characteristics caused by weathering. The weathered intervals could result from limestone dissolution, as described by Phan (1992). Dissolution of the nanofossils will cause the collapse of the micro-caves and a change in internal structure of the material in the weathered zones. The calcite oversaturation of water that flows through these preferential flow paths could then result in secondary calcite deposition. This could explain why the low CEC-values coincide with high carbonate concentrations. So far these changes have not been measured independently with e.g. X-ray diffraction.

An alternative check was done by comparing CEC and exchanger composition of surface (mudflow) material, with the results found in the core. If the geochemistry of the weathered surface material and that of the weathered intervals in the core are identical, it is likely that the same chemical processes are involved. The CEC of weathered surface material is around 15 meq/100g with less than 10 % sodium possession and around 50 % calcium possession. The geochemistry found in the disturbed weathered layers resembles

the surface sample. This indicates that the disturbed layers in the core could have been subject to the same weathering process.

Bogaard and Van Asch (1996) suggest that the high concentration water that originates from scarps of fresh Albian-Aptian blue marls and that is characterised by very high sodium and sulphate concentrations, is the result of pyrite oxidation. Pyrite is abundantly available in the Albian-Aptian blue marls. This causes an increase of acid (H^+), which is immediately neutralised by limestone dissolution. The Ca^{2+} concentration in the water increases rapidly causing an imbalance between the water chemistry and the exchanger composition. As a consequence, sodium at the complex is replaced with calcium. While these processes need oxygen, this would lead to low sodium concentration at the cation complex near the surface and increasing sodium fraction with depth. This is in very good agreement with the measured cation fractions of both cores A and B (figures 3.5 and 3.6). The general decrease of the sodium fraction towards the surface in cores A and B suggests that the described weathering process takes place over a large depth. The pronounced dips in the sodium fraction in core A at 9.5 and 19.5 m depth can indicate that this process is more active here and would point to preferential flowpaths. Although it is not clear whether pyrite oxidation causes these preferential flowpaths, or the opposite.

Of the geochemical measurements on the Alvera core, only the results of the cation fraction could be explained, not the CEC and $CaCO_3$ analysis. On the basis of the geochemical results for the Alvera I2 borehole, two distinct intervals were identified (see figure 3.7). Till 5 m depth Ca^{2+} dominates the exchanger complex, below 5 m Ca^{2+} and Mg^{2+} prevail. These intervals point to two distinct water types with compositions related to the exchanger composition. At 16 m depth the sodium fraction has increased at the expense of Ca^{2+} and Mg^{2+}. The increase of Na^+ with depth is in agreement with the change from $CaHCO_3$ to $NaHCO_3$ found in the ground water (see § 3.3).

Figure 3.9 shows a similar development, but less distinct, of different cation composition for the Boulc-Mondorès cores. The sodium fraction is compared to the calcium and magnesium fraction in cores A and B. Both show an upper section till around 10 m depth with low Na^+ and high Ca^{2+}-Mg^{2+} concentrations. Below that a gradual increase in sodium concentration is perceptible. This could point to the depth of the influence of precipitation in the local water system.

The hydrological system of the Boulc-Mondorès landslide was schematised as a superficial hydrological system, fed by precipitation. On basis of the cation composition, this ‘infiltration’ system seems to reach as deep as 10 m (figure 3.9). Furthermore, the subsurface seem to have several important preferential flowpaths. Lastly, some additional arguments for pyrite oxidation were come across, but no decisive answer about the origin of the water quality can be given. The Alvera hydrological schematisation gave a ‘root zone’ of 0.5 to 2 m deep and underneath a clay zone of unknown depth. The geochemical analyses indicate an infiltration zone to a depth of 5 m below surface at I2 drilling. This enforces the idea of so-called ‘dead-end’ cracks infiltrating the clay zone.

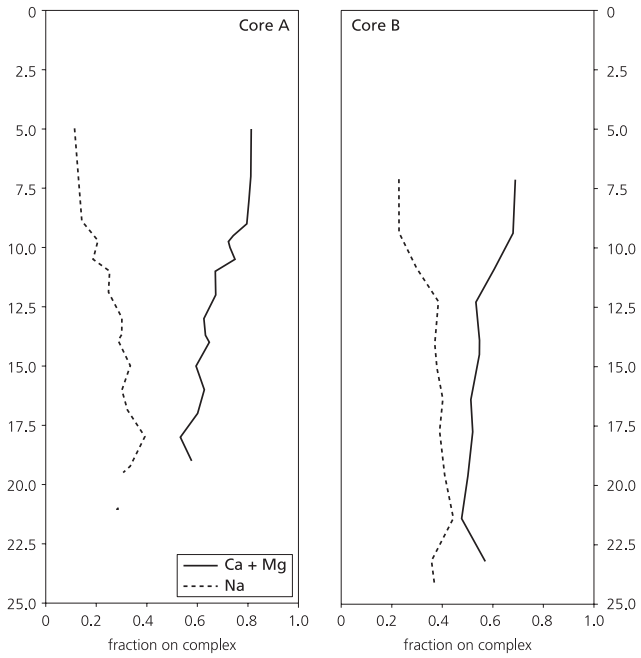

Figure 3.9 Profile of cation fraction possession from cores A and B of the Boulc-Mondorès landslide: Mg^{2+}+Ca^{2+} vs. Na^{+}.

Knowledge of the depth of the transition between water types can improve understanding of the hydrological system of a landslide significantly, if the origins of these water types are known. This would in particular be the case if the upper water type is representative for locally infiltrated water and the lower water type for regional ground water. However, it is too early to make statements with respect to this without more spatial geochemical information to support the findings, and some more detailed hydrochemical measurements to better characterise the water types.

3.8 Conclusions / further outlook

The aim of this chapter is not to come up with the definitive interpretations of the hydrological systems for the two landslides presented here. For such a purpose the presented data are rather limited. However, it was shown in what respect geochemistry can be used in landslide investigations. Because many landslides are very difficult to unravel using standard geohydrological methods, it is proposed to add hydro- and geochemical techniques to such studies. If borehole columns are available, these techniques are relatively cheap and fast. CEC and cation fraction analyses are applicable in marls, although some caution should be taken considering carbonate dissolution. It is furthermore recommended to try $SrCl_2$ as displacement fluid.

The Boulc-Mondorès example showed that a large amount of information on the subsurface can be extracted from geochemical analyses. In the Boulc-Mondorès cores distinct weathered layers could be identified. The weathered layers could develop or may

already have been developed into slipsurfaces. Geotechnical analysis of the weathered material should reveal that.

With this geochemical information it has also been possible to explain the water chemistry found in the Boulc-Mondorès landslide. In less complex settings the combination of hydro- and geochemistry could reveal the extension of the ground water catchment delivering water towards the landslide area. Both Alvera and Boulc-Mondorès examples show that geochemical techniques may be useful in locating boundaries between water types where this is not possible with lithological data. The geochemical results obtained from boreholes can be used in planning depth-specific hydrochemical sampling to characterise a change in water type. The above-mentioned information can be of great importance in landslide interventions for which the hydrological system and the origin of the water have to be known in detail. It is also plausible that knowledge of the hydrogeochemical evolution of clayey landslides may improve long-term predictions of slope stability.

A slipsurface of only several millimetres thick will not be found with geochemical techniques, unless it was already visible in the core and thus sampled deliberately. The proposed methods work on a decimetre scale, not smaller. As the CEC analyses may reveal ‘internal differences’ that could have severe influence on the slope stability. As stated in the introduction, chemical composition can have a very large effect on the strength parameters of the soil. The here described technique can also be used for purposive sampling for laboratory strength tests.

From the above it is clear that geochemistry is a potentially valuable technique for e.g. landslide research, but it is recognised that still a large amount of work has to be done before all practical uncertainties are solved.

4 PHYSICAL AND HYDROLOGICAL CHARACTERISTICS OF THE BELINE STUDY SITE

4.1 Topographical information of the Beline slope

The Beline slope is situated in a small village called Salins-les-Bains in the Jura department, France (figure 4.1). It is located in the lower part of the Jura mountain chain with regional elevation ranges from 300 m to 800 m. The Beline slope lies between the 'Furieuse' stream (345 m) and the Clucy limestone plateau (± 600 m), has an average slope of 17° and covers 36 hectares. The Beline slope is bordered on the north side by two different limestone scarps, on which in the northwest edge Fort Belin is built. The Furieuse flows on the southwest side. The slope continues on the east side and turns after approximately half a kilometre northeast into the Gouaille valley (figure 4.2).

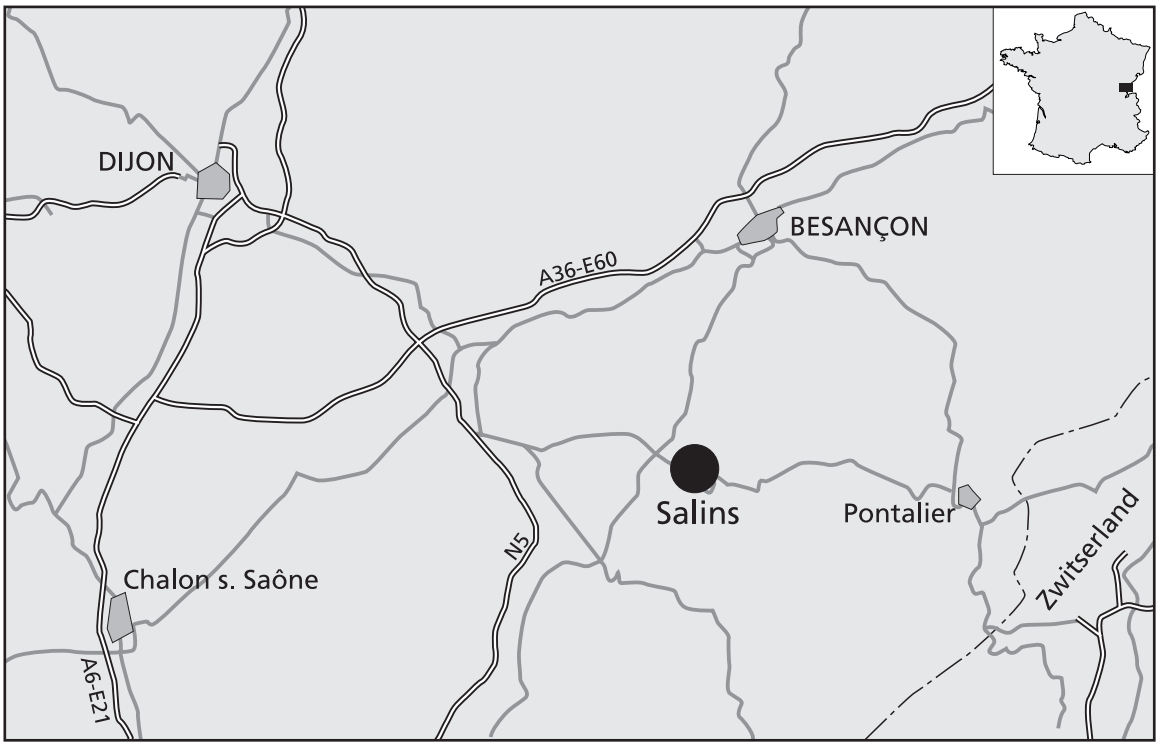

Figure 4.1 Location of the study area.

The Beline slope has had different land use types; viticulture, agriculture and presently the area consists of private gardens of grass and fruit trees (figure 4.3). On the site, a few remnants of an old drainage system are found, called “Raie pavée”. The drains were superficially built and had the shape of a canal of approximately 40 cm wide and 20 cm high. They were made of limestone stones that were simply placed on or in the soil. The system has collapsed after the site was abandoned for agriculture and viticulture. The current state and distribution of the system is unknown.

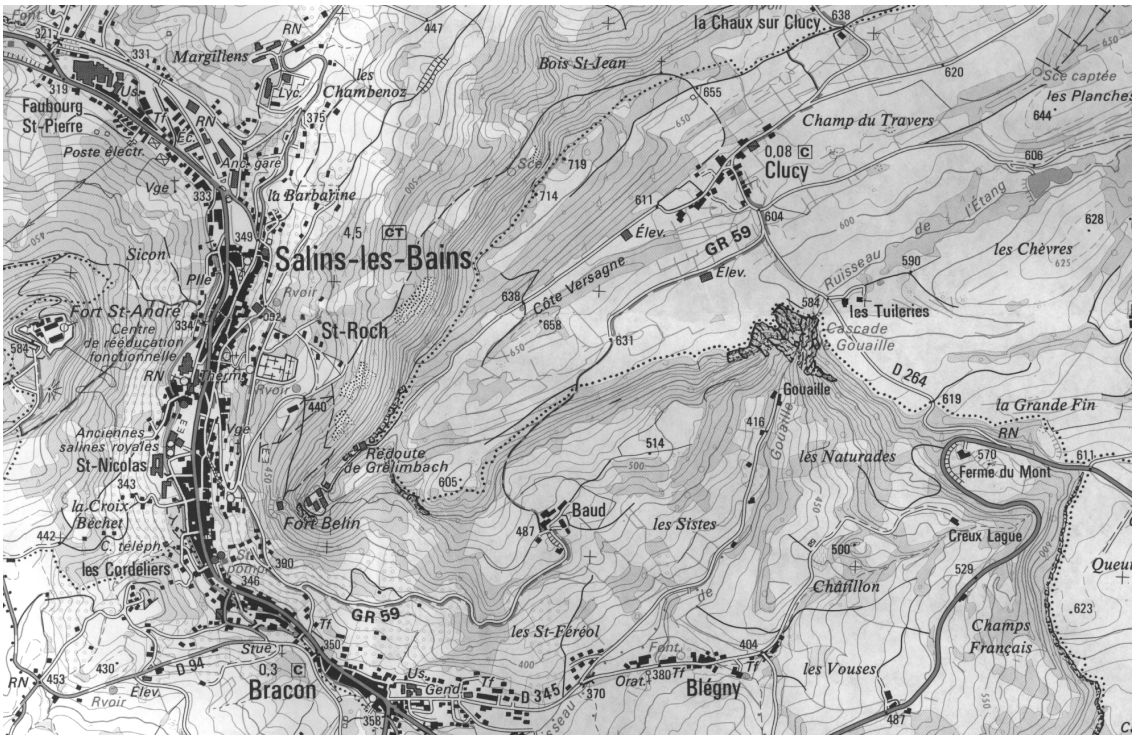

Figure 4.2 Topographical map of Salins-les-Bains and surroundings (from IGN 3325 ouest).

Figure 4.3 Detailed topographical map with land registration information of the Beline slope.

4.2 Previous research at the Beline slope

A Children's Medical Home, abbreviated as MES, was built in 1985 at the lower part of the slope (371 m). The construction work induced a mass movement, which initiated a substantial research attention. Lainé (1989) studied the behaviour of the unsaturated zone of a small test area (5000 m^2) next to the MES. This area has moved after the excavation work for the MES started (figure 4.4).

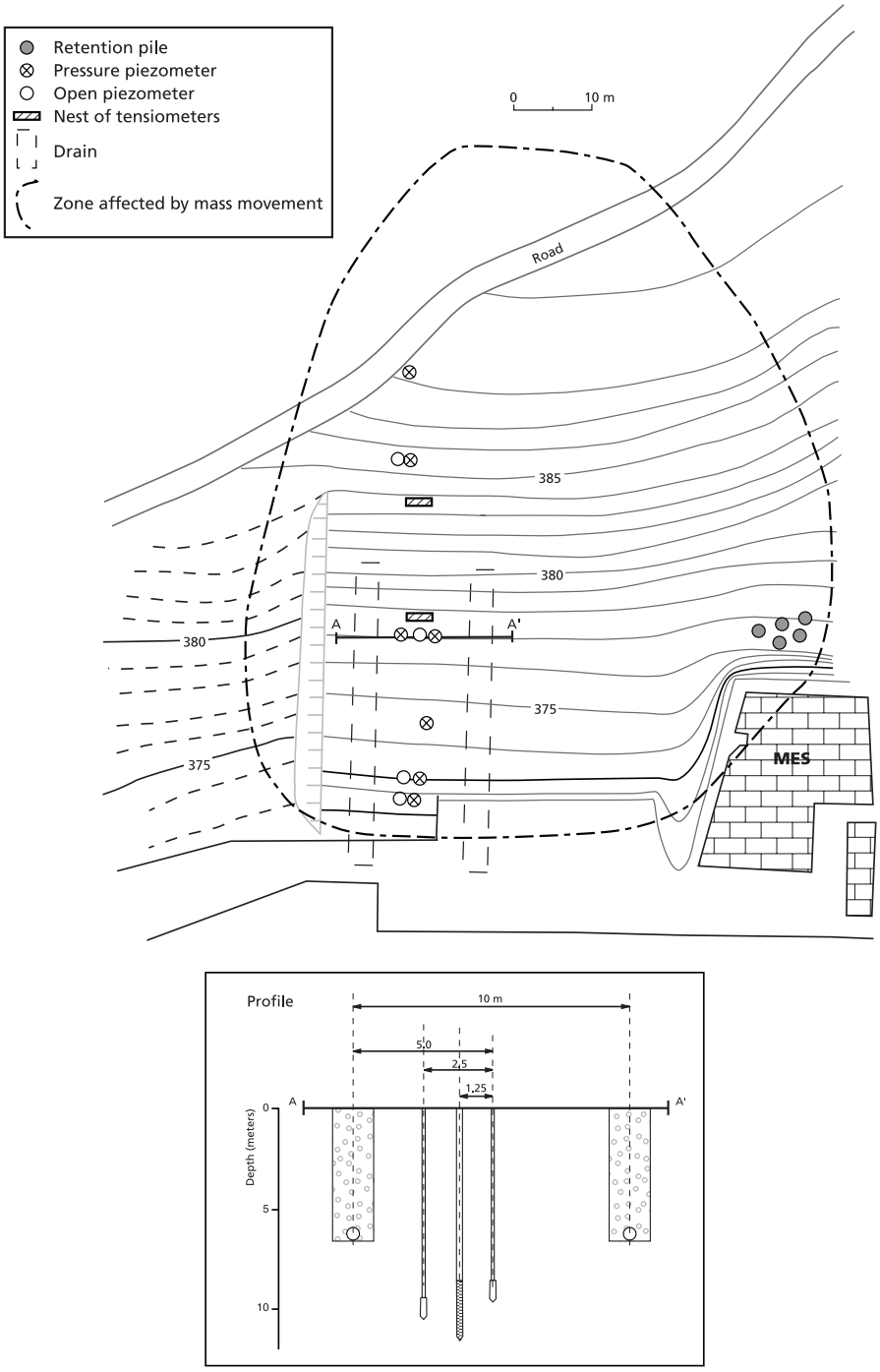

Figure 4.4 Landslide delimitation and instrumentation set-up in 1988 (after Lainé, 1989).

The test area consisted of one densely equipped profile of approximately 75 m length. The test site was instrumented in two steps (June 1988 and February 1989) whereas the total measuring period ranged from June 1988 to July 1989. In total 12 piezometers (7 pressure devices, 5 open standpipes) and two nests of 4 or 5 tensiometers were installed. The profile was situated in the middle of two, 10 m separated, drains. The drains were buried downslope at 3.5 m and upslope at 7.5 m (figure 4.2). This dense instrumentation provided Lainé to make a detailed subsurface schematisation of the first 10 m (figure 4.5).

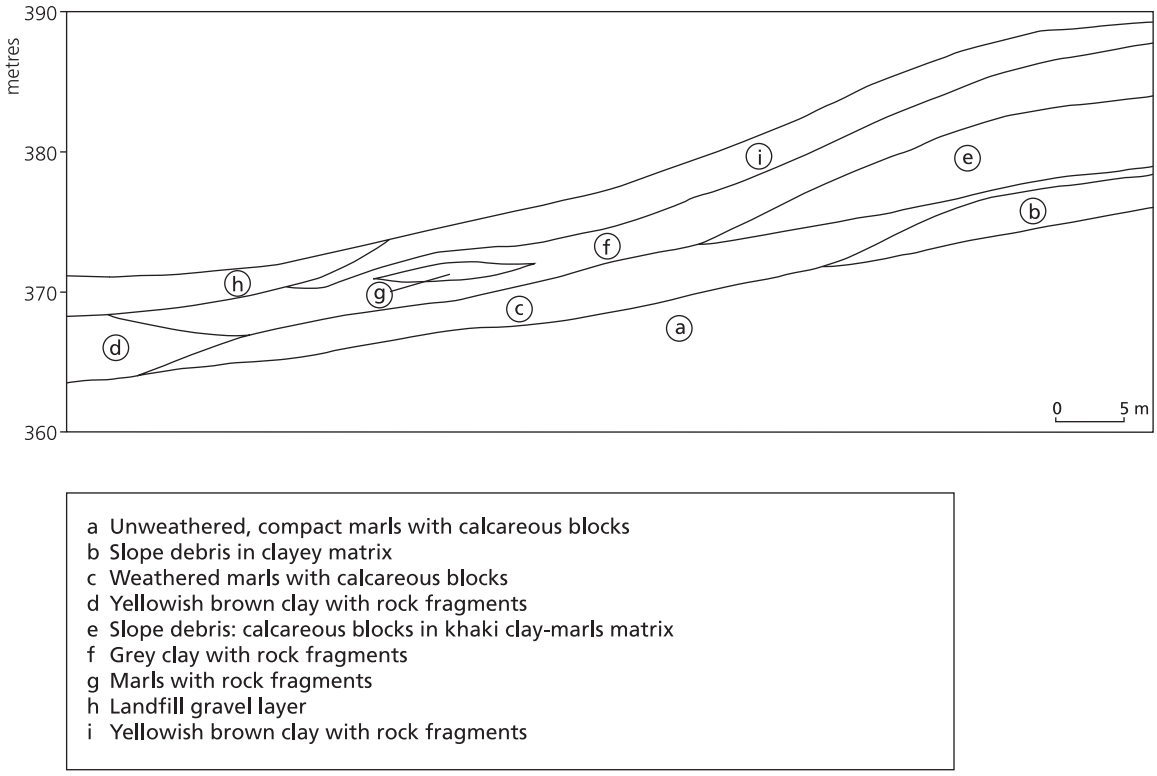

Figure 4.5 Detailed lithological profile through the MES landslide area (after Lainé, 1989).

Lainé (1989) concluded that the ground water system was replenished by the unsaturated zone and not according to the "Chateau d'eau"-concept (rainwater infiltration at the limestone plateau followed by lateral downslope saturated flow). In the unsaturated zone clear vertical flow was recorded but also some subsurface lateral flow. Lainé also stated that due to several problems with the field instrumentation, the short measuring period and the complexity of the hydraulic behaviour of the soil, it has not been possible to fully prove the vertical ground water recharge at depth. Also the influence of perched ground water lenses could not be demonstrated. On the basis of model calculations, Lainé concluded that water flow through fissures towards the ground water system must exist.

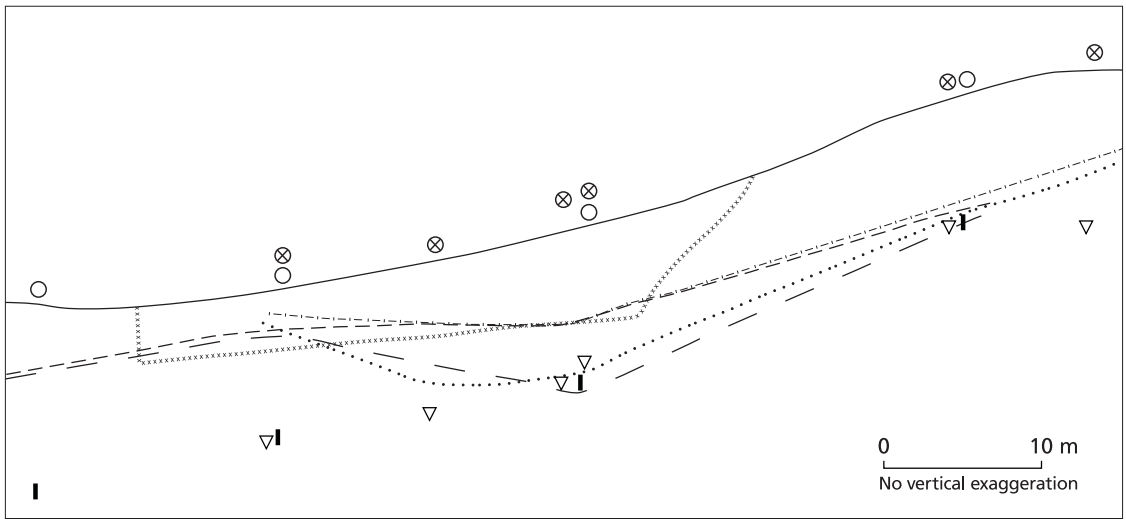

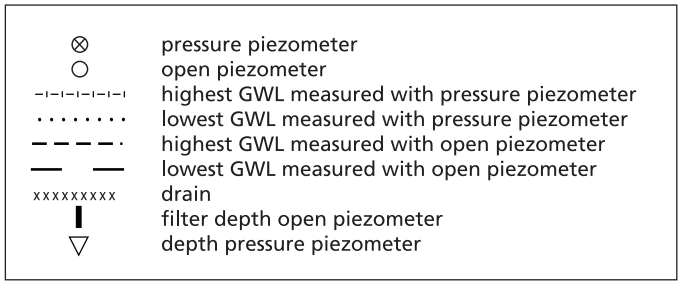

Figure 4.6 Maximum and minimum observed ground water levels in the research area of Lainé between 1988 and 1989.

Besides the very localised instrumentation and short duration of the measuring period, the largest drawback is that the instrumentation was placed between two drains. Lainé showed that the highest measured ground water levels coincide well with the depth of the two drains (figures 4.4 and 4.6). These aspects limit the use of the data in case of natural ground water recharge.

The Hycosi-project (Leroi, 1997) extended the research attention from a local, geotechnical, scale to a medium, process-oriented, scale for the entire upper slope area.

4.3 Regional and local geology

The Jura is the northwest outmost arc-shaped part of the Alps. The Salins-les-Bains region belongs to the so-called external zone of the Jura (Chauve, 1975) and is built-up by a group of Mesozoic deposits, consisting mainly of marls and limestones (figure 4.7). The Beline slope is built up mainly of marly deposits of Lias age with a total thickness of almost 200 m. At the lowest point – in the Furieuse stream – a massive 10 m thick limestone bed is exposed, buried by alternating marl layers and some marly to sandy limestone beds. The marly beds are followed by limestone formations of the upper Lias

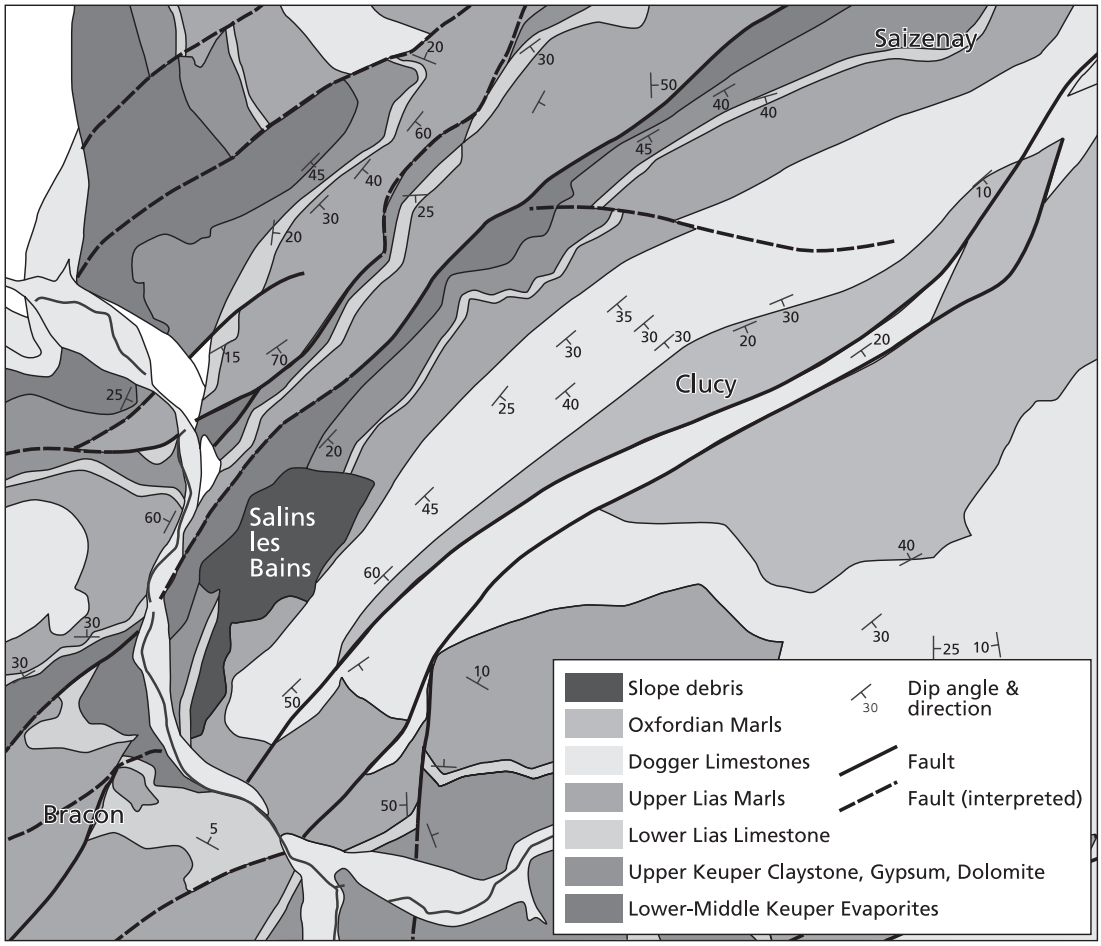

Figure 4.7 Regional geological map (adapted after the 1.50.000 geological map, issue Salins-les-Bains, BRGM, 1967).

(iron-rich oolite limestone) and various, often massive, limestone beds of Dogger age. The Beline slope is furthermore covered with debris, which depth differs locally. The debris originates from the limestone scarps bordering the slope on the entire north site.

Six boreholes were drilled in the marly slope to install equipment and to provide a detailed description of the superficial lithology. The borehole locations (figure 4.8) were chosen after geophysical survey. The main lithologies described (Leroi and Monge, 1996) in all the boreholes were:

- Small limestone gravel pieces embedded in grey clay
- Abundant limestone gravel in a yellow matrix of clay silt and sand, observed only in the cored borehole
- Silty grey marls of average density with variable gravel content and sometimes gravel beds, found in all destructive boreholes
- Stiff, dark blue and grey marls

From the destructive drillings the depth of the unweathered marls was determined at 11 and 17 m below surface. The other four boreholes did not reach the unweathered marls. All boreholes showed a disturbed surface layer with description 1) and with a thickness

of 4.1 to 5 m. In between the surface layer and the marl bedrock an intermediate layer is found of silty grey marls with variable gravel content (description 2). This intermediate layer has a thickness of up to 12 m. The interpretation fails to take into account the cored drilling (SC1) which was placed in a geophysical anomaly (see § 4.4). The intermediate layer in this borehole consists of abundant gravel in a silt-sand matrix (description 2). A geological interpretation is difficult. It can be argued that this coarse material is a scree deposit in a local paleovalley.

In the MES construction work reports, it was written that black marls were encountered at ± 8 m depth. Asté (1997) also described the observation of organic material at 9 m depth in an open trench. Both observations indicate a former surface, which has been covered with remoulded marls in an ancient mass movement(s).

For more detailed information about the first 2 meters of the unsaturated zone, manual auger holes were drilled and described. Overall, the shallow unsaturated zone (0 – 2.5 m) consists of a loam to silty clay lithology with enclosed concentrations of loose, angular stones of on average 1-5 cm in diameter. In some auger holes relatively firm, partly weathered, marls are encountered at a shallow depth. In two auger holes thin stone layers are present. The concentration of the stones differs enormously. The size of the stones also differs, but sizes of up to 50 cm in diameter can be encountered. The upper 5-10 cm has a high concentration of organic matter. Furthermore, visual observable macropores characterise the upper part or infiltration layer. On basis of all the available information the thickness of the infiltration zone is set at 40 cm. The deeper part of the unsaturated zone (percolation zone) varies in thickness between 3-6 m.

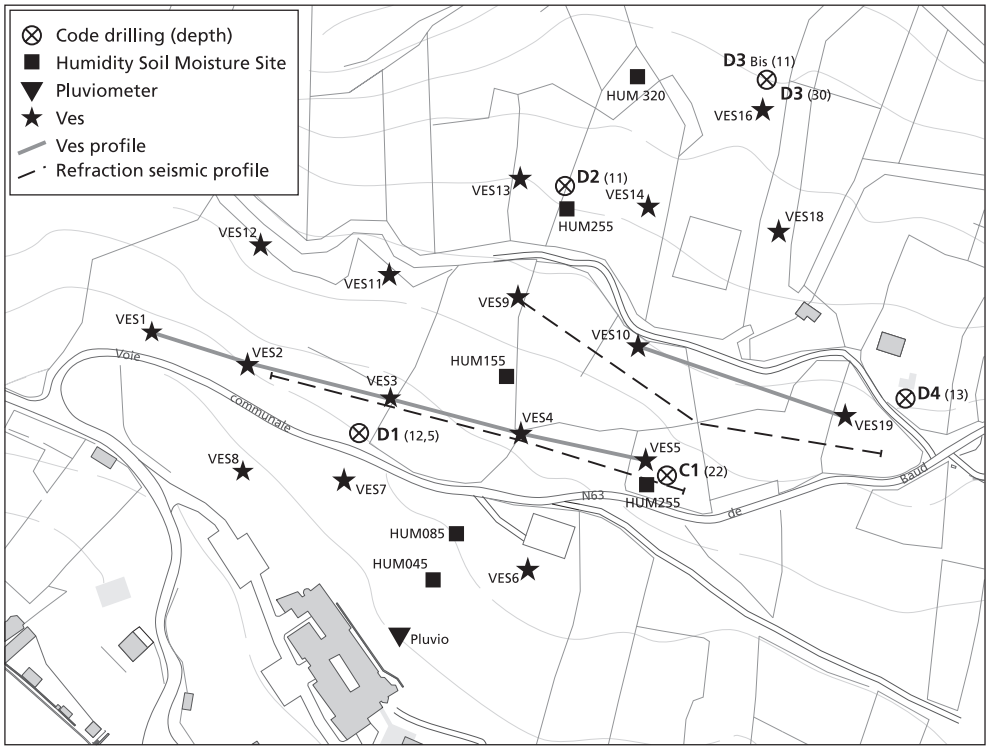

Figure 4.8 Field survey locations, borehole locations and drilling depth. D = destructive drilling and SC = cored drilling.

4.4 Geophysical surveys at the Beline site

In May and June 1995 a geophysical investigation was conducted (Baltassat & Charbonneyre, 1995) on the Beline slope. In September 1996 a microgravimetry survey was executed on the limestone plateau immediately adjacent to the Beline slope (Le Jeune & Besse, 1996). On the Beline slope the aim was to gain better understanding of the subsurface structure through geo-electrical and seismic refraction measurements. Additionally, the geophysical surveys were used to plan the borehole locations for ground water and soil moisture monitoring. At the limestone plateau of Clucy microgravimetric profiles were run nearby the limestone scarp bordering the Beline slope to envisage karstic features and linked to this, the supply of water towards the Beline slope. The interpretation of the geophysical investigations has benefited from the borehole information, which was used to calibrate the interpretations.

The geo-electrical method was used in vertical (vertical electric soundings, VES) and horizontal (profiling) configuration. The former configuration uses an expanding-spread traverse, i.e. the centre of the electrode spread is fixed and the current electrode spacing is systematically increased. The latter configuration uses a constant-spread traverse, i.e. the electrode spacing is held constant and the entire spread is moved. Fifteen vertical electric soundings with a depth of maximum 200 m were made, and a total of sixteen electrical profiles were taken with a total of 350 measurement points (260 points with 60 m spacing, 90 points with 120 m spacing).

All measurements show low resistivity variations with values not exceeding 100 Ohm.m (see Baltassat & Charbonneyre, 1995). These values are in conformity with those expected for marls and clay. In the VES the resistivity generally decreased with depth. From the two sections made of the soundings (figure 4.9), two resistivity layers came forward:

- A first layer with resistivity varying between 12 and 95 Ohm.m and a thickness of 12 to 25 m. The interpretation of this layer is one of remoulded marls and clay with debris embedded.
- A second layer with lower resistivity values (5-15 Ohm.m), which was interpreted as stiff, compact, unweathered marls.

The overall limited contrast in resistivity between the two layers leads to uncertainty about the exact depth of the interface between the layers.

The seismic refraction measurements can be used to determine the depth of a principle refractor, like that of unweathered marls. The measured velocities give an indication of the compactness and type of material present in the subsurface. Above the communal road to the hamlet of Baud, nine, 100 m long seismic lines were measured using explosives as the seismic source. Downslope of the road, nearby the MES, two 60 m long and six 120 m long lines were measured using a sledgehammer as seismic wave source. The geophones were spaced 2.5 m between the energy source and first geophone, and 5 m between the following geophones (Baltassat & Charbonneyre, 1995).
From top to bottom, three layers were distinguished based on their seismic velocities:

- a surface layer with seismic velocities between 200-850 m/s
- an intermediate layer with seismic velocities between 800-1400 m/s
- the main refractor with seismic velocities between 2000-3000 m/s

Table 4.1 Typical values of compressional wave velocity (V_p) (after Burger, 1992, Cordier, 1985, Kleyn, 1983, Parasnis, 1997).

Material/lithology	Compressional wave velocity (V_p) [m/s]
Air	330
Water	1400-1500
Unsaturated, weathered soil	300-900
Saturated sand (with clay or gravel fraction)	900-2000
Saturated clay (glacial moraine, Tertiary clay)	1100-2700 (according to compaction)
Limestone	2000-6000
Marls	1800-3800

Table 4.1 shows some typical values for compressional wave velocity. Together with table 4.1 the first layer can be interpreted as unsaturated weathered material. The intermediate layer contains probably more water, but still consists of unconsolidated material. The main refractor or third geophysical layer has wave characteristics of very compact clay, marls or some limestone. The depth of the principle refractor varies between 3 and 11 m below surface and tends to be deeper towards the east side of the slope.

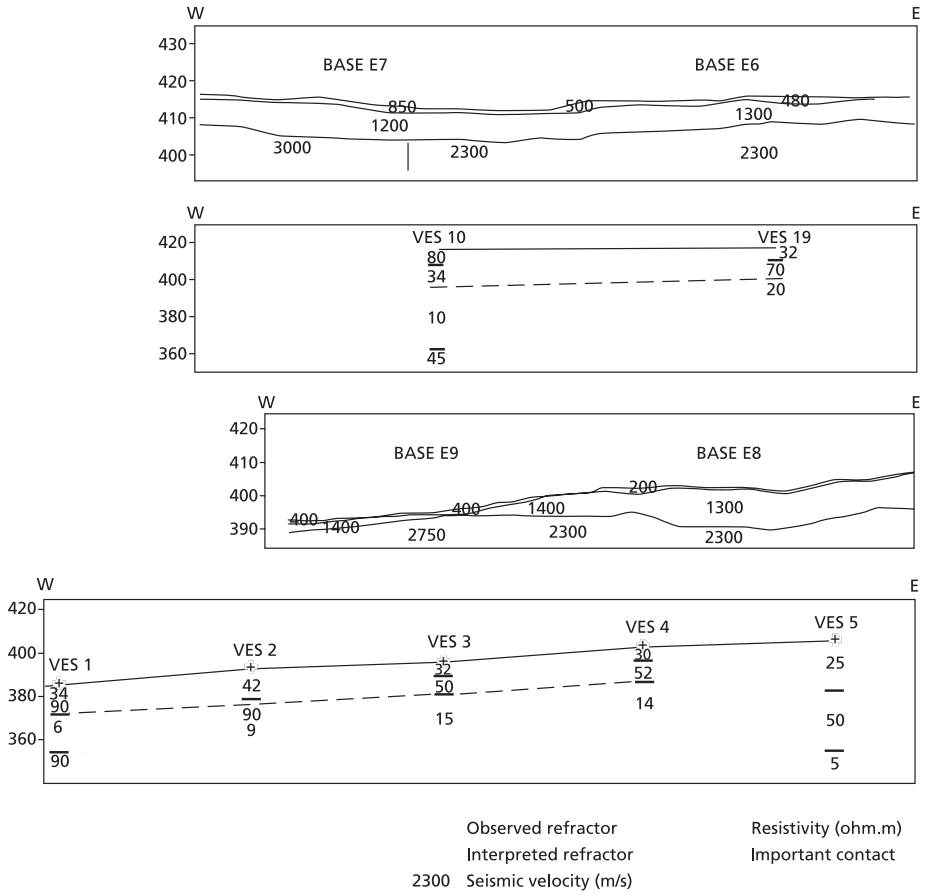

Figure 4.9 Two transect of geophysical results of VES and of refraction seismic. Location of transects at the slope are shown in figure 4.8.

The isobaths of the main refractor show similarity with the high resistivity measurements by electrical profiling. However, the interface identified by geo-electrical methods is systematically deeper. Borehole observations tend to agree better with the geo-electrical interface.

The microgravimetrical survey was carried out in September 1996 (Le Jeune & Besse, 1996) to determine if and where cavities exist in the oblong part of the limestone plateau between Fort Belin and the village Clucy. Four profiles separated by about 100 m were measured using a measurement interval of 5 m.

The results demonstrate a low 'anomaly' in the centre of the profiles and three 'plus anomalies'. The 'low anomaly' can correspond with cavities, karst or a decompressed zone. It is however, impossible to specify the depth or extension of the features that create the microgravimetrical anomaly. Most remarkable is that the low anomaly is located at the highest point of the area, and not –as expected- in the lower areas which correspond with geological faults. The low anomaly is located in the middle of a weakly synclined structure. The results indicate that the assumption of karstic water supply from a part of the Clucy plateau (see also § 4.6 and figure 4.11) towards the Beline slope could be valid.

4.5 Geomorphology of the region and the Beline site

The Salins-les-Bains region is characterised by large local differences in relief and by karstic features like sinkholes, dolines and caves as observed on the Clucy limestone plateau. The region furthermore shows abundant small-scale mass movements like soil slips, slumps and creep at the marly river valley sides. Although not so many disastrous mass movements occur, the on going slowly moving deformation of the slopes is a continuous economic problem.

The valley of the Furieuse is one of the larger 'reculées' of the region (Chauve, 1975). A reculée is a valley, which migrates backwards under the influence of one or more springs underneath the valley headscarp. This results in a plateau landscape of limestone and river valleys with marly slopes.

Asté (1997) concludes after geomorphological analysis that the Beline slope is an ancient landslide. His vision is supported by the detection of organic material at 8 m depth in an open trench at the Beline slope made during the construction of the MES.

The geomorphological map is (figure 4.10) shows a very complex, steep terrain. In first impression no global structure can be distinguished. One presently active landslide area is shown in the north-eastern part of the map. A second area with the characteristics of movement is the western part, next to the forest underneath Fort Belin. Other features are a central valley and several closed depressions.

In general the area can be characterised as a slope with abundant bulges, niches and scarps without clear large-scale structure. The interpretation is highly complicated by the different land use activities of the dozens of owners both in past and present. For example some terracing is present while an adjacent parcel shows a smooth slope.

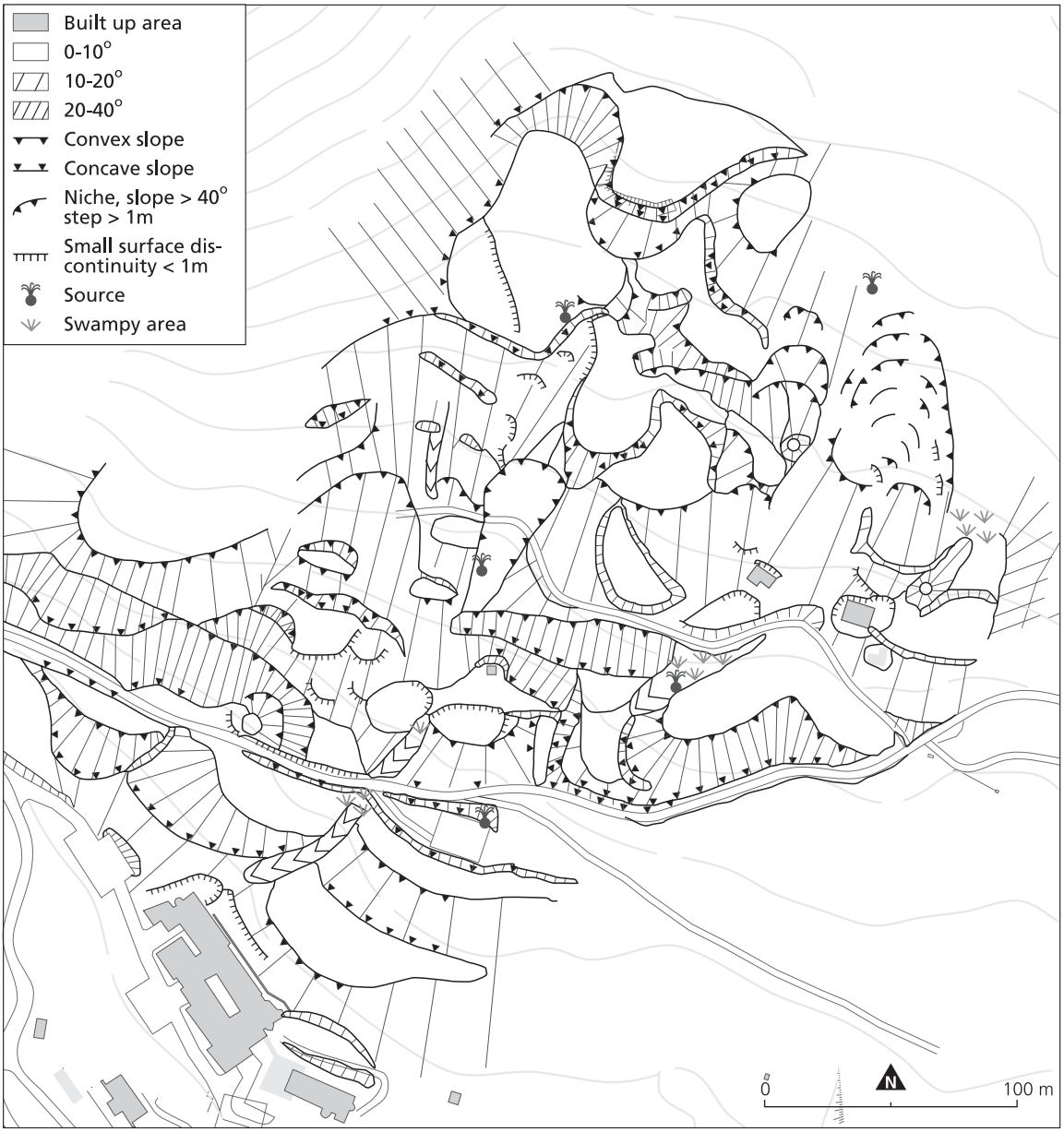

Figure 4.10 The geomorphological map of the Beline slope.

4.6 Regional hydrological setting of the study area

A large-scale karst tracer study by Mangin (1975) southeast of the line Cernans to Nans-sous-St-Anne showed that this part of the karst plateau drains towards the Source du Lison. To study the possible water flow from the limestone plateau towards the Beline slope, a karst research at the Clucy plateau (northwest of the line Cernans to Nans-sous-St-Anne) was set up between May 1996 and September 1996 (Roelandse & Blatter, 1996, Hemel, et al. 1997). During four months all springs adjacent to the Clucy limestone plateau were monitored. Furthermore, two tracer tests were performed in collaboration

with the Direction Regional de l'Environnement (DIREN), Besançon. The results are summarised in figure 4.11.
Based on the results of the study at the Clucy plateau, Hemel et al (1997) concluded that the largest part of the plateau drains towards the Gouaille spring and waterfall. Only the oblong part of the limestone plateau between Clucy and Fort Belin may possibly (partly) drain towards the Beline slope. Here the microgravimetrical survey was performed (see § 4.4).

The Stiff-diagrams in figure 4.11 show that the stream Vaux and the karst sources Lison and Gouaille have the same Ca^{2+} and HCO_3^- water type, which is typical for limestone areas. The other two diagrams from the Beline slope and a location northwest of the Clucy plateau show besides HCO_3^-, SO_4^{2-} as additional important anion, and Mg^{2+} besides Ca^{2+} as additional cation. Especially the sulphate concentration indicates that this water has also flown through marls. This is in agreement with the lithology found there (figure 4.7). To see if different water sources could be distinguished at the Beline slope, the different seepage zones were sampled. All water sources had limited discharge throughout the year (< 1 l/s), showed spatially identical water composition, and no fluctuations of the water chemistry through the year.

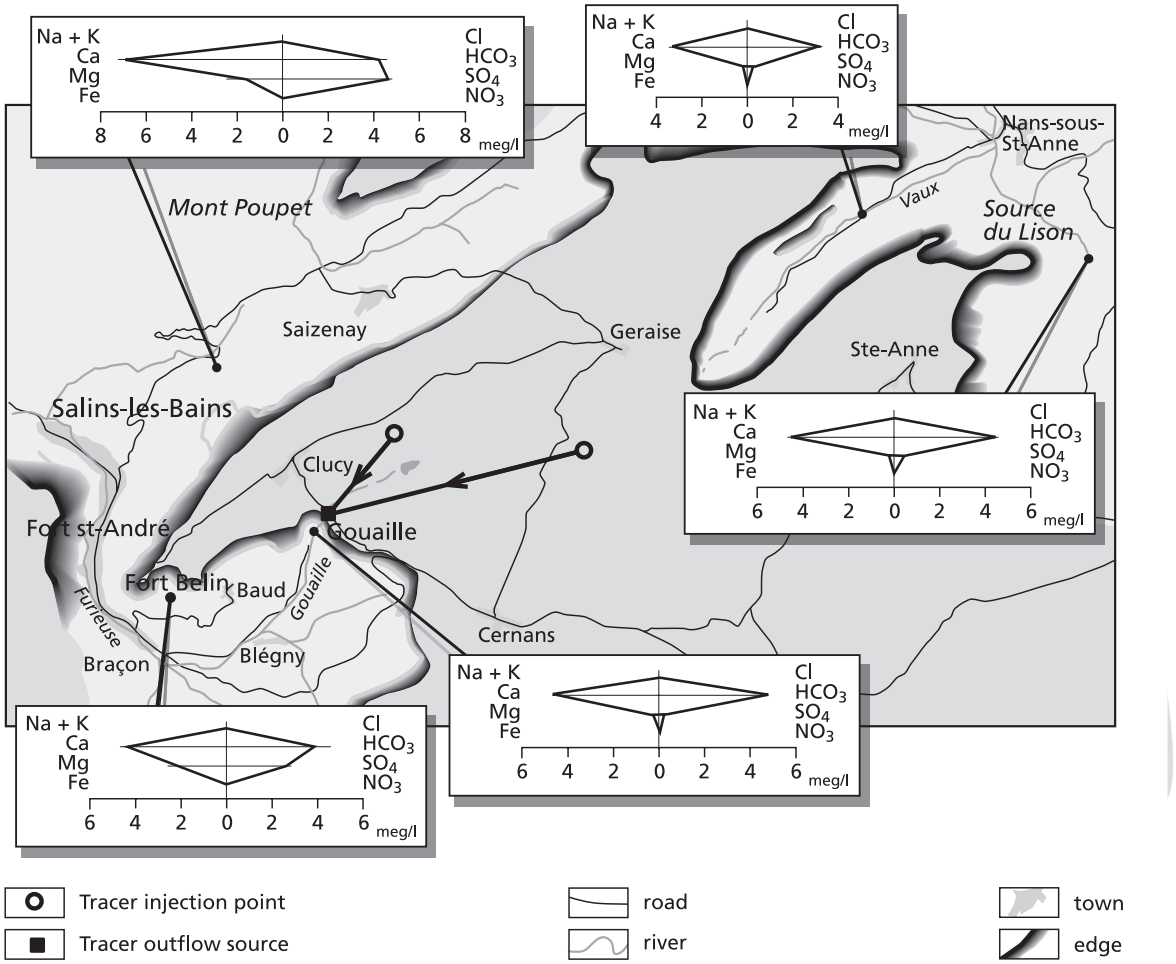

Figure 4.11 Overview of regional hydrology and hydrochemistry around the Clucy plateau.

4.7 Determination of the soil water hydraulic parameters of the Beline slope

Soil water retention curves

A soil water retention curve is a soil characteristic relating soil water content to pressure head tension. The retention curve and K_s can be used to calculate unsaturated permeability as a function of soil water content (Van Genuchten 1980, Mualem 1986). The retention curve analyses also reveal porosity (saturated water content) and bulk density. In total 26 samples were taken at 6 sample locations in 1996. In 1997 an additional 30 bulk density samples were taken (Van den Eijnden, 1998).

The soil retention samples were taken using 100 cm^3 Kopecky rings, which were carefully driven into the soil followed by the removal of soil surplus, taking care not to seal the sample. The samples were covered and stored at 7 °C. Together with the Kopecky cylinders also some loose aggregates were collected for the determination of soil water content at pF=4.2 in a pressure vessel. Retention curves were determined in the laboratory using the suction table method (Klute, 1986). In this method only suction is imposed on the samples. The samples are placed on a body of 'Blokzijl' sand (air-entry resistance of 100 mbar) for pF range 0-2, and on a body of 'Kaolinite' sand (air-entry resistance of 500 mbar) for the pF range of 2-2.7. pF=4.2 is determined in a membrane pressure pan with 16 bar pressure.

In total 58 bulk densities were determined using the Kopecki rings of 100 cm^3. The lowest bulk density of 0.98 gr/cm^3 was measured at the surface, the highest was 1.94 gr/cm^3 at 2.5 m depth. The average bulk density is 1.51 gr/cm^3 with a standard deviation of 0.20 gr/cm^3; the median was 1.53 gr/cm^3. A weak relationship of increasing bulk density with depth was found (figure 4.12).

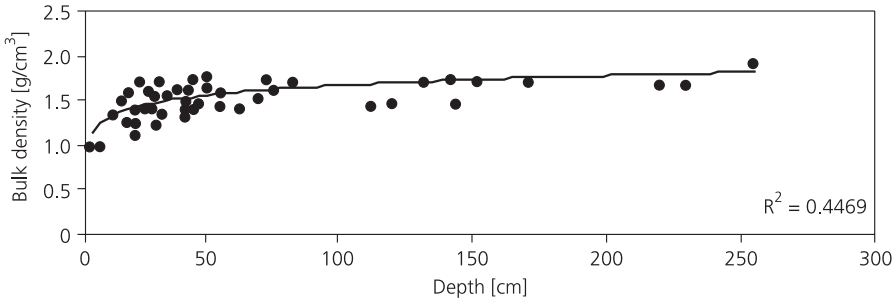

Figure 4.12 Dry bulk density as a function of depth.

The 26 soil water retention curves that were determined, resemble a fine textured soil category (Wösten and Van Genuchten, 1988). All retention curves were expressed in terms of effective soil moisture content and then compared. The effective soil moisture content is defined as:

$$\Theta_e = \frac{\theta - \theta_r}{\theta_s - \theta_r} \tag{4.1}$$

Θ_e = effective soil moisture content [-]
θ = actual soil moisture content [m^3/m^3]
θ_r = residual soil moisture content [m^3/m^3]
θ_s = saturated soil moisture content [m^3/m^3]

From the 26 retention curves porosity values were determined. The average value of the porosity is 43 % with a standard deviation of 5 %. The median value for porosity using all data is 42 %, the highest and lowest measured porosity is 59 % and 36 % respectively. No clear relationship with depth was found. The average soil moisture content for the first layer (0-40 cm) is 45 %, for the second layer 41 %. Using these porosity data, the average retention curve was calculated for both layers (see figure 4.13).

The average effective soil moisture per pressure head per layer was then calculated. This resulted in two average retention curves, one for the first layer from 0 to 40 cm depth and one for the second layer below 40 cm. With the average porosity per layer, the actual soil moisture contents can be calculated.

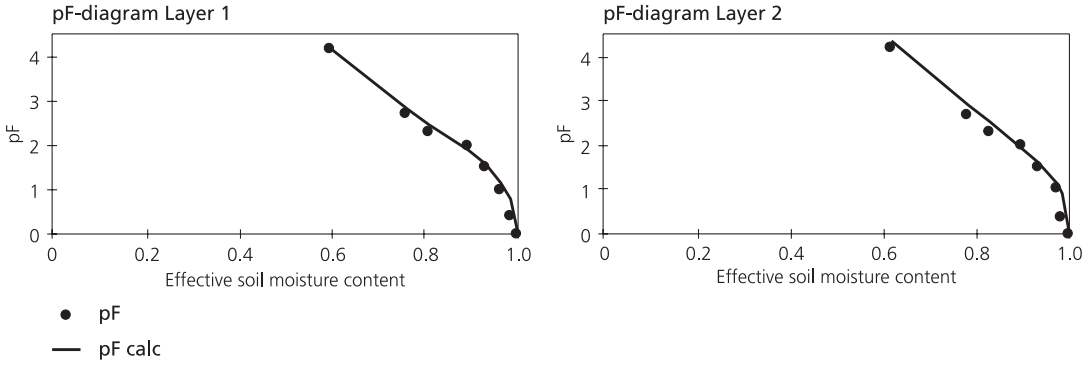

Figure 4.13 Soil water retention curves and the fit of the hydraulic function.

Hydraulic function

In unsaturated zone modelling the most critical parameter is the unsaturated hydraulic permeability. Excluding the numerous empirical relationships of unsaturated permeability and soil suction that exist, two physical approaches can be distinguished (Kutilek and Nielsen, 1994). One states that the relative permeability ($K(h)/K_s$) is a power function of the effective soil moisture content (Kozeny equation). The second theoretical method is based on statistical pore-size distribution models that assume water flow through cylindrical pores and incorporate the equations of Darcy and Poiseuille. This latter method derives information on the pore size distribution from the pore water retention data of the soil. The soil water retention data can be given in tabular form or by means of analytical soil water retention functions, which can then be incorporated in a pore-size distribution model. The resulting equation for the relative permeability has no unique solution. Several

authors come up with the same number of solutions for this equation using different assumptions (many based on mathematical convenience). See Mualem (1986) for a thorough review on unsaturated hydraulic models.

The Van Genuchten-Mualem model (Van Genuchten, 1980) is used to determine the unsaturated permeability using the average soil water retention curves as displayed in figure 4.13. The RETC computer code (Van Genuchten et al, 1991) was used for non-linear least-square fitting of the Van Genuchten-Mualem equation (see formula below) using the retention curves.

$$\Theta_e = \left[1 + (\alpha \cdot |h|)^n\right]^{-m} \qquad (4.2)$$

With m = 1 - (1/n).

The unsaturated permeability can be calculated with the Van Genuchten-Mualem model, if the actual soil moisture content (or pore pressure) and the saturated permeability are known by using:

$$K(\theta) = K_{sat} * \Theta_e^b [1 - (1 - \Theta_e^{1/m})^m]^a \qquad (4.3)$$

with: a=2, b=0.5, m=1-(1/n) and Θ_e the effective soil moisture content.

Saturated permeability

The saturated permeability was determined in-situ using the inverse-auger hole method (Kessler and Oosterbaan, 1974). The inverse auger hole test is an infiltration test, which is executed in the unsaturated zone. A hole with diameter of 5-5.5 cm is made to a certain depth (mainly 40 cm), filled with water and the rate of water level fall is measured. In the study area 78 tests were executed in the summer of 1996 and 1997.

The saturated permeability can be found with Darcy's law assuming that the hydraulic gradient is 1.

$$Q(t_i) = K * A(t_i) * 1 = K * (2\pi r\, h(t_i) + \pi r^2) = 2K\pi r\,(h(t_i) + r/2) \qquad (4.4)$$

With:
$Q(t_i)$ = water flux [m^3/s]
K = saturated permeability [m/s]
$A(t_i)$ = time dependent flow area [m^2]
$h(t_i)$ = time dependent water height in auger hole [m]
r = radius of auger hole [m]

The amount of infiltrated water is also known:

$$Q(t_i) = -\pi r^2 \frac{dh}{dt} \qquad (4.5)$$

Combining the two formulas and rearranging gives:

$$K = 1.15\,r\,\frac{\log(h(t_1)+\frac{r}{2}) - \log(h(t_n)+\frac{r}{2})}{t_n - t_1} \qquad (4.6)$$

By plotting $h(t_i)+r/2$ against t_i on semilog paper a straight line with tangent alpha is obtained. This is done using a linear regression calculation between $\log(h(t_i)+r/2)$ and t_i.

The saturated permeability tests showed a very large variation of the permeability within the surface layer of the Belin-slope. The range of saturated permeability for 79 tests was $1.4*10^{-3}$ m/d to 46.5 m/d. The geometric mean saturated permeability is 1.5 m/d whilst the median was $8.7*10^{-2}$ m/d. The frequency-distribution of the logarithmic values of the saturated permeability values is shown in figure 4.12. This figure shows a left-skewed distribution of $\log(K_s)$. From the figures one can conclude that the (spatial) variability of the saturated permeability is very large. The measured saturated permeabilities range four orders of magnitude. It indicates the existence of both micropore flow and preferential flow.

The saturated permeability has been associated with surface characteristics like slope angle. No relationship between the two was found. Both lower and higher permeabilities were found at relatively flat terrain and on the steep slopes. All test were performed in soils with grass cover. The measurements show the range of permeabilities encountered in the Beline slope, thus the (geometric) average should be handled with care and can only be used as an 'order of magnitude' or first approximation for the saturated permeability of the surface layer.

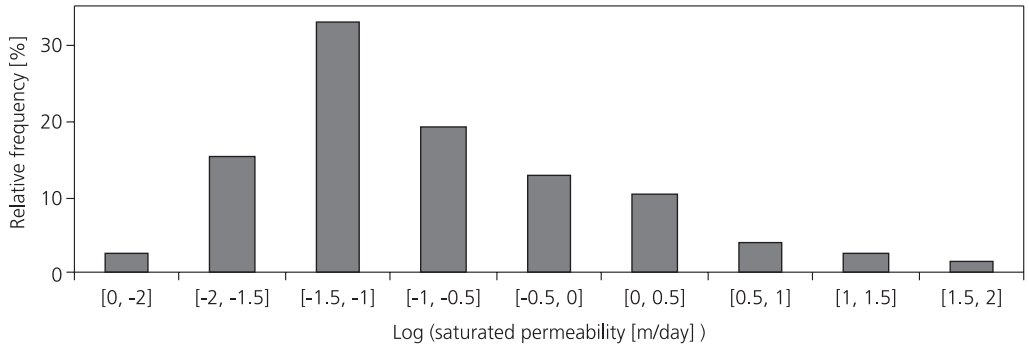

Figure 4.14 Frequency distribution of saturated permeability values at the Beline site.

5 COLLECTION, EVALUATION AND CORRELATION OF HYDROLOGICAL TIME SERIES

5.1 Introduction

This chapter aims at describing and evaluating the hydrological and meteorological time series. It gives a description of the sites where the instruments were installed and, where necessary, additional technical information. The gross measurements are then analysed and errors in e.g. time are corrected (paragraphs 5.2 and 5.3). This quality check results in clean and reliable time series, which will be used for further analyses. The time series will also be described statistically to search for the trends and quantify their amplitude.

In paragraph 5.4 statistical relationships between meteorological input variables and hydrological variables are explored, using cross-association and cross-correlation techniques. The results demonstrate the hydrological processes acting in the research area. The techniques moreover help to quantify relationships and to analyse their significance.

In paragraph 5.5 the hydrological and meteorological data and the results of the statistical analyses are used to interpret the hydrological system within the slope. This provides a conceptual basis for modelling the hydrological behaviour in the slope assuming a causal relationship between precipitation, soil moisture and ground water. In paragraph 5.6 the conclusions of this chapter are drawn.

5.2 Meteorological data

Precipitation measurements

The objectives of the analyses of the meteorological time series are twofold. The first is to present an overview of the precipitation regime during the measurement campaign in Salins-les-Bains. The second is that the on-site data collection is not continuous and not always reliable. It must be examined whether the data from the Météo France climate station at Arbois are representative for the Salins-les-Bains region and thus of use (with possible corrections) in further hydrological research.

Precipitation was measured continuously at three locations: two on-site locations and the nearest Météo France climate station. The first on-site rain gauge was located near the children's hospital on the slope (called 'La Beline') and the second on the limestone plateau in the small village called Clucy (figure 5.1). Both rain gauges are tipping buckets with 400 cm^2 collecting surface and a measurement resolution of 0.2 mm (table 5.1). The rain gauge in Clucy sampled every 10 minutes, the one on the Beline slope every three hours. The rainfall data were compared with the data coming from the Météo France climate station at Arbois, 10 km southeast of Salins-les-Bains.

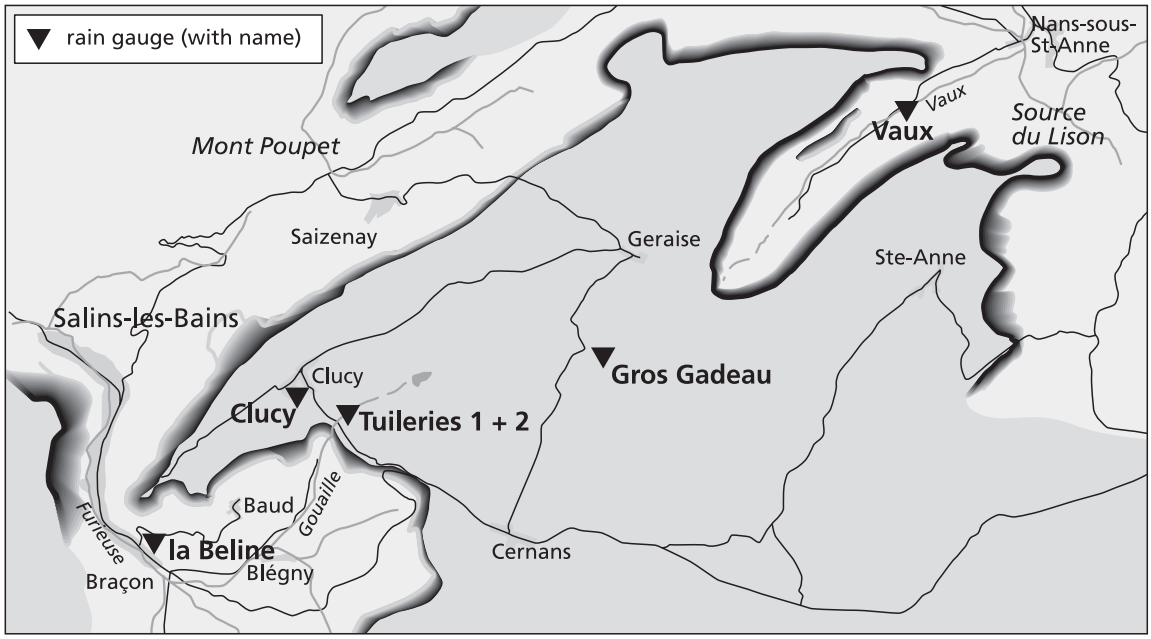

Figure 5.1 Locations of precipitation gauges between Salins-les-Bains and Nans-sous-ste-Anne.

During three months in the summer of 1996 an additional tipping bucket was installed, together with two nonrecording or total rain gauges for a hydrological research of the karst plateau east of Salins-les-Bains (Hemel et al., 1997). The tipping bucket was installed on the karst plateau near the 'cascade de Gouaille', next to the farm 'les Tuileries' (figure 5.1, table 5.1) and is called 'Les Tuileries1'. One of the two total rain gauges was installed east of the karst plateau in the Valley of Vaux (called 'Vaux'). The other one was located first near the farm 'les Tuileries' (called 'Tuileries2') and thereafter replaced to the sinkhole Gros Gadeau in the centre of the karst plateau (called 'Gros Gadeau') (figure 5.1). Table 5.1 gives further specification of the instruments. In figure 5.2 the time schedule of all precipitation measurements is given.

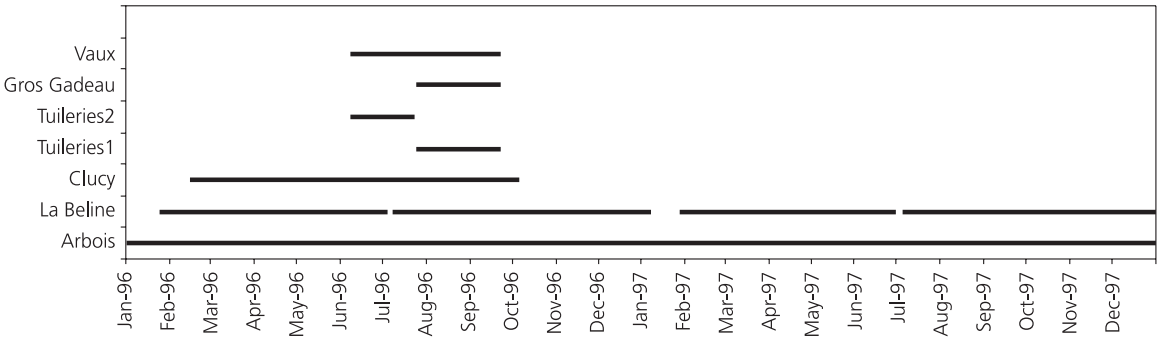

Figure 5.2 Overview of operation periods of the precipitation measurements in the Salins-les-Bains region.

Table 5.1 Specifications of the precipitation measurements near the Beline slope. The locations of the precipitation measurements are shown in figure 5.1.

	Altitude	Specifications
Arbois	311 m	Meteo France daily data 1996 hourly data (summed to daily precipitation 0000-2400); 1997 daily data (0900-0900), 1 m above surface
La Beline	379 m	Tipping bucket, receiver surface 400 cm^2, precision 0.2 mm, frequency every 3 hours, 2 m above surface
Clucy	608 m	Tipping bucket, receiver surface 400 cm^2, precision 0.2 mm, frequency every 10 minutes, 1.50 m above surface
Tuileries1	590 m	Tipping bucket, receiver surface 400 cm^2, precision 0.2 mm, frequency every 15 minutes, 50 cm above surface
Tuileries2	590 m	Non recording, receiver surface 314 cm^2, 30 cm above surface
Gros Gadeau	640 m	Non recording, receiver surface 314 cm^2, 30 cm above surface
Vaux	444 m	Non recording, receiver surface 314 cm^2, 30 cm above surface

Daily rainfall and potential evapotranspiration data of 1996 and 1997 were obtained from Météo France climate station at Arbois. In 1996 both daily totals and hourly data were available while in 1997 only daily rainfall measurements were obtained.

Table 5.2 shows some of the precipitation characteristics. The Arbois rain station registered 156 rain days (1133 mm) and 177 rain days (1142 mm) in 1996 and 1997 respectively, which is 3.1 mm/day on average. The Arbois station's daily maxima were 44 and 53 mm for these years. The Clucy rain gauge registered for a period of 235 days, showing 131 days with rain. In total this station recorded 555 mm of rain against 594 mm in Arbois during the same time period, which is a difference of 7 %. On average 2.4 mm/day (excluding dry days: 5.3 mm/day) of rain was registered in Clucy and a maximum of 41 mm/day.

The Beline rain gauge cumulated 645 and 343 mm of rainfall in respectively 1996 and 1997, which is very low. Field observations in these periods revealed that the Beline rain gauge was not cleaned and maintained sufficiently, leading to an underestimation of the precipitation. The Beline rain gauge was cleaned on 13 October 1996 and functioned well for the next month, but after this the collecting funnel seemed to get clogged again and rainfall collection fell behind that of the Arbois station. In summary, it seems that the Beline rain gauge functioned normally in its first three months (February - April 1996) and for approximately one month following 13 October 1996.

The rainfall intensity was calculated from the Clucy data (10 minutes frequency) and the Arbois hourly data in 1996 (see table 5.3). In Clucy the maximum 10-minute rainfall was 10.2 mm. The average 10-minute rainfall during rain events was calculated as 0.33 mm. In Arbois a maximum intensity of 10.4 mm/hour was measured with an average rainfall intensity of almost 1 mm/hour (table 5.3). Although the maximum measured rainfall intensity in Clucy is larger than the maximum storm intensity in Arbois, the average rainfall intensities measured at both stations are much more similar.

Table 5.2 Precipitation characteristics measured at three rain gauges in Salins-les-Bains region.

	Maximum daily precipitation 1996		Maximum daily precipitation 1997		Cumulative 'annual' precipitation		Average daily precipitation 1996 / 1997	
	Amount	Date	Amount	Date	1996	1997	Including dry days	Excluding dry days
Arbois	44.0	18/11	52.6	21/06	1132.6	1141.8	3.1 / 3.1	7.3 / 6.5
Beline[a)]	28.0	12/11	26.0	21/06	645.0	343.1	- / -	- / -
Clucy [b)]	41.0	08/07		-	-554.8		2.4 / -	5.3 / -

[a)] Period of functioning 25/01/96 – 31/12/97, average calculation not useful because of malfunctioning of the rain gauge (see annual rain totals 1996 – 1997).
[b)] Period of functioning 15/02/96 – 06/10/96

Table 5.3a Rainfall intensity characteristics of Clucy rain gauge measured between 15/02/96 and 06/10/96.

	Including dry days			Excluding dry days		
Total days: 235 Rainy days: 131 Dry days: 104	Precipi-tation [mm/day]	Maximum intensity [mm/10 min]	Average intensity [mm/10 min]	Precipi-tation [mm/day]	Maximum intensity [mm/10 min]	Average intensity [mm/10 min]
Maximum	41.00	10.20	1.42	41.00	10.20	1.42
Average	2.36	0.38	0.15	5.33	0.87	0.33

Table 5.3b Rainfall intensity characteristics of Arbois rain gauge in 1996.

	Including dry days			Excluding dry days		
Total days: 366 Rainy days: 156 Dry days: 210	Precipi-tation [mm/day]	Maximum intensity [mm/hour]	Average intensity [mm/hour]	Precipi-tation [mm/day]	Maximum intensity [mm/hour]	Average intensity [mm/hour]
Maximum	44.00	10.40	5.80	44.00	10.40	5.80
Average	3.09	0.95	0.41	7.26	2.23	0.97

The different rainfall measurements during summer 1996 are given in figure 5.3. First, it shows that the overall patterns of all registrations are similar. But at the same time it shows that the nonrecording rain gauges (Tuileries2 and Vaux) and the recording tipping bucket (Tuileries1) collected 20-50 % more rain than the Clucy and Arbois rain gauges. The Tuileries1 tipping buckets received more precipitation in almost all rain events even though the Tuileries1 and Clucy station are less than 1 km apart. A further analysis shows that 30 mm of the 50 mm difference between the Tuileries and Clucy stations occurred in two summer storms (10/11 August and 28 August).

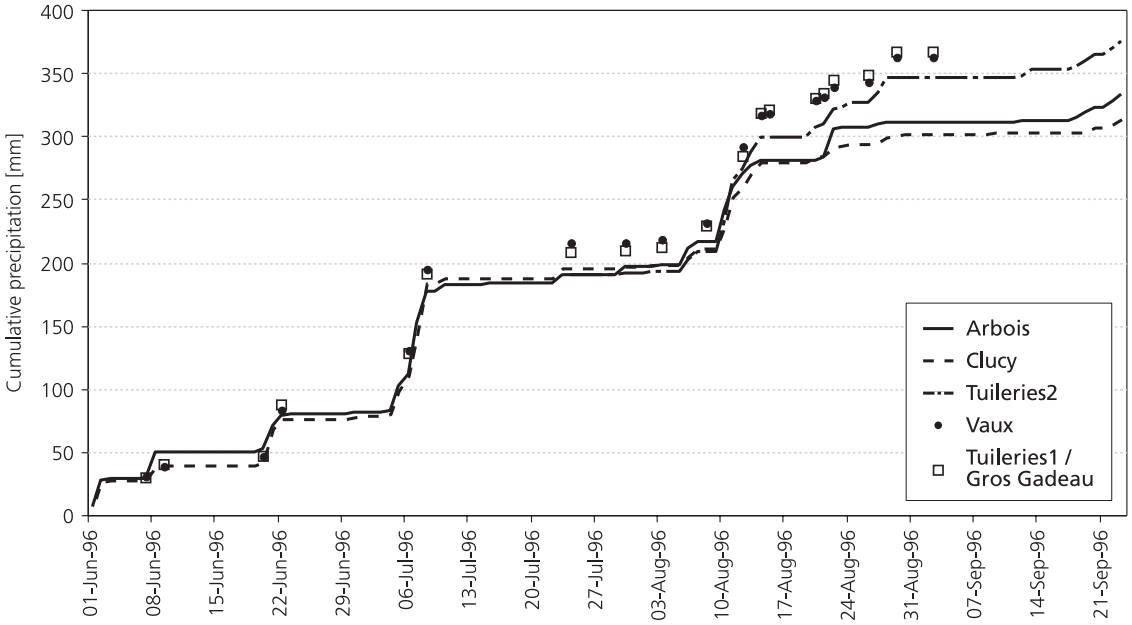

Figure 5.3 Cumulative precipitation at Clucy limestone plateau in summer 1996.

One explanation for this could be that the total rain gauges and the Tuileries tipping bucket are located 30 to 50 cm above ground surface whereas the Clucy and Arbois rain gauges are 1.50 m from the ground. Lower installed rain gauges are known to collect significantly more rainfall than higher installed rain gauges. This is mainly the result of wind velocity patterns around unshielded rain gauges (e.g. Brakensiek et al, 1979). The spatial distribution of the local summer storm could be an explanation, too.

Comparison of the Beline and Arbois data is difficult, due to the clogged funnel of the Beline rain gauge. Figure 5.4 shows a 14 days running total precipitation in the longer wet periods in 1996 and 1997. The window of 14 days is arbitrarily but is a compromise between too much details and a too generalised overview. Six periods in which more than 100 mm of rain fell within a period of 14 days are present. Especially November 1996, May 1997 and the end of June 1997 were wet periods. It is also clear that the rainfall patterns in time between the Arbois and Beline stations are comparable. The first three months that the Beline rain gauge functioned normally and October 1996, after cleaning, the Beline rain gauge results equal the Arbois data. The Clucy and Arbois data are very similar except for the first wet period in May 1996.

There exists a strong correlation ($r = 0.88$) between the rain gauges of Arbois and Clucy (table 5.4). The Arbois station did receive 7 % more precipitation than the Clucy station. A correlation between the Beline rain gauge and the Arbois data was calculated only for the four months that the Beline station worked properly. A correlation of 0.95 (0.92 taking only the rainy days into account) was found. The Beline rain gauge collected almost 20 % less precipitation than the Arbois station in these four months. But the majority of this deficit occurs in only two rain events at the end of the periods with a ‘clean’ funnel, being the first week of April 1996 and the second week of November 1996. This may be caused by the earlier mentioned clogging problem. The remaining difference can be caused by an exposure limitation of the Beline rain gauge.

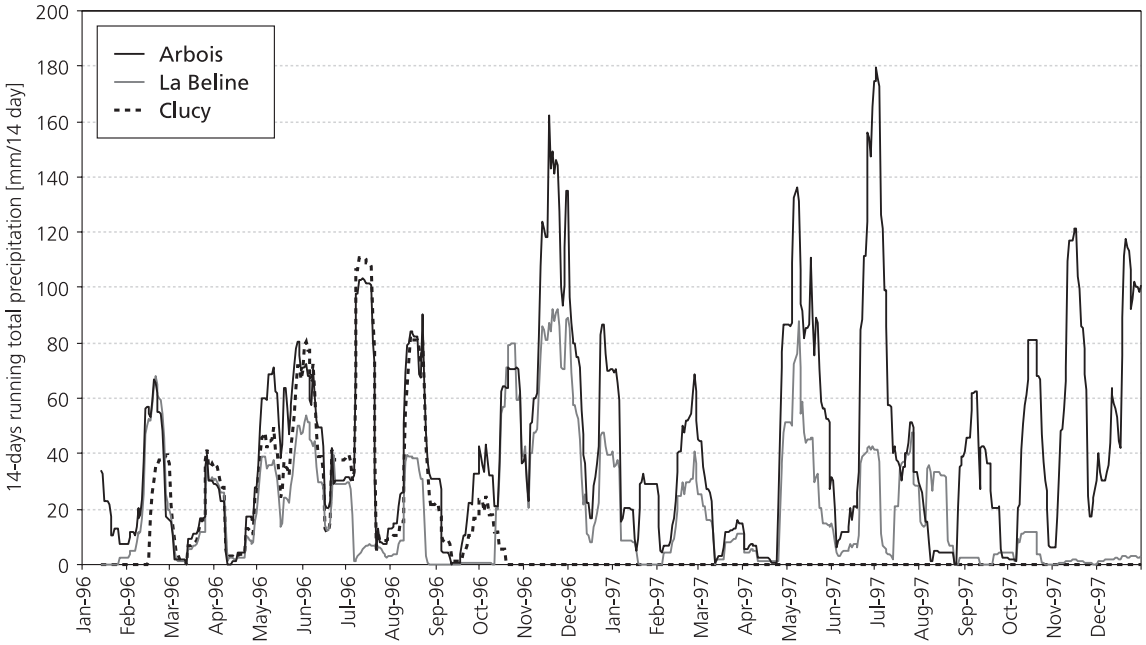

Figure 5.4 Comparison of precipitation measurements of Arbois, Beline and Clucy stations in 1996-1997.

Table 5.4 Linear correlations (r) between the rain gauges of Arbois, Beline and Clucy.

	Beline 25/1/96 - 30/04/96 14/10/96 - 15/11-96	Clucy 15/2/96 – 6/10/96 [a)] 15/2/96-30/04/96 [b)]
Arbois	0.95 (0.92)	0.88 (0.82)
Beline	-	0.78 (0.68)

[a]) For correlation Clucy versus Arbois
[b]) For correlation Clucy versus Beline
( ) The results are given in brackets if the dry days are excluded from the calculation

The precipitation data show that the precipitation regime in and around Salins-les-Bains shows a temperate precipitation regime with on average low intensities. Except for some storms in summer, the spatial variability of the precipitation seems to be limited. It is recognised that the precipitation measurements of the on-site tipping buckets Clucy and Beline are difficult to relate to the Météo France rainfall data from Arbois. The Clucy data period consists of eight (spring and summer) months in 1996 and the Beline period was reduced to four months. During these periods the correlation with the Arbois rainfall data is quite high, although some 10 % more rainfall is recorded in Arbois than on the Beline slope. The overlapping period, however, is too short for a sound quantitative correlation between the Arbois and on-site rainfall data.

Combining all precipitation measurements in this field area, it is concluded that the Arbois precipitation data are the most reliable data available and that they are representative for the field area although some differences can exists between the precipitation in Arbois and in Salins-les-Bains, especially in the summer period.

Evapotranspiration

Together with the precipitation data, data on the daily potential evapotranspiration were obtained from the Arbois Météo station. No on-site information was available. The daily potential evapotranspiration was calculated using to the Penman-Monteith method. This method combines the profile method and the energy budget method. The data used by Météo France are the daily average temperature, wind velocity and vapour pressure, together with the incoming solar radiation (fixed by latitude and season), number of hours with sunshine and the theoretical maximum number of hours of sunshine in one day. Météo France uses the average of the maximum and minimum daily temperature for the daily average temperature calculations. Wind velocity and vapour pressure are the averages of eight daily measurements. A wind measurement is the 10-minute average wind velocity at 10 m above the surface.

The potential evapotranspiration has a maximum of almost 8 mm/day and an average of 2.2 mm/day. Table 5.5 gives an effective precipitation of 0.9 mm/day in the Salins-les-Bains region taking potential evapotranspiration equal to actual evapotranspiration. Figure 5.5 shows the precipitation surplus as a function of time. In the months March until October a precipitation deficit exists, in the months October until March precipitation excess prevails.

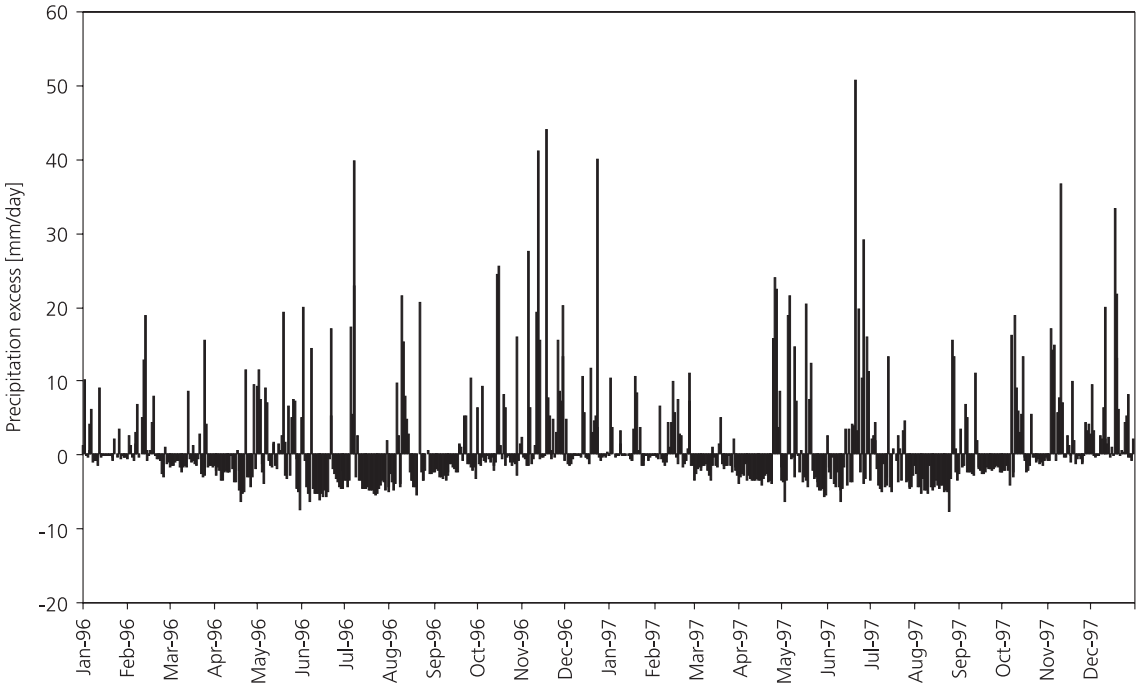

Figure 5.5 Precipitation excess calculated at Arbois meteo station in 1996-1997.

Table 5.5 Precipitation excess calculated for the Arbois Météo station.

	1996		1997		1996+1997	
	[mm/year]	[mm/day]	[mm/year]	[mm/day]	[mm/year]	[mm/day]
Precipitation	1132.6	3.1	1141.8	3.1	1137.2	3.1
Potential ET	754.3	2.1	827.5	2.3	790.9	2.2
Precipitation excess	378.3	1.0	314.3	0.9	346.3	0.9

5.3 Hydrological data

Pore water pressure measurements

Pore water pressure was measured in 1996 and 1997 at 5 locations in the Salins-les-Bains research area (D1, D2, D3, D4, and SC1: see figure 4.8). The drillings were located in such a way that they covered the slope in an adequate manner with also taking into account the accessibility for the drilling equipment. Technical information about the drillings, the installation of the pore water pressure devices and their calibration was given by Leroi and Monge (1996). Table 5.6 summarises the depth of the drilling and sensor installation and average ground water levels. The monitoring of pore water pressure by D2, D3 and D4 stopped at 6 August 1997 (figure 5.6) because of technical problems, probably after a thunderstorm in the area. Ground water levels were measured 8 times a day from January 1996 till December 1997.

Table 5.6 Basic information of the ground water level data.

	Depth drilling [m]	Depth sensor [m]	Average GWL[a] depth [m]	σ_{avg} of daily GWL [m]	σ_{max} of daily GWL [m]
D1	12.5	4.5	3.40	0.004	0.011
D2	11	7.5	6.46	0.006	0.014
D3	11	9.0	4.17	0.007	0.067
D4	13	6.0	5.2 [b]	0.027	0.292
SC1	22	19.5	± 14 [c] ± 5 [d]	-	-

[a]) GWL denotes Ground Water Level.
[b]) Average GWL D4 was estimated; D4 time series not stable.
[c]) According to the measurements of the pore water pressure cell.
[d]) According to descriptions made by the drilling company.

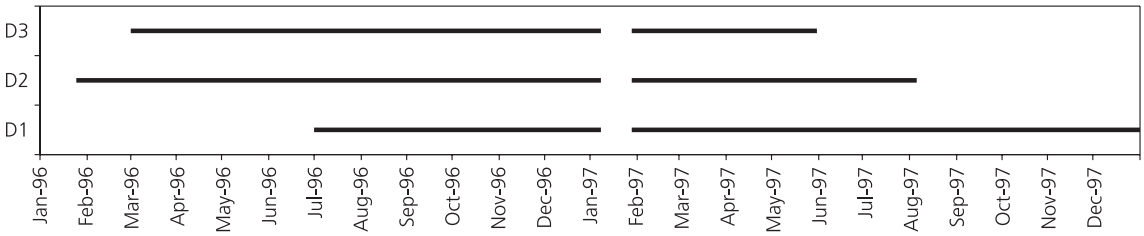

Figure 5.6 Overview of operation periods of the ground water level measurements at the Beline site, Salins-les-Bains.

The three hourly ground water level measurements were averaged to daily values. The standard deviations of the daily record of 8 ground water levels were used as a measure for the soundness of the measurements (table 5.6). The standard deviation of the ground water level measurements within 1 day was generally small (less than 1 cm). Larger standard deviations were checked manually. In most cases a high standard deviation was the result of one extreme ground water level measurement, deviating more than 25 cm from the other measurements. If such an outlier or missing value was found, it was removed. Sensors D1 and D2 were very stable whereas sensors D3 and D4 showed more outliers and missing values (see table 5.6). Remarkably, the larger standard deviations of daily ground water level measurements occur in the summer periods. A second check was made visually. The sensors needed some time to recover from the installation disturbance before equilibrium was reached. The time period of representative data was visually estimated.

Figure 5.6 shows the time bars of the measurement periods of the different sensors. If necessary for calculations or analyses, missing ground water levels are linearly interpolated between the nearest measurements before and after that moment.

In figure 5.7 the coarse ground water level data are shown and in table 5.7 the minimum and maximum ground water levels and their time of occurrence is given. Below follows a short description.

Table 5.7 Highest and lowest ground water level (GWL) measurements in meters below surface and the time of occurrence.

	Avg GWL 1996-1997	Maximum GWL 1996		Minimum GWL 1996		Maximum GWL 1997 [b]		Minimum GWL 1997 [b]	
		GWL	Date	GWL	Date	GWL	Date	GWL	Date
D1	-3.40	-3.32	2/8	-3.56	31/10	-3.24	4/8	-3.55	6/12
D2	-6.46	-6.30	16/7	-6.67	18/10	-6.34	27/7	-6.57	23/4
D3	-4.17	-4.03	22/8	-4.21	23/11	-4.18	1/4	-4.37	5/8
D4	-5.2 [a]								

[a] Visually estimated
[b] Early stop time series D2 and D3 at 6 August 1997

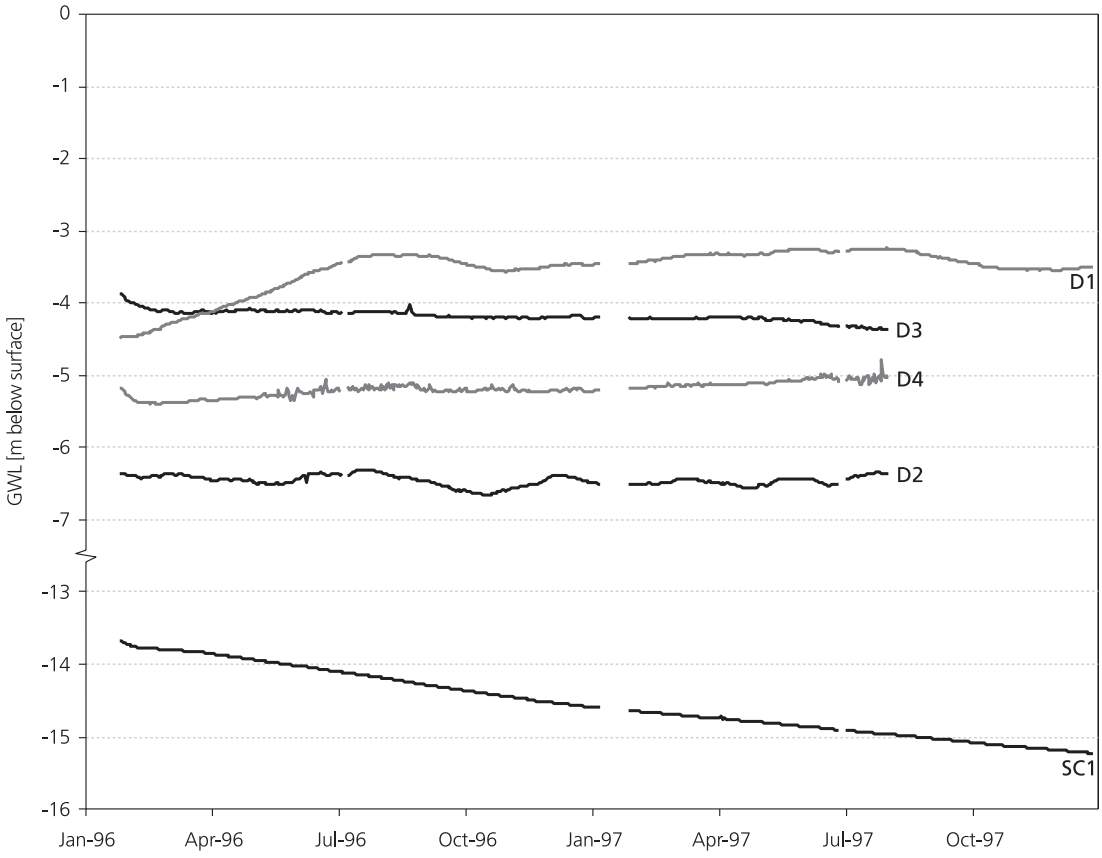

Figure 5.7 Ground water level data measured at the Beline slope in 1996-1997.

The pore water sensor D1 starts around 4.5 m below surface, then rises more than 110 cm and finally gives a stable signal around 3.40 m below surface. The ground water level fluctuated between –3.32 m and –3.56 m in 1996 and between –3.24 m and –3.55 m in 1997. Pore water pressure sensor D2 seems to be stable directly after the datalogger was installed (two months after installation of the pore water pressure devices). It rose to –6.30 m in 1996 and than dropped to –6.67 m in November 1996. In 1996 the water level fluctuated between –6.40 m and –6.57 m below surface although it went up to –6.34 m in august 1997 after which the sensor stopped working. The D3 pore water sensor seems to be stabilised in March 1996. After that, three periods can be distinguished. First, a ground water level of –4.10 m till September 1996 was found, than a small drop in water level height was recorded, followed by a period with again a very stable ground water level of –4.20 m below surface till May 1997. The ground water level time series then drops to almost –4.40 m. D3 stopped functioning in August 1997. The short-term fluctuations are within the 1-2 cm range. Ground water level measurements of D4 rise continuously from February 1996 to August 1997. The short-term fluctuations remain a few centimetres. The unstable character of the measurements of D4 together with the climbing average ground water level seems to make D4 unreliable for further analysis of the ground water level fluctuations. Sensor SC1 shows a continuously decreasing ground water level of around –14 m below surface whereas in the drilling description of this cored drilling a ground water level of around -5 m below surface has been found (Leroi and Monge,

1996). The extreme deep ground water level, which also decreased in time, led to the decision to exclude this sensor from further analysis.

The ground water level data (figure 5.7) show that D1 and D2 are complete and stable time series with ground water level fluctuation of approximately 30 cm. The time series of D3 and D4 show more instability and limited fluctuations. The ground water level at D1 increases from November 1996 until August 1997 whereas the measurements of D2 remain constant. The D2 series show clear fluctuations whereas D1 shows small fluctuations on the increasing ground water level, whereas the timing of both series overlaps. The ground water level fluctuations are smooth and gradual, indicating that there are no fast reactions to rainfall events.

Figure 5.8 shows the autocorrelation function of the ground water level fluctuations of the three pore water pressure sensors used. The autocorrelation function of D1 shows an autocorrelation of around 0.25 for time lags up to 14 days. The fact that D1 has long gradual rising and falling stages is the explanation for this high autocorrelation. D2 shows much less autocorrelation. A possible explanation for this is that the D2 fluctuations are more influenced by external factors than by 'system memory'. The ground water level fluctuations of D3 have almost no autocorrelation. This is what could be expected from D3 with its small, short-term fluctuations around a constant average value.

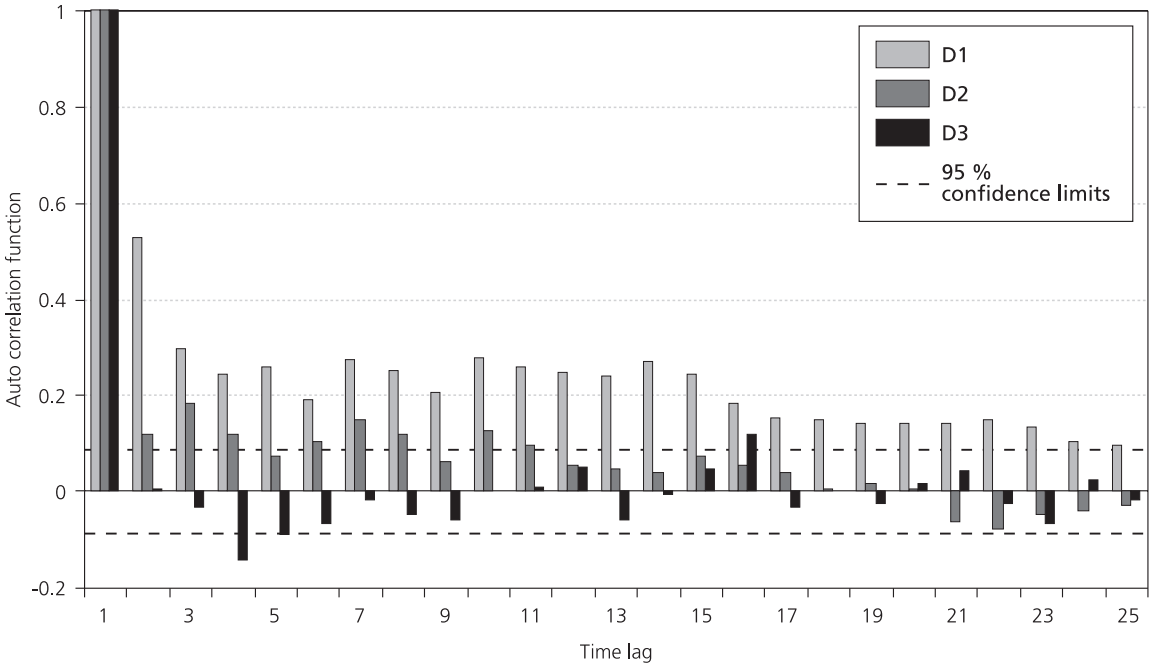

Figure 5.8 Autocorrelation function for ground water level fluctuations of D1, D2 and D3 monitoring locations.

Soil moisture measurements

Soil moisture and soil temperature were measured at 6 locations at three depths (figure 4.8) with Humilog instruments (Monge and Leroi, 1997). All Humilogs were installed in manually drilled auger holes till 1.3 m depth. A Humilog consists of conductivity and temperature measurements. The latter serves to correct for the temperature dependence of soil and water conductivity (Iris Instruments, 1996 in Monge and Leroi, 1997). The soil moisture nests were located across the slope in one line, except for Hum225, which was located near D4. Four of the six soil moisture nests were located underneath grass. Hum045 has more or less a lawn grass cover whilst Hum225 and Hum255 have hayland grass cover. Hum085 also has a cultivated grass cover but is located adjacent to some high trees. Hum155 is located underneath trees with grass undergrowth, whereas Hum320 was placed in a forest environment (table 5.8).

The Humilog's measurement frequency was eight measurements per day. These values were averaged to daily values in order to be related to daily precipitation and ground water level measurements. The absolute values of the soil moisture content together with the standard deviation of the eight daily measurements were used as an indication for soundness of the measurements. All time series (both soil moisture and temperature) were then manually checked, outliers and missing values removed and prepared for further use.

Table 5.8 Basic information of the Humilog soil moisture data collection at the Beline slope.

	Depth	% elements [a]		Vegetation	Remarks
	[m]	<2 mm	<0.08 mm		
HUM045	0.4	91	75	Short cultivated	Altitude 383m
	0.8	97	87.5	grass	Slope 0-10°
	1.1	99	87.5		
HUM085	0.4	90	78	Short cultivated	Altitude 390m
	0.8	84	65	Grass with trees	Slope 0-10°
	1.3	-	-		
HUM155	0.35	90	73	Long grass with	Altitude 404m
	0.45	90	75	trees	Concave slope profile,
	0.8	85	50 [b]		Hum155 in flat part
HUM225	0.5	94	78	Long grass	Altitude 404m, Slope 10-20°
	0.75	89.5	74		Soil moisture has no T-
	1.3	-	-		correction after 7/8/97
HUM255	0.4	70	51	Long grass	Altitude 430m
	0.8	75	56		Slope 10-20°
	1.0	-	-		
HUM320	0.4	77	62	Forest	Altitude 445m, Slope 0-10°
	0.6	93	83		Soil moisture has no T-
	1.3	99.5	92		correction after 17/05/97

[a] Analyses by ANTEA (Antea, 1996 in Monge and Leroi, 1997)
[b] Between 0.45 and 0.8 m depth a sharp clay/sand contact was found. The granumetrical analysis above this contact resulted in: 86.5% < 2mm and 68% < 0.08 mm.

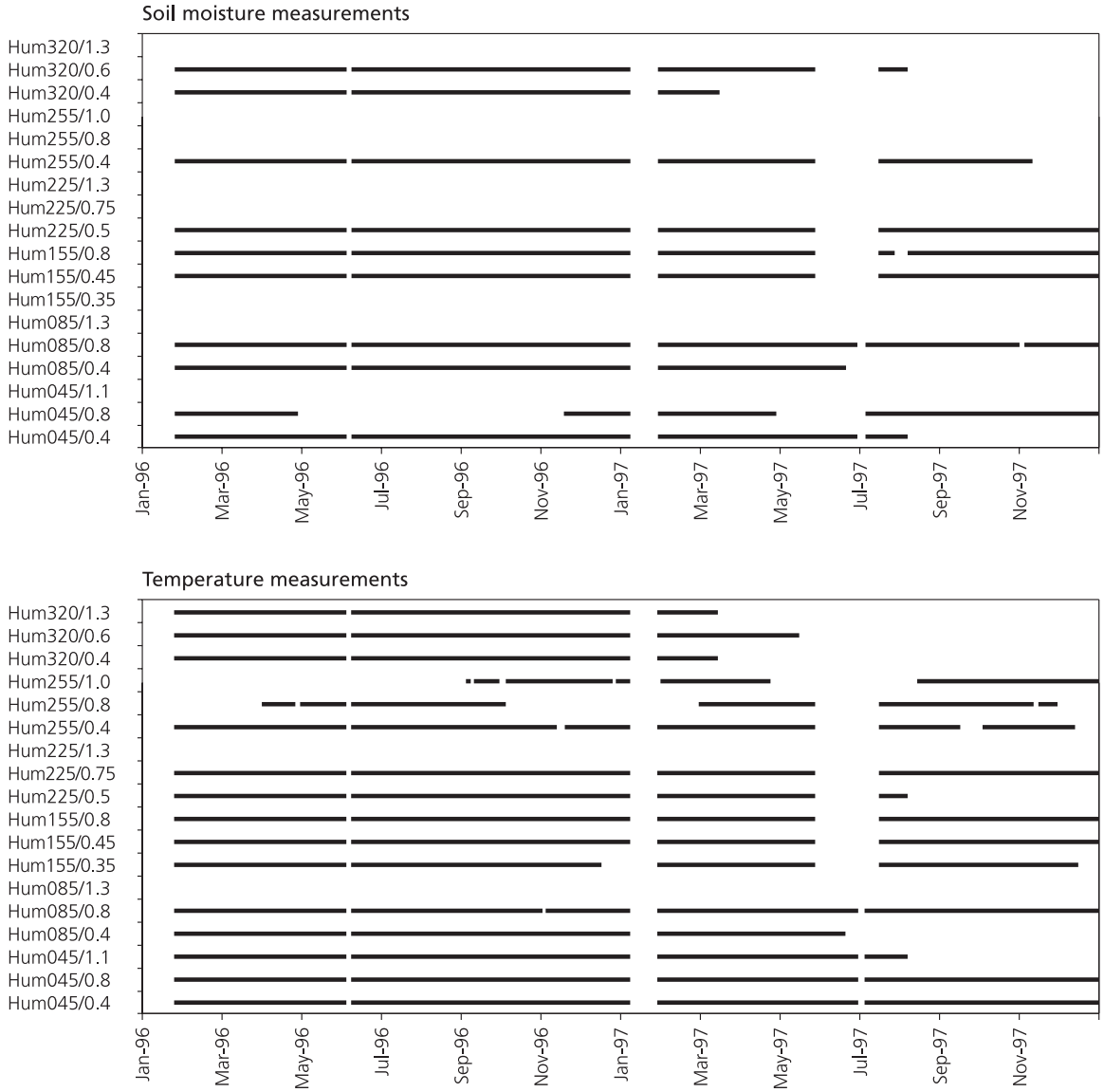

Figure 5.9 Overview of operation periods of the soil moisture and temperature measurements at the Beline site, Salins-les-Bains.

Eight time series of volumetric soil moisture content of more than 12 months were gathered. All sensors installed deeper than 1 m failed, most probably because the manual installation in the stony soils damaged the soil moisture sensors. The temperature sensors behaved less problematic. Fourteen temperature time series of more than 12 months were collected.

The soil temperature ranged between 0.9 °C and 22.7 °C, so no frost has been recorded below 35 cm soil depth in 1996 and 1997. Around 1 m depth the temperature fluctuated between 4 and 15 °C. Generally, one observes (as expected) an attenuation of the temperature amplitude and diminishing short term fluctuations with increasing depth and a shift in timing of the maxima and minima of the soil temperature with depth. The temperature measurements underneath grass are on average more peaked whereas the

measurements underneath forest are smoother. Furthermore, the former shows a slightly larger range in seasonal temperature than the latter.

The soil moisture content on the research slope fluctuated between 20 % and 55 % . Generally the driest soil was encountered in October while the wettest conditions were found in February. The shallow sensors (0.4-0.5 m) show faster fluctuations than the deeper sensors (0.6-0.8 m) that give a more gradual image (table 5.9). The soil moisture measurements underneath trees give the largest and fastest (short term) fluctuations. The measurements in grass-covered soils are generally smoother. None of the soil moisture time series show autocorrelation in their daily differences.

Table 5.9 Summary of the soil moisture measurements at the Beline slope, Salins-les-Bains. Soil moisture content is expressed in percentage.

	HUM 045		HUM 085		HUM 155		HUM 225	HUM 255	HUM 320	
Depth [cm]	40	80	40	80	45	80	50	40	40	60
Range 96	24	2	17	6	19	19	12	16	28	24
Range 97	21	2	15	10	22	14	12		13	11
Average daily differences	0.62	0.07	0.31	0.16	0.50	0.57	0.18	0.61	1.65	0.44
Total measurements	532	238	491	677	637	629	637	289	394	490

Figure 5.10 gives the soil moisture time series for each location. The maximum recorded values of Hum045 sensor at 40 cm depth are between 47 % and 50 %. The time series of the sensor at 85 cm depth is too short to draw conclusions about maximum and minimum values. Hum085 gives two fairly good time series (40 and 80 cm deep). Both sensors show an upper limit of 46-47 % water content in the soil if we disregard the last two months of data from 1997. Where the shallow sensor shows a dry soil with some 30 % soil water content, at 80 cm depth the soil water content hardly falls underneath 40 %. The image given by Hum155 shows distinct fluctuations of which some drying stages seem unrealistic, e.g. February to April 1996 of the sensor at 80 cm depth. The soil moisture saturation is slightly above 40 % at 45 cm depth and 43 % at 80 cm depth.

Remarkable is the low maximum soil water content at a depth of 80 cm of 35-36 % in the winter of 1996-1997. Furthermore the average 0.57 % difference in daily soil water content is very high compared to the other, deeper located, sensors. This suggests that Hum155 at 80 cm depth has some (electronic) instability. Hum225 at 50 cm depth shows a smooth variation of soil moisture fluctuating between 32 and 45 %. The short time series of Hum255 at 40 cm depth is peaked and, as with Hum155 at 80 cm depth, shows some sharp decreases in soil moisture content (average daily soil moisture content differences of 0.61 %). The measurements have a maximum of 41 % and a minimum of 25 %. Hum320 has the most peaked time series of all Humilogs.

Both the 40 cm and 60 cm Humilogs show sharp reactions on rain events. The sharp decreases normally follow after sudden increases of soil moisture, except in May 1996. At 40 cm depth the maximum soil moisture content is 50 %, the minimum value is 26 %. The sensor at 60 cm depth gives a less peaked time series with a maximum around 42 %. But remarkably the measured soil moisture content decreases to a minimum of almost 20 % and this is lower than the Humilog at 40 cm depth.

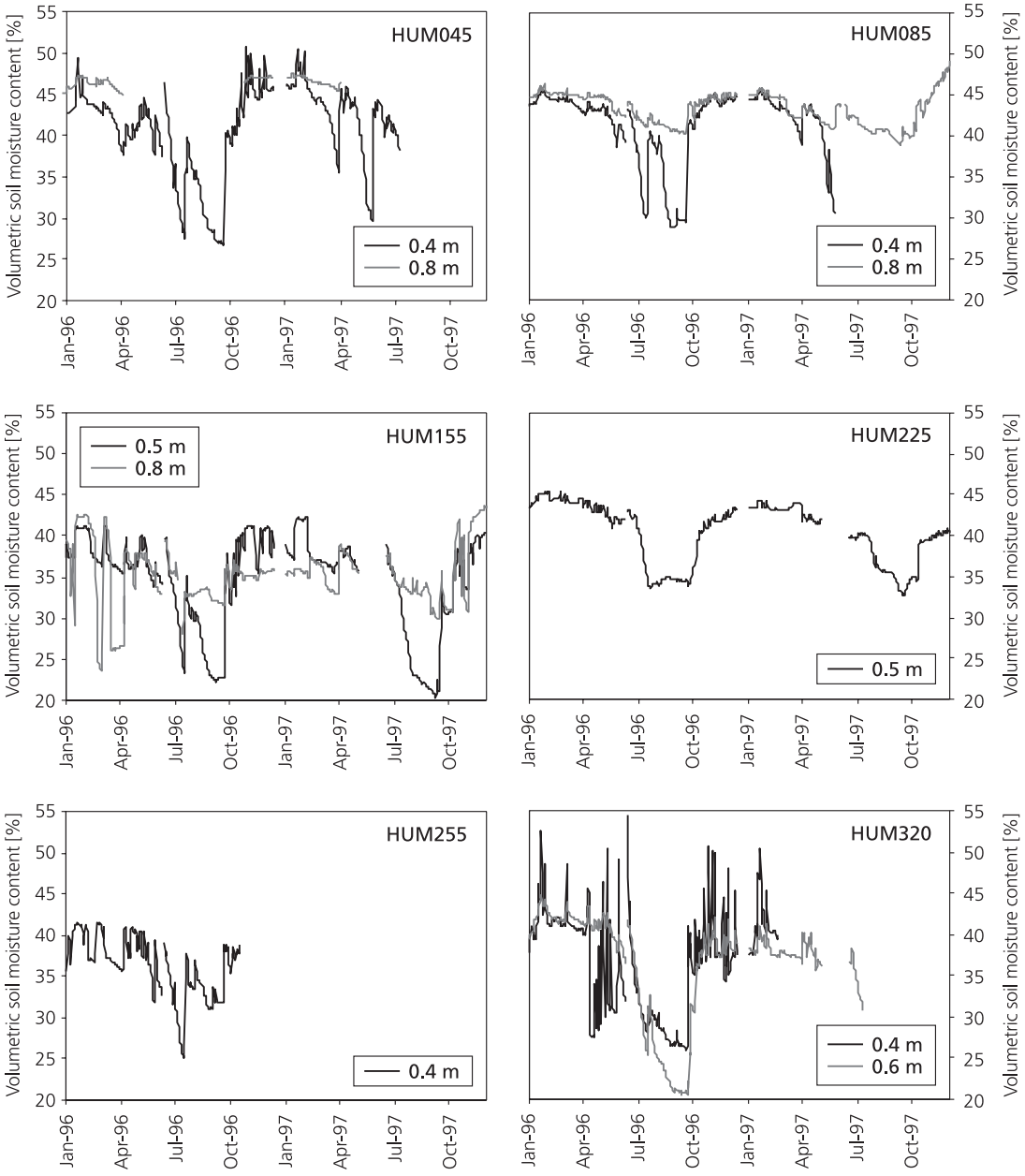

Figure 5.10 Results soil moisture measurements with Humilog system in 1996-1997.

5.4 Statistical relationships between meteorological and hydrological time series

Cross-association or matching

Cross-association analysis or 'matching' is a statistical technique to relate two sequences of nominal data at successive time lags (Davis, 1986). A 'match' is the condition that the 'value' of both series is the same. The number of matches between the two sequences is counted as well as the number of possible matches. The ratio of the number of matches over the possible number of matches (the relative number of matches) can be used as an index for the similarity between the two sequences. When relating precipitation and ground water level fluctuation series, one is not interested in counting matches of the same value but rather in counting the matches when both series fulfil a certain condition, such as matches of precipitation exceeding 5 mm/day and rising ground water level. Such conditions serve two goals. It transforms ordinal time series into binary (nominal) time series (true or false), which can be matched. Secondly, applying the (variable) threshold can filter some of the noise in the time series and thus the cross-association may reveal correlations which otherwise could have remained unnoticed.

The input series for the cross-association analyses are precipitation and effective precipitation. Effective precipitation is defined here as daily precipitation minus daily potential evapotranspiration. To filter the short-term noise also the 3 days backward moving average filter is applied on the effective precipitation input series. The output series are the time series of daily changes in soil moisture content and daily ground water level fluctuations. The output series are thus time series of the difference between two subsequent days in soil moisture content or ground water level. The thresholds for the input data are 2.5, 5 and 10 mm. For the output data the thresholds are 0, 0.1 and 0.5 m^3/m^3 for the soil moisture series and 0, 2.5 and 5 mm for the ground water level fluctuations. Table 5.10 summarises the cross-association analyses done here. The number of matches can be analysed with a χ^2-statistic to test whether the number of matches can result from two randomly distributed series. The χ^2-statistic was calculated for each cross-association analysis.

The cross-association between (effective) precipitation and soil moisture changes was performed to determine the time delay in the infiltration process. The precipitation data are on a daily basis, which impels the matching to be performed on the same time scale. It is recognised that this time resolution is large for the infiltration process.

All soil moisture time series give similar results for the cross-association analyses. In figure 5.11 the cross-association results of Hum085 for all given combinations (table 5.10) are shown as an example. The arbitrary thresholds do not change the pattern of the results, although the largest threshold combination (10, 0.5) left too less matches. All results show a time lag of maximum two days (except Hum225). The percentage of matches decreases between time lag 2 and 5 and then remains almost constant. The percentage of matches with no time lag or small time lags (1-2 days) is generally twice the matching percentage of the constant value with increasing time lags. The deeper installed soil moisture probes have a slightly larger time lag than the shallow soil moisture probes. Also the matching percentage with the shallow soil moisture values is higher than that of the deeper soil moisture values. The results described above show that the unsaturated zone (to 1 m depth) reacts generally within 48 hours on a rain event.

Table 5.10 Overview of the cross-association and cross-correlation calculations analyses.

Test number		Input	Output	Input threshold	Output threshold
1	A	P	θ	2.5	0
	B	P	θ	5	0.1
	C	P	θ	10	0.5
2	A	P(eff)	θ	2.5	0
	B	P(eff)	θ	5	0.1
	C	P(eff)	θ	10	0.5
3	A	MA3 P(eff)	θ	2.5	0
	B	MA3 P(eff)	θ	5	0.1
	C	MA3 P(eff)	θ	10	0.5
4	A	P	GWL	2.5	0
	B	P	GWL	5	2.5
	C	P	GWL	10	5
5	A	P(eff)	GWL	2.5	0
	B	P(eff)	GWL	5	2.5
	C	P(eff)	GWL	10	5
6	A	MA3 P(eff)	GWL	2.5	0
	B	MA3 P(eff)	GWL	5	2.5
	C	MA3 P(eff)	GWL	10	5
7		P	θ	0	-
8		P(eff)	θ	0	-
9		MA3 P(eff)	θ	0	-
10		P	GWL	0	-
11		P(eff)	GWL	0	-
12		MA3 P(eff)	GWL	0	-

Test numbers 1-6 are cross-association calculations
Test numbers 7-12 are lagged cross-correlation calculations
P = Precipitation [mm]
P(eff) = Effective precipitation = Precipitation minus potential evapotranspiration [mm]
MA3 = 3-day backward moving average
θ = Soil moisture content fluctuation
GWL = Ground water level fluctuation

The cross-association technique was also used at the Beline slope to determine the time delay between (effective) precipitation and ground water level reaction. The ground water fluctuation data of field stations D1, D2 and D3 are used. For three arbitrary threshold combinations the cross-association between the input series and the ground water level fluctuations are shown in table 5.10 (tests 4-6).

Figure 5.12 shows the results of the matching analysis for D2. The figure shows that the lowest threshold results in a high number of matches (up to 20 %) and gradually changing graphs with an optimum at 4-5 days time lag. The cross-association graphs are more distinct using the intermediate thresholds for the time series. A time lag of 5 days gives the maximum number of matches between the input series and the ground water level fluctuation output. The analysis with the highest thresholds result in identical pattern of the graph as in case of lower thresholds, but the image is more capricious because such a small number of matches is left. The results with the ground water level time series of D1 and D3 showed identical results although less distinct. Figure 5.12 shows that the choice of the input time series has no effect on the cross-association results.

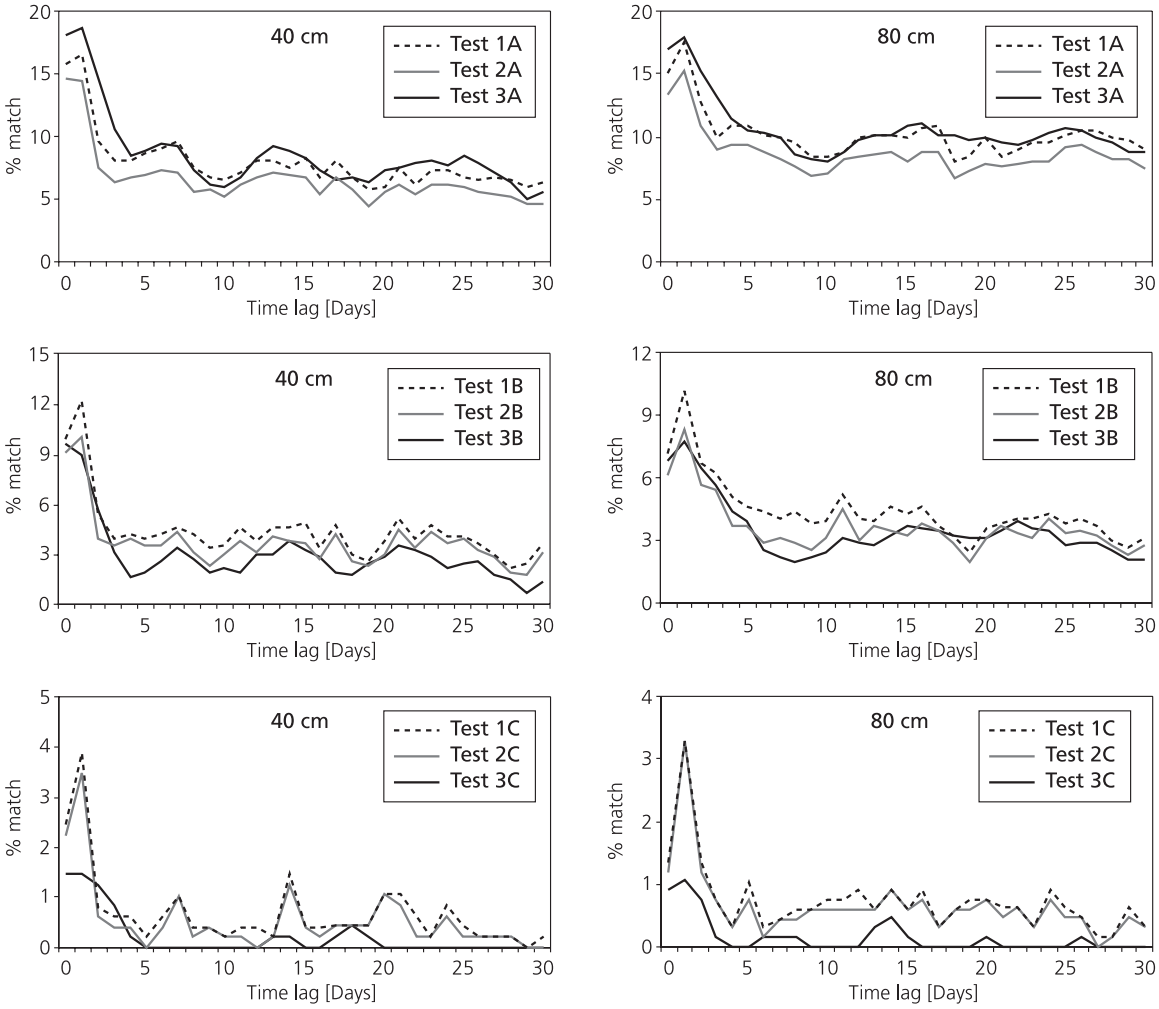

Figure 5.11 Cross-association results of hum085 soil moisture fluctuation. Test numbers correspond with table 5.10.

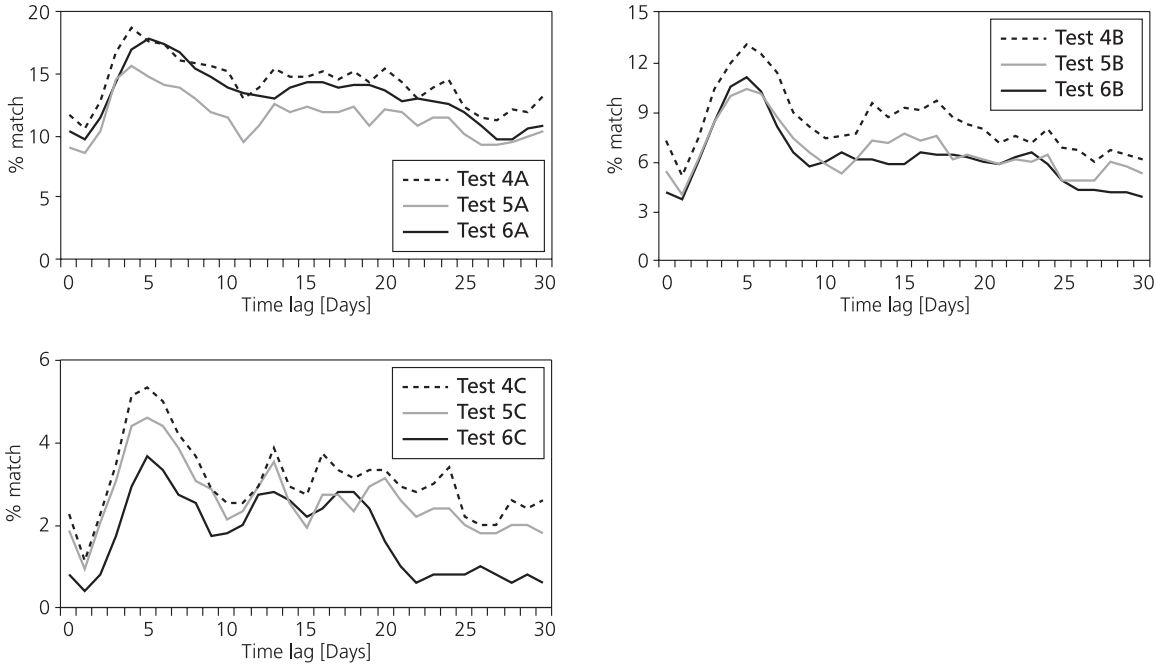

Figure 5.12 Cross-association results of D2 ground water level fluctuation. Test numbers correspond with table 5.10.

The cross-association analysis indicates an average time delay of 5 days before ground water level reacts on a rainfall event. The peaks in matching are not very distinct, but at a 95 % significance level it was unlikely that the peak in percentage of matches was the result of random, unrelated variation, i.e. that there was no relationship between both time series.

Cross-correlations

Lagged cross-correlation is a statistical technique for comparing two ordinal time series at successive (time) lags. It quantifies the linear relationship between two series at a certain lag (or offset) in time between them. The correlation between the two time series at every time lag is calculated and is visualised by plotting the correlation versus time lag (cross-correlogram). The difference with cross-association is that cross-correlation relates ordinal data while cross-association uses nominal data. So, cross-association analysis calculates the relative number of matches of precipitation larger than 5 mm/day and ground water level fluctuations larger than 2.5 mm/day, whereas cross-correlation linearly relates the measured values of the two data.

For the cross-correlation calculations the same input time series as with the cross-associations are used. The output series are the daily changes in soil moisture content and the daily ground water level fluctuations (see table 5.10, tests 7-12). In the cross-correlations only rainy days were used in order to prevent correlation bias caused by the large number of dry days.

In table 5.11 the maximum correlation, the 95% confidence limit and the time lag for which they apply are given for the lagged correlations between (effective) precipitation and soil moisture content changes. As an example, the correlograms of Humilog 085 and

the 95 % confidence limits are given in figure 5.13. The soil moisture content changes are maximally correlated with the meteorological input at one day time lag. At a time lag of two days or more, correlation between the two time series is no longer significant (figure 5.13). The soil moisture measurements at 40 cm depth show the strongest cross-correlation with the meteorological input. The deeper soil moisture measurements show weaker correlations (table 5.11).

Table 5.11 Results of the cross-correlation between soil moisture content changes with effective precipitation.

	Depth [m]	Maximum correlation	95% Confi-dence limit	Time lag
HUM045	0.4	0.38	0.13	0
	0.8	0.29	0.22	1
HUM085	0.4	0.41	0.14	1
	0.8	0.34	0.11	1
HUM155	0.45	0.37	0.12	1
	0.8	0.21	0.12	1
HUM225	0.5	0.20 [a)]	0.12	7
HUM255	0.4	0.39	0.19	1
HUM320	0.4	0.44	0.16	0
	0.6	0.37	0.14	0

[a)] At a time lag of 1 day a cross-correlation of 0.16 exists

The correlations between soil moisture content changes and effective precipitation (here defined as precipitation minus potential evapotranspiration) are lower than the correlations between soil moisture content changes and gross precipitation. Of all soil moisture locations, Hum320 gives the strongest correlogram having a clear correlation with zero time lag and no correlation with increasing time lag. All other soil moisture measurements have positive correlations with a day time delay.

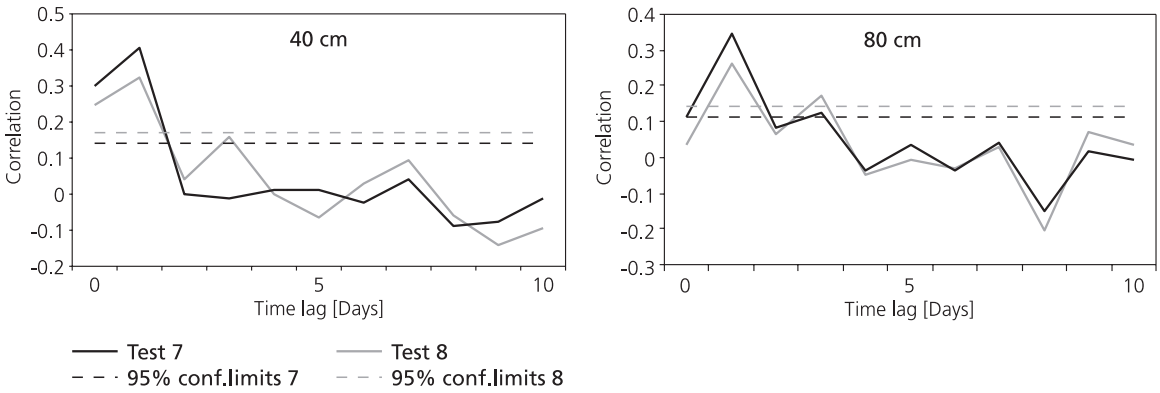

Figure 5.13 Cross-correlation results of Hum085 soil moisture fluctuations. Test numbers correspond with table 5.10.

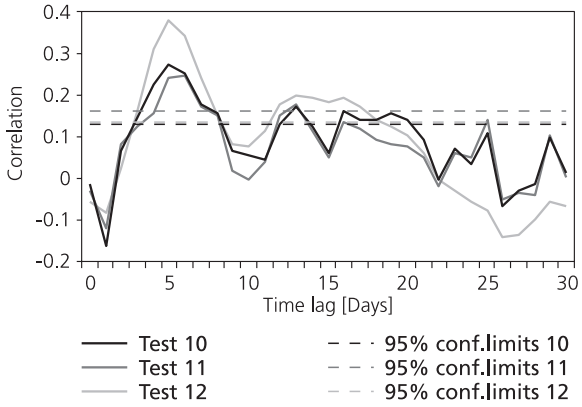

Figure 5.14 Cross-correlation results of D2 ground water level fluctuations. Test numbers correspond with table 5.10.

All three pore water fluctuation measurements have low correlations with the input data. The correlograms of input time series with D1, D2 and D3 ground water level fluctuations time series give smoother correlograms and higher correlations with the 3-days backward moving average operation (which was applied to filter the short-term noise in the input time series). The correlograms of D2 are shown in figure 5.14 together with the 95 % confidence limits for the null hypothesis (no correlation). The confidence limits can differ because different number of data pairs result from the analysis.

The correlations with pore water pressure cell D1 (not shown) has the highest correlation (0.27) with a time lag of 6 days using the 3-day backward moving average in- and output data. It also shows a relatively high correlation (up to 0.23) with a time lag of 12 to 19 days. The correlation with effective precipitation remains predominantly under the 95 % confidence limit of not rejecting the null hypothesis. D2 (figure 5.14) has the most pronounced correlogram of the three series. At a time lag of 5 days, a clear peak in the correlation exists. With increasing time lag the correlation diminishes and noise and possibly non-linear relationships remain. D3 (not shown) starts with a negative correlation, then shows a weak positive correlation (max. 0.17) at a 6 days time lag and finishes with a correlogram fluctuating around zero. The correlations of piezometer D3 with the climatic input parameters do no exceed the 95 % confidence limits.

This analysis shows that gross climatic variables and ground water level fluctuation are linearly correlated with a time lag of 5-6 days. A smoothing operation like the 3-day backward averaging of the ground water level fluctuation data firms up existing correlations. The low linear correlation values indicate that the influence of the antecedent conditions is important and thus that the non-linear behaviour of the unsaturated zone cannot be omitted in the Beline slope.

5.5 Conceptual model of the physical processes at the Beline slope

The final part of this chapter is to interpret all former analyses in terms of the physical behaviour of the hydrological system at the Beline slope. This results in a conceptual model of the hydrological system assuming a causal relationship between precipitation, soil moisture content and ground water level. Such a comparison between the different time series can illustrate the seasonal patterns of the hydrological system. To compare the time series, all data were standardised. Standardisation is defined as:

$$y_i = (x_i - x_{avg})/\sigma_x \, .$$

y_i = standardised value of time series
x_i = value of time series at timestep i
x_{avg} = average value of time series
σ_x = standard deviation of time series
i = subsequent timestep

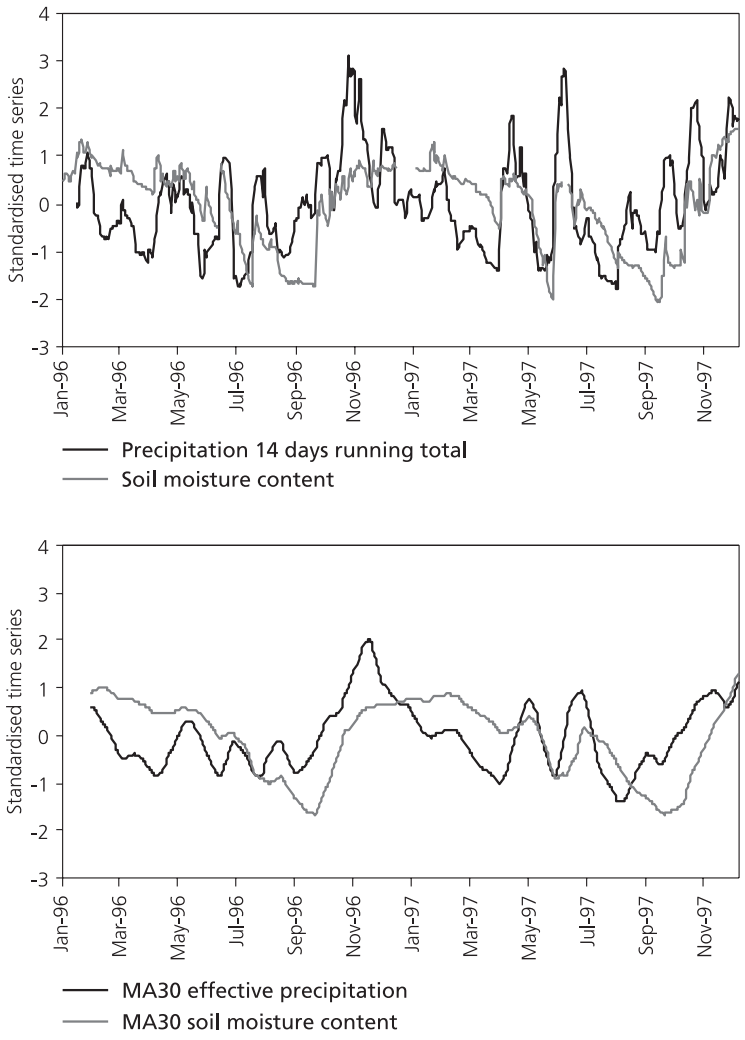

Figure 5.15 Relationship between precipitation and soil moisture content.

Subsequently, the different standardised soil moisture data and ground water level time series were summarised in one representative time series. Regardless of depth or location, the median of the standardised time series was calculated per day to come to one representative (median) time series for both soil moisture content and ground water level. The effective precipitation (precipitation minus potential evapotranspiration) was first add up to 14-days running totals and then standardised.

The results are plotted in figures 5.15 and 5.16. The standardised soil moisture time series has its minimum in October and maximum in February, and shows some skewness. It decreases slowly (February to September) but increases fast (October and November) and increases slightly in winter. The figure can be cleared up if the high-frequency variations are filtered by a 30-days backward moving average of the soil moisture content time series. This part of the figure shows that periods with positive standardised effective precipitation have rising soil moisture content whereas periods with negative standardised effective precipitation show decreasing soil moisture content.

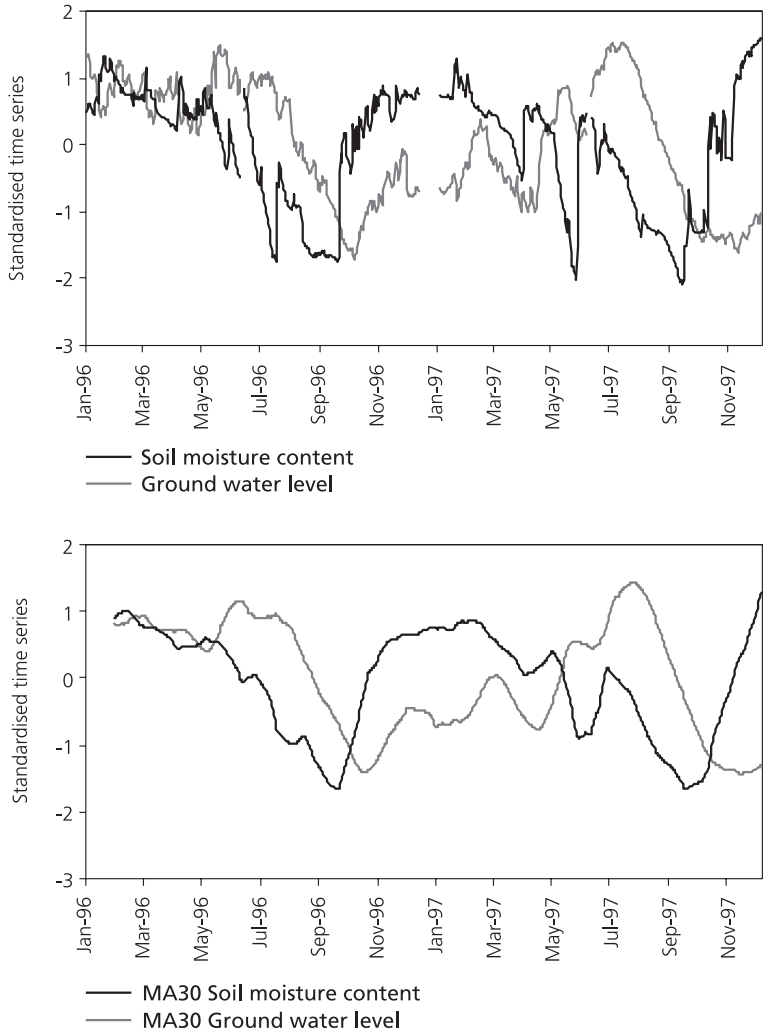

Figure 5.16 Relationship between soil moisture content and ground water level.

The ground water levels (figure 5.16) show a maximum in summer (July and August), and minimum ground water levels are encountered at the beginning of the winter period (October - November). The figure shows an asymmetrical ground water level fluctuation. The ground water level remains high until the end of the summer, then it drops in three months to its minimum. After that the ground water level slowly recovers in the next nine months. The moving averages of figure 5.16 enhance this picture. Figure 5.16 shows that if negative standardised soil moisture content occurs, the ground water system becomes (partly?) disconnected from the meteorological system and deflates. In the period of positive standardised soil moisture content a slow but continuous ground water recharge fills the ground water system again. Only in summer 1997 this relationship is not met totally.

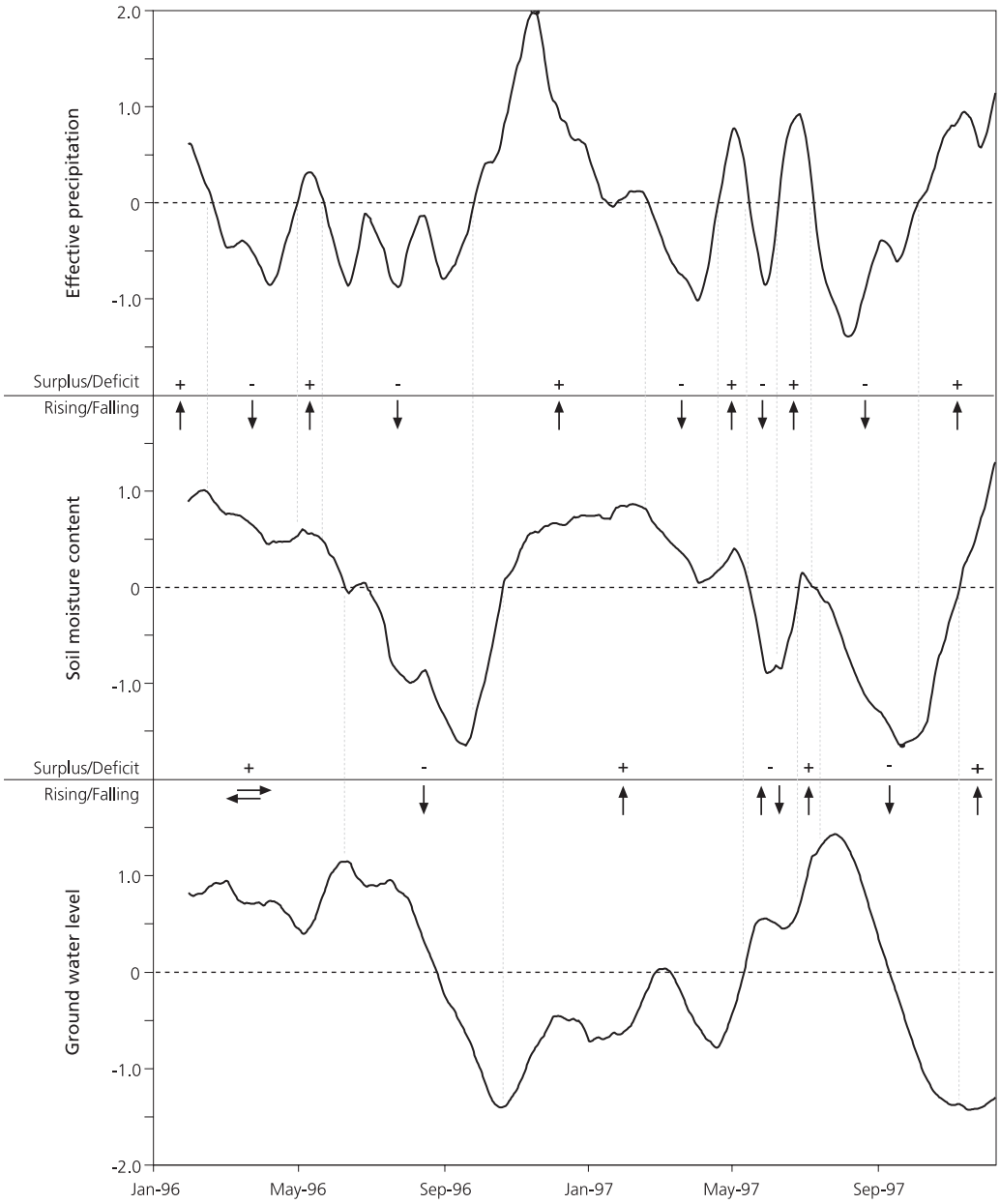

Figure 5.17 Summary of hydrological system in the Beline slope.

Figure 5.17 summarises the above and explains the time delay between the peaks in effective precipitation and soil moisture content and between soil moisture content and ground water level fluctuations. As long as a positive standardised effective precipitation exists, the soil moisture content will rise even though the standardised effective precipitation diminishes. The time delay between the peaks in soil moisture content and ground water level also logically follows from the standardised curves. As long as the standardised soil moisture content is above zero, the ground water level will rise. Figure 5.17 shows that if the standardised effective precipitation curve crosses the zero-line it corresponds with a local minimum or maximum of the standardised soil moisture content graphs. The same is valid if the latter crosses the zero-line, which corresponds with a local minimum or maximum of the standardised ground water level curves. This implies that, on a long time scale, the subsurface hydrological system at the Beline slope is in equilibrium with the climatic conditions and that, on a shorter time scale, a transient situation exists. Figure 5.17 also suggests that some causal relationship between the amplitude of a standardised input time series (e.g. soil moisture content) and the rate of increase or decrease of the output time series (e.g. ground water).

In figure 5.18, every three months one schematic total soil suction profile is drawn together with the zero flux plane(s), which explains figure 5.17. The development of a zero flux plane can explain the seasonal dynamics of the unsaturated zone in the Salins-les-Bains slope. The surplus of evapotranspiration in spring develops a soil suction gradient towards the surface.

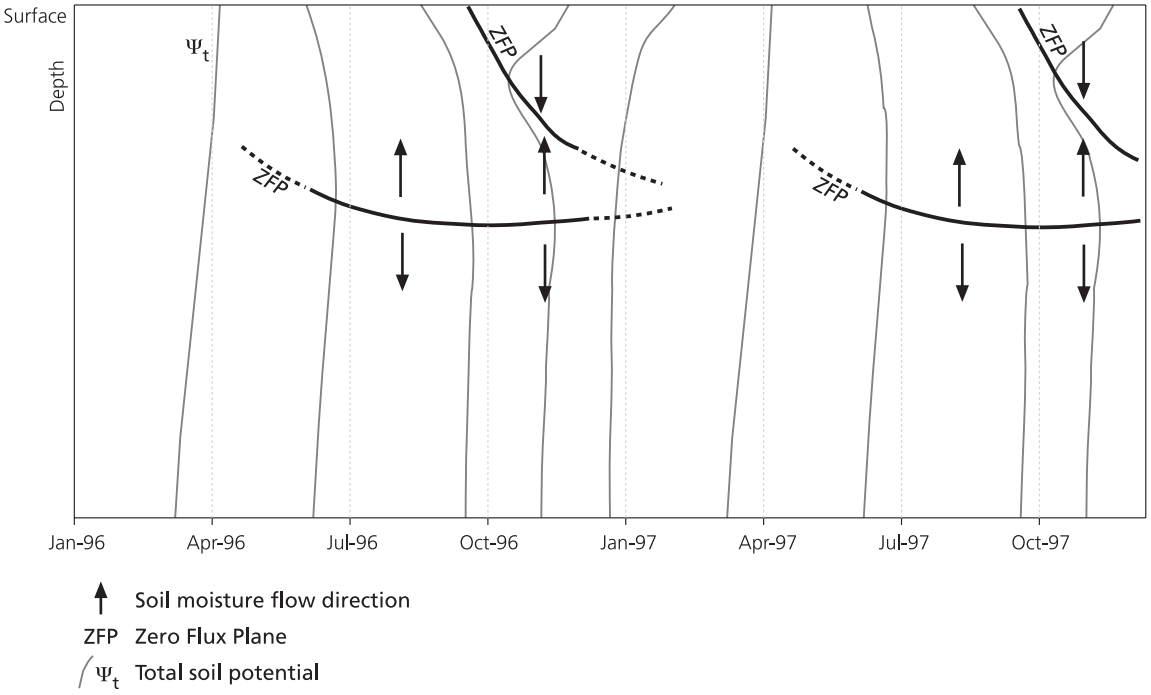

Figure 5.18 Explanation of hydrological system in the Beline slope using zero flux planes in the unsaturated zone.

This results in a zero flux plane because diverging flow paths develop in the upper unsaturated zone. During the summer, surplus of evapotranspiration increases, the soil suction gradient increases and the zero flux plane moves deeper. This results in a lower soil suction gradient above the saturated zone and thus a decreasing ground water recharge. In autumn a wetting front infiltrates and thus a new, second, zero flux plane develops because of converging flow paths in the upper unsaturated zone. Still, the soil suction gradient above the ground water table decreases and ground water recharge declines. When the converging zero flux plane reaches the diverging zero flux plane, a continuous soil suction gradient exists again and slowly the soil pressure gradient increases and ground water recharge augments (see also figure 5.17).

The cross-association and cross-correlation analyses (paragraph 5.4) showed significant correlations between (effective) precipitation and fluctuations of soil moisture content or ground water level. A time lag of on average one day was found between precipitation and soil moisture changes. A time lag of 5-6 days was encountered between precipitation and ground water level fluctuation. These relatively fast reactions on precipitation seem to be contradictory with the observations just described.

The unsaturated zone reacts fast following a rain event. Individual storm events have a direct effect on the shallow soil moisture content and with a small time lag on the deeper soil moisture content. The meteorological and unsaturated zone systems are closely related and have two temporal scales; one event based (see results cross-correlation and cross-association) and one seasonal based (see results standardised time series).

For the ground water system a more complex picture comes forward. On a seasonal time scale the ground water system reacts with a large time delay (months). On a small time scale a 5-6 days time delay is encountered between fluctuations in the ground water level and rainfall. These smaller fluctuations are secondary. During rainfall events relatively fast ground water recharge (preferential flow e.g. in soil cracks) seems to exist but its quantity is limited. A time delay of 5 days was encountered between effective precipitation and these secondary ground water level fluctuations, which is not extremely fast. This means that it is unlikely the result of bypass flow through large fissures between the meteorological and ground water system. It could be the result of partially penetrating (saturated) fissures or other, slower, preferential flow paths through the unsaturated zone, which are still part of the matrix system.

5.6 Conclusions

In this chapter the meteorological and hydrological data collected at the Beline slope, Salins-les-Bains, France were analysed. It was shown that the precipitation data from the Météo France station in Arbois are representative for the situation at the Beline slope except for convective summer storms. Furthermore, the rainfall intensities are on average low. The meteorological data show that from March until October a precipitation deficit exists, and in the months October until March a precipitation surplus prevails.

The soil moisture measurements within the first meter generally performed properly, whereas below 1 m no data were gathered. As expected the shallow sensors show high amplitude fluctuations whereas the deeper sensors show more attenuated soil moisture fluctuations. Under forest the fluctuations were most peaked. In general, the soil moisture measurements show a consistent picture. The ground water level data of field stations D1,

D2 and D3 could be used and D4 and SC1 were rejected. The amplitude of the fluctuation was some 30 cm. The ground water level fluctuations showed no or limited autocorrelation.

On a time scale of days, it was shown that the soil moisture content reacts within 48 hours on meteorological input. The ground water system showed a tendency to react on effective precipitation after a time delay of around 5 days. Both cross-association and cross-correlation techniques show the same result. Both analyses also show that the linear correlation between precipitation and ground water level fluctuation is weak. This is partly the result of the assumption of a linear relationship between the input system and the ground water system, whereas the unsaturated zone in reality behaves non-linear. This is also valid for a preferential flow system in the unsaturated zone.

Another point of discussion is whether the use of effective precipitation, defined here as gross precipitation minus potential evapotranspiration, is influencing the short-term relationships as described above. The input system is in reality net precipitation minus actual evaporation and actual transpiration. First of all, only the relationships between meteorological system and the soil hydrology systems was analysed during rainfall events. No attention has been paid to possible relationship of evapotranspiration and soil moisture or ground water decrease. Secondly, the found relationships with cross-association and cross-correlation techniques are identical notwithstanding the choice of the input series (gross precipitation, effective precipitation or the filtered effective precipitation). Lastly, it is felt that the error which is introduced by the here used definition of effective precipitation is to be preferred over the uncertainty which is associated with the calculation of on-site actual evapotranspiration.

On a longer, monthly time scale, clear causal relationships in the hydrological system could be visualised. It was shown that the time lag between the meteorological and soil moisture systems is a consequence of periods of above or below average effective precipitation input. Between the soil moisture and ground water systems it was shown that a change from positive to negative standardised values of soil moisture content correspond to a local maximum ground water level and vice versa. The whole system can be explained with the temporal behaviour of zero flux plane development. It is concluded that the ground water system is in equilibrium with the local climate. The rate of increase or decrease of e.g. the ground water level could well be explained by the amplitude of the positive or negative standardised soil moisture content at that moment.

In summary, the ground water level within the Beline slope fluctuates especially on a seasonal time scale as response to the climatological system (with emphasis on the evapotranspiration). The fluctuations are phase-shifted and attenuated in the unsaturated zone. Fast preferential flow through the 4 m thick unsaturated zone exists but does not contain large quantities of ground water recharge. Furthermore these faster fluxes have a too large time delay (5-6 days) to be the result of an open fissure system. In the following two chapters, the hydrological modelling is addressed to try to explain and quantify this observation.

6 HYDROLOGICAL MODELLING OF THE UNSATURATED ZONE

6.1 Introduction

The aim of this chapter is to describe, through mathematical modelling, the hydrological time series as presented in chapter 5 and to predict the water fluxes through the unsaturated zone that cause ground water level fluctuations. Thus the reaction of the hydrological unsaturated zone system at the Beline slope to precipitation and evapotranspiration is quantified. An important aspect of this research is the predictive value of the models, the validation.

In this chapter the one-dimensional water transfer is studied from the surface towards the ground water system through the unsaturated zone using deterministic models. Two types of deterministic models will be used to analyse their ability to describe and predict hydrological time series: empirical and physically based models. First several empirical models are used (§ 6.2) for relating meteorological time series to ground water level time series. All empirical models are transient and are fitted using the RMSE as objective function to minimize the differences between measured and calculated ground water levels. Paragraph 6.3 handles physically based modelling of the unsaturated zone of the landslide area using Hydrus 1D software (Simunek, et al, 1998). This model is transient and the equations are solved numerically. In paragraph 6.4 the hydrological behaviour of the unsaturated zone of the Beline site and the model performance are discussed.

6.2 Empirical models for water transfer through the unsaturated zone

Table 6.1 shows eight different empirical models that were used to describe the ground water level time series as measured at field stations D1 (1 July 1996 – 31 December 1997), D2 (25 January 1996 – 5 August 1997) and D3 (1 March 1996 – 1 June 1997). The models differ in concept, complexity and the number of parameters. All models are fitted (or 'trained') on the first year of ground water level measurements and validated by using the remnant ground water level time series. The standardised soil moisture content (§ 5.5) and effective precipitation are used as input variables. Effective precipitation is defined as precipitation minus potential evapotranspiration.

The first model describes the average ground water level without fluctuations. This model has no parameters and serves as reference. The second model assumes the ground water fluctuation to behave as a sine around the average. The parameter 'a' determines the amplitude of the ground water level fluctuation and 't_L' the time lag or timing of the maximum and minimum ground water levels. The third model adds effective precipitation with a five days delay. This has been selected because the time series analyses (chapter 5) showed a time lag of on average 5 days between precipitation and ground water level response. Model 4 uses effective precipitation as input to model the ground water level, model 5 uses the standardised soil moisture content and model 6 combines the models 4 and 5. Model 7 allows for asymmetry in the ground water level

Table 6.1 List of the empirical ground water level models.

No.	Model		Tuning parameters
1	$GWL_t = GWL_{avg}$		-
2	$GWL_t = GWL_{avg} + a \cdot \sin(t + t_L)$		a, t_L
3	$GWL_t = GWL_{avg} + a \cdot \sin(t + t_L) + b \cdot Pe_{t-5}$		a, t_L, b
4	$GWL_t = GWL_{t-1} + b \cdot Pe_{t-5}$		b, initial GWL
5	$GWL_t = GWL_{t-1} + c \cdot \Theta_{t-1}$		c, initial GWL
6	$GWL_t = GWL_{t-1} + c \cdot \Theta_{t-1} + b \cdot Pe_{t-5}$		b, c, initial GWL
7	$GWL_t = GWL_{t-1} + c_1 \cdot \Theta_{t-1}$	$\wedge\ \Theta_{t-1} \geq 0$	c_1, initial GWL
	$GWL_t = GWL_{t-1} + c_2 \cdot \Theta_{t-1}$	$\wedge\ \Theta_{t-1} < 0$	c_2, initial GWL
8	$GWL_t = GWL_{t-1} + c_1 \cdot \Theta_{t-1} + b \cdot Pe_{t-5}$	$\wedge\ \Theta_{t-1} \geq 0$	b, c_1, initial GWL
	$GWL_t = GWL_{t-1} + c_2 \cdot \Theta_{t-1} + b \cdot Pe_{t-5}$	$\wedge\ \Theta_{t-1} < 0$	b, c_2, initial GWL

GWL	Ground Water Level	t	Day
Θ	Standardised soil moisture content	t_L	Lag time
Pe	Effective precipitation	a, b, c	Fit parameters

fluctuation in that the ground water level decline is faster than the ground water level rise (chapter 5). Model 7 therefore separates the calculation of the ground water level in case of a positive or negative standardised soil moisture content. Model 8 adds effective precipitation to model 7.

The root mean squared error (RMSE) was used as an objective function for the goodness of fit between observed and calculated ground water level data. The RMSE is a measure for the (average) absolute error: 0 is a perfect fit.

$$RMSE = \sqrt{\frac{\Sigma(x_i - x_{obs})^2}{n}}$$

x_i calculated value
x_{obs} observed value
n number of observations

The parameters listed in table 6.1 were adjusted unrestrictedly to come to the smallest RMSE for the observed versus modelled time series. These calculations were executed with the Excel iteration program (Solver). It uses a non-linear optimisation with a quasi-Newton iteration scheme. The convergence limit was set at 0.001. Figure 6.1 shows the measured and modelled time series of the ground water level for the field station D2. Table 6.2 gives the resulting parameter values.

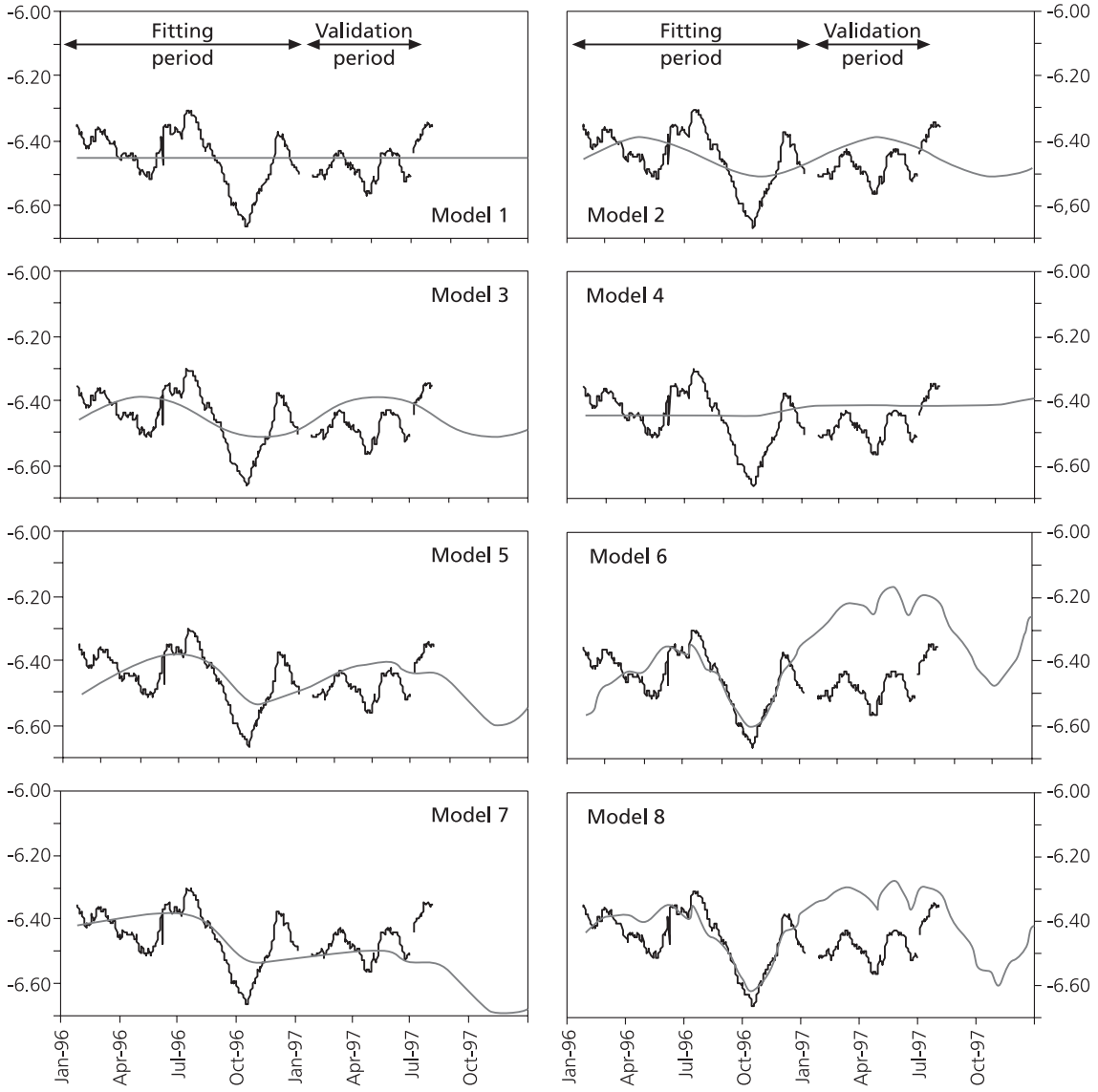

Figure 6.1 Time series of the observed (bold line) and predicted (thin line) ground water level for monitoring station D2 using empirical models as listed in table 6.1. The y-axis shows the ground water level in meters below surface.

An important aspect of a model is its performance after the training period: the validation. Table 6.3 shows the results of the objective function calculated for the training period as well as for the validation period and also the ratio of the RMSE for the two periods. Both figure 6.1 and table 6.3 show that the model performance is generally poor in the validation period. The RMSE for the validation period is in most cases much larger than for the fitting period. This implies that the training data set is too short. Would the model results improve when all data are used for fitting the empirical models or does one see an increase of the absolute error with a growing data set? This does, however, imply that a validation data set is no longer available. The RMSE for the models results fitted on all available data and the ratio of the RMSE for model results fitted on two different time spans are given in the last two columns of table 6.3.

Table 6.2 Overview of the fit parameters for the different empirical models (see also table 6.1). GWL is an abbreviation for ground water level, (ini) denotes initial value and (avg) means average value.

	Parameter	D1	D2	D3
model 1	GWL(avg)	-3.39	-6.45	-4.16
model 2	a	0.11	0.06	0.05
	t_L	-56.71	-30.00	-61.43
model 3	a	0.11	0.06	0.05
	t_L	-55.51	-40.00	-61.41
	b	-5.59E-04	1.67E-04	-1.18E-04
model 4	GWL(ini)	-3.41	-6.45	-4.14
	b	2.11E-04	8.36E-05	-2.24E-04
model 5	GWL(ini)	-3.26	-6.51	-4.17
	c	2.53E-03	1.42E-03	9.13E-04
model 6	GWL(ini)	-3.29	-6.57	-4.16
	c	2.35E-03	2.08E-03	8.65E-04
	b	6.94E-05	5.39E-04	-1.04E-04
model 7	GWL(ini)	-3.31	-6.42	-4.11
	c_1	2.66E-03	4.41E-04	-7.30E-05
	c_2	2.13E-03	1.37E-03	7.70E-04
model 8	GWL(ini)	-3.32	-6.44	-4.11
	c_1	3.23E-03	6.26E-04	-1.04E-04
	c_2	1.92E-03	2.04E-03	7.78E-04
	b	-1.51E-04	6.40E-04	9.86E-06

The following observations can be made from the empirical model results (see tables 6.2, 6.3 and figure 6.1):

- The model results indicate that models 7 and 8 perform in most cases better than the other 6 models. This is independent of the calibration time span and is also true for the validation period.
- Modelling ground water level fluctuations with only precipitation and evapotranspiration data (model 4) performs worse in all cases than using only soil moisture content.
- The model performs only slightly better when the effective precipitation is added (models 3-4-6-8) to the empirical models. Unfortunately, the effective precipitation is sometimes subtracted (a negative parameter b). This, of course, is not in agreement with the physical reality.
- The model parameters (table 6.2) derived for the three ground water time series differ a lot and sometimes even change sign.
- To fit the empirical models using different parameters to represent rising and falling stages of the ground water level seems useful. Models 7 and 8 represent the ground water level times series better than models 5 and 6.
- When the fitting period was enlarged from one year to the whole data set, the D1 and D3 ground water time series show an increase in absolute error, and D2 shows improvement of the model performance.
- The ratio of RMSE during fitting and validation shows that the model performance decreases significantly in the validation period.

Table 6.3 Results of the goodness of fit calculations for the empirical modelling. The fitting was done using the first year of ground water data and using all data, the validation used the remnant data of the different ground water time series. RMSE = Root Mean Squared Error, [val/fit] = ratio of RMSE of validation period over fitting period, [fit1/fit2] = ratio of the RMSE of 1 year fitting period over fitting with all data.

	Fitting 1 year	Validation	Ratio	Fitting all data	Ratio
D1	RMSE [m]	RMSE [m]	[val/fit]	RMSE [m]	[fit1/fit2]
Model 1	0.086	0.118	1.37	0.098	1.14
Model 2	0.037	0.057	1.52	0.043	1.15
Model 3	0.036	0.055	1.52	0.041	1.15
Model 4	0.080	0.153	1.90	0.096	1.21
Model 5	0.043	0.095	2.19	0.052	1.20
Model 6	0.038	0.081	2.13	0.042	1.11
Model 7	0.033	0.052	1.61	0.034	1.02
Model 8	0.030	0.039	1.30	0.032	1.07
D2					
Model 1	0.085	0.056	0.66	0.076	0.90
Model 2	0.074	0.084	1.15	0.073	0.98
Model 3	0.074	0.083	1.13	0.072	0.97
Model 4	0.085	0.075	0.89	0.076	0.89
Model 5	0.070	0.068	0.97	0.067	0.96
Model 6	0.065	0.243	3.73	0.067	1.04
Model 7	0.069	0.077	1.12	0.065	0.94
Model 8	0.053	0.158	2.98	0.054	1.03
D3					
Model 1	0.043	0.058	1.34	0.045	1.05
Model 2	0.020	0.093	4.55	0.038	1.90
Model 3	0.020	0.093	4.55	0.038	1.90
Model 4	0.039	0.013	0.32	0.033	0.84
Model 5	0.026	0.081	3.14	0.039	1.49
Model 6	0.022	0.046	2.11	0.024	1.07
Model 7	0.015	0.013	0.87	0.015	0.99
Model 8	0.015	0.013	0.88	0.015	0.99

The results show the importance of soil moisture content for the estimation of the ground water level fluctuations in a clayey soil with relatively deep ground water levels. The inclusion of effective precipitation can improve the performance of the empirical models only slightly. In some cases, however, this can be in a contra-productive physical way, i.e. subtraction of water in rainy periods and adding water during periods of precipitation deficits.

A clear problem in the described method is that both the training and validation periods are too short to calibrate the empirical models. The model performance decreases sharply in the validation period, indicating that the empirical models do not sufficiently describe the system. A measurement error or an extreme event can easily distract empirical models from the general, average, image. In the practice of landslide research, however, a time series as presented here is quite extraordinary. Shortage of data is far more common than the existence of large databanks with hydrological time series. A

second problem with this exercise is the small ground water amplitude of the system. This results in a less clear 'cause-effect' relationship.

It is therefore concluded that the proposed empirical models for the given periods are unreliable when they are to be used for prediction purposes. Only models 7-8 have some predictive value. Furthermore it is shown that the soil moisture content of the unsaturated zone has a higher predictive value for ground water level response than effective precipitation.

6.3 Physically based unsaturated zone modelling

6.3.1 Aim and parameterisation of the Beline unsaturated zone model

The purpose of deterministic modelling of the unsaturated zone is to gain insight in the hydrological behaviour of the unsaturated clayey soil and to quantify the influence of land use and climate changes on the hydrological behaviour of the unsaturated zone. For this, time series of ground water, soil moisture and meteorology were used. Secondly, it will be attempted to model the ground water level fluctuations on a daily basis using generally available meteorological information. Lastly, model sensitivity was analysed and its robustness was assessed (validation). The model was calibrated with a transient inverse modelling approach using one year of soil moisture and ground water level data. The transient calibration avoids problems in transferring steady-state calibrated models towards transient models (Anderson and Woessner, 1992). The Hydrus1D software package (Šimunek, et al, 1998) was chosen because it is capable of modelling the water flow in the unsaturated zone with numerous different boundary conditions, works with flexible time discretisation, can handle modelling of longer time series (not only event based) and because of its inverse modelling option. Furthermore it is extensively tested and calibrated and has a user-friendly interface as pre- and postprocessor.

Model description

Hydrus-1D (version 7.0) is a finite element software package for simulating water, heat and solute transport in one-dimensional variably-saturated media. The program numerically solves the Richards' equation for variably-saturated water flow (Šimunek, et al, 1998). The subsurface can be heterogeneous, non-uniform and the soil column may have an inclined angle. The upper boundary conditions can be transient head or flux controlled and can deal with atmospheric conditions. The lower boundary condition can be a time series of ground water levels (Dirichlet type), water fluxes (Neumann type), deep drainage, horizontal drains as well as free drainage conditions.

The governing flow equations are solved numerically using a standard Galerkin-type linear finite element scheme. The inverse modelling uses a Marquardt-Levenberg type parameter optimisation (Šimunek, et al, 1998). The hydraulic parameter models that are included are the Mualem-Van Genuchten model (with air-entry value option), the modified Mualem-Van Genuchten model and the Brooks-Corey model. If parameter estimation is not available use can be made of an included database for hydraulic parameters. The unsaturated zone model can furthermore include a sink-term for plant root water uptake and a plant root growth model.

Parameterisation

In deterministic modelling the assumption is that with sufficient knowledge of the mathematical equations describing the physical processes, one only has to make a discretisation of the subsurface and determine its intrinsic parameters. In hydrological unsaturated zone modelling the intrinsic parameters are, among others, the saturated and unsaturated permeability. The former was determined with the inverse auger hole method, the latter with the Van Genuchten-Mualem model (§ 4.7). The unsaturated zone was discretised using field data of porosity, bulk density and auger hole descriptions.

As described in § 4.2 the unsaturated zone consists of a 40 cm thick infiltration zone and a percolation zone. The infiltration zone is characterised by a lower bulk density, a higher porosity and a higher saturated permeability. The percolation zone underlies the infiltration zone and varies in thickness between 3 and 6 m and is considered to have homogeneous hydrological characteristics.

The input variables are daily precipitation and potential evapotranspiration, calculated by using the Penman-Monteith equation (see § 5.2). For representation of the soil moisture conditions, time series were constructed for the first and second layer. First all the soil moisture time series were expressed in terms of effective soil moisture after which they were averaged per layer. The average effective soil moisture time series was transformed into average soil moisture by multiplying with the layer porosity under the assumption of negligible residual soil moisture content.

The initial parameters were taken from the field data as gathered in 1996 and 1997 (§ 4.6) and are listed in table 6.4. As with the empirical models, the first year of soil moisture and ground water level data was used for calibration. The model was calibrated with an inverse modelling approach in which the hydraulic parameters were allowed to be optimised within certain limits (table 6.4.). The inverse modelling uses the sum of the squared errors as objective function. The inverse modelling used the average daily soil moisture content per layer as objective time series. The porosity was fixed at 45 % for the topsoil layer and 41 % for the second layer. The soil moisture time series of the first layer was attached to 30 cm depth and the series for the second layer to 80 cm depth. The upper boundary condition is a Neumann-type boundary and consists of a time series of precipitation and potential evapotranspiration. The actual calculated flux is equal or lower than the potential boundary condition. In other words: the model has a variable meteorological boundary condition with surface runoff. The lower boundary condition is a Dirichlet-type boundary and consists of ground water level time series of stations D1, D2 or D3. This implies that the thickness of the unsaturated zone varies between 3.5 and 6.5 m.

Initial soil moisture conditions in the unsaturated zone are set equal to the equivalent soil moisture profile (Salvucci and Enktekhabi, 1994a-b). The equivalent soil moisture profile was calculated with a steady-state unsaturated flow scenario with an upper boundary condition of net precipitation surplus of 1 mm/day. The lower boundary condition is the average ground water level. The model results are shown in figure 6.2. The influence of the first layer is clearly visible and results in relatively high initial soil moisture conditions.

Table 6.4 Parameterisation for the Beline inverse unsaturated zone model.

	Depth [cm]	Position observation node [cm]		θ_s [-]	α [cm^{-1}]	n [-]	K_{sat} [cm/day]
Layer 1	0 - 40	-31.5	Initial	0.45	0.045	1.08	21.8
			Minimum	-	0.001	1.001	-
			Maximum	-	0.15	2.5	218
Layer 2	> 40	-81.5	Initial	0.41	0.041	1.07	12.9
			Minimum	-	0.001	1.001	-
			Maximum	-	0.15	2.5	129
			Optimisation allowed ?	No	Yes	Yes	Yes

6.3.2 Inverse model

Table 6.5 shows the hydraulic parameter set that results from the inverse modelling. Hydrus-1D also specifies the upper and lower bounds of the 95 % confidence levels around each fitted parameter. Large confidence limits indicate that the results are not very sensitive to the value of a parameter (Šimunek, et al, 1998). The optimised hydraulic parameters do not resemble the initial set which was determined using field and laboratory tests. Almost identical hydraulic parameter sets result from inverse modelling using the ground water data of D2 and D3 as lower boundary condition. Kutilek and Nielsen (1994) state that α normally ranges from 10^{-2} to 10^{-3} cm^{-1}, and n between 1.2 and 4. As table 6.5 shows, the average hydraulic parameter value and 95 % confidence limits are within this range. The results of the inverse modelling using D1 ground water data are not plausible. The saturated permeability of the second layer is larger than that of the first layer. This is not very likely. Furthermore, the value of α for the second layer is very high. The differences in model behaviour are partly reflected by the regression coefficient between observed and modelled soil water content. The squared regression coefficient is lower for data coming from ground water field station D1 than for stations D2 and D3.

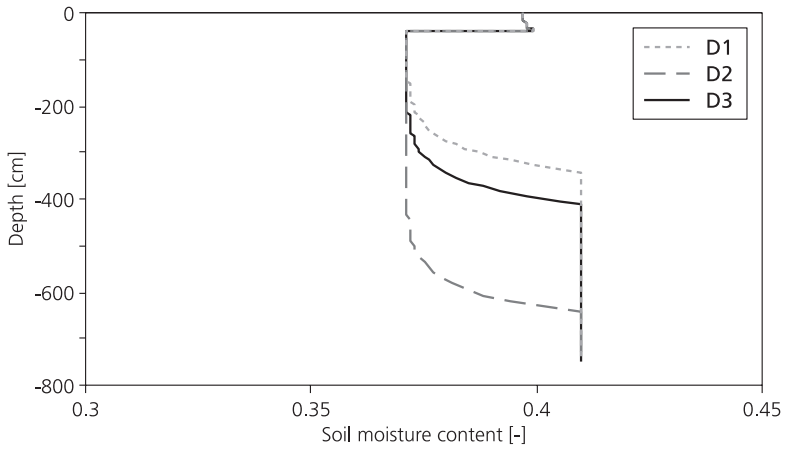

Figure 6.2 The equivalent soil moisture profiles that are used as the initial soil moisture content for the unsaturated zone model.

Inverse modelling is sensitive to initial settings. Because of this, a sensitivity analysis was performed on the inverse model or more specifically, the sensitivity of the hydraulic parameter outcome to changes in initial settings was tested. In the most favourable condition all inverse model runs should come up with the same parameter values and confidence limits. If this is not the case, equivalent model performance can be reached with different parameter sets. The following initial settings were used:

1) initial values of hydraulic parameters
2) porosity
3) lower boundary condition and
4) meteorological time frame.

Table 6.5 Results of the inverse modelling: α (cm^{-1}) and n (-) are van Genuchten-Mualem parameters, K_s (cm/day) is the saturated permeability. Furthermore the 95 % confidence limits are given. R^2 is the squared regression coefficient for the observed versus calculated soil moisture data. The mass balance error is the percentage of water balance error of the unsaturated flow model in the last run using the optimised hydraulic parameter values.

			95 % confidence level	
	Parameter	Value	Lower	Upper
D1				
Layer 1	α	7.30E-03	4.91E-03	9.69E-03
	n	1.265	1.214	1.316
	K_s	8.60	2.21	14.98
Layer 2	α	2.78E-02	1.35E-02	4.21E-02
	n	1.143	1.106	1.179
	K_s	51.57	-4.51	107.65
	R^2	0.55		
	Mass balance error %	0.00		
D2				
Layer 1	α	4.46E-03	3.08E-03	5.85E-03
	n	1.199	1.165	1.233
	K_s	40.76	-2.84	84.37
Layer 2	α	4.20E-03	3.10E-03	5.29E-03
	n	1.252	1.200	1.304
	K_s	4.40	1.68	7.12
	R^2	0.69		
	Mass balance error %	0.47		
D3				
Layer 1	α	4.93E-03	3.56E-03	6.30^{E}-03
	n	1.225	1.179	1.270
	K_s	31.87	4.82	58.92
Layer 2	α	5.92E-03	4.69E-03	7.15^{E}-03
	n	1.255	1.211	1.299
	K_s	5.07	2.55	7.58
	R^2	0.69		
	Mass balance error %	0.77		

Ad 1)
Per test one initial hydraulic parameter was 20 % increased or decreased as compared to the values shown in table 6.4.

Figure 6.3 shows the optimised hydraulic parameters and 95 % confidence interval for all inverse model runs. The D2 test 3 is not shown because of the numerical instability of the test run. Figure 6.3 clearly shows that the saturated permeability has the largest range of most likely values and confidence limits, indicating that it is not a sensitive parameter. A second observation is that the parameters of layer 1 are less scattered than those of layer 2. This suggests that the inverse model is more sensitive to changes in the upper layer than to changes in the lower layer. The figure also shows that in general the differences between the ground water level data sets (using D1, D2 or D3) are larger than between the different sensitivity model runs. This implies that the choice of ground water level time series and matching meteorological time series is (at least) as important as the initial parameter values.

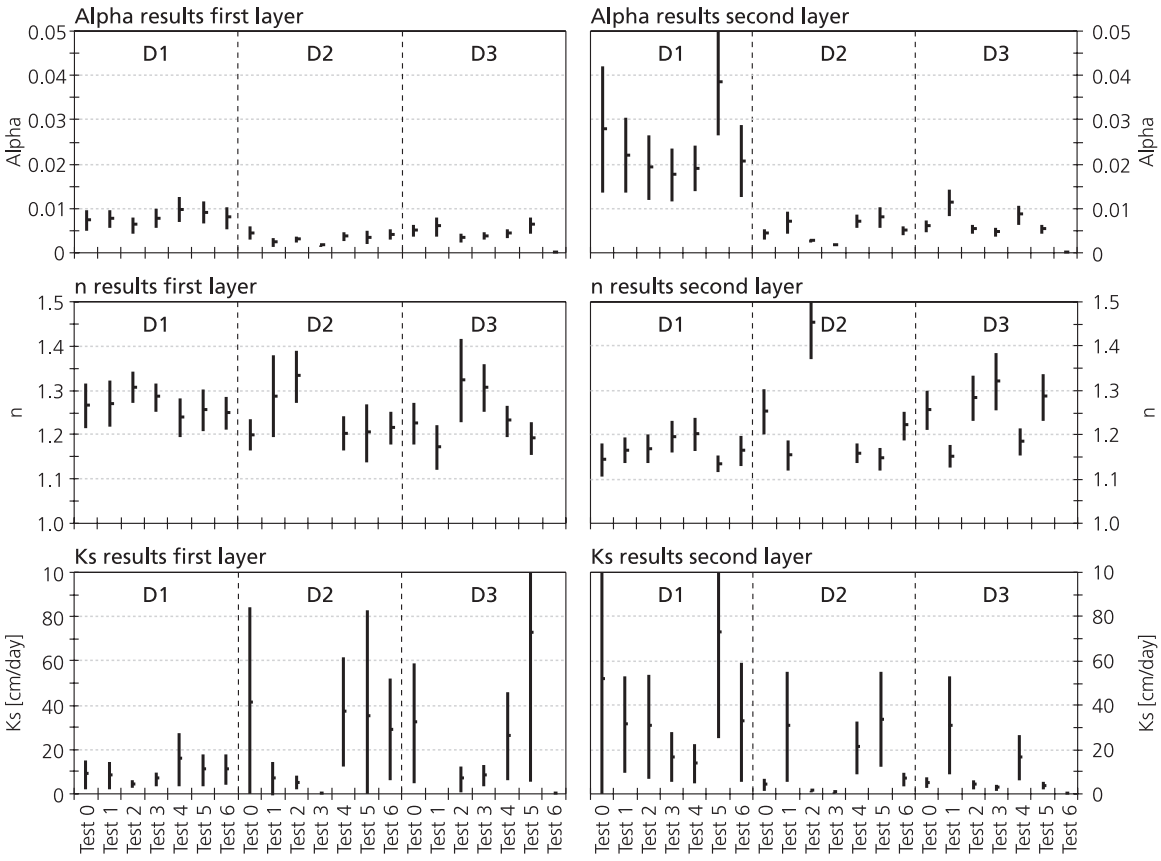

Figure 6.3 Results of the sensitivity analyses of the inverse model on initial parameter setting. Results are shown per parameter and layer. The horizontal line is the parameter value outcome, vertical line indicates 95 % confidence limits. Test 0 is the initial inverse model (for results see table 6.5), test 1 initial α-value +20 %, test 2 initial α-value -20 % , test 3 initial n-value +20 %, test 4 initial n-value -8 % (=minimum), test 5 initial K_s-value +20 % and test 6 initial K_s-value -20 %.

Table 6.6 Indicative correlogram of parameters used in the inversed model. The correlation coefficients are median values of the correlograms of all sensitivity runs as shown in figure 6.3.

		Layer 1			Layer 2		
		α	n	K_s	α	n	K_s
Layer 1	α	1.00					
	n	-0.90	1.00				
	K_s	0.65	-0.86	1.00			
Layer 2	α	0.45	-0.36	0.19	1.00		
	n	-0.01	0.28	-0.08	-0.75	1.00	
	K_s	-0.15	-0.07	-0.10	0.66	-0.94	1.00

For a better insight in the sensitivity results, the mutual dependency of the hydraulic parameters was calculated. For all inverse model runs correlations were determined between the optimised hydraulic parameters. Table 6.6 shows an indicative correlation matrix which gives the median values of the correlation coefficients of all inverse model results as shown in figure 6.3. No correlation exists between the parameters of the two layers. Within both layers a strong negative correlation exists between n and K_s. In the upper layer α and n are strongly negative correlated, whereas in the second layer this correlation is a little less evident. The positive correlation between α and K_s is for both layers weaker. The strong correlations between the parameters (especially with parameter n) hinder the determination of a unique parameter set and thus the calibration of the unsaturated zone model.

Ad 2)
Porosity is known to have a significant influence on the hydrological behaviour of the unsaturated zone. Sensitivity analysis on the parameter porosity is not straightforward, because the soil moisture time series were obtained by multiplying the average effective soil moisture per layer by the average measured porosity. Changing porosity of a layer changes the average soil moisture time series.

Figure 6.4 shows the effect of increasing porosity of both layers on the model performance (expressed in the correlation coefficient between modelled and observed soil moisture time series), and on the resulting hydraulic parameters. The explained variance increases if the porosity increases to 55 % for the first and 45 % for the second layer. A further increase in porosity did not improve the model results. The hydraulic parameters show no trend with increasing porosity, and do not deviate from the range of results shown in figure 6.3. However, increasing porosity diminishes the lower boundary flux and slightly delays the timing of these fluxes (figure 6.5).

Ad 3)
The effect of the ground water level fluctuations on the unsaturated zone model was also tested. The lower boundary condition was set at a constant value equal to the average ground water level instead of using the ground water level time series. The parameter outcome (α, n and K_s for both layers) did not vary much from the results observed in the

sensitivity analysis (figure 6.3). The change from variable ground water data to a constant ground water level did not influence the lower boundary flux.

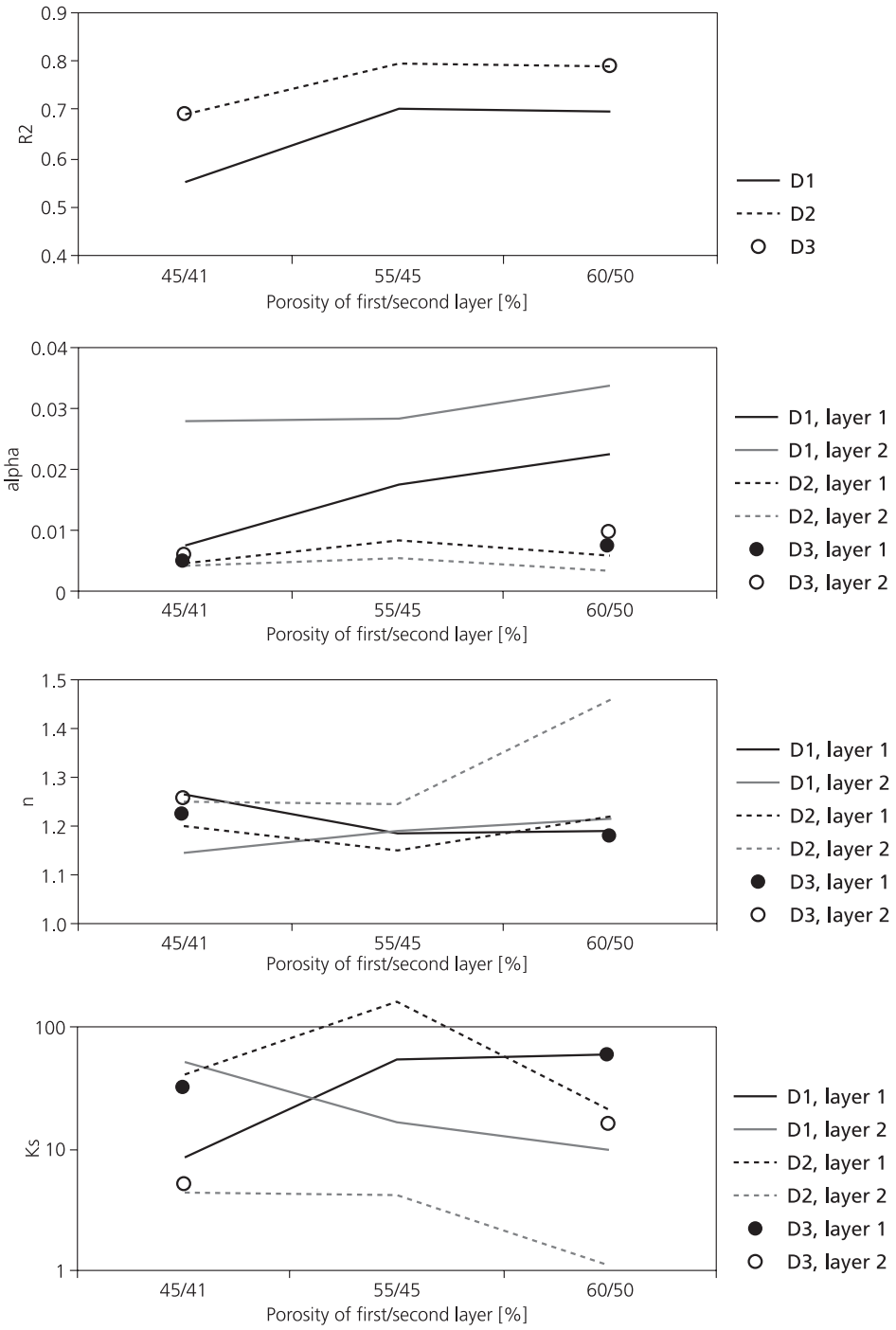

Figure 6.4 Sensitivity of increased porosity on the parameter optimisation. The x-axis labels (e.g. 45/41) denote the porosity of the first and second layer respectively.

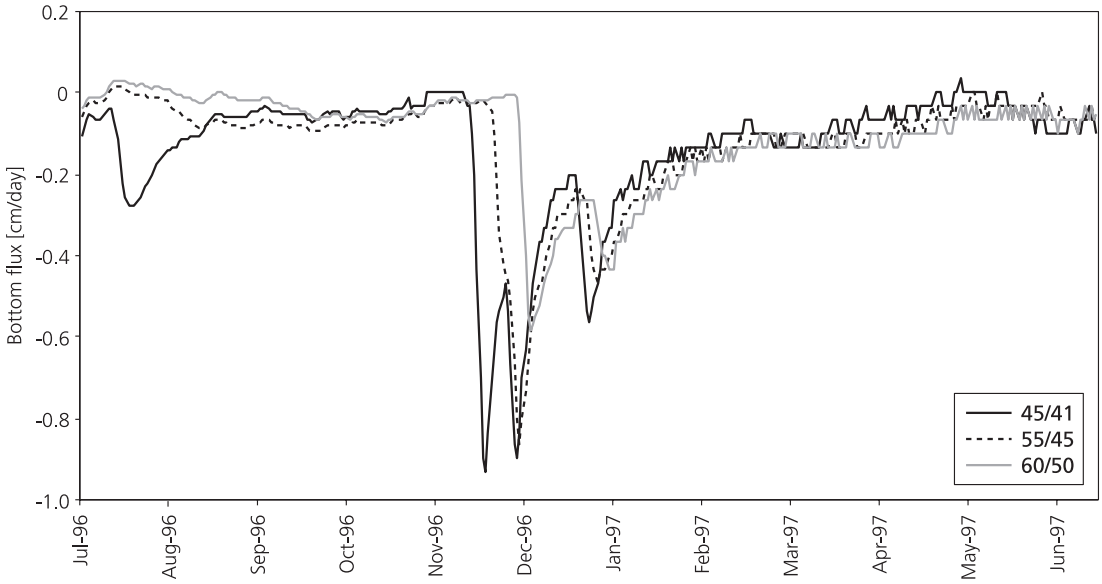

Figure 6.5 Example of the unsaturated zone bottom flux as function of the porosity for ground water time series D1. The numbers in the legend indicate the porosity in percentage of the first and second layer respectively.

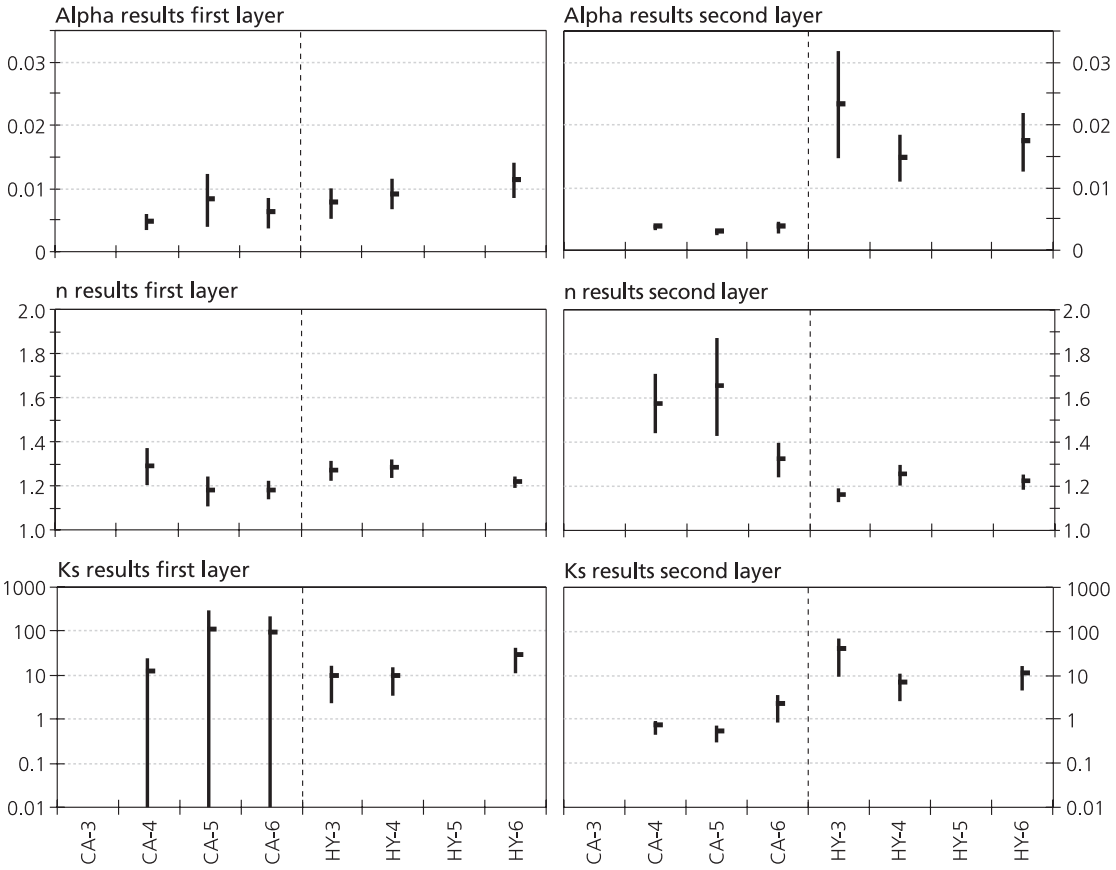

Figure 6.6 Results of the parameter optimisation (inversed modelling) using hydrological (HY) and calendar (CA) year of data combined with constant ground water levels at -3, -4, -5 or -6 m. CA-3 and HY-5 suffered from numerical instability.

Ad 4)
From the above results it was questioned whether the depth of the ground water level or the accompanying meteorological data influenced the inverse model outcome the most. The influence of these two aspects was tested separately by running the inverse model with two meteorological input periods and 4 different constant ground water levels. The two data periods were 25 January 1996 to 24 January 1997, approximately a calendar year (abbreviated as CA and previously used for ground water data series D2) and 1 July 1996 to 30 June 1997, a hydrological year (abbreviated as HY and previously used for ground water data series D1). The ground water levels were 3, 4, 5 and 6 m below surface. The initial (or equivalent) soil moisture profiles were recalculated using these ground water levels. The calendar year receives 1144 mm of precipitation and has a potential evapotranspiration of 753 mm whilst the hydrological year has 1304 mm of precipitation and 790 mm potential evapotranspiration.

The results are shown in figure 6.6. Two inverse model runs had important numerical instability (CA-3 and HY-5) and did not converge. Figure 6.6 shows that the influence of the meteorological period is large. It furthermore shows that the influence of the ground water depth on the hydraulic parameter outcome in both layers is small.

The following conclusions can be derived from the sensitivity analysis of the inverse model:
- the influence of ground water level fluctuation is negligible, both on the parameter optimisation and the ground water flux. This indicates that no back coupling of the ground water level reaction for the unsaturated zone behaviour exists. This implies that a coupled saturated – unsaturated zone model is not necessary, because both systems do not really interact.
- the choice of the meteorological data of one year is short to calibrate this highly non-linear unsaturated zone model. The difference in model performance as shown in table 6.5 is mainly related to the differences in input time series (precipitation and evapotranspiration).
- the porosity of the subsurface does influence the model performance as represented with the regression coefficient between observed and calculated soil moisture content, but does not influence the parameter outcome of the inverse modelling. Porosity does influence the bottom flux calculated by the model: a higher porosity delays and diminishes the ground water flux at the bottom.
- the analyses show that the intrinsic parameters as determined in the field and laboratory are not useful for the numerical modelling of the unsaturated zone. This is most probably the result of the limited scale of the samples.

Notwithstanding the obvious problems of non-unique parameter optimisation, an attempt was made to use the Beline unsaturated zone model for direct modelling. It is recognised that no simple or unique way exists to establish the optimal parameter combination. The following decisions were made on basis of the sensitivity analysis:
- the averaged constant ground water level was used because fluctuations in the ground water level had no influence on the inverse model.
- consequently all available meteorological and soil moisture data were used, starting on 25/1/96. The inverse modelling used the calendar year data (25/1/96 – 24/1/97).

- the parameter n of both layers was assigned a fixed value because the correlogram (table 6.6) shows that a high correlation between n - α and n - Ks exists. The range of model output could be narrowed down when n was fixed in the inverse modelling. Therefore the average n-value per layer was determined using the calendar time series (CA in figure 6.6). This gives n(1)= 1.2 and n(2)=1.5.

Table 6.7 Results of the inverse unsaturated zone modelling with n(1) = 1.2 and n(2) = 1.5.

			95 % confidence level	
	Parameter	Value	Lower	Upper
- 4 m				
Layer 1	α	6.71E-03	6.10E-03	7.32E-03
	K_s	57.57	25.67	89.47
Layer 2	α	3.96E-03	3.62E-03	4.30E-03
	K_s	0.76	0.66	0.86
	R^2	0.69		
	Mass balance error %	0		
- 5 m				
Layer 1	α	5.96E-03	5.41E-03	6.51E-03
	K_s	46.98	21.08	72.88
Layer 2	α	3.18E-03	2.87E-03	3.48E-03
	K_s	0.78	0.68	0.87
	R^2	0.70		
	Mass balance error %	0		
- 6 m				
Layer 1	α	5.52E-03	5.01E-03	6.02E-03
	K_s	42.31	13.79	70.83
Layer 2	α	2.82E-03	2.52E-03	3.11E-03
	K_s	0.80	0.70	0.90
	R^2	0.70		
	Mass balance error %	0		

The inverse model was run again, now with the ground water level at 4, 5, and 6 m below surface. Table 6.7 shows the results of the inverse model using the calendar year of meteorological data and three different ground water levels as lower boundary condition leaving only α and K_s to be optimised. As expected, the confidence limits of α and K_s are narrowed down considerably. Simultaneously, the correlation between parameters α and K_s was cancelled out.

6.3.3 Direct modelling

The aim of direct modelling is to analyse the model performance using a validation procedure and thus to study the possibility to predict ground water level changes using this 1D unsaturated zone model. For direct modelling the optimised parameters from Table 6.7 are used. Besides the selection of the parameter values, the boundary conditions should be changed in a direct model procedure because it is the ground water level, which is to be calculated.

Boundary conditions

The ground water level data were used as a Dirichlet-type boundary condition in the inverse model. In the direct modelling the ground water levels should be predicted and are thus not set a-priori. The lower boundary has to be changed in a Cauchy-type of boundary condition (head dependent flow boundary). The relation between head on the bottom boundary and the bottom flux should be known for this type of boundary condition. But as stated earlier, the ground water level fluctuations do not influence the model performance, nor do they influence the bottom flux as calculated by the Beline model. An average ground water level as lower boundary condition performed as well. In fact, even no change in bottom flux occurred while working with a fixed average ground water level as lower boundary condition. Thus there is no relationship between pressure head and bottom flux. This eliminates the possibility of working with a Cauchy lower boundary condition.

The second option is working with a Neumann boundary condition. The change towards a Neumann boundary condition is quite difficult. First of all, no information is known about the variable flux across the lower boundary. Working with a steady-state flux across the lower boundary is unrealistic and leads to unstable models, but information on transient bottom fluxes is not available.

There only remains to model the lower boundary with the Dirichlet boundary condition and give up the aim of direct modelling the ground water level. As was shown in § 6.4.2, the Beline model was not sensitive for the lower boundary condition. In the direct modelling lower boundary fluxes are reported and those can than be used as ground water recharge fluxes (upper boundary conditions) for a saturated zone model (see chapter 7). For the direct modelling, the lower boundary condition was set on a ground water level of 4, 5 and 6 m below surface.

Validation of the Beline model

The Beline model was validated on the second year of data using three different ground water levels, respectively 4, 5 and 6 m below surface. Figures 6.7 gives the measured and modelled soil moisture time series using the optimised parameter configuration of table 6.7. The modelled time series shows more dynamic behaviour than the measured time series. This is the case for both 30 and 80 cm depth. All model runs were numerically stable and showed a perfect water balance. The model performances are quantified in table 6.8.

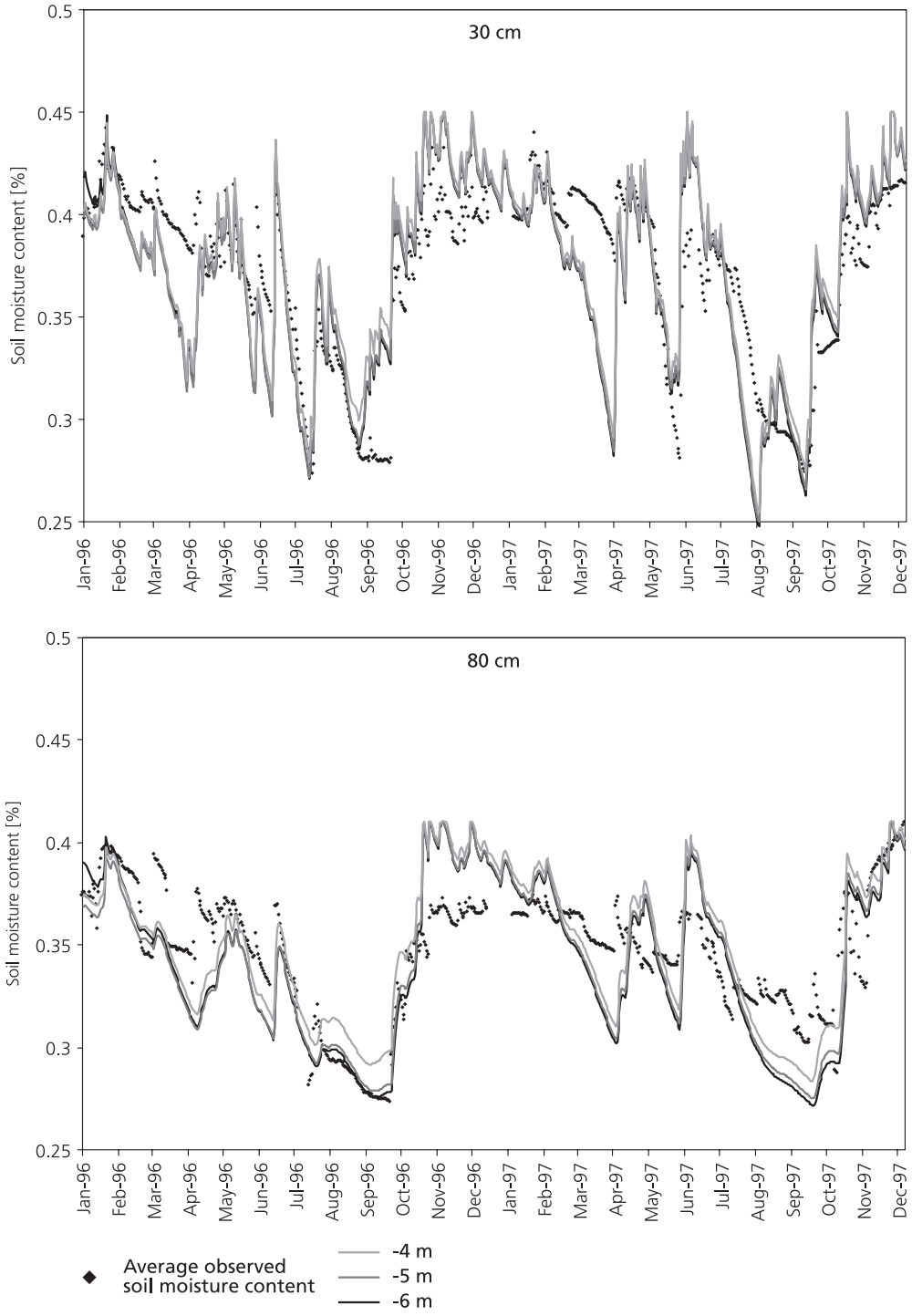

Figure 6.7 Measured and modelled soil moisture (30 and 80 cm depth).

Table 6.8 shows the RMSE of the model for both the calibration and validation year and the ratio between the two is given. A ratio of more than 1 means that the RMSE has increased. The RMSE is largest for the soil moisture time series at 30 cm depth. Also the increase in RMSE going from calibration to validation is largest for the shallow soil moisture data. This signifies that the absolute error is largest in the shallow zone.

Table 6.8 Validation results of the Beline unsaturated zone model: 'tot' stands for all data, '30' for soil moisture data at 30 cm depth and '80' for soil moisture data at 80 cm depth.

	Calibration	Validation	Val/Cal
GWL at -4 m			
RMSE_tot	0.026	0.028	1.07
RMSE_30 cm	0.029	0.034	1.15
RMSE_80 cm	0.023	0.022	0.95
GWL at –5 m			
RMSE_tot	0.026	0.030	1.13
RMSE_30 cm	0.028	0.034	1.21
RMSE_80 cm	0.023	0.024	1.02
GWL at –6 m			
RMSE_tot	0.025	0.030	1.21
RMSE_30 cm	0.027	0.035	1.26
RMSE_80 cm	0.022	0.025	1.12

Overall, figure 6.7 and table 6.8 show that the unsaturated zone model is a stable model, which describes the soil moisture time series well. The absolute model error of the predicted soil moisture content is relative small (2.2 – 3.5 % volumetric soil moisture content) during the calibration as well as validation periods compared with the validation results of the empirical models (table 6.3).

The error increases on average 13 % from the calibration to the validation period. This is entirely the effect of the model results in the first layer, which is the most fickle in its behaviour. The second layer has only limited model error increase. This shows that the Beline unsaturated zone model gives a good description of the unsaturated zone system at the Beline slope and has good predictive value.

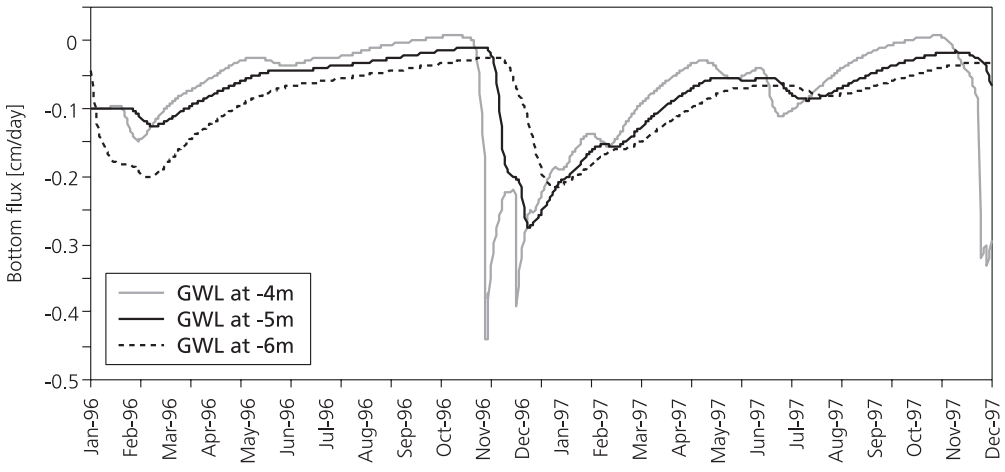

Figure 6.8 Model results of the bottom flux of the Beline model as a function of the ground water level.

Figure 6.8 shows the calculated lower boundary flux for the three different lower boundary conditions, i.e. the defined constant ground water levels. The maximum flux is diminished in case of lower ground water level and shifted forward in time. Analysis of the upper boundary flux – the atmospheric condition – showed that all precipitation infiltrated, whereas almost all evapotranspiration could exfiltrate the Beline model. This is the effect of modelling on a daily time basis. All precipitation is evenly distributed over 24 hours, resulting in a very low rainfall intensity. This is thought to be an acceptable assumption because the analysis of the rainfall intensity in chapter 4 showed that rainfall intensities are rather low near the study site.

6.3.4 The effect of changes in input variables on ground water recharge

One of the main reasons for using a numerical model is to quantify the effect of system changes. In the case of the Beline unsaturated zone model, it is interesting to know the increase or decrease of ground water recharge after (large scale) meteorological boundary conditions changes. Changes is upper boundary condition can be the result of a prolonged wetter period than average, or be the result of structural climate change or be the effects of changes in land use.

In climate change research a mean annual temperature increase in the next century is foreseen. How this translate into changes in precipitation and evapotranspiration is very uncertain and under intensive study in climate change research. As an example, the POPSICLE-project (Kilsby et al., 1998) calculated the precipitation change for a spatial homogeneous warming for several points in western-Europe. Precipitation increases with 2.5-5 % per °C warming, with both summer and winter periods have increased precipitation.

The effects of land use changes are also very difficult to quantify. An increase in evapotranspiration is foreseen when forest should replace the current grass land use. Also interception will increase. At the same time land use change could change infiltration capacity and thus facilitating infiltration. The qualitative, net effect can often be determined, but the quantification of a change will remain highly disputable.

Because all the uncertainties in climate change scenarios and effects of land use changes, the choice was made to study the effect of changes in meteorological regime with a sensitivity analysis. Table 6.9 gives the scenarios that were calculated.

Figure 6.9 shows the relative change in ground water recharge (the bottom flux of the Beline model) as a result of changes in input parameter. The relative change was calculated by comparing the cumulative bottom flux of the scenario model with the calibrated model with ground water at 5 m below surface (figure 6.8). Changes in precipitation have slightly more effect than changes in potential evapotranspiration. This is shown as both precipitation and potential evapotranspiration decrease with the same percentage. A decrease of potential evapotranspiration has a relatively large effect on the ground water recharge. A 20 % decrease of potential evapotranspiration results in a 45 % increase in ground water recharge. Vice versa, the effect diminishes because in case of a high potential evapotranspiration and a low available soil moisture, the actual evapotranspiration is limited. However, the influence of increase and decrease in precipitation on the ground water recharge remains very large as is shown in figure 6.9.

Table 6.9 Scenario definitions for the Beline unsaturated zone modelling. P = change in precipitation, PET = change in potential evapotranspiration.

Name	Scen1 %	Scen2 %	Scen3 %	Scen4 %	Scen5 %	Scen6 %	Scen7 %	Scen8 %
P	0	0	0	0	-10	-20	+10	+20
PET	-10	-20	+10	+20	0	0	0	0

Name	Scen9 %	Scen10 %	Scen11 %	Scen12 %	Scen13 %	Scen14 %	Scen15 %	Scen16 %
P	-10	-20	+10	+20	+10	+20	-10	-20
PET	-10	-20	+10	+20	-10	-20	+10	+20

Figure 6.10 shows the effect of precipitation increase and potential evapotranspiration decrease and vice versa. If precipitation would increase with 20 % and at the same time potential evapotranspiration would decrease 20 %, the Beline slope would undergo a doubled ground water recharge. The opposite would reduce the ground water recharge with 'just' 60 % while the limited soil moisture availability would reduce actual evapotranspiration.

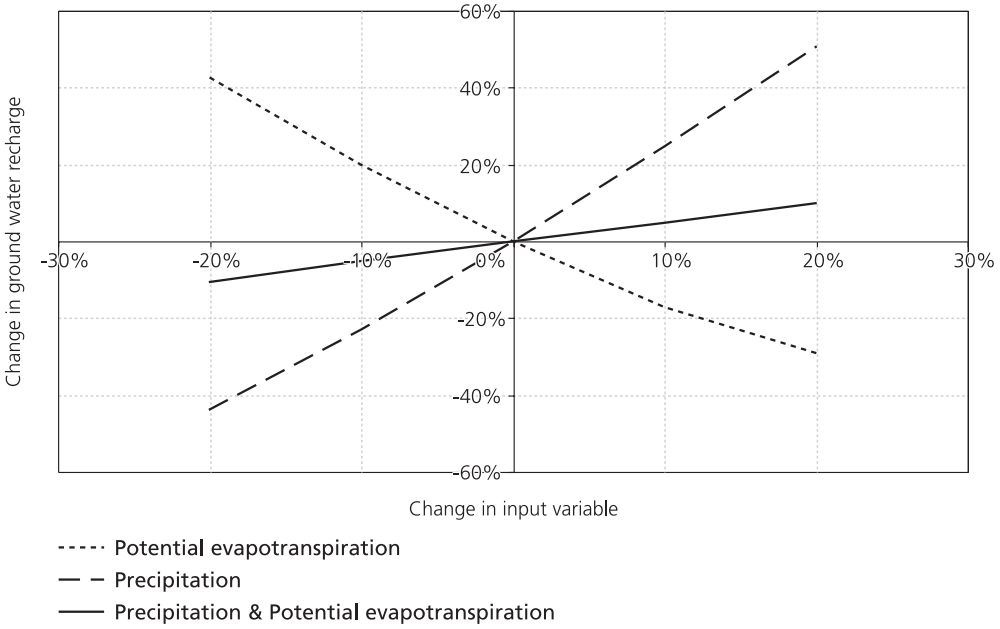

Figure 6.9 Relative effect of input changes on the change in ground water recharge (=increase in cumulative recharge compared to the situation of figure 6.8 for ground water at 5 m).

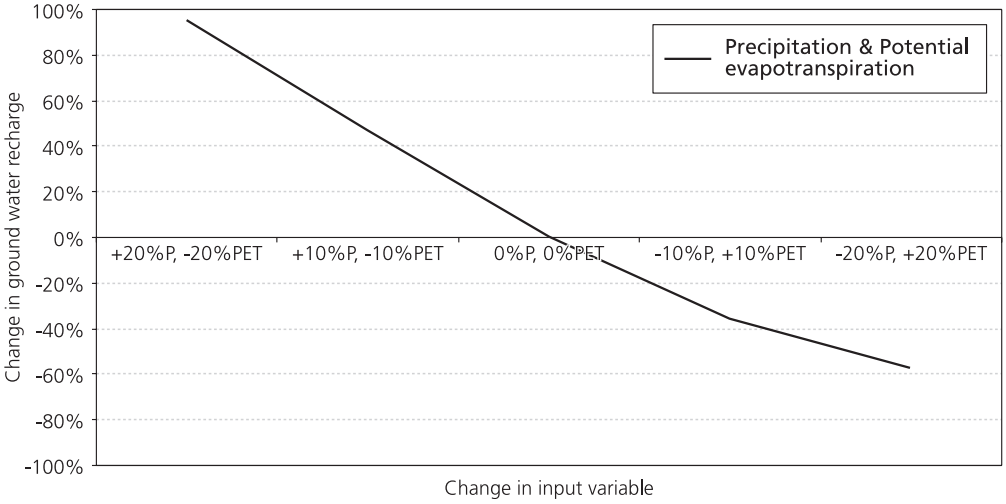

Figure 6.10 Relative effect of the combination of input changes on the change in ground water recharge.

6.3.5 Discussion and conclusions of the physically-based unsaturated zone model

The analyses that are described so far work with the assumption of a matric flow environment. It does not incorporate preferential flow. This assumption can be defended for the model presented here, as it only describes the soil moisture content. This model is not calibrated against the ground water level fluctuations. Already with matric flow the modelled soil moisture content shows more dynamics than the observed soil moisture time series.

The Beline model functions very well in describing the soil moisture distribution for the first meter of the unsaturated zone, also in the validation period. The model is stable and follows the soil moisture measurement. The bottom flux will be used as ground water recharge upper boundary condition in a saturated zone model.

It was shown that the saturated and unsaturated zone are decoupled, meaning that the ground water level fluctuations do only very limited influence the unsaturated zone model. Ground water level differences of 1 or 2 m do, however, affect the behaviour of the bottom flux (amplitude and timing).

The model shows that the unsaturated zone plays a major and decisive role in transferring the water to the ground water system or keeping it away from it. Only in case of a very moist unsaturated zone environment will the transfer of water result in a ground water level rise. This is in good agreement with the conclusions of chapter 5 (figure 5.17).

Changes in input variables have a large influence on the ground water recharge. A decrease in PET with 10 % or increase in P with 10 % results in a 20-25 % increase in ground water recharge. The effect of an increase in PET on the ground water recharge is limited because the soil moisture deficit will limit the actual evapotranspiration. Of course vegetation will suffer water stress in this situation.

The Beline 1D unsaturated zone model is not capable of calculating ground water level fluctuations. This is a major disadvantage of 1D unsaturated zone modelling.

6.4 Discussion and conclusions of the unsaturated zone modelling

The aims of this chapter were given in the first paragraph and can be summarised with the question: Are we capable of quantifying the hydrological behaviour of the Beline unsaturated zone with deterministic models and what is the predictive value? Both a set of empirical models was defined and a physically-based model was built with the Hydrus1D computer code (Simunek, et al, 1998). The empirical models used effective precipitation and standardised soil moisture time series as input and tried to describe and predict the ground water level fluctuations. The physically-based model used precipitation and potential evapotranspiration to describe and predict the soil moisture content and subsequently the unsaturated zone water flux or ground water recharge of the Beline slope. One year of calibration data was used, ground water level data for the empirical models and soil moisture content for the physically-based model.

The linear empirical models were 'trained' on one year of ground water level data. The model performance in the validation period was very variable. None of the proposed eight linear empirical models showed a RMSE during the validation period that was less than 25 % higher than during calibration for all ground water time series (table 6.3). Fitting these models on all available ground water data did in most cases not improve the model performance. Assuming that a validation is a good measure for the predictive value of a model, it is concluded that none of the linear empirical models can be used for effect calculations.

However, the linear empirical models were very useful in analysing the hydrological time series. They showed that precipitation has only a very limited contribution to ground water level fluctuations. The soil moisture content seemed a much better predictor for that. This is in good agreement with the finding in chapter 5 (figure 5.17).

The physically-based model was calibrated against soil moisture content using an inverse modelling procedure. The calibration data set of one year was short and resulted in a non-unique set of parameter values, which were highly correlated. The inverse modelling learnt that the ground water level fluctuations (decimetre scale) had no impact on the unsaturated zone water transport. Even the influence of the absolute depth of the ground water could vary between 3 and 6 m and showed only limited effect on the unsaturated zone dynamics. The latter did influence, however, the behaviour of the unsaturated zone water flux or ground water recharge, i.e. the timing and amplitude of the water flux. On basis of the correlogram and the sensitivity analysis on the inverse model, the ground water depth was set constant and the n-values from the Van Genuchten Mualem model were fixed at the values resulting from the first inverse model run.

The validation of the Beline unsaturated zone model showed the model to be very robust. This model can be used for quantification of changes in the hydrological system. Changes in the input time series were addressed with a sensitivity analysis. A two year wetting scenario (10 % more precipitation or 10 % less evapotranspiration) results in a more than doubled ground water recharge in that period. When precipitation and evapotranspiration both increase 20 %, it is shown that ground water recharge increases 10 %. With changes in input variables over a time frame of two years the effect of wetting is much more problematic than of drying. This is explained by the condition that all precipitation can infiltrate (low rainfall intensities) and that actual evapotranspiration is limited by the availability of soil moisture in the upper part of the soil.

The last conclusion of the unsaturated zone modelling is that both type of models were not capable of describing the ground water level time series. The fitting period was to short for the empirical models to result in a reliable description of the ground water level fluctuations. The 1D physically-based model can only model ground water level fluctuation with a lower Cauchy boundary condition, which describes the relationship between hydraulic head and bottom flux. Because this relationship is normally not known, a 1D model will not be able to give ground water levels. For landslide research the behaviour of the pore pressures (ground water) is of utmost importance. A saturated zone model will be presented in the following chapter which will use the ground water recharge fluxes of the Beline unsaturated zone model. Then also the effects of the changes in ground water recharge as result of changes in the input time series will be addressed.

7 THE EFFECTS OF GROUND WATER RECHARGE ON THE HYDROLOGICAL MODELLING OF THE SATURATED ZONE OF THE BELINE SLOPE

7.1 Introduction

To establish the stability of a slope, the pore pressure distribution in the slope has to be known. A 2D groundwater model was made of the Beline slope using the Modflow code (McDonalds and Harbaugh, 1988) of release 1996. To study the effects of land use changes on slope stability, one has to quantify the influence of land use changes on the ground water behaviour, in terms of changes in ground water level fluctuations.

The aims of this chapter are:

- Modelling the spatial distribution of pore water pressure for slope stability calculations
- Finding an effective way to determine ground water recharge using precipitation data and unsaturated zone models
- Quantifying the influence of changes in land use or climate on the hydrological behaviour of the slope by means of ground water recharge modelling

In paragraph 7.2.1 the ground water model is described and its geometry and parameterisation is discussed. The ground water model is calibrated with the ground water level data of D1, D2 and D3 of 1996 and is validated with the 1997 data set (§ 7.2.2). The ground water model is tested on its capability to model ground water level fluctuations using hypothetical recharge time series. Then the focus shifts to the estimation of the recharge time series. In general, there is a focus on the schematisation and parameterisation of ground water models while limited attention is paid to the input variable: the recharge time series. These are constructed by means of the bottom flux of the unsaturated zone hydrological model and precipitation series (§ 7.2). To incorporate preferential flow, a methodology is proposed where recharge time series are constructed using a combination of soil moisture content and precipitation (§ 7.3). In paragraph 7.4 the influence of land use change scenarios on the hydrological behaviour of the Beline slope is quantified. The chapter finishes with a summary and discussion in which the aims of this chapter are evaluated.

7.2 The Beline saturated zone model

7.2.1 Model description and parameterisation

In the Hycosi project (Leroi, 1997), several ground water models have been reviewed (van Esch, 1995). This study showed the Modflow software to be one of most suitable hydrological software packages for describing pore pressure fluctuations in slopes. Modflow has been developed by the USGS (McDonald and Harbaugh, 1988) and is one of the most commonly used ground water models in the world. The physical part of the Modflow ground water modelling software is capable of modelling both steady-state and transient conditions in two and three dimensions and includes heterogeneity and

anisotropy of the subsurface layers. The model needs a pre- and postprocessor to help with input and output of the model. The widespread use of the Modflow software has the advantage that a large number of additional software is available, the so-called graphical user interfaces (GUI's). In this study the PMWIN software (Chiang and Kinzelbach, 1996) is used as a pre- and post-processor. The PMWIN software also supports the automatic calibration program PEST (Doherty et al, 1994). Also the Excel spreadsheet software is used for both pre- and post-processing of the data.

The Beline model uses the digitised 1:25.000 IGN topographical map of the Salins-les-Bains region with a 25 by 25 m^2 discretisation as the digital elevation model of the surface. The 2D model is a SW-NE orientated transect along the steepest gradient of the slope with a cell length of 25 m (figure 7.1). The surface elevation was interpolated from the digital elevation model of the Beline slope. Along this transect three pore pressure measurement sites are located: D1, D2 and D3 (figure 7.1). The model covers an area, which extends from the river La Furieuse till the plateau of Clucy (see also chapter 4). The part southwest of the river La Furieuse was excluded from the Modflow model as was the plateau of Clucy.

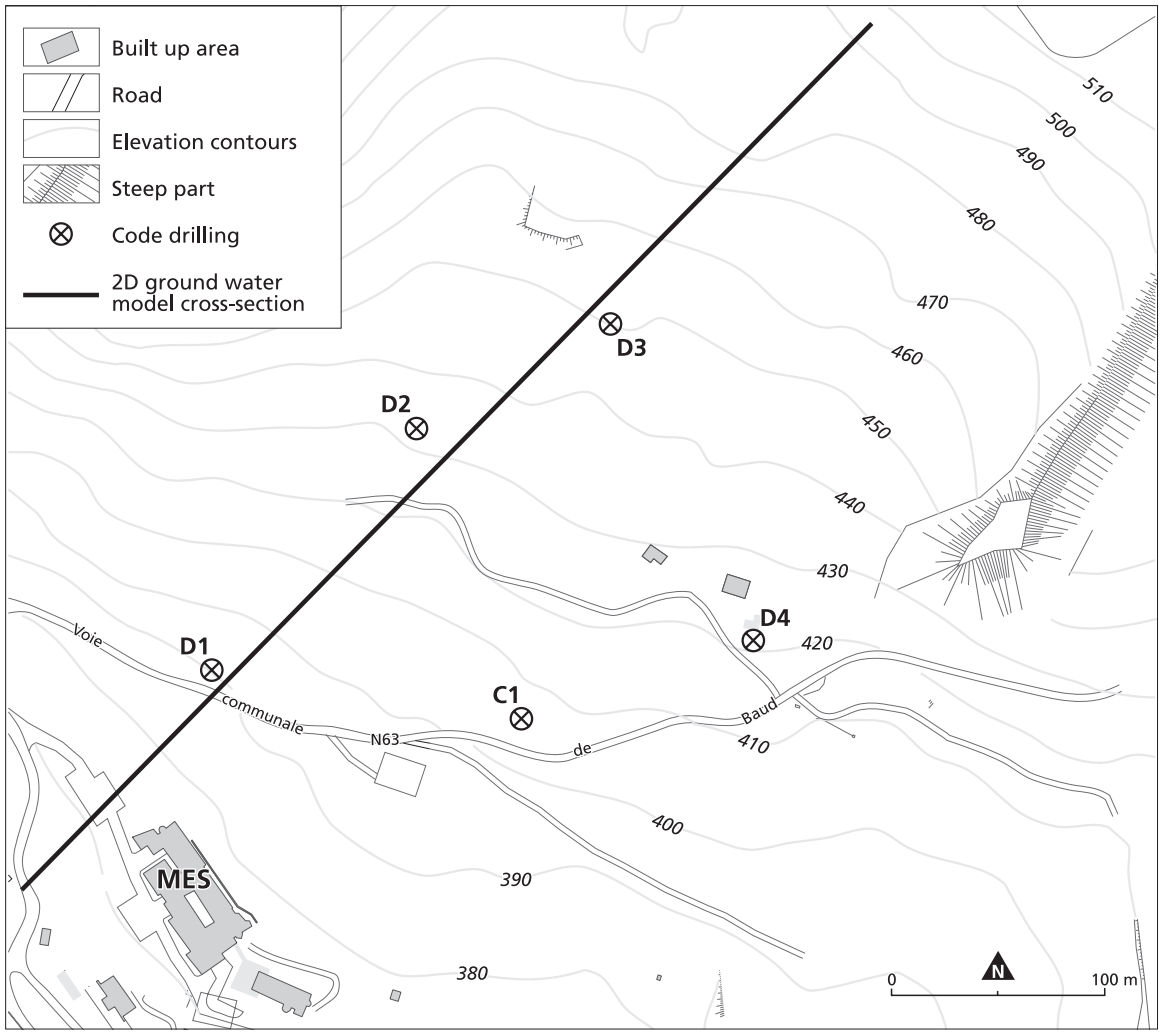

Figure 7.1 Overview of the observation sites and a 2D ground water model cross-section at the Beline slope, Salins-les-Bains, France (see also figure 4.8).

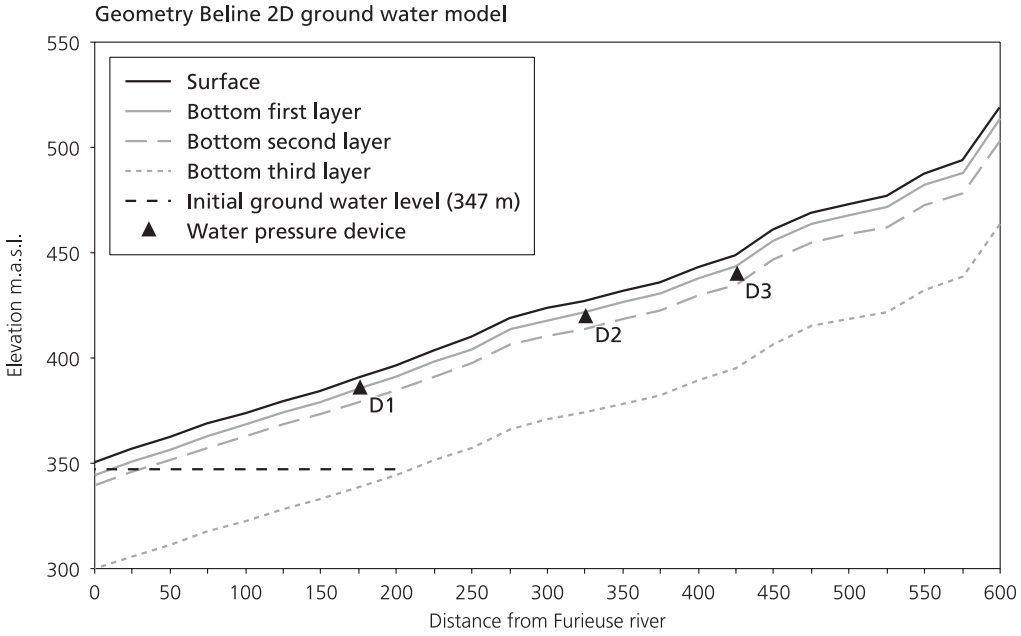

Figure 7.2 Geometry of the 2D Beline ground water model and the initial, horizontal, ground water setting.

The hydrological model schematisation (figure 7.2) was derived from the geological schematisation as presented in chapter 4. Three layers were identified using borehole information, drilling progress and geophysical surveys:

- a disturbed surface layer, with relatively low bulk density and abundant gravel content and with an average thickness of 5 m;
- a zone of remoulded marls with silty layers, a variable gravel content, an average bulk density and a variation in thickness of 5 m at the bottom of the slope to more than 10 m in the upper part of the slope;
- compact, blue marls, with generally no gravel, but with some limestone fragment concentrations.

The Beline ground water model was built up with these 3 layers only. Instead of the often used horizontal cell geometry with inclined definition of hydrological parameters (like saturated permeability), here the layers have variable elevation definition such that they coincide better with the slope parallel layering. The saturated permeability values of these layers decrease from the surface downwards. The saturated permeability was determined to be on average 0.129 m/d between 40 cm and 1.5 m below surface (see chapter 6). No saturated permeabilities could be obtained from the deeper lithologies. Table 7.1 gives an overview of the initial hydrological model parameters.

The surface was modelled using the drainage package of Modflow. By defining drains in the upper layer near the surface (20 cm below surface) with a high conductance, exfiltration of ground water was modelled. With the drain option water can exfiltrate but not re-infiltrate, so it is withdrawn from the hydrological process. The main advantage of the drain option for surface modelling over other options, like modelling air as a very permeable layer, is its numerical stability. Main disadvantage is the irreversible loss of

Table 7.1 Initial values of the hydrological parameters of the Beline ground water model.

	Thickness [m]	Saturated Permeability [m/day]	Specific Yield [-]	Specific Storage [1/m]
Layer 1	5	0.129	0.25	0.001
Layer 2	5 to 10	0.0129	0.2	0.001
layer 3	40	0.00129	0.2	0.001

the seepage water. Re-infiltration, however, has never been observed on the Beline slope. The seepage that was found at the Beline site, was drained in the local sewage system. The average ground water recharge (upper boundary flux) was set at 0.75 mm/day, equal to the average bottom flux in the unsaturated zone model (chapter 6).

Analysis during the construction of the model learned that the horizontal and vertical discretisation (subdivision of a layer into more model layers with the same parameterisation) did not influence the model outcome. However, for the transmissivity of the layers the model is very sensitive. In this model approach the thickness of the layers was fixed and the saturated permeability was calibrated.

7.2.2 Model calibration and validation

The calibration of the ground water model was carried out in two steps. First, the calibration consists of modelling the steady-state ground water level using a transient ground water model with constant upper boundary flux. This first calibration phase leads to a set of permeability values for the three layers of the Beline slope and initial ground water levels for the second part of the calibration. The second calibration phase of the Beline ground water model was to tune the ground water fluctuations by adjusting the porosity related parameters.

The calibration was performed using the ground water level measurements of water pressure devices D1, D2 and D3. As described earlier, the average ground water level at D1 was 3.5 m, at D2 6.5 m and at D3 4.2 m below surface (figure 7.3). The final and steady-state ground water level will be used as initial values for the modelling of the measured ground water level fluctuations.

The calibration starts with an initial, horizontal ground water level equal to the river Furieuse (347 m, see figure 7.2), and stops when the model reaches a steady-state ground water level. Using the average recharge flux of 0.75 mm/day, saturated permeability values of 0.4 m/d for the first layer, 0.1 m/d for the second layer and 0.0075 m/d for the third and lowest layer were found, by method of trial and error. The calculated ground water level provides an average for the three observation points (figure 7.3). After the trial and error calibration the measured and modelled ground water depth are respectively 3.5 m and 3.6 m below surface for observation point D1, 6.4 m and 2.2 m below surface for D2 and 4.1 m and 8.0 m below surface for observation point D3. This parameterisation of the saturated permeability is not a unique solution. However, equivalent ground water levels can be obtained only when the saturated permeabilities do not deviate more than 25 % of the ones described above with the given schematisation and average recharge flux.

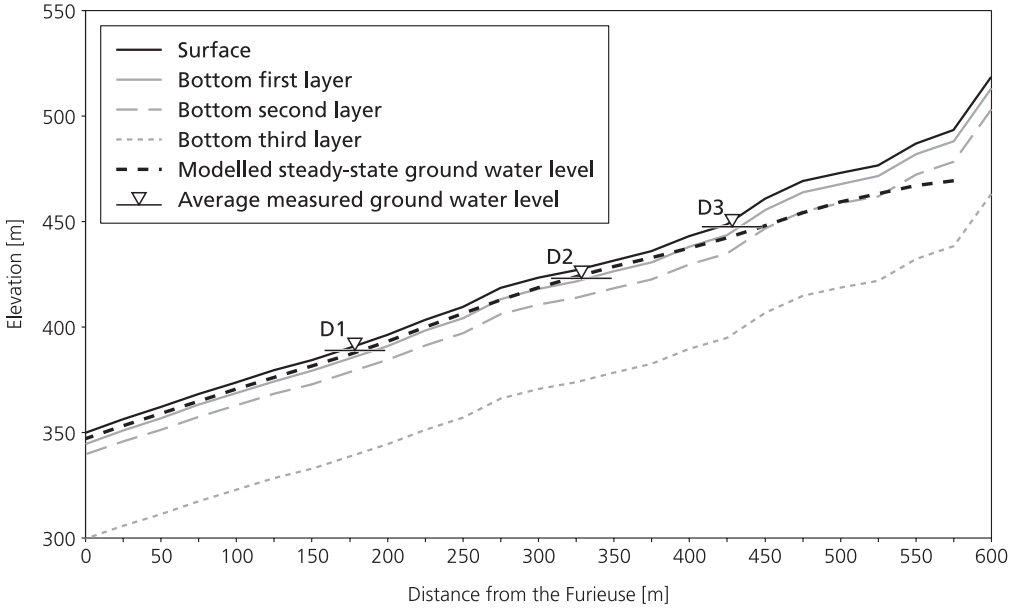

Figure 7.3 Modelled and measured steady-state ground water level at the Beline slope.

These large differences at D2 and D3 have several reasons. First of all, the result of the coarse interpolation of the surface height, which is caused by the 25*25 m2, cells. On a small scale, large topographical differences exist at the Beline slope. Secondly, a ground water level error of a few meters is a relatively small error compared to the level change along the slope. Thirdly, there is the aspect of the uncomplicated subsurface schematisation of three continuous layers that results in a smooth water table whereas small-scale heterogeneity has important influence on the local ground water table.

The model's capability to model ground water level fluctuations was then tested with a hypothetical recharge fluctuation (table 7.2). After reaching a steady-state ground water level, 25 stress periods (model time periods in which the values of the input parameters do not change) of one year followed in which the recharge fluctuates between 0.53 mm/day (30 % decrease) and 0.98 mm/day (30 % increase) in steps of 10 % per model stress period. After this the model continues with monthly stress periods in which the recharge also fluctuates in steps of 10 %. The model run ends with a stress period in which the average recharge flux (0.75 mm/day) is used again to check the numerical stability of the ground water model.

Figure 7.4 shows the results of this model run for the three observation boreholes D1, D2 and D3. The results show that the Beline ground water model is capable of modelling transient recharge fluxes, both for longer and shorter stress periods. The final heads are used as initial ground water heads in further analysis.

Table 7.2 List of the stress periods with hypothetical recharge values to test the Beline ground water model on its capability to model ground water level fluctuations.

Stress Period	Period length [Days]	Recharge [mm/day]	Remarks
1	20000	0.75	Initiation
2	20000	0.75	
3	20000	0.75	
4	20000	0.75	
5	360	0.75	Annual fluctuation
6	360	0.75	
7	360	0.75	
8	360	0.68	
9	360	0.6	
10	360	0.53	
11	360	0.6	
12	360	0.68	
13	360	0.75	
14	360	0.83	
15	360	0.9	
16	360	0.98	
17	360	0.9	
18	360	0.83	
19	360	0.75	
20	360	0.68	
…		…	
30	360	0.83	
31	30	0.75	Monthly fluctuation
32	30	0.68	
…		…	
599	30	0.6	
600	30	0.68	
601	10000	0.75	Final average recharge

In the first calibration phase the saturated permeability of the three layers was adjusted. In the second calibration phase the ground water level fluctuation was calibrated by adjusting porosity related parameters (specific yield and specific storage). The 1996 ground water level data of D1 and D2 were used for calibration. The validation data set consists of the ground water level data of 1997.

As recharge input, the ground water model uses the time dependent bottom flux of the Beline unsaturated zone model (chapter 6). This bottom flux of the unsaturated zone model depends slightly on the ground water depth. For reasons of conciseness and clarity, only the bottom fluxes that result from calculation of the unsaturated zone model with the ground water level defined at 4 m below surface are used (see chapter 6). As calibration criteria, the RMSE and the ground water fluctuation range were chosen.

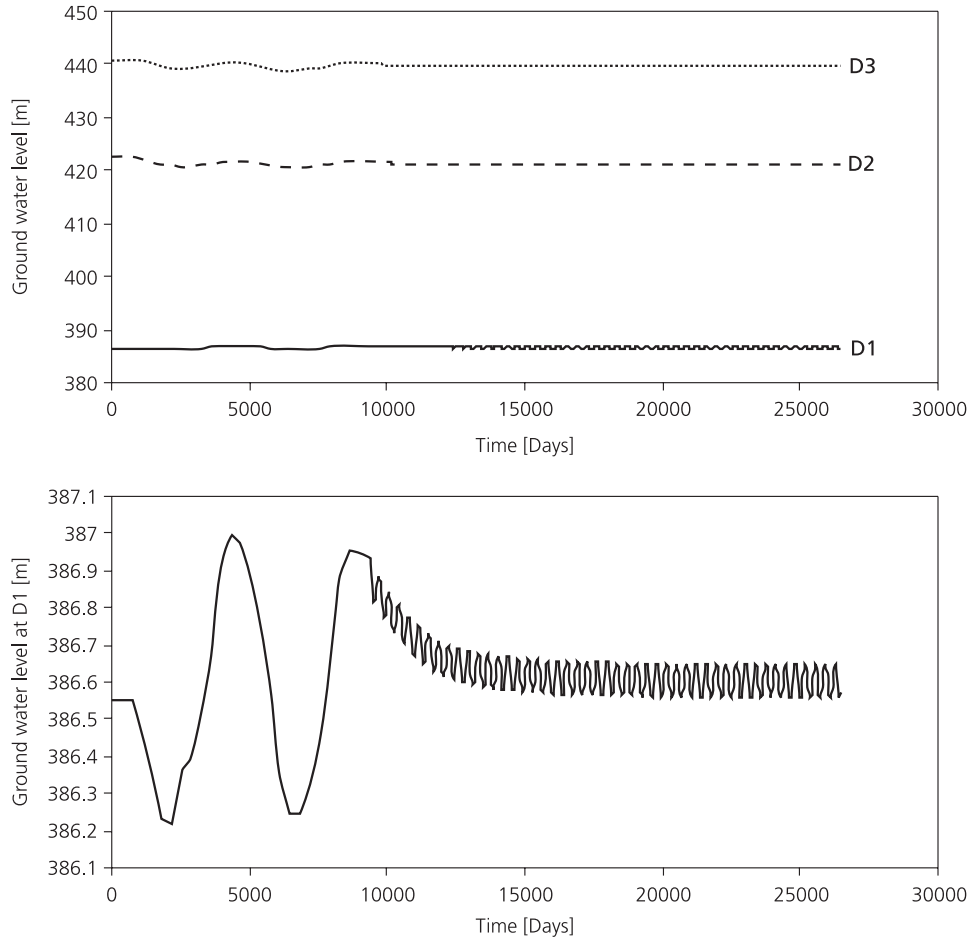

Figure 7.4 Results of modelled ground water level fluctuation (stress period 5-600 from table 7.2) in observation points D1, D2 and D3 (above) and in D1 (detail below) using hypothetically fluctuating long and short term recharge series.

Table 7.3 The final hydrological parameter setting of the 2D Beline ground water model after calibration. The ground water model uses the ground water recharge series from the unsaturated zone model with ground water at 4 m below surface as input series.

	Thickness [m]	Saturated Permeability [m/day]	Specific Yield [-]	Specific Storage [1/m]
Layer 1	5	0.4	0.375	0.0075
Layer 2	5 to 10	0.1	0.325	0.0075
Layer 3	40	0.0075	0.2	0.0075

Figure 7.5 shows the modelled and measured ground water level for 1996 and 1997 for observation points D1 and D2. The fluctuations are plotted against the average ground water level of 1996. The corresponding values of the calibrated porosity related parameters are given in table 7.3. The modelled range of ground water level fluctuation corresponds well with the measurements. The timing of the ground water level maximum

and minimum is not represented, especially in the calibration year 1996. Only the high ground water level in summer 1997 in observation point D1 is well represented. The ground water model fails to represent the individual maxima and minima for observation point D2. Also the velocity of ground water level fall and rise does not match the measurements. Remarkably, the validation period (1997) seems to fit field measurements better than the calibration period (1996).

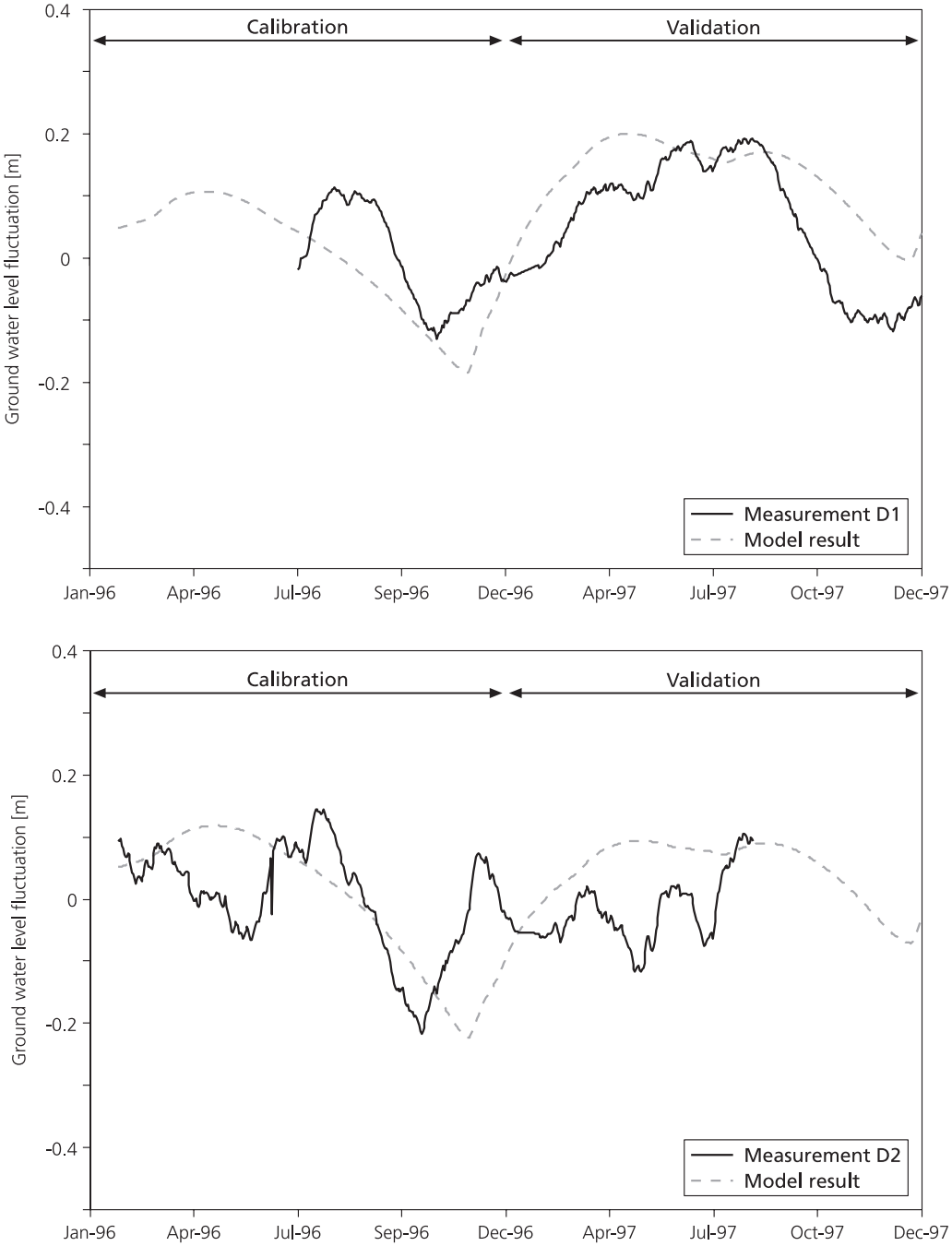

Figure 7.5 Results of the ground water modelling at the Beline slope for 1996 (calibration) and 1997 (validation) for two recharge time series. The model run used the bottom flux of the unsaturated zone with a ground water table at 4 m below surface as ground water recharge.

Table 7.4 The RMSE values and the range of ground water level fluctuations, both measured and modelled for the calibration (SC, 1996) and validation (SV, 1997) of the Beline ground water model.

		D1		D2	
		RMSE [m]	Range [a)] [m]	RMSE [m]	Range [a)] [m]
Measured	1996-1997		0.322		0.361
Modelled	SC (1996)	0.083		0.100	
	SV (1997)	0.091	0.385	0.098	0.342

[a]) The range was determined over 1996 and 1997.

The RMSE values are given in table 7.4. Statistic objective functions like RMSE to quantify the goodness of fit between measured and modelled time series are very sensitive for phase shifts of the peak values. This means that if two identical time series are evaluated with a RMSE, while they only differ by a time lag, they will show high RMSE values. Figure 7.5 shows such a shift in peak timing. Therefore especially the range of fluctuations was used as calibration criterion. The RMSE does, however, show that the model performs likewise in the validation and calibration periods.

Although the model represents the general trend of the ground water dynamics, the short-term fast dynamics are not modelled. The explanation for the lack of modelled dynamics and the difficult timing is not hidden in the ground water model (schematisation, parameterisation) but in the relatively smooth recharge time series, which equals the bottom flux of the unsaturated zone model. Figure 7.6 relates the bottom flux of the unsaturated zone model with the measured and modelled ground water results.

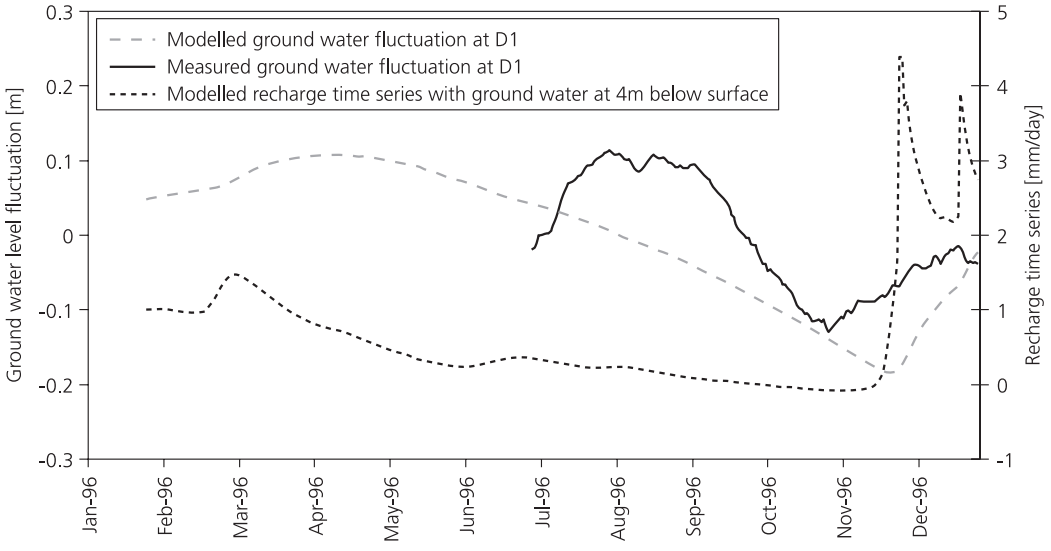

Figure 7.6 Comparison of modelled and measured ground water level at D1 with the recharge time series.

Figure 7.6 learns that the modelled ground water level fluctuations react directly on the recharge input series. The unsaturated zone model retains and thus attenuates the ground water flux considerably but represents the (seasonal) amplitude of the fluctuations reasonably well. The reason for this is that only matric flow was incorporated and that any kind of preferential flow was ignored. Figures 7.5 and 7.6 indicate that the ground water model is calibrated as well as possible with the available data and that the input series need more refinement. The results lead to the question whether there are more suitable recharge time series like the direct use of the precipitation time series.

7.2.3 Precipitation as recharge series

Not all precipitation is converted to ground water recharge. Most of the precipitation is buffered in the unsaturated zone and evapotranspiration will take away most of that water. In the Beline area the precipitation was on average 3.1 mm/day. The ground water system was calibrated while receiving on average 0.75 mm/day, equal to 24 % of the total precipitation. If only precipitation is used as recharge series, one has to multiply the daily precipitation with 0.24 to obtain the recharge series. The same parameter configuration was used as was given earlier in table 7.3. So no additional calibration of the porosity related parameters was carried out.

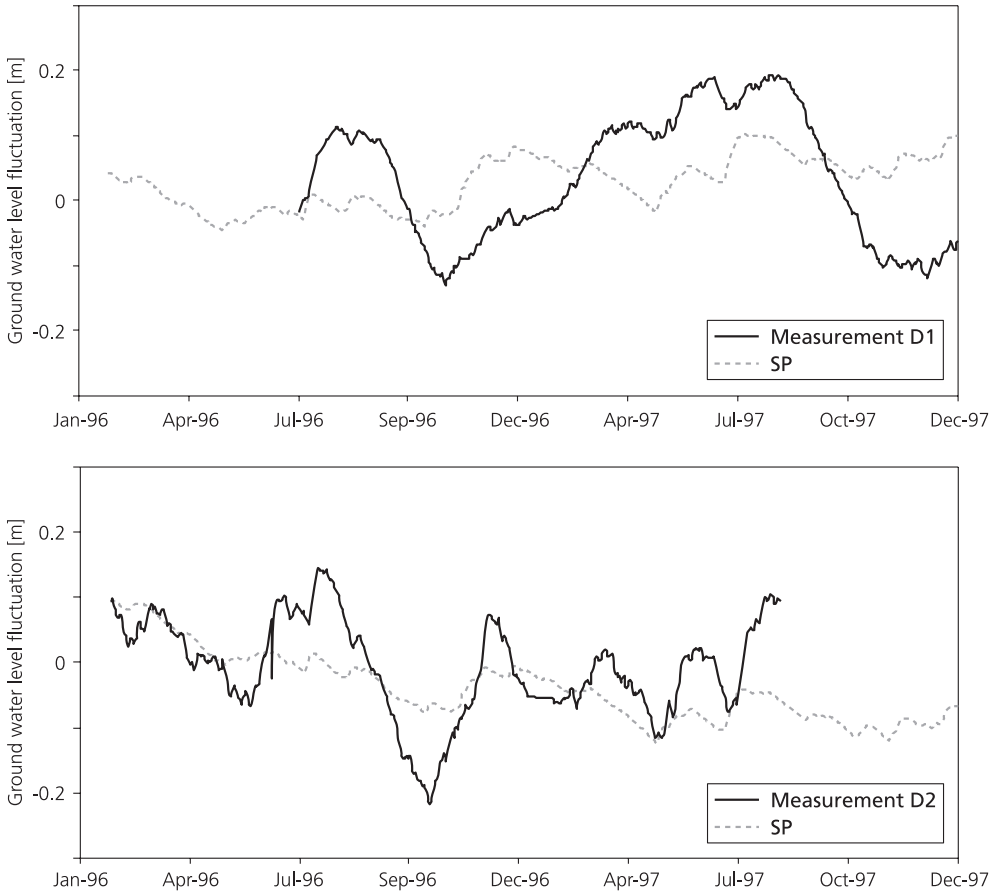

Figure 7.7 Ground water level modelling results using a fraction of the daily precipitation data as recharge series (SP) for observation sites D1 and D2.

Figure 7.7 shows the model results of observation point D1 and D2. The modelled range of the ground water level fluctuations is much smaller than the measurements. However, the timing of the individual peaks is represented better than in figure 7.5. Especially for observation point D2 the results have improved. This suggests that at least a part of the ground water level fluctuations observed in D2 is the result of the direct influence of precipitation. In the D1 case, the general trend of the ground water level fluctuations is modelled well by the unsaturated zone flux as input data (figure 7.5), but the second order fluctuations of D1 are reflected better by the ground water model with direct precipitation input. Additional calibration of the porosity related parameters only resulted in a slightly higher amplitude of the modelled fluctuations when the values of these parameters outranged their normal values.

The model runs can be interpreted as follows. In addition to matric flow through the unsaturated zone, also direct influence of precipitation on the ground water level takes place (see also chapter 5). Ground water modelling using only a constant fraction of the precipitation time series as recharge series does not lead to the desired results because it does not represent the seasonal fluctuations of the unsaturated zone behaviour.

7.3 State dependent recharge

As described in section 2.5, in the subsurface especially seasonal and some short-term ground water reactions takes place on precipitation. The seasonality in the recharge comes from the state in which the unsaturated zone is. The 'state' of the unsaturated zone refers to the moisture condition in which the soil is. The state-dependency on ground water recharge of the unsaturated zone involves that after dry periods significant amounts of water can be stored in the unsaturated zone and after prolonged wet periods the storage capacity is limited. It is only after the soil is saturated that preferential flow actually transports water downwards (see e.g. Van Asch et al, 2001).

The main consequence for the modelling of ground water level fluctuations is that the recharge time series should be based on state-dependent preferential flow. How to combine matric and preferential flow in one input time series for a ground water model without introducing additional parameters and thus additional uncertainty?

The bottom flux of the unsaturated zone model (chapter 6) is a good indicator whether unsaturated or near-saturated conditions prevail in the upper subsurface. In the case of no downward flux (dry conditions), precipitation is likely to be stored more easily in the unsaturated zone and ground water recharge will be limited. In the case of a large downward flux (wet conditions), a large fraction of the precipitation is likely to recharge the ground water system. At the same time, it should be taken into account that the hydrological model has calibrated the (unknown) saturated permeability values of the subsurface, using a daily average recharge flux of 0.75 mm.

The following conditions are respected when modelling with state-dependent recharge: 1) the average (annual) recharge flux should remain unchanged, and 2) recharge should be derived directly from precipitation but also as a function of the state of the unsaturated zone.

So it is proposed to define the recharge time series as:

$$R_t = \frac{v_t}{\bar{v}} \cdot f \cdot P_t \tag{7.1}$$

R_t = Recharge time series at time t
v_t = Bottom flux of the unsaturated zone at time t
$\bar{v}$ = Average (annual) bottom flux unsaturated zone
f = Optimalisation factor, or factor of proportionality
P_t = Precipitation at time t

The f-factor has to be introduced to ensure that the water balance of the unsaturated zone is correct. In other words, the f-factor ensures that the sum of the unsaturated bottom flux (Σv_t) equals the sum of the newly calculated recharge (ΣR_t).

f is defined as:

$$f = \frac{\sum_{t_1}^{t_n} v_t}{\sum_{t_1}^{t_n} \left(\frac{v_t}{\bar{v}} \cdot P_t \right)} = \frac{\sum_{t_1}^{t_n} R_t}{\sum_{t_1}^{t_n} \left(\frac{v_t}{\bar{v}} \cdot P_t \right)} \tag{7.2}$$

The proposed equation for calculating the state-dependent recharge also has to be restrained to prevent the recharge (R_t) from exceeding the precipitation (P_t). Otherwise, in case of a relatively wet unsaturated zone ($f^*(v_t/v_{avg}) > 1$), more recharge could be calculated than has been fallen.

$$\text{IF } R_t \geq P_t \text{ THEN } R_t = P_t \tag{7.3}$$

Given the precipitation and unsaturated zone model bottom flux time series, the recharge time series (R_t) and the f-factor can easily be determined iteratively in a spreadsheet model. Figure 7.8 shows the results of the model run with the 'state-dependent recharge function'. The ground water model has not been calibrated with this recharge option, and uses the parameter settings as given in table 7.3. The ground water model represents the measurements in observation points D1 and D2 better than in figure 7.5, where the ground water level fluctuations are modelled with a fluent line. Figure 7.8 shows model results, which depict both the seasonal effects and the direct influence of precipitation on recharge.

One deficiency of the model results as shown in figure 7.8 is the time delay between the measured and modelled ground water level rise in October - November 1996. Figure 7.9 visualises the calculation of the ground water recharge as a function of the state of theunsaturated zone. The bottom flux time series of the unsaturated zone model with a lower boundary condition of 4 m below surface is shown. It is shown that in October and November 1996 a significant amount of precipitation has to fall before the unsaturated zone reacts, i.e. larger amounts of precipitation are transported to the ground water system.

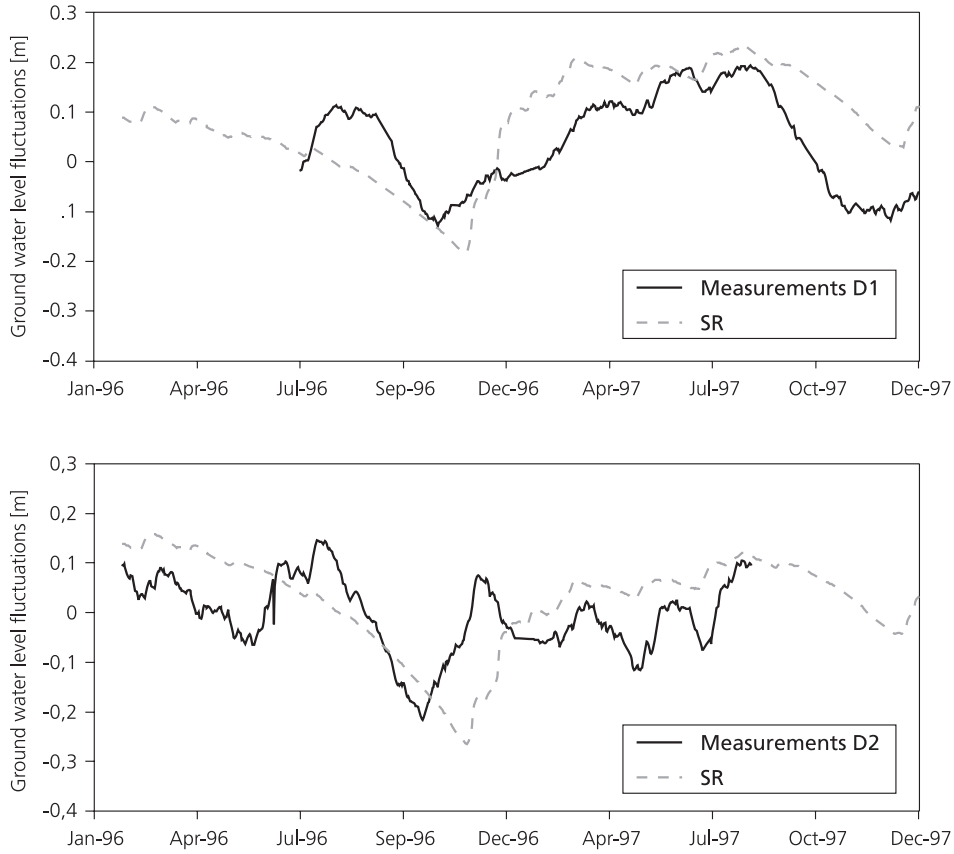

Figure 7.8 Ground water model results using the state-dependent ground water recharge time series (SR) for observation sites D1 and D2.

The time delay is the direct consequence of the fact that v_t – as calculated by the unsaturated zone model in chapter 6 – is near 0 and thus the ground water recharge is near 0. But the ground water observations show earlier reaction on prolonged precipitation. The proposed model to calculate recharge assumes that only limited rainfall can replenish the ground water system when the upper subsurface is not near saturation ($v_t \rightarrow 0$). This assumption does not always have to be true. A particular hydrological system could have some direct contact via (large) preferential flow.

Therefore the proposed equation can be improved easily for this situation in the following way:

$$R_t = \left(f_{dir} + \frac{v_t}{\bar{v}} \cdot f \right) \cdot P_t \qquad (7.4)$$

With f_{dir} being the direct recharge fraction, a constant fraction of the precipitation. $f_{dir}*P_t$ is the amount of precipitation per rain event that is passed directly to the ground water system. Main disadvantage, however, is the introduction of a new -not measurable- parameter.

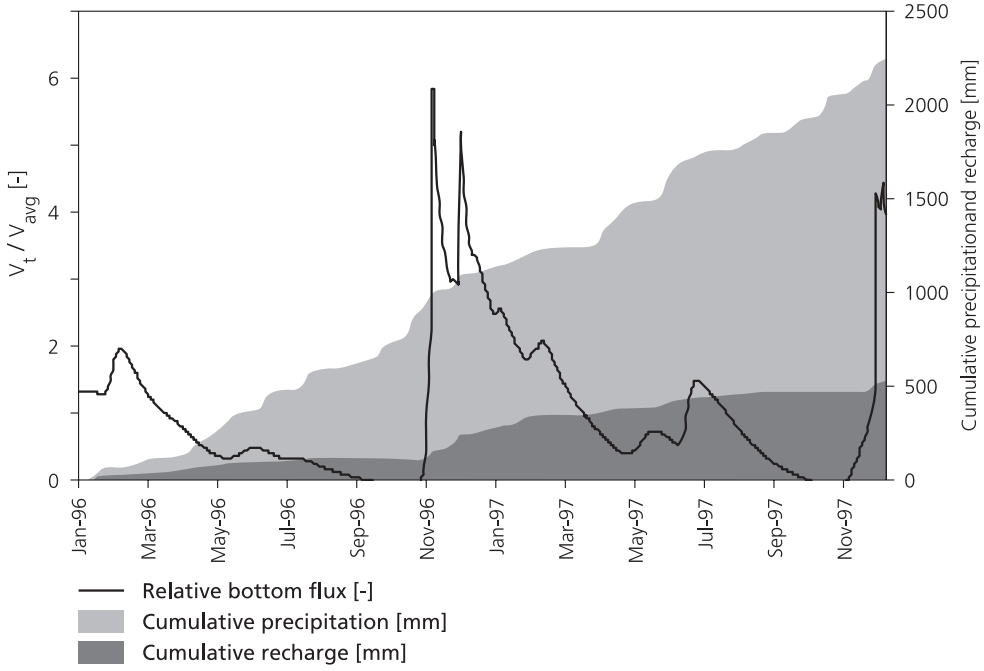

Figure 7.9 Overview of cumulative precipitation and recharge in relation to the relative bottom flux of the unsaturated zone model.

Figure 7.10 shows the results of the ground water modelling with the extended recharge model (SER) together with the results of the recharge model (SR). In general, the graphs have not changed. The ground water level calculations with the SER are a little attenuated. The extended recharge model did not move the modelled ground water level rise forward in time.

Remarks and discussion

It should be stressed that the results given in this paragraph were calculated without additional calibration. This to make the comparison of the effects of the different recharge models easier. As recharge input, the ground water model uses the time dependent bottom flux of the Beline unsaturated zone model (chapter 6). This bottom flux of the unsaturated zone model depends only slightly on the assumption of the ground water depth. For reasons of conciseness and clarity only the bottom fluxes that results from calculation of the unsaturated zone model with a ground water level defined at 4 below surface are presented. The bottom flux of the unsaturated zone model with a lower boundary of ground water at 5 m below surface has also been used as recharge time series in the ground water model. This does not alter the model results and consequently the insight in the hydrological behaviour of the Beline slope.

The model results have improved significantly when using a more realistic recharge input series. Still, the model results as shown in figures 7.8 and 7.10 show that the ground water level fall in dry periods is significantly faster in the measurements than in the model results. One way to overcome this, is to increase the saturated permeability causing the modelled ground water system to drain more rapidly. However, a set of

higher permeabilities needs a proportionally larger average recharge flux. Higher permeability values also result in a less inclined ground water level within the slope, i.e. downslope a larger area will have ground water seepage and upslope the ground water level will be deeper. Also, the calibrated saturated permeabilities are already relatively high considering the silty clay and marly environment. Another solution is to decrease the porosity, but this also leads to a larger, undesired range of ground water level fluctuations. Also a decrease in porosity would reduce the performance of the unsaturated zone model (chapter 6). The fast decline of ground water in dry periods could also come from 3D effects (diverging flowlines) which can not be taken into account in the 2D set-up as used here.

The state-dependent ground water recharge function is not developed for water transport from the ground water to the unsaturated zone (negative R_t). In a clayey slope with a thickness of the unsaturated zone between the 3 and 6 m, in a temperate climate, the unsaturated zone is generally very moist (see e.g. the equivalent soil moisture profiles in figure 6.2). A situation that the hydraulic gradient above the ground water table will be directed upwards, is not likely (see also figure 5.18 with the interpretation of the unsaturated zone behaviour at the Beline slope).

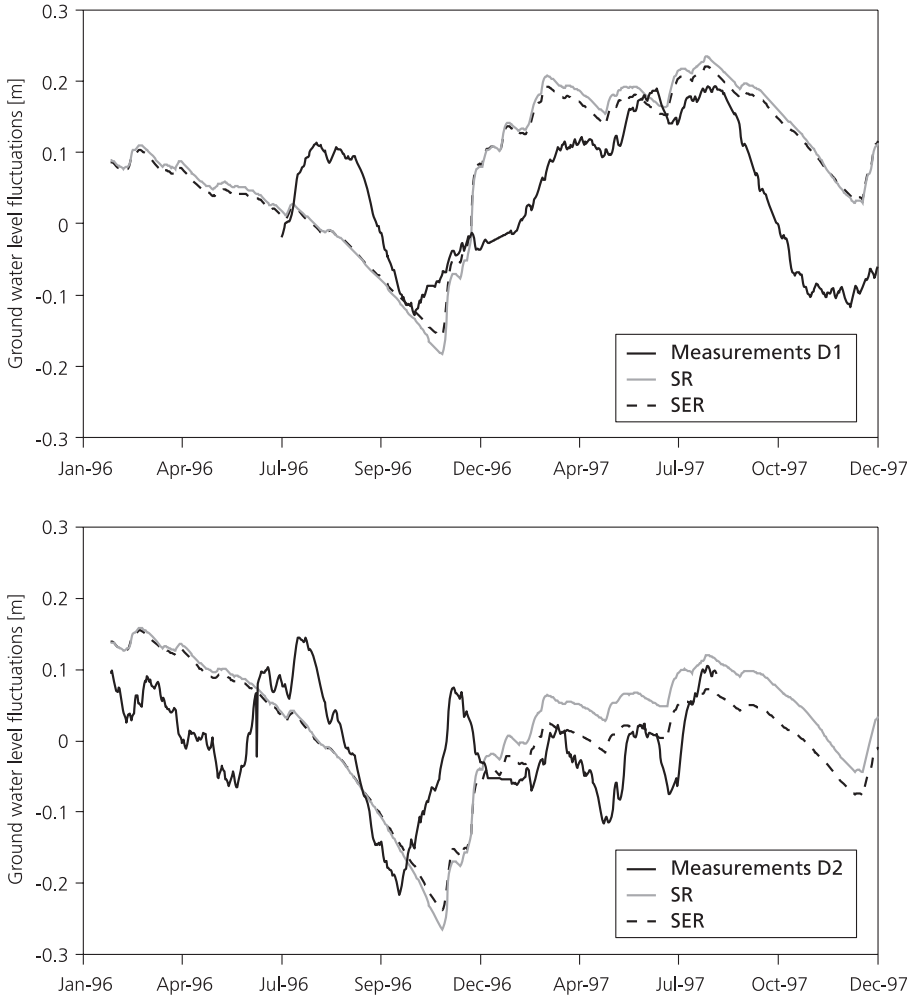

Figure 7.10 Ground water model results using state-dependent recharge time series (SR) and its extended version (SER, with f_{dir}=0.10) for observation sites D1 and D2.

The state-dependent recharge function, as proposed here, assumes the availability of an unsaturated zone model. If this is not so, the state-dependent recharge function can also be approximated with a sinusoidal function (see Bogaard et al, 1998). The recharge function then becomes:

$$R_t = \left[f_{avg} + \alpha \cdot \sin\left(\left(\frac{\text{daynumber} + \text{dayoffset}}{366} \right) \cdot 360 \right) \right] \cdot P_t \qquad (7.5)$$

with:

f_{avg}	= Average recharge fraction
α	= Amplitude recharge fraction
daynumber	= Julian day
dayoffset	= Time delay parameter

The average recharge fraction (f_{avg}) is forced to be larger than the amplitude of the recharge fraction (α), otherwise the recharge function becomes negative during some periods. f_{avg} * P_t equals the average recharge flux that is used to calibrate the ground water model using its steady-state ground water level. The remaining parameters α and 'dayoffset' should be optimised using ground water level measurements.

7.4 A scenario study on the impact of environmental changes on the ground water level

Since the ground water level fluctuations could be modelled well, it is possible to study the effects of changes in the input time series on the ground water system. Changes in land-use and climate can be represented by changes in potential evapotranspiration and fluctuations in precipitation (see also chapter 6). A change in potential evapotranspiration or precipitation (or both) results in a change in unsaturated zone behaviour and thus has an effect on the ground water recharge. This results in changes in the ground water system and finally in slope stability. In chapter 5 different scenarios are introduced. With these the transient effects of changes in boundary condition on the hydrological system can be studied starting with the same initial conditions, i.e. a prolonged wet or dry period, or the effects of land-use change.

For the scenario studies, the reader is referred to table 6.9, where the scenarios are defined. The scenarios can be divided into four groups: 1) changes in potential evapotranspiration, 2) changes in precipitation, 3) changes in both potential evapotranspiration and precipitation with opposing effects and 4) changes in both potential evapotranspiration and precipitation with similar effects.

The changed bottom flux of the unsaturated zone model was used directly for the ground water model. This ensures that the non-linear behaviour of the unsaturated zone is taken into account. The effects of preferential flow in the recharge input time series, as described and discussed in § 7.3, are also studied, by recalculating the recharge series using formulas 7.1 to 7.3.

First of all, figure 7.11 shows that the Beline hydrological system can buffer around one year of changes in input variables. It is after this period that the hydrological system

starts to react. Secondly, the general trend of all the scenario calculations, as depicted in figure 7.11, is that the effects of wetting are larger than the effects of drying. In other words, a decrease of the potential evapotranspiration with 10 % has more effect than an increase of potential evapotranspiration with 10 %. This can be explained by a high

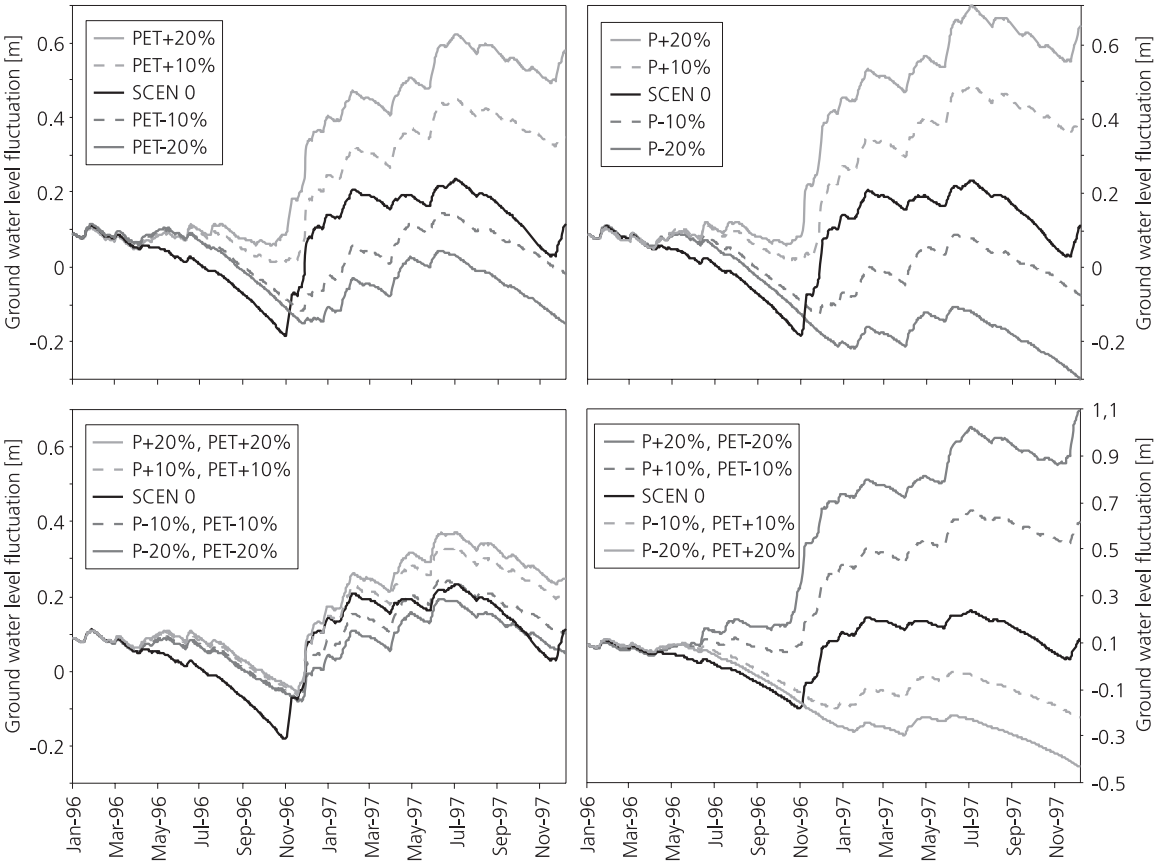

Figure 7.11 Ground water fluctuations as response to different input change scenarios for observation point D1 using the state-dependent recharge function.

evapotranspiration demand, which does not have to lead to actual evapotranspiration. In case the soil is already dried out the actual evapotranspiration will be low, whereas in wet periods the soil seems to be able to absorb the surplus of precipitation and thus percolation and ground water recharge increase.

Thirdly, the scenarios show that a change in potential evapotranspiration has slightly less effect than a change in precipitation. Scenarios 9 to 12 (changes in precipitation (P) and potential evapotranspiration (PET) with opposing effects) show this effect most clearly. A decrease of rainfall and potential evapotranspiration results in almost no change in ground water behaviour, whereas an increase of both variables results in a ground water level rise.

One of the reasons that no limitation seems to exist for additional precipitation to infiltrate is because all precipitation falling in 1 day is spread over that day and thus results in very low rainfall intensities. In reality this does not have to occur, when

increased rainfall leads to increased rainfall intensities and thus the occurrence of overland flow when rainfall intensities exceed the soil infiltration capacity.

Is it necessary to use the state-dependent recharge model for providing the input of the ground water model when seasonal changes are calculated? Figure 7.12 shows the results of scenarios 1, 3, 5 and 7, calculated with both the recharge input directly from the bottom flux of the unsaturated zone model and the state-dependent recharge model. As shown, for the overall trend of the ground water level fluctuations and the maximum ground water level rise, the choice of input time series does not seem very relevant. However, when the distribution of precipitation changes a lot, the state-dependent recharge model will give more realistic ground water reactions. Secondly, for creep calculations (see chapter 7) the time span that a certain ground water level is sustained, can be of importance.

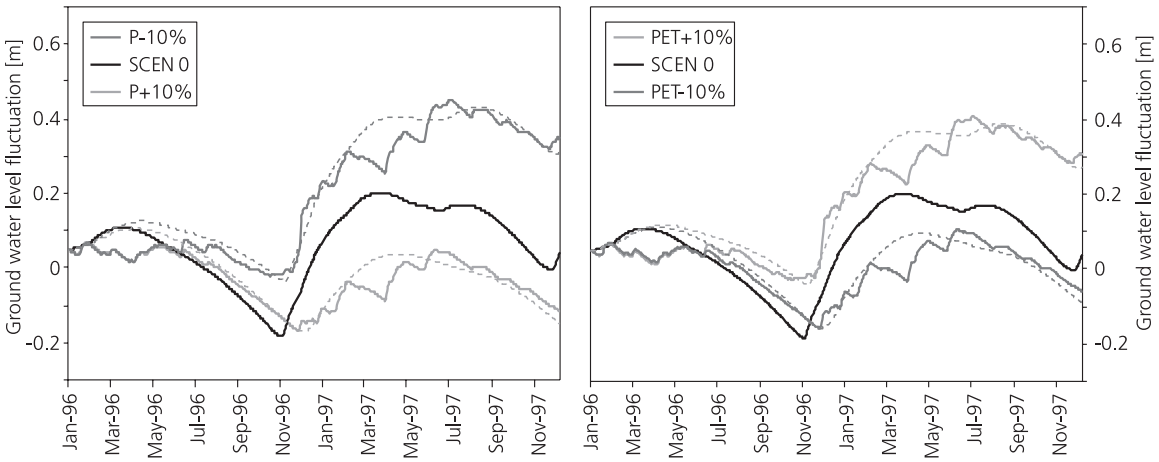

Figure 7.12 Comparison of scenario results using the recharge input series of the unsaturated zone model (thick grey line) and of the state-dependent recharge model (thin grey line).

7.5 Summary and discussion

This chapter describes the modelling of ground water level and its fluctuations using the Modflow model for clayey slopes. It focuses on the effects of ground water recharge time series. The proposed methodology to study the ground water level fluctuations in clayey slopes consists of modelling the unsaturated and saturated zone separately. The unsaturated zone model results in a bottom flux or ground water recharge flux. Using the annual average value for recharge, the ground water model is calibrated on its steady-state ground water level by adjusting the hydraulic conductivity. The dynamics of the ground water system are modelled by calibrating the porosity related parameters.

The calibration of the saturated permeability is performed on the average, steady-state, ground water level as deduced from only three observation sites. With the used geometry, it was difficult to fit all three observations exactly. The modelled average ground water level is a smooth line through the observations, which resulted from a trial and error approach. The fixed average recharge of 0.75 mm/day also indirectly limits the saturated permeability values for the subsurface. Recharge flux and saturated permeability in a steady-state situation are related.

It was tried to perform this calibration automatically using the PEST program. Two important problems came up using this approach. First of all, the measured depth of the ground water table is too irregular to model with the geometry as described above. Secondly, the automatic calibration program changes the selected parameters within certain boundaries. By automatically selecting an 'extreme' parameter value or combination of parameter values, the model becomes numerically unstable. This puts an end to the inverse modelling exercise, resulting in no optimisation. Narrowing the optimisation range for a parameter (e.g. permeability) can prevent this problem from occurring. But tests showed that the range should be narrowed to unpractical small values, leaving no free optimisation. Lastly, the presented results show that it is very hard, if not impossible, to work with an objective function like RMSE if the input time series (ground water recharge) have a phase shift in the time series (measured ground water levels). In such a case, the best statistical fit does not necessarily represent the best model result, and thus remains manual control on the calibration process indispensable.

In this chapter it was shown that the ground water level fluctuations in the clayey Beline slope could neither be explained with matric flow (from the unsaturated zone model) nor with (fractional) precipitation input. The role of the saturation grade of the unsaturated zone is indispensable. The (preferential) recharge flux depends on antecedent moisture conditions in the unsaturated zone. A model is proposed to combine the state of the unsaturated zone and the precipitation input in a simple determination of the recharge time series: the so-called 'state-dependent recharge function'. It transforms precipitation to recharge by scaling it with soil moisture conditions. As a function for the soil moisture condition the ratio of the matric bottom flux and the average matric bottom flux is used. In this way, the highly non-linear behaviour of the unsaturated zone is incorporated in the ground water recharge time series.

The model results, as shown in figures 7.8 and 7.10, show that the ground water level fall in dry periods is significantly faster when measured than when modelled. So, it is fair to state that the saturated permeability should be set higher in order to make the ground water system drain more rapidly. However, a higher set of permeabilities also results in a less inclined ground water level within the slope, i.e. downslope a larger area will have ground water seepage and upslope the ground water level will be much deeper. Also, the calibrated saturated permeabilities are already relatively high for a silty clay and marly environment.

Besides the mathematical aspects of the model calibration, the spatial uncertainty caused by spatial heterogeneity is also responsible for imperfection of the model results. Other error sources are the absence of on-site actual evaporation, transpiration and rainfall data. In this research it was tried to exclude the effects of spatial variability as much as possible and to focus on the effects of ground water recharge on ground water level fluctuations. It was shown that with the available data a good insight can be reached in the behaviour of the hydrological processes in clayey slopes that are prone to mass movement.

One aim of the ground water modelling was to determine the spatial distribution of the pore water pressure in the Beline slope. This aim is not fulfilled. Using the available data it is not possible to come to a pore pressure distribution in the Beline slope, which improves the ground water level measurements that were the starting point of this study. However, it was possible to quantify the ground water level fluctuations.

The second aim was to determine an effective way to obtain ground water recharge from precipitation data and unsaturated zone models. The recharge and extended recharge models proved to be straightforward and useful methods to determine the important recharge time series that are used as input for ground water modelling.

The next aim was to quantify the influence of changes in ground water recharge on the ground water level fluctuations. The general trend of all the model scenarios was that changes resulting in wetting had more effect than changes resulting in drying. Furthermore, wetting by an increase in precipitation has more effect than by a decrease in potential evapotranspiration. This is mainly caused by the fact that an increase in precipitation is almost totally absorbed by the soil because of the artificially low rainfall intensities caused by modelling on a daily time scale. However, the measured rainfall intensities at the Beline slope and the Arbois Météo France station revealed that the maximum rainfall intensities during a rainfall event were on average between 1 and 2 mm/hour. This in contrast with changes in potential evapotranspiration, which do not automatically lead to changes in actual evapotranspiration. The availability of water in the upper few centimetres of the soil controls the evapotranspiration flux. In clayey soils the unsaturated hydraulic conductivity already becomes very low with a small decrease in soil moisture content, resulting in very slow moisture transport through a dry soil/atmosphere interface layer.

8 SLOPE STABILITY AND DEFORMATION IN RELATION TO GROUND WATER LEVEL FLUCTUATIONS

8.1 Introduction

This chapter aims to quantify the influence of ground water level changes on slope mobility. For this it is necessary to evaluate and quantify the mechanisms of movement at the Beline slope. Slope movement mechanisms can roughly be divided in sudden (plastic) and continuous (visco-plastic) deformations. The former mechanism prescribes rigidity until a certain stress threshold is exceeded. The latter mechanism has a deformation range from a deformation threshold to a failure threshold. This process is generally referred to as (continuous) creep.

This chapter first of all describes the field and laboratory measurements (§ 8.2 and 8.3). In paragraph 8.4 the slope stability is evaluated using the limit equilibrium method for plastic failure with a plane parallel slipsurface (infinite slope model) and circular slipsurface (Bishop's method). In paragraph 8.5 creep is modelled by means of the Yen creep model.

8.2 Subsurface schematisation and field deformation measurements

For the geotechnical analysis, the same schematisation as for the hydrological modelling was used. This follows from the geological schematisation as given in chapter 4. Three layers were identified using borehole information, drilling progress and geophysical surveys:

- a disturbed surface layer, low density and abundant gravel content, with an average thickness of 5 m;
- a zone of remoulded marls with silty layers, a variable gravel content, an average density and a thickness of 5 m at the bottom of the slope towards more than 10 m in the upper part of the slope;
- compact blue marls, in general no gravel, but with some limestone concentrations.

In order to measure deformation with depth, the Beline slope in Salins-les-Bains was equipped with one inclinometer tube, which was installed at drilling location D3 (see figure 4.8). The flexible tube reached as far as 28 m below surface level. It was manually monitored once a month from January 1996 till December 1997. The displacement was measured in two directions (8-188°N and 98-278°N) of 50 cm vertical intervals. The measurement error of these deformation measurements is in the range of 1-2 mm. With the two measurements both the absolute displacement and the direction can be calculated. Figure 8.1 shows the cumulative displacement in the first 6 m. No displacement was recorded below 6 m depth. During all other months no displacement could be distinguished. Two clear moments of distinctive movement were recorded: July 1996 and November 1996. In 1997 some movement took place, but not as notably as in November 1996. The direction of the movement changes slightly with depth. Near the surface it is in a southerly direction, at 2 m depth in a SW direction and below 3 m the movement has a SSW orientation.

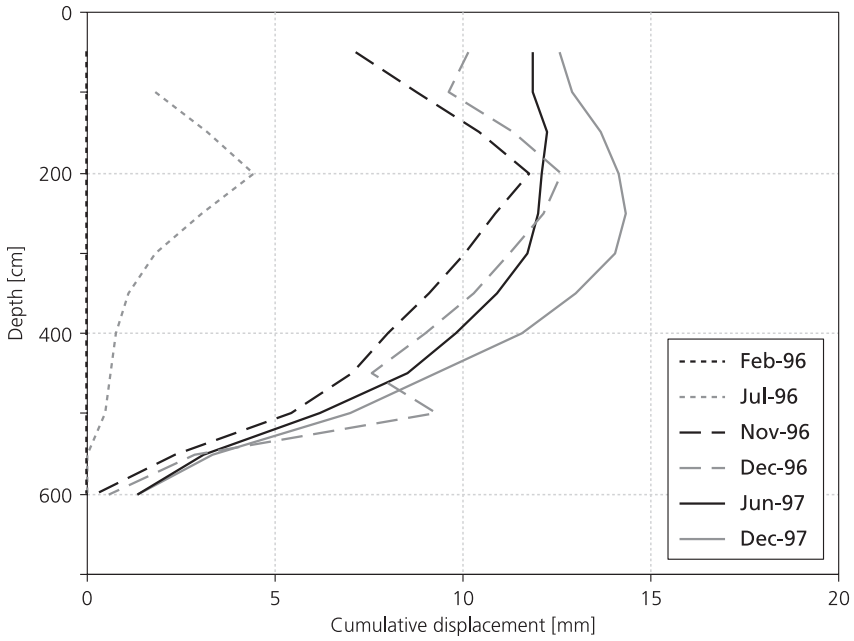

Figure 8.1 The total cumulative displacement recorded with the inclinometer at the Beline slope (January 1996 - December 1997).

The inclinometer measurements can be interpreted in two ways. At the location of the inclinometer tube a creep zone is situated between 3 and 6 m below surface. Another explanation can be that the deformation takes place in a thin slipsurface or zone around 4.5 m below surface. The firmness of the inclinometer tube then spread the (small) displacement over 3 m tube. Another observation from the displacement measurements is that the surface displaces less. An explanation could be that the grass surface cover mobilises additional shear strength and thus holds back the upper part of the profile from displacement.

8.3 Laboratory measurements of geotechnical soil parameters

To determine the strength parameters cohesion and angle of internal friction of the soil (see § 2.2), direct shear and triaxial laboratory tests were executed. For the determination of viscosity and creep threshold an experimental creep test was set up.

In total 37 direct shear tests were performed, 32 with undisturbed samples and 5 with disturbed samples. The direct shear samples were collected in the central part of the slope at depths varying from 20 to 160 cm. The samples were stored at 7 °C before testing. The samples were cut into slices of 6*6 cm with a thickness of 2 cm and saturated for the duration of one week. After this, the samples were consolidated for 2-3 days (while saturated) using an oedometer. The single stage drained direct shear tests were executed with an axial load varying from 50 to 250 kPa and with a deformation velocity of 0.08 to 0.12 mm/hr (2 to 3 mm/day). The tests were stopped when the shear strength reached a constant value or were stopped automatically after ± 9 mm of displacement.

Furthermore 6 triaxial tests were performed. Three triaxial samples were taken from the cored drilling SC1 (see figure 4.8) in the interval of 1.4-2.7 m and three from 21.3-21.6 m below surface. The height and diameter of the shallow samples were 10 and 5 cm respectively and of the samples from 21 m depth 7.6 and 3.8 cm respectively. The drained triaxial tests used an all-round (fluid) pressure of 50, 150 and 400 kPa and a deformation velocity of 0.24 mm/hr.

The results are shown in table 8.1. The cohesion and angle of internal friction are peak strength values for the undisturbed samples and residual strength for the disturbed sample. The soil cohesion ranges from 11 to 20 kPa, and the angle of internal friction ranges from 23 to 28 degrees.

Table 8.1 Results of the strength tests at the Beline slope: n= number of tests, c'=effective cohesion, φ'= effective angle of internal friction and ρ_d=dry bulk density.

Test type	Depth [m]	n [-]	c' [kPa]	φ' [°]	ρ_d [g/cm^3]	Remarks
Direct shear	0.2-0.4	11	20	26	-	Some grass roots
Direct shear	0.6	6	12	24	1.6	
Direct shear	0.68	5	11	23	-	
Direct shear	0.96	5	17	28	-	
Direct shear	1.6	5	13	23	1.7	
Direct shear	1.2	5	14	19	-	Disturbed test samples
Triaxial	1.4-2.7	3	17	27	1.64	2 tests showed a barrelling type of failure
Triaxial	21.3-21.6	3	0	21	1.58	Unweathered marls

An experiment was set up to measure the viscosity and creep threshold values under laboratory conditions, the simple shear viscosity test. The apparatus, which was designed for viscosity tests, consists of two retention plates of 10 by 20 cm^2 with 3 cm of soil samples in between. The lower plate is fixed and the upper plate is pulled using a dead weight (figure 8.2). The samples were inundated till the upper retention plate. The retention strips on the retention plates were placed perpendicular to the direction of movement and penetrated the sample 0.5 cm. This leaves 2 cm of soil free to deform. Plastic transparent sides prevented lateral soil displacement.

The normal stress load was applied to the upper retention plate and the shear stress load was hung below the pulley. The displacement rate was measured with a strain gauge behind the upper retention plate. The samples were consolidated on average one week before the viscosity tests were performed. The viscosity test stopped after the displacement rate became constant, which was generally within one week. The average displacement velocity was calculated between 1 and 7 days after the start of the test.

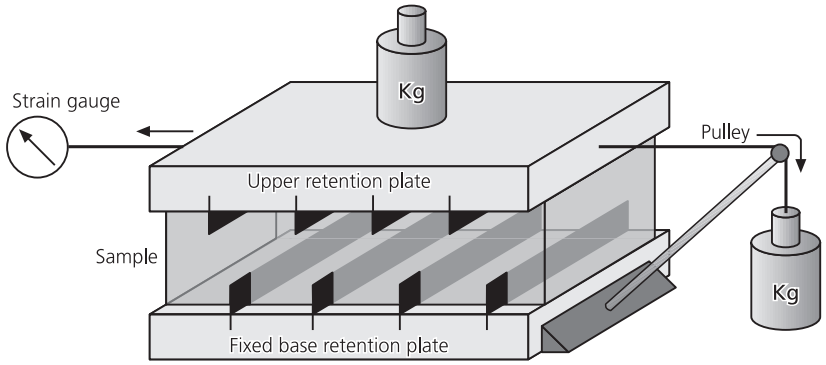

Figure 8.2 Schematic representation of the viscosity apparatus.

In total 24 tests were performed with 4 different normal loads. The analysis of the viscosity was performed assuming Bingham rheological behaviour of the material (e.g. Nieuwenhuis, 1987, Van Asch and Van Genuchten, 1990). The linear Bingham visco-plastic flow equation is:

$$\tau = \tau_0 + \eta \cdot \frac{du}{dy} \tag{8.1}$$

with:

τ	= shear stress	[kN/m^2]
τ_0	= threshold value for creep (yield strength)	[kN/m^2]
η	= dynamic viscosity	[kNs/m^2]
u	= displacement velocity	[m/s]
y	= depth	[m]
du/dy	= shear strain rate	[s^{-1}]

under the assumption that the thickness of the deforming layer does not change in time (dy/dt=0). The shear strain rate is defined as:

$$\frac{du}{dy} = \frac{\left(\frac{dx}{dt}\right)}{dy} \tag{8.2}$$

where:

dx/dt	= displacement velocity in x-direction	[m/s]

The displacement velocity can be determined from the straight line in the displacement-time graph. The thickness over which the sample deforms (dy) was taken equal to the sample height between the retention strips, i.e. 2 cm. The shear stresses and corresponding shear strain rates were plotted as shown in the example of figure 8.3. A linear regression results in the creep threshold (τ_0) and the dynamic viscosity η of the material (eq. 8.1).

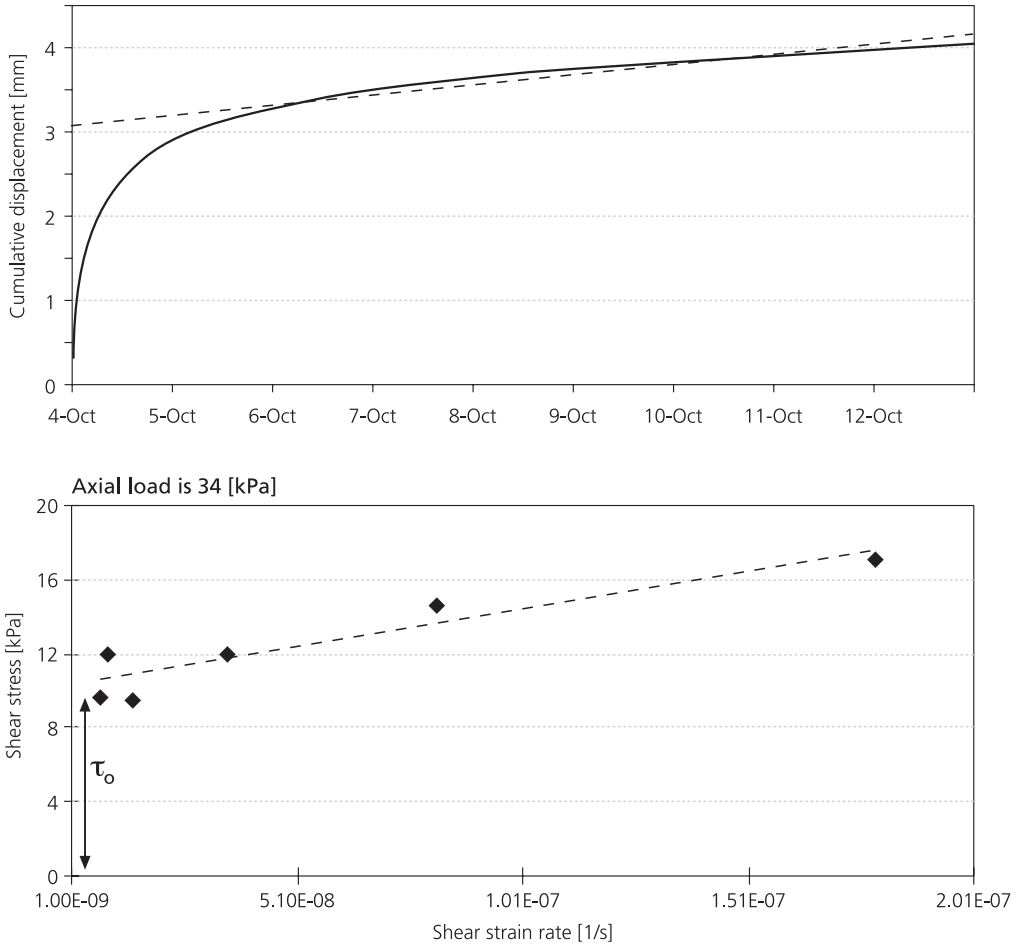

Figure 8.3 Example of the determination of viscosity from a laboratory test. First of all the shear strain rate (displacement velocity divided by creep height) is calculated between 1 and 7 days after the test started (first graph). Then the shear strain rates are plotted against their shear stresses. The linear regression through these points gives the creep threshold (τ_0) and the dynamic viscosity (η).

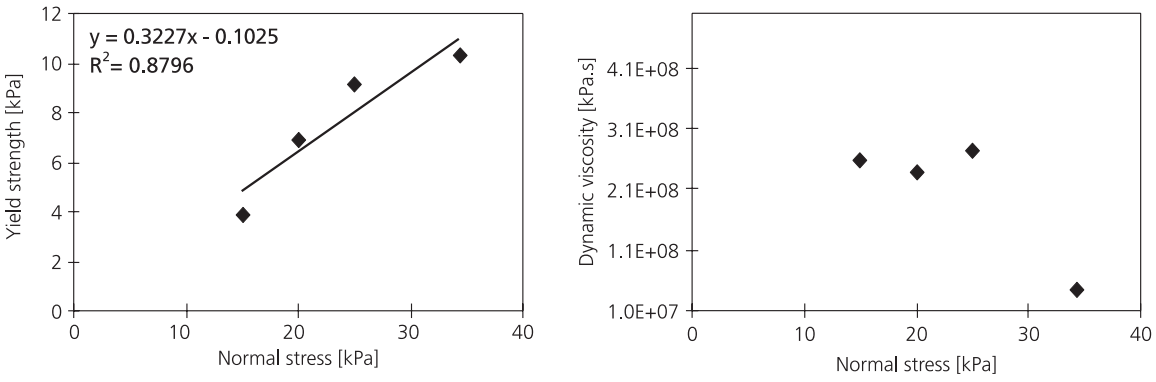

Figure 8.4 Relationships of the yield strength and dynamic viscosity with the normal stress in the soil, as determined with the laboratory viscosity tests.

The results of the laboratory viscosity tests are shown in figure 8.4. Both yield strength (creep threshold) and dynamic viscosity were plotted against the normal stress that was applied: 15, 20, 25 and 34 kPa. The creep threshold (τ_0) shows to be linearly related to the applied normal stress. The viscosity could not be related with the normal stress.

8.4 Static stability model

A general approach to obtain an indication of the stability of a given area is to analyse the stability of potential failure mechanisms. For any mechanism both the maximum resisting force and the driving force are calculated. An instable situation is predicted when the driving force exceeds the maximum resisting force. The ratio of the maximum force and actual driving force can be used to predict the likelihood of failure. This ratio is often referred to as Factor of Safety, FS. A static stability model only evaluates the equilibrium between driving and resisting forces. It does not take into account transient mass movement processes. The aim of the stability calculation in this research is to evaluate changes of slope stability as results of changes in ground water levels within the slope.

In the framework of the Hycosi project several models have been used and developed for slope stability analysis. Boeije and Teunissen (1997) developed a 3D stability model called 3DSTAB, Asté (1997) used the 3D.PENT program. The 3D stability computer codes are capable of evaluating the Factor of Safety of three-dimensional spheres. The above-mentioned researchers performed a detailed analysis of the possibility of using such models for the evaluation of slope stability at the Beline slope. Boeije and Teunissen (1997) worked with a highly simplified schematisation of the slope and concluded: "It is difficult to define or predict the precise geometry of the landslide. There is not sufficient data available for the characterisation of the soil strength in different areas and layers. This limits the quantitative capabilities of the method for 3D stability analysis presented here." Asté (1997) evaluated and combined the existing data. He analysed three predefined spheres with regard to their stability using the actual topography and one on a hypothetical ancient topography for evaluating the existence of an ancient landslide. He made it plausible that the slope has been subject to an ancient large-scale landslide. For recent landslide analysis his 3D stability calculations are also strongly dependent on input data and pre-information on movement.

For stability analysis one needs information on the strength parameters and on the geometry. For both 2D and 3D models the former information is equally necessary, but a 3D stability model requires much more spatial information on the geometry than 2D models. As outlined above, this geometry information is limited available. It was therefore decided to perform the analysis using 2D slope stability models. Plane parallel failure is studied using an infinite slope model and for circular failure Bishop's method was used.

Parameterisation

The geotechnical parameterisation of the three layers (§ 8.2) is given in table 8.2. Only 3 strength tests were executed on the unweathered marls and none on the intermediate layer. Boeije and Teunissen (1997) and Asté (1997) did not have the triaxial test results of the deeper material when they investigated the slope stability of the Beline site. They

used another parameter configuration (see table 8.2). Boeije and Teunissen (1997) discussed the first assumption that the angle of internal friction was 13° is implausible and that a value of 30° is more reliable. Such a low angle of internal friction for the marls leads to deep-seated slipsurface. This is not supported by any field evidence. The shear strength values from the triaxial test (c=0 kPa and φ=21°) on the sample from the Beline slope at 21 m below surface (layer 3) are doubtful.

Table 8.2 The initial parameter setting for the 2D Beline stability analysis.

Layer	Thickness [m]	c' [kN/m^2]	φ' [°]	γ_s [kN/m^3]	Remarks	*c' [a)] [kN/m^2]*	*φ' [a)] [°]*
1	5	15	25	20	DS and Triaxial tests	*20*	*26*
2	5 to 10	10	22.5	20	No laboratory tests	*30*	*20*
3	-	0	21	20	Triaxial tests	*40*	*13*

[a)] In italic the strength values used by Boeije and Teunissen (1997) and Asté (1997).

The geotechnical characteristics of marls have a large range depending on the degree of limestone cementation in the marls. They can behave as a rock with cohesion values in the range of 1000-10000 kPa (Carson and Kirkby, 1972). De Joode (2000) did several strength tests on undisturbed black marls rock from Oxfordian age ("Terres Noires"), unconfined compression tests as well as direct shear test. With the latter, the angle of internal friction was determined with broken material using the contact plane between two slices of Terres Noires as shear plane. A value of 30.5° was determined for the peak strength and a value of 24.5° for the residual strength. Under the assumption of an angle of internal friction of 30.5°, the compressive strength tests showed cohesion of more than 3000 kPa.

Antoine et al (1988), however, find Terres Noires marls with c'=72 kPa and φ'=29°. Jibson et al (1998) assigned cohesion values on the basis of available strength tests and expert knowledge of many different geological formations near Los Angeles, California. They come up with cohesion values in the order of 25-40 kPa for geological formations as shale, mud or clay.

Of course every lithology has different characteristics and consequently different strength characteristics. There is, however, severe doubt on the shear strength value of the 'fresh' marls from the Beline slope determined by the triaxial tests. Therefore the marls have been assigned a cohesion value of 100 kPa and an angle of internal friction of 30° in the rotational slip analysis.

The ground water level monitoring (chapters 4 and 7) gave ground water levels between 3.4 and 6.4 m depth at the central part of the slope. The maximum ground water level that was measured was at 3.24 m below surface (table 5.7). Furthermore, at the central part of the slope clear signs of deformation have been mapped (figure 4.10). For the stability calculation a ground water level of 3 m below surface will be used as a reference ground water level, a first approximation for the critical ground water level. This is to ease comparison between several stability calculations.

Infinite slope model

The infinite slope model calculates the factor of safety as:

$$FS = \frac{c' + \left(\gamma^* \cdot z \cdot \cos^2(\beta) - h_w \cdot \gamma_w \cdot \cos^2(\beta)\right) \cdot (\tan(\varphi'))}{\gamma^* \cdot z \cdot \sin(\beta) \cdot \cos(\beta)} \qquad (8.3)$$

with:

$\gamma^* = (1-m) \cdot \gamma + m \cdot \gamma_s$

where:

c’	= Effective cohesion	[kN/m^2]
ϕ’	= Angle of internal friction	[°]
β	= Slope angle	[°]
γ*	= Average unit weight soil	[kN/m^3]
γ_w	= Unit weight water	[kN/m^3]
γ	= Unit weight unsaturated soil	[kN/m^3]
γ_s	= Unit weight saturated soil	[kN/m^3]
z	= Thickness soil layer	[m]
h_w	= Height water above slip surface	[m]
m	= fraction layer saturated, h_w/z	[-]

The infinite slope model uses a slipsurface parallel to the surface and it reasons that the interslice forces are cancelled out because of the symmetry. The infinite slope model was used to subject some parameters to sensitivity analysis; parameters that have a large uncertainty or are difficult to determine. Three parameters were studied on their effect on the FS of the slope: the depth of the slipsurface (z), relative height of the water table (m, also written as r_u, the pore pressure ratio) and strength parameters (c’ and φ’). The slope angle is a very sensitive parameter (see e.g. Mulder, 1991) but relatively accurate to measure. The Beline slope angle measures 17°. Figure 8.5 shows the influence of these three factors on the slope stability. First of all it can be deduced that slope instability cannot occur in the first layer (5 m). All strength parameter combinations result in a stable slope. Instability by a deeper located slipsurface in the second layer is more likely. For the stability at 10 m depth the angle of internal friction is more important than the cohesion due to higher stress levels. On the other hand, the value of the angle of internal friction has almost no influence on the stability of superficial slipsurfaces.

In the situation of a slipsurface at 10 m depth with c’=10 kN/m^2 and φ’=22.5°, the slope becomes unstable for a ground water level of 2.5 m below surface (m=0.75). If a local steepness of 20° is assumed, the slope with a slipsurface at 10 m below surface will become instable with a ground water level at 5 m below surface (c’=10 kN/m^2 and φ’=22.5°). A slope of 17° with a slipsurface at 5 m below surface, will become unstable with a ground water level at 3 m below surface if the c’ and φ’ reduce to e.g. 5 kPa and 18°. A slipsurface at 7.5 m will need a reduction of c’ and φ’ to 7.5 –10 kPa and 19 - 20° with the same ground water level (-3 m). Especially the reduction of the cohesion seems quite drastic, when it is compared to the shear strength results of the disturbed samples (c’=14 kPa and φ’=19°), which can be seen as an approximation of the reduced strength of the soil.

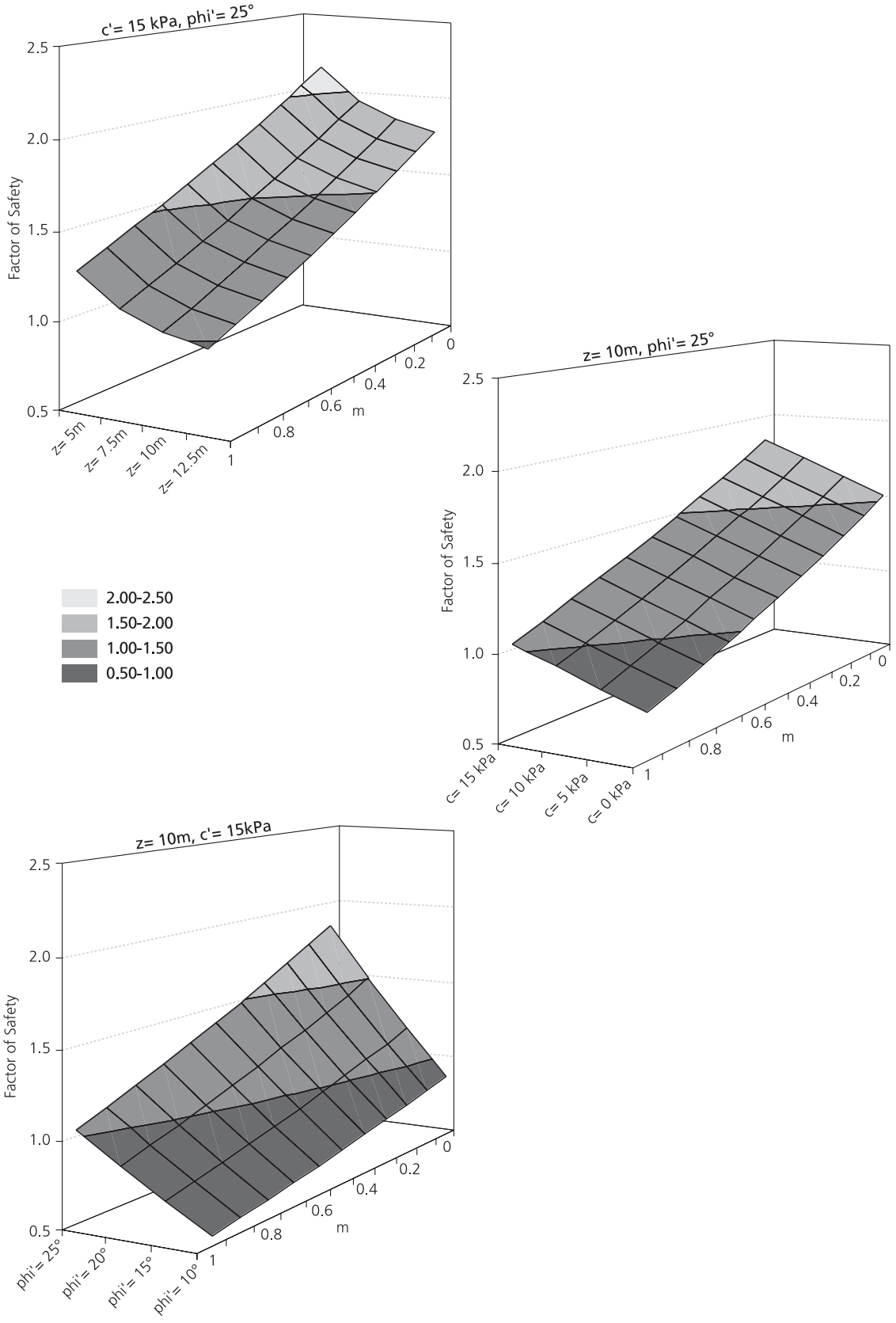

Figure 8.5 Relationship between the Factor of Safety (FS) and ratio pore pressure/soil depth (m) with the depth of the slipsurface (z), cohesion (c') and the angle of internal friction (φ').

Bishop's method

Rotational slips can also be analysed with limit equilibrium methods by applying the method of slices. The factor of safety is defined as the ratio of the available shear strength to the shear strength, which must be mobilised to maintain a condition of limit equilibrium (Craig, 1992). In several 2D models (Bishop, Fellenius), the slipsurface is assumed to be a circle, along which the shear stresses can be calculated. These stresses result in a resisting moment around the axis of the circle. The gravitational forces on the mass in the soil circle itself create a driving moment around the axis of the circle.

The slope stability calculations of these rotational slips were executed with the SLIDE computer code. This program calculates slope stability according to the method of slices. It is capable of analysing a rotational slipsurface for lowest FS of circular as well as ellipse shape, according to Fellenius, Bishop (ordinary), Janbu (simplified and rigorous), Spencer, Morgenstern and Price (see e.g. Craig, 1992). It can perform a slope analysis if the toe and the scarp of a slipsurface are defined and can work with a non-rotational slipsurface if it is predefined.

Stability calculation along the Beline slope learnt that the part around inclinometer tube (D3) was the most unstable. Further analyses were therefore focussed on this higher part of the slope. Calibration of the slope stability model was strongly limited by data shortage, both of strength parameters and soil and slipsurface geometry. For these analyses the strength parameters of the unweathered marls (layer 3) were set on c=100 kPa and φ= 30° while for the intermediate layer c=10 kPa and φ=22.5° was assigned (see table 8.2). The slope around the inclinometer tube showed a slipsurface at maximum 10 m depth (6.2 m below surface at D3) with a FS=1.12 with a ground water level at 3 m below surface (figure 8.6). This is a FS of 0.11 more than when using the infinite slope model. A FS=1.0 can be reached by setting φ of the second layer at 21° instead of 22.5°.

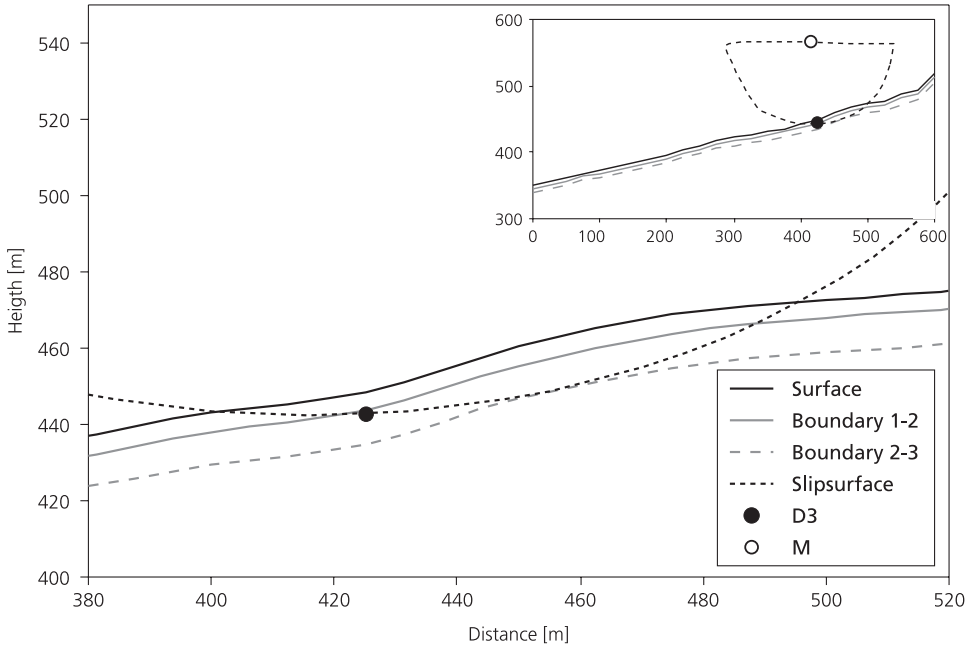

Figure 8.6 Location of the slipsurface of a rotational slide using the Bishop's method of slices at the Beline slope.

Quantification of the effects of ground water level changes on the slope stability

In chapter 7 changes in land use or climate were modelled by changing the input variable precipitation and potential evapotranspiration with 10 or 20 %. The reaction to these changes is an increase of the ground water level in the order of decimetres. How does this affect the slope stability?

In case of the Beline slope (c=10 kN/m^2, φ=22.5° for the second layer), an increase of ground water level from 3 to 2.5 m below surface results in a decrease of FS of 0.035 using the infinite slope model and in case of a rotational slipsurface the FS decreases 0.033. The change in FS seems independent of the model assumptions.

It could be interesting to analyse when the subsurface is most sensitive for ground water level changes. Sensitivity of a slope to ground water level changes is defined as a change in the derivate of FS with water level increase (dFS/dh). This is calculated with the infinite slope model. Figure 8.7 shows the effect of a change in the depth of the slipsurface, cohesion or angle of internal friction on the sensitivity of the slope to changes in pore water pressure. It shows that the deeper the slipsurface is located, the less will the FS decrease when ground water increases with 1 m. This is generally known as the effects of the pore pressure ratio. The same is valid for soils with a low angle of internal friction. Changes in cohesion do not affect the decrease of FS with 1 m ground water level increase. This shows that slopes with a frictional soil and shallow slipsurfaces are most sensitive to changes in pore water pressure. This is the situation, which is encountered at the Beline site. It must be stressed that the 1 m ground water level rise is only a calculation example (unit water level rise), and not expected at the Beline slope.

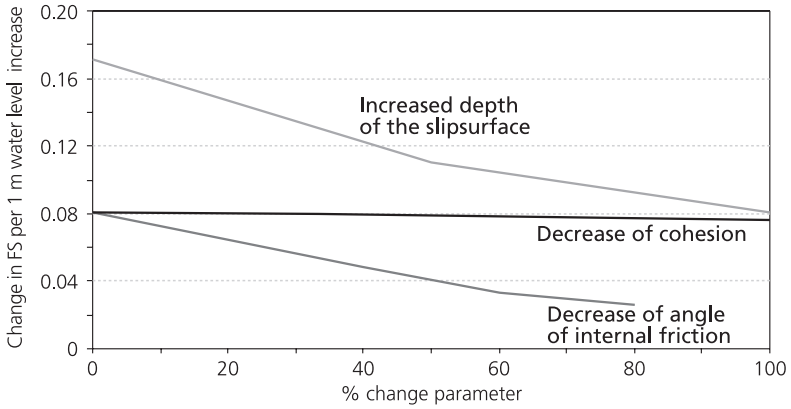

Figure 8.7 Effects of the depth of the slipsurface and the strength parameters (cohesion and angle of internal friction) on dFS/dh. Depth of the slipsurface runs from 5 m to 12.5 m, cohesion from 15 kPa to 0 kPa and φ from 25° to 5°.

Conclusions

The following conclusions can be drawn from the 2D static stability analyses:
Using the peak strength values determined in the laboratory (table 8.1) and assuming a correct subsurface schematisation, the Beline slope is stable under the ground water conditions encountered in the field.

- On the Beline slope the FS lowers with 0.035 when the ground water level rises from 3 to 2.5 m below surface. This will not cause catastrophic failure.
- The area most prone to landslides is the part around the inclinometer tube. This is also observed in the field and in the inclinometer tube.
- The static stability analysis shows that in the event that a landslide will occur, it can be expected to have a slipsurface with a maximum depth of 10 m depth.
- Ground water level changes have a relatively larger effect on the stability of a slope with frictional soils and shallow potential slipsurfaces.
- The strength parameters as determined in the laboratory have to be reduced to c' is 5 to 7.5 kPa and φ' is 18° to 20° in order to come to a FS around 1 when the ground water level is 3 m below surface. This reduction in strength is in agreement with the reduced strength analysed with the viscosity tests (see paragraph 8.4).

8.5 Displacement model

Static slope analysis classifies a slope either as stable or unstable. They do not give information about the movements. This limits their use to relative changes in slope stability and the evaluation of catastrophic mass movements. But accelerating sliding along a slip surface is not the only mechanism of slope movement. An additional movement mechanism is creep. The creep process may be of great importance in the development of landslides because initial movement of the slope may start with creep processes at stress values that lie far below the peak strength of the soil material (Van Asch and Van Genuchten, 1990). These slow creep movements can also lead to accelerated creep and shear failure. The aim of the displacement modelling is to evaluate the slope movement in terms of creep and to quantify the effects of ground water level changes on the slope movement of the Beline slope.

On the basis of the Bingham rheological behaviour of material (Equation 8.1) several so-called creep models were developed. Nieuwenhuis (1987) describes and compares the performance of the models of Ter-Stepanian (1963) and of Yen (1969). The former states that the dynamic viscosity (η) and the yield strength (τ_0) are a function of the normal stress. Yen (1969) and Suhaydu and Prior (1978) define the yield strength by the residual strength parameters c_r' and φ_r' of the material. The dynamic viscosity (η) is constant and independent of the existing isotropic stress conditions in the soil as in the Bingham fluid.

The laboratory viscosity tests show that the yield strength is a function of the normal stress and indicates that the dynamic viscosity is stress independent (figure 8.3). These results support Yen's creep model and it was therefore decided to further explore the Beline slope using this model.

Yen describes the yield strength (τ_0) as:

$$\tau_0 = c_r' + \sigma' \cdot \tan(\varphi_r') \qquad (8.4)$$

c_r'= residual effective cohesion
φ_r'= residual effective angle of internal friction

Using the laboratory data (figure 8.4) the effective residual strength of the surface material (c_r' and φ_r') can be determined. The effective residual cohesion is negligible and

$\tan(\varphi_r') = 0.32$, thus $\varphi_r' = 18°$. For the dynamic viscosity the average value of the four tests was taken: $2*10^8$ kNs/m^2. As comparison, Van Asch and Van Genuchten (1990) found a dynamic viscosity for varved clay in the French Alps of $2.4*10^8$ kNs/m^2. Ter-Stepanian (1965) reports in-situ determined dynamic viscosity values, calculated after 7 year of displacement in Oligocene claystone and sandstone in the Caucasus, of $1*10^{10}$ kNs/m^2. Yen (1969) calculates in his creep analysis of a silty clay profile near Malibu, California a dynamic viscosity value of $1.6*10^8$ kNs/m^2.

The creep model of Yen has the basic assumption of the static infinite slope model (Van Genuchten 1989, Van Asch and Van Genuchten 1990). Ground water is assumed to flow parallel to the ground surface. Considering the stress behaviour of the soil, the soil should consist of isotropically consolidated material and there should be no changes in stress distribution due to creep. The viscosity is a time independent material characteristic. Yen's creep model implicitly assumes that the subsurface, which is subject to creep, is in residual strength condition. As the Beline slope is the result of an ancient landslide (Asté, 1997) and has numerous mass movement features indicating recent displacement, the assumption of residual strength condition of the subsurface seems to be met.

Calibration of the Yen creep model at the Beline slope

Given the coordinate system as shown in figure 8.8, the effective normal stress (σ') and shear stress (τ) are given by the following expressions:

$$\sigma' = \left((z - z_w) \cdot \gamma' + z_w \gamma_u \right) \cdot \cos(\beta) + P \qquad (8.5)$$

$$\tau = \left((z - z_w) \cdot \gamma_s + z_w \gamma_u \right) \cdot \sin(\beta) + S \qquad (8.6)$$

z	= Soil depth measured perpendicular to the soil surface	[m]
z_w	= Depth of phreatic surface perpendicular to the slope	[m]
β	= Slope angle	[°]
γ_u	= Unit weight unsaturated soil	[kN/m^3]
γ_s	= Unit weight saturated soil	[kN/m^3]
γ'	= Submerged unit weight of soil (γ_s-γ_w)	[kN/m^3]
γ_w	= Unit weight of water	[kN/m^3]
S	= Shear stress overburden	[kN/m^2]
P	= Normal stress of overburden	[kN/m^2]

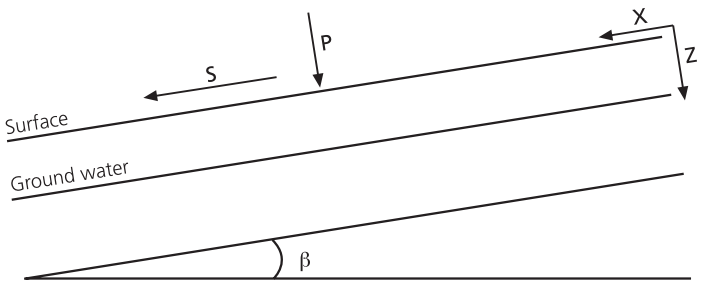

Figure 8.8 Coordinate system for the creep description.

Table 8.3 Parameterisation of the Yen creep model.

	Value	Unit
β	17	[°]
γ_u	16.5	[kN/m^3]
γ_s	20	[kN/m^3]
c_r	0	[kN/m^2]
ϕ_r	18	[°]
η	$2.00*10^8$	[kNs/m^2]

The ground water levels were compiled using the average ground water depth of the measurements at D3 (4.1 m below surface) and adding the modelled ground water level fluctuations (see chapter 7). This was necessary because severe doubts had emerged on the registration of ground water level fluctuations at D3. The creep modelling was executed on a monthly time scale for the first 6 m. The parameterisation is given in table 8.3. It is stressed that the exact point in time of occurrence of displacement is disregarded in this analysis. The phase-shift between observed and modelled ground water level fluctuations is the direct consequence of the unsaturated zone modelling and has been discussed in chapters 6 and 7.

The Yen model was calibrated using the inclinometer results of figure 8.1. The optimisation was performed with the total cumulative displacement as objective criterion. This is 14 mm of displacement in 1996 and 1997 (figure 8.1). Consequently, the calculated displacement velocities are integrated over time to come to the cumulative displacement values. The calibration focuses on the determination of the thickness of the creep zone and its absolute depth. This is also studied as a function of the dynamic viscosity values.

As it is generally very hard to deduce a unique parameterisation for a creep model, a sensitivity analysis is performed in order to narrow down the number of possible solutions for the Beline slope. With a creep model, it is necessary to delimit the creep zone, both in absolute depth (compared with the ground water level) and in total thickness. Two extreme interpretations of the inclinometer results can be given with respect to the deformation zone: a) a creep zone between 3 and 6 m, or b) a thin slipsurface or interval around 4.50 m below surface (see also § 8.2).

The depth where the shear stress (τ) exceeds the yield strength (τ_0) is the upper limit of the creep zone. Therefore one needs the ground water level at which movement was initiated. Starting with the parameterisation of table 8.3 and taking a ground water level of 4 m depth, the top of the creep zone then lies at 4.44 m depth. With a ground water level at 4.1 m below surface the subsurface starts to deform at 4.55 m below surface. As the exact ground water level, which initiated the movement, is unknown, in further analysis, the top of the creep zone was set at 4.5 m below surface.

Displacement by creep can occur, in its extreme, by either a combination of a thick creep zone with relatively high viscosity values or a combination of rigid material and a thin slipsurface with a relatively low viscosity value. This implies that either the creep zone thickness or the viscosity value needs to be tuned in such a way that the modelled cumulative displacement in two years equals the measured displacement under the given ground water level data. As a first step in the analysis of the displacement of the Beline

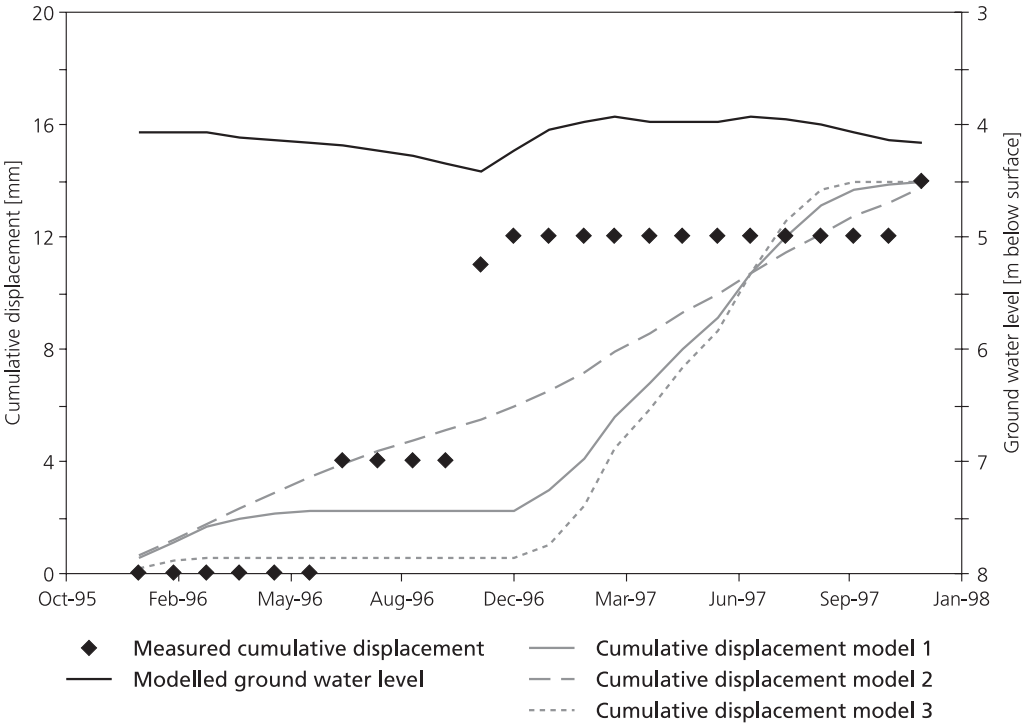

Figure 8.9 Results of the Yen creep model with different combinations of creep zone thickness and viscosity values. The dynamic viscosity and creep zone thickness are: model 1: $\eta=2.0*10^{8}$ kNs/m^2, creep zone from 4.50-4.67 m.; model 2: $\eta=1.3*10^{10}$ kNs/m^2, creep zone from 4.50-6.00 m.; model 3: $\eta=6.0*10^{6}$ kNs/m^2, creep zone from 4.50-4.51 m. Other parameterisation is given in table 8.3.

Table 8.4 Relationship of the thickness and depth of the slipsurface with the calibrated dynamic viscosity.

Slipsurface	Interval [cm]	Dynamic viscosity [kNs/m^2]
10 cm	445-455	6.00E+07
	450-460	8.00E+07
	455-465	1.20E+08
	460-470	1.60E+08
1 cm	440-441	1.20E+06
	445-446	3.50E+06
	450-451	6.00E+06
	455-456	9.00E+06
	460-461	1.40E+07
	465-466	1.80E+07
	470-471	2.50E+07

slope, the laboratory viscosity value (table 8.3) was used. This gives a creep zone of 17 cm thickness. Figure 8.9 (model 1) shows the calculated displacement using the creep model with a deformation layer between 4.50 and 4.67 m depth compared with the measured inclinometer cumulative displacement.

In contrast, the calibration of the creep model can also start assuming that the thickness of the creep zone is known from the inclinometer tube registration: from 4.5 to 6 m depth. The laboratory viscosity results are in that case assumed to be less reliable. Under these assumptions, it is necessary to increase the dynamic viscosity value for the soil almost 100 times to tune the calculated and measured cumulative displacement (figure 8.9, model 2). This results in an almost continuous creep velocity for two years. Model 3 in figure 8.9 assumes a creep zone of only 1 cm, from 4.50 to 4.51 m below surface. In this case the dynamic viscosity has to decrease to $6*10^6$ kNs/m^2 to match measured and calculated cumulative displacement.

From the above it is clear that when the dynamic viscosity is allowed to be optimised too, an infinite amount of parameterisation can be obtained to tune measured and calculated displacement. Table 8.4 gives a few examples of combinations of creep zone thickness, absolute depth and dynamic viscosity values.

Table 8.4 shows that creep patterns with a slipsurface of e.g. 1 cm need much lower dynamic viscosities, and are very sensitive for absolute depth. A subsurface with a creep zone of low viscosity is also very sensitive for the height of ground water above the slipsurface. Figure 8.10 shows the resulting displacement in one month when the maximum ground water level would increase with maximum 25 cm. Here also the example models 1, 2 and 3 of figure 8.9 are used.

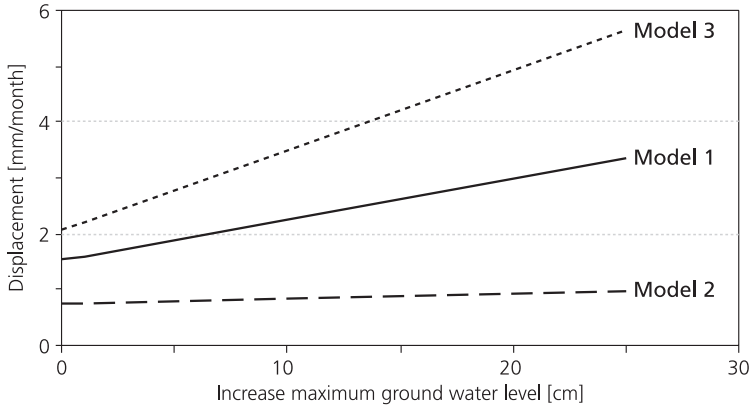

Figure 8.10 Changes in monthly displacement as a function of an increase of the maximum ground water level (March 1997) for example models 1, 2 and 3 (see figure 8.9).

The displacement at the Beline site that was measured with the inclinometer shows intermittent steps of movement (with a temporal resolution of a month). From the above it can be deduced that the displacement at the Beline site cannot be the result of a creep zone of several meters. In that case continuous creep should have been recorded. On the other hand, a slipsurface of e.g. 1 cm results in discontinue steps of displacement but would show significant acceleration of displacement as a consequence of only minor ground water level rises. This is hard to check while no reliable ground water level time

series at the inclinometer is available. The measured ground water time series of D1 and D2 suggest that high ground water levels hold for one week to more than a month. Such prolonged periods of high ground water points in the direction of a somewhat more gradual creep process.

The combination of a measured viscosity value of $2*10^8$ kNs/m^2, the intermittent character of the inclinometer displacement and the measured time span of high ground water levels suggest that the Beline site is subject to a displacement process of creep in a limited creep zone of several cm's to dm's. Therefore, the creep model of 17 cm thickness from 4.50 to 4.67 m below surface with a dynamic viscosity equal to the laboratory tests of $2*10^8$ kNs/m^2 , was chosen to represent the Beline slope and was taken as point of departure for the scenario study.

Quantification of the effects of ground water level changes on dynamic slope movement

As an example the effects of changes in potential evapotranspiration (PET) on creep behaviour of the Beline slope was studied. Figure 8.11 gives the changes in ground water level at location D3 on the changes in potential evapotranspiration. Figure 8.12 gives the resulting changes of monthly displacement. It shows a doubling of the displacement in case of a 10 % decrease of PET and a 4 to 7 times higher displacement velocity in case of a 20 % decrease in PET. An increase in PET will generally stop the creep process in the Beline slope.

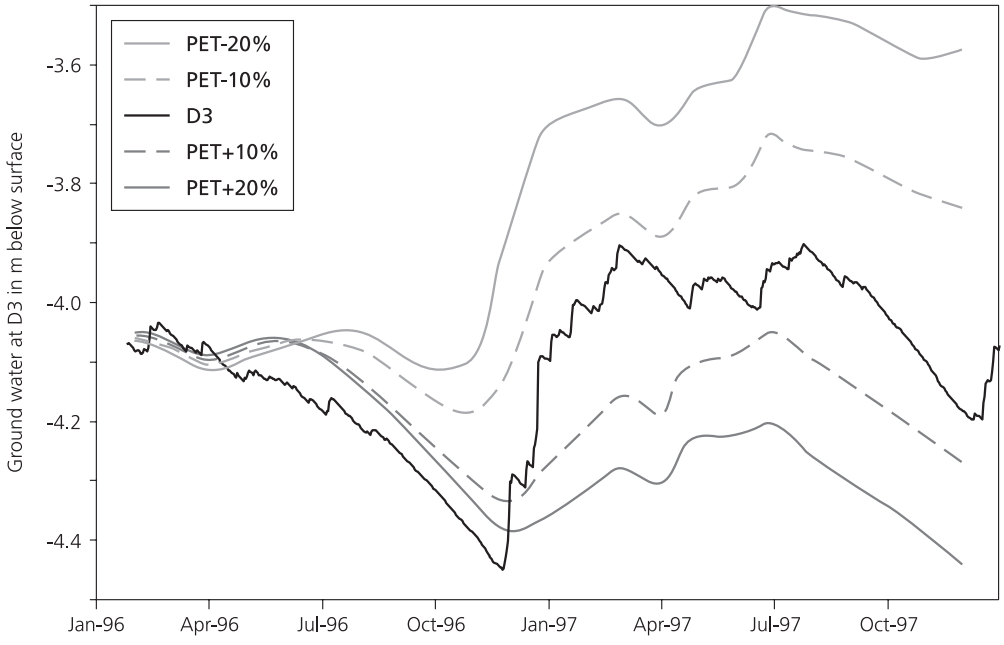

Figure 8.11 Changes in ground water level as a result of changes in potential evapotranspiration.

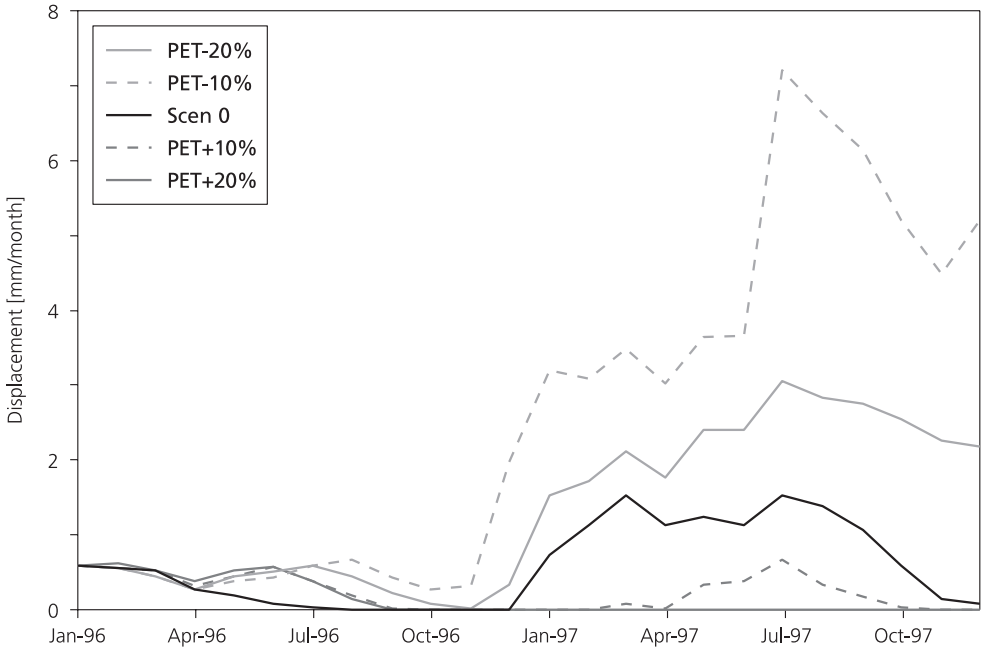

Figure 8.12 Effects of changes in potential evapotranspiration on the displacement velocity of the Beline slope.

In a two years period, a total displacement of 14 mm was measured whereas a decrease of PET with 10 % results in a total displacement of 30 mm and a PET decrease of 20 % gives 70 mm of displacement. This is the reaction on an increase of ground water level of respectively 20 and 40 cm. These increases in ground water level seem very realistic compared to the ground water level measurements. Clearly, not (only) the absolute ground water level increase but rather the duration of the higher ground water level is important for the total displacement.

Another aspect is well illustrated in figure 8.12. The first year the slope is subject to wetting, the effects are nearly negligible. In this period the system has the resilience to buffer the increased input. After the buffer is full, the ground water levels climb and the displacement accelerates.

Conclusion for the study of the displacement of the Beline slope.

A study was performed to analyse the creep behaviour of the Beline slope. The following points should be highlighted:

- The interpretation of the inclinometer data showed that the Beline system exhibits intermittent displacement (on a monthly temporal scale).
- It is interesting to note that the creep tests (simple shear viscosity tests) delivered indeed a residual strength value with nearly zero cohesion and a lower friction angle. Therefore, it can be concluded that the laboratory viscosity tests supported the (theoretical) creep model of Yen. This model assumes viscosity to be independent of normal stress and the creep threshold (yield strength) to be related to the residual strength of the material.

- The direct shear tests of disturbed samples (table 8.1), the sensitivity analysis of the static slope stability failure (§ 8.3) as well as the analysis of the viscosity tests in terms of residual strength, show residual angle of internal friction of around 18-19°.
- Using the parameterisation of table 8.3 it was recognised that the soil deformation behaviour of the Beline slope had to be limited to a small creep zone. The exact thickness of the creep zone could not be determined. As the Beline site showed only limited displacement, but was subject to ground water level fluctuations of decimetres, it can tentatively be concluded that the displacement at the Beline slope is not concentrated in a slipsurface of a few millimetre thick but in a creep zone with cm or dm dimensions. The creep zone is presumably situated between 4.5 and 5 m depth.
- The kinematic sensitivity for ground water level changes is strongly influenced by the thickness of the creep zone. A creep zone of 1.5 m is not sensitive to ground water level changes. Such a system has a continuously slow displacement under its own weight. On the contrary a thin slipsurface is highly sensitive to ground water level fluctuations, especially if it has limited ground water above the slipsurface. A few centimetres of ground water level rise may then lead to a catastrophic acceleration of the displacement.
- The changing ground water conditions as a result of changes in climate or land use have two important consequences for the creep displacement at the Beline slope. Acceleration of the displacement will occur because of an increased ground water level. Probably more significant is the impact of prolonged periods of high ground water level. This prolonged period of movement is for slopes, which encounter creep features, probably the most important factor for catastrophic failure.
- Although the creep process seems to be responsible for the measured displacement at the Beline site, the data limitations make it impossible to unravel the mass movement process beyond doubts. The assumptions of isotropic and time independent material and stress conditions cannot be validated. The lack of well-recorded ground water level data at the inclinometer tube limits strongly the interpretation. Even more important is the absence of information on the depth and the thickness of the slipsurface or creep zone. Every study on the transient behaviour of a slope remains largely hypothetical if the latter information is missing. The analyses described above show that new techniques for displacement observations which follow the deformation profile without constraints are very important.

9 SUMMARY

PART I GENERAL INTRODUCTION

This thesis is a follow-up of the 1993-1997 EU-funded Hycosi project (Leroi, 1997). The aim of the Hycosi project was to improve the knowledge of water circulation in the ground, from site scale to basin scale, in order to understand the impact that hydrometeorological changes have on slope stability. The data gathered in this project formed the starting point of the research described here.

The objective of this thesis is to analyse and quantify hydrological processes in clayey slopes susceptible to landsliding.

The following questions are raised:

- What can hydro- and geochemistry add to our knowledge of a hydrological system in an unstable clayey slope?
- What processes dominate the ground water recharge in unstable clayey slopes and how can the ground water recharge be quantified?
- What is the consequence of changes of land use or climate for unstable slopes?

2 Literature review on hydrology and mass movement

In mass movement research (ground) water plays an important role in both the saturated and unsaturated zones. The influence of pore water is incorporated in the effective stress model for strength calculations of the soil.

In order to understand the influence of water on mass movements better, in chapter 2 a classification is presented of landslide triggers and causes. Temporal aspects of the development of a landslide have up till now not received due attention in such classifications. The words ‘cause’ and ‘trigger’ of a landslide are not synonymous. The trigger is the final external stimulus of a landslide, but the cause can be a long-term process like weathering or a change in ground water regime or land use. Cause and trigger can coincide when processes act on a short time scale, as with an earthquake trigger. For thorough understanding of landslide processes, it is necessary to determine both the trigger and the cause of a landslide. This, however, is not always a straightforward procedure.

Chapter 2 also presents a review of hydrological research in mountainous terrain. With the development of computer modelling, deep ground water circulation is modelled and nested ground water systems are quantified. A lot of research attention is spent on hillslope processes. These studies focus to a large extent on surface water, surface erosion and stream flow response. The infiltration process received a lot of attention in order to determine overland flow. Research on hillslope infiltration has shown that slope downward water transport through the unsaturated zone is very unlikely, unless clear heterogeneity or anisotropy exists parallel to the slope. In most cases one can safely state that percolation of water in hillslopes is a near-vertical, 1D process.

Enormous research attention over the past decades was spent on unsaturated zone hydrology from a more agricultural point of view. This often very detailed, process-

related research specifically concentrated on the root zone. In these studies the water availability and not the ground water recharge was the most important research objective. A general conclusion is thus that the unsaturated zone and ground water recharge in hillslopes received only very limited attention, especially so for clayey slopes.

All the hydrological research in relation to agriculture gained us enormous insight in the behaviour of water in the unsaturated zone. The piston flow concept of matric flow is nowadays almost totally replaced by the concept of preferential flow. The words 'preferential flow' do not specifically refer to macropore or fissure flow, but more to flow as a consequence of state-dependent anisotropy or heterogeneity, that is: prolonged wet (moist) 'subsurface fingers' transport water from the surface to the ground water system.

The literature review showed that many different hydrological models exist (most of them 2D) of which some are linked to stability models. This is to facilitate scenario calculations for slope stability. Some are built within a GIS environment and some use GIS for pre- and post-processing.

PART II GEOCHEMICAL STUDY

3 The potential of geochemical techniques in identifying hydrological systems

This chapter's objectives are twofold:

- to test the potential of cation exchange capacity (CEC) analysis for refinement of the knowledge of the hydrological system in landslide areas, and
- to examine two laboratory CEC analysis techniques on their applicability to partly weathered marls.

Two laboratory techniques, the NH_4Ac and NaCl methods, are tested. Also, the geochemical results are compared with the core descriptions and interpreted with respect to their usefulness.

Both analysis techniques give identical results for CEC, and are plausible on the basis of the available clay content information. The determination of the exchangeable cations was more difficult, since part of the marls dissolved. With the ammonium-acetate method more of the marls are dissolved than with the sodium-chloride method. This negatively affects the results of the exchangeable cations. Therefore, the NaCl method is to be preferred for the determination of the cation fractions at the complex, be it that this method has the disadvantage that the sodium fraction cannot be determined. To overcome this problem it is recommended to try and use another salt e.g. $SrCl_2$ as displacement fluid.

Both Alvera and Boulc-Mondorès examples show transitions in cation composition with depth. It was shown that the exchangeable cation fractions can be useful in locating boundaries between water types, especially the boundary between the superficial, rain fed hydrological system and the lower, regional ground water system. The above-mentioned information may be of great importance for landslide interventions since the hydrological system and the origin of the water need to be known in detail. It is also plausible that long-term predictions of slope stability may be improved by knowledge of the hydrogeochemical evolution of clayey landslides.

In the Boulc-Mondorès example the subsurface information that can be extracted from CEC analyses was presented. In the Boulc-Mondorès cores deviant intervals of CEC could be identified. These are interpreted as weathered layers that may develop or have already developed into slipsurfaces. The CEC analyses of the cores revealed 'differences in chemical composition' that can have an influence on slope stability. It is known that the chemical composition of a soil may have a large effect on the strength parameters of the material. The technique described in chapter 3 can also be used before core sampling for laboratory strength tests. The major problem of the CEC analyses turned out to be the explanation of the origin of the differences found in the core samples.

From the above it is concluded that geochemistry is a potentially valuable technique for e.g. landslide research, but it is recognised that still a lot of work has to be done before the technique can be applied in engineering practice.

PART III PHYSICAL AND HYDROLOGICAL ANALYSIS

4 Characterisation of the Beline study area

This chapter describes the Beline study site and presents an overview of previous work. This previous research is characterised by a geotechnical, small-scale investigation in the direct vicinity of the endangered children's hospital (MES). The artificial drainage structures that were present next to the MES posed a problem for the hydrological research. With the onset of the Hycosi-project the research was extended from a local, geotechnical scale to a medium, process-oriented scale including the entire upper slope area.

After the geological, geomorphological and geophysical surveys followed six drillings for the installation of pore water pressure devices and an inclinometer. Moreover, manual drillings for soil moisture probes and for soil sampling were undertaken. As the Beline slope is situated adjacent to a karstified limestone plateau (Clucy plateau), a tracer study was set up to determine the karst drainage direction. The tracer test showed that most of the Clucy plateau does not drain towards the Beline slope. Only the drainage direction of the small area directly adjacent to the Beline slope could not be ascertained.

The Beline area consists of abundant small to medium scale, slow mass movements. The area covers 36 ha, has an average slope of 17° and an elevation ranging from 345 to 600 m. The intermittent slow movements occur in the remoulded weathered marls consisting of silty clay materials with local intercalations of gravel deposits. A combination of different field techniques such as geophysical surveys and manual and mechanical auger holes revealed the existence of three layers. At the surface lie five meters of disturbed silty loam deposits characterised by low sorting, high gravel content and low density. Underneath this lies a layer, varying from five meters thickness downslope to ten meters thickness upslope, consisting of remoulded silty marls with variable gravel content. Compact blue marls that sometimes contain limestone concentrations underlie the two layers. The ground water level varies between three and six meters below the surface. Moreover, field observations show that the unsaturated zone is characterised by a permeable topsoil of 40 cm. An impression of the hydraulic characteristics of the Beline slope was perceived by the results of numerous field and laboratory tests.

5 The evaluation of the hydrological time series

In chapter 5 the meteorological and hydrological data collected at the Beline slope were analysed. On-site precipitation measurements were compared with the nearest climate station of Météo France, Arbois to evaluate their representativeness for the Beline site. Also a quality control was performed on the hydrological data. The meteorological and the hydrological time series were statistically related. These statistical relationships were integrated in a conceptual model of the hydrological processes of the slope.

It was shown that the precipitation data from the Météo France station in Arbois are representative for the meteorological situation encountered at the Beline slope with the logical exception of locally occurring, convective summer storms. Furthermore analyses showed that the rainfall intensities in general are rather low. For evapotranspiration only the daily potential evapotranspiration as determined for the Arbois climate station using the Penman-Monteith method was available.

The results from the 18 soil moisture probes placed at six locations at three depths and the five pore pressure devices were evaluated. The soil moisture probes within the first meter generally functioned properly, whereas below one meter no data could be gathered. Two representative soil moisture time series were constructed from these data, one extending from the surface to 40 cm depth and one from 50 to 100 cm depth. The soil moisture content on the research slope fluctuated between 20 % and 55 %. The driest soil was encountered in October at the end of the meteorological precipitation deficit period, whilst the wettest conditions were encountered in February at the end of the precipitation surplus period. Of the five pore pressure devices, three performed properly during (part) of the monitoring period (1996-1997). The ground water level within the Beline slope lies between three and six meter below surface and the amplitude of the fluctuations is some 30 cm.

The meteorological and hydrological time series were statistically analysed using different lagged time intervals to reveal time delay and correlations between the two. Both cross-association (or ‘matching’) and linear cross-correlation analyses were used. The results showed that the soil moisture content increases within 48 hours after the onset of a rain event. The correlation between precipitation and shallow soil moisture values is stronger than with deeper soil moisture values. The ground water system showed a tendency to react on precipitation after a time delay of approximately five days. The analyses show that the correlation between precipitation and ground water level fluctuation is weak.

The analyses described above are especially useful to determine short term relationships or fast responses. To analyse seasonal relationships a method of relating standardised (and filtered) time series was used. Causal relationships in the hydrological system could be visualised on a monthly time scale. It was shown that the soil moisture system reacts on periods of above or below average effective precipitation input. It was also shown that between the soil moisture and ground water systems changes from positive to negative standardised values of soil moisture content correspond to a local maximum ground water level and vice versa. This is a strong indication that the Beline slope, when considering a longer time-scale, is in perfect (steady-state) balance with the local climatological circumstances.

This led to the description of a conceptual model of the hydrological system at the Beline site. The ground water level within the Beline slope fluctuates, especially on a seasonal time scale, as a response to the climatological system (with emphasis on the

evapotranspiration). The response is attenuated and delayed in the unsaturated zone. Fast preferential flow through the four meter thick unsaturated zone exists, but does not cause large quantities of ground water recharge. Furthermore it was concluded that these faster fluxes have too large a time delay (5-6 days) to be the result of an open fissure system.

6 The unsaturated zone

The main objectives of this part of the research can be summarised with the question: Is it possible to quantify the hydrological behaviour of the Beline unsaturated zone with a deterministic model and what is its predictive value? A further objective is to quantify the effect of changes in land use or climate on ground water recharge. A set of empirical models was defined. Also a physically-based model was built with the Hydrus 1D computer code. The physically-based model used precipitation and potential evapotranspiration to describe and predict the soil moisture content and subsequently the unsaturated zone water flux or ground water recharge at the Beline slope. One year of data was used for calibration: ground water level data for the empirical models and data on soil moisture content for the physically-based model. The remaining data was reserved for validation.

The empirical models used effective precipitation and standardised soil moisture time series as input and tried to describe and predict the ground water level fluctuations. After validation, it was concluded that none of the proposed linear empirical models was capable of quantitatively describing the hydrological system. However, the linear empirical models were very useful for analysing the hydrological system. They confirm the finding of chapter 5 that precipitation only offers a very limited predictive value for ground water level fluctuations and that the soil moisture content is a much better predictor for ground water level fluctuations.

The hydraulic parameters of the Van Genuchten-Mualem unsaturated permeability model were calibrated with the physically-based unsaturated zone model using an inverse modelling procedure with soil moisture content as objective time series. This did not result in a unique set of hydraulic parameters. The parameter outcome showed high correlations between the hydraulic parameters within each layer. Also, sensitivity analysis of the inverse model showed that a calibration set of one year was too limited. It was shown that the ground water level (a lower boundary condition in the unsaturated zone model) did not seemingly influence the model calibration (parameter optimalisation). It did however influence the timing and amplitude of the unsaturated zone water flux or ground water recharge. After the fixation of ground water depth and the hydraulic parameter with the highest correlation with the other parameters, a second inverse model was run to finalise the model calibration. Validation of this unsaturated zone model showed the robustness of the model.

As the validation results of the model were positive, the unsaturated zone model was used to quantify the effects of land use or climate changes. These changes affect the input time series and were addressed with a sensitivity analysis. A two year wetting scenario (10 % more precipitation or 10 % less evapotranspiration) results in a more than doubled ground water recharge for that period. The opposite, an increase in potential evapotranspiration with 10 %, has very limited effect on the ground water recharge, because the soil moisture deficit near the surface restrains actual evapotranspiration.

Generally, it was concluded that (on a short-time scale) wetting is much more influential than drying.

7 The saturated zone

This chapter describes the 2D modelling of ground water level fluctuations, i.e. the schematisation, calibration and validation. It focuses on the effects of ground water recharge time series on the modelling of the saturated zone. The objectives of this chapter are

- to model the spatial distribution of pore water pressure for slope stability calculations,
- to determine the ground water recharge, and
- to quantify the influence of changes in land use or climate on the hydrological behaviour of the slope.

The proposed methodology to study the ground water level fluctuations in clayey slopes consists of separately modelling the unsaturated and saturated zone. Since the results of the unsaturated zone model in chapter 6 showed a decoupling of the unsaturated zone water transport and the saturated zone water level this could be done in such a way. The unsaturated zone model results in a bottom flux or ground water recharge flux, which is the upper boundary condition of the ground water model.

After calibration of the steady-state ground water level at the Beline slope, the modelled ground water levels could not match all measured ones. Therefore, the first objective of the ground water level modelling could not fully be met. The subsurface schematisation of the slope turned out to be way too simplified for modelling the spatial distribution of the ground water level.

Using the ground water recharge time series from the unsaturated zone model of chapter 6, the ground water level fluctuations could not be modelled. The calculated ground water patterns were much too attenuated and smooth. Identically, it was shown that the ground water level fluctuations in the clayey Beline slope could not be explained using a fraction of the precipitation as ground water recharge. The results showed no seasonal variation. The role of the saturation grade of the unsaturated zone is indispensable, but also that of the rain events. Therefore, for the calculation of a ground water recharge time series a model is proposed that combines the state of the unsaturated zone with precipitation data, the so-called ‘state-dependent recharge function’. It transforms precipitation to recharge by scaling it with soil moisture conditions. The ratio of the matric bottom flux and the average matric bottom flux is used as a function of the soil moisture condition. This ground water recharge series was shown to better describe the ground water level fluctuations. When no soil moisture data are available, an empirical sinusoidal function was proposed which imitates the state of the unsaturated zone. The state-dependent recharge model proved to be a straightforward and useful method to determine the important recharge time series that are used as input for ground water modelling.

The last objective of this chapter is to quantify the influence of changes in ground water recharge on the ground water level fluctuations. The ground water recharges have been calculated with the unsaturated zone model as response to changes in input time series. It was shown that the hydrological system could buffer almost one year of changed ground water recharge. It is just after this year that ground water really starts to react. In this second year the ground water level can rise 20-30 cm higher than under the

formerly normal situation as a reaction on only a 10 % increase in precipitation or 10 % decrease in potential evapotranspiration. The general trend of all the (short term) model scenarios was that changes resulting in wetting had more effects than changes resulting in drying.

PART IV GEOTECHNICAL ANALYSIS

8 Stability and displacement

The aim of this chapter is to analyse the movement of the landslide at the Beline slope and to determine the effect of ground water level fluctuations on the stability of the Beline slope. The outcome of this investigation largely depends on the geotechnical characteristics of the slope and the mass movement processes. In this chapter the field and laboratory geotechnical analysis are presented.

The inclinometer measurements show a total displacement of 14 mm in two years. Besides the standard geotechnical strength tests like direct shear and triaxial tests, simple shear viscosity tests were executed with different levels of normal stress. The results of the creep tests, being simple shear viscosity tests, support the (theoretical) creep model of Yen. This model assumes viscosity not to be a function of normal stress and the creep threshold (yield strength) to be related to the residual strength of the material.

The analysis showed that the detected displacement pattern at the Beline slope appeared to be a creep process. The creep zone was dimensioned in the order of 10-20 cm and is most likely to be located between 4.5 and 5 m depth.

Changing ground water conditions as a result of changes in climate or land use have two important consequences for creep displacement at the Beline slope. An acceleration of the creep displacement will occur when ground water level increases. Probably more important is that also the time span of relatively high ground water levels increases which results in an increase in cumulative displacement. Such periods of prolonged displacements are probably the most critical factor for the occurrence of catastrophic failure. In this respect a long-term change in vegetation pattern is likely to have much more effect than a short-term change in meteorological input.

SYNTHESIS

Conceptual model of the hydrological processes in clayey slopes.

The main objective of this thesis is to “analyse the hydrological processes in unstable clayey slopes”. This objective is the central theme of the thesis. From the analyses described in this thesis a conceptual model of the hydrological behaviour of the studied slope can be given. It concerns a fine-grained (silt-clay) slope in a temperate climate with grass cover.

The ground water level within such a slope fluctuates especially on a seasonal time scale. The unsaturated zone attenuates and delays the precipitation. The seasonality of ground water recharge implies that only in the case of a moist unsaturated zone, recharge

occurs during rain events. Therefore precipitation has only a very limited predictive value for ground water level fluctuations. Combined with soil moisture content, a much better predictor for ground water level fluctuations arises.

It is hypothesised that the recharge through a fine-grained subsurface with low (matric) permeability is facilitated by preferential matric flow paths ("fingers"). These paths distinguish themselves not as much by texture differences, but more by state-differences, i.e. differences in soil moisture content and consequently differences in hydraulic conductivity.

Recommendations for further research

With this work the research on the ground water recharge processes over several meters of fine grained (clayey) material is not finished. Especially the visualisation of the patterns of water transport in the deeper unsaturated zone lacks. The following recommendations for further hydrological landslide research are given:

- The use of geochemical techniques for visualising hydrological processes should be evaluated further.
- Further research should be aimed at improving both the measurement techniques and equipment for measuring hydrological variables in clayey soils.
- Displacement research is hampered by a lack of detailed in-situ subsurface displacement information, in part due to the stiffness of inclinometer tubes. Also, the measurements should at least have a vertical resolution in the order of centimetres. Improvements in this field must thus be sought.

ANALYSE VAN HYDROLOGISCHE PROCESSEN IN ONSTABIELE KLEIHELLINGEN

SAMENVATTING

Dit proefschrift komt voort uit het door de EU gesubsidieerde Hycosi project dat liep van 1993 tot 1997. De belangrijkste doelstelling van het Hycosi project was om de kennis op het gebied van de stroming van water in de ondergrond van onstabiele hellingen te vergroten om zo de gevolgen van veranderingen in het hydrologische en meteorologische systeem op stabiliteit van een helling beter te kunnen inschatten. De gegevens die zijn verzameld in het Hycosi project vormde de basis voor dit promotie-onderzoek.

De doelstelling van dit proefschrift is om de hydrologische processen in kleihellingen die gevoelig zijn voor aardverschuivingen te analyseren en kwantificeren. De volgende vragen zijn daarbij opgeworpen:

- Wat kan hydro- en geochemie bijdragen aan onze kennis van het hydrologische systeem in kleihellingen?
- Welke processen domineren de grondwater aanvulling in onstabiele kleihellingen en hoe kunnen die worden gekwantificeerd?
- Wat zijn de consequenties van veranderingen in landgebruik of klimaat voor onstabiele hellingen?

2 Literatuur overzicht

In massabewegingen speelt water een belangrijke rol. De invloed van poriewater zit verwerkt in het zogenaamde effectieve spanningsmodel voor sterkte berekeningen van de bodem. Dit beschrijft hoe door stijging van het grondwater de druk op de gronddeeltjes afneemt, waardoor de bodem minder interne sterkte kan ontwikkelen.

Om de invloed van water op aardverschuivingen goed te kunnen begrijpen wordt er in hoofdstuk 2 eerst een klassifikatie gegeven van de oorzaken en de triggers van aardverschuivingen. De factor tijd heeft tot nu toe redelijk weinig aandacht gekregen bij zulke klassificaties, terwijl dat het principiële verschil is tussen een ‘oorzaak’ en een ‘trigger’ van een aardverschuiving. De trigger is de laatste externe ‘prikkel’ voor een aardverschuiving, maar een oorzaak kan een langdurig proces zoals verwering of grondwaterregime verandering zijn. De oorzaak en trigger kunnen samenvallen als het om processen met een korte tijdschaal gaat, zoals een aardbeving. Hoewel het erg lastig is om zowel de trigger als de oorzaak van een aardverschuiving te bepalen is het voor een goed begrip van de onderliggende processen van aardverschuivingen wel noodzakelijk.

Dit hoofdstuk geeft ook een overzicht van hydrologisch onderzoek in bergachtig gebied. Met de ontwikkeling van computer modellering van grondwater stroming, bleek het goed mogelijk om diepe grondwater circulatie in bergachtig gebied te berekenen. Hieruit bleek dat grondwater stroming op zowel lokale als regionale schaal kan optreden. Deze systemen liggen op elkaar gesuperponeerd.

Veel onderzoek is gedaan naar de hydrologische processen in en op (beboste) hellingen. Deze studies hebben zich sterk gefocussed op oppervlaktewater, erosie en de gevolgen hiervan voor het riviersysteem. Het infiltratieproces was hierbij van belang om

te bepalen hoeveel water overbleef om direct naar de rivier te stromen. De processen van grondwater percolatie (infiltratiewater dat verder stroomt naar het grondwater systeem) kregen in deze studies veel minder aandacht. Het infiltratie onderzoek op hellingen heeft wel aangetoond dat er geen hellingafwaartse transport in de onverzadigde zone plaatsvindt, anders dan in gevallen van extreme heterogeniteit of anisotropie parallel aan de helling. Percolatie van water in hellingen is dan ook te zien als een vertikaal, één dimensionaal proces.

In meer landbouwkundig hydrologisch onderzoek heeft de onverzadigde zone heel veel aandacht gekregen, maar deze studies bleven veelal beperkt tot de eerste meter van de bodem. Recent, en zeer gedetailleerd, hydrologisch onderzoek in de onverzadigde zone heeft een enorme hoeveelheid kennis opgeleverd over de preferente stroming van water in het bovenste deel van de bodem. Dit duidt niet noodzakelijkerwijs op stroming door macroporiën of breuken, maar meer op stroming als gevolg van toestand afhankelijke anisotropie of heterogeniteit. Dat wil zeggen: persistente natte structuren (‘vingers’ genaamd) transporteren het neerslag water van het bodemoppervlak richting het grondwater systeem.

In zijn algemeenheid kan gesteld worden dat aan de grondwater aanvulling in hellingen weinig onderzoek is verricht.

3 Wat is het potentieel van geochemie voor hydrologisch onderzoek in kleihellingen?

Dit hoofdstuk heeft de volgende doelstellingen:

- Het testen van de mogelijkheden van cation uitwisselingscapaciteit (CEC) analyse voor het verbeteren van de kennis van het hydrologische systeem in aardverschuivingsgebied
- Het vergelijken van twee laboratorium methoden voor geochemische bepalingen op hun toepasbaarheid op gedeeltelijk verweerde mergels

De NH_4Ac en NaCl methoden ter bepaling van de CEC gaven identieke resultaten. De bepaling van de uitwisselbare cationen met deze methoden bleek lastiger, aangezien een deel van de mergels oploste. Met de ammonium-acetaat methode loste meer van de mergel op dan met de natriumchloride methode. Hierdoor heeft de NaCl methode de voorkeur gekregen, al heeft dat als nadeel dat de natriumconcentratie bepaling moest komen van de NH_4Ac methode. Om dit probleem te voorkomen wordt voorgesteld om een ander zout, bijvoorbeeld $SrCl_2$ als verplaatsingoplossing te gebruiken.

De geochemische analyses van zowel de Alvera modderstroom als die van Boulc-Mondorès gaven duidelijke verschillen van chemische samenstelling van het uitwisselingscomplex met de diepte aan. Vooral het verschil tussen natrium aan het complex (mariene oorsprong) en calcium aan het complex (zoetwater oorsprong) was duidelijk waarneembaar. Dit toont aan dat de uitwisselbare cation fractie een potentieel waardevolle techniek is voor het begrenzen van hydrologische systemen in de ondergrond: bijvoorbeeld de grens tussen het oppervlakkige, door regen gevoede systeem en dieper liggende regionale grondwater systeem. Deze informatie is van belang om de oorsprong van het water in de ondergrond te achterhalen. Het is bijvoorbeeld mogelijk dat de lange termijn stabiliteit van een helling beter ingeschat kan worden als er inzicht is in de lokale hydrogeochemische processen.

In het geval van de Boulc-Mondorès boorkernen kon ook veel informatie van de ondergrond verkregen worden met behulp van de CEC bepalingen. Lagen met verschillende CEC waarden konden worden onderscheiden. Deze lagen zijn geïnterpreteerd als lagen met een hogere graad van verwering die zich zouden kunnen ontwikkelen (of al hebben ontwikkeld) tot een glijvlak. De CEC bepalingen toonden interne verschillen aan in chemische samenstelling die mogelijke de stabiliteit van de helling beïnvloeden. Het is bekend dat de chemische samenstelling van een bodem grote invloed kan hebben op de sterkte karakteristieken van het materiaal.

Het grootste probleem met de hier beschreven techniek bleek de verklaring voor de oorsprong van de gevonden chemische verschillen te zijn. Uit bovenstaande kan daarom worden geconcludeerd dat geochemie in potentie een bruikbare techniek is voor onder andere in aardverschuivingsonderzoek, maar dat er nog veel werk verricht zal moeten worden voordat de techniek bruikbaar zal zijn in de dagelijkse geotechnische praktijk.

4 De karakterisatie van het Beline onderzoeksgebied

Dit hoofdstuk beschrijft de Beline onderzoekhelling en geeft een overzicht van het werk dat hier is uitgevoerd. In het begin vond het onderzoek vooral plaats in de directe omgeving van het bedreigde kinderziekenhuis en werd het gekarakteriseerd door kleinschalig, geotechnisch onderzoek. Met het Hycosi onderzoeksproject werd het onderzoeksgebied ruimer gedefinieerd, namelijk de hele bovenliggende helling en werd het onderzoek veranderd in medium-schaal en proces geörienteerd.

Na het geologisch, geomorfologisch en geofysisch onderzoek werden zes boringen voor de plaatsing van één inclinometer en vijf waterdrukopnemers gezet. Tevens werd de helling voorzien van zes locaties met drie bodemvochtmeters. Monsters werden genomen van de ondergrond voor hydrologische en geotechnische bepalingen. Aangezien de Beline helling in een karstgebied ligt, is tevens een karst hydrologisch onderzoek uitgevoerd in het naastgelegen kalkplateau. De tracertesten toonden aan dat het grootste deel van het karstplateau van Clucy niet draineert richting de aardverschuiving.

De Beline helling beslaat 36 ha, heeft een helling van gemiddeld 17°. De ondergrond bestaat uit opnieuw afgezette verweerde mergels (siltige klei) met ingesloten kalkgrind afzettingen. Uit het veldonderzoek bleken drie lagen te onderscheiden. Aan het oppervlakte ligt zo'n 5 m dikke afzetting van siltige klei/leem die wordt gekarakteriseerd door een slechte sortering, hoog grindgehalte en lage dichtheid. De laag daaronder varieert in dikte van 5 m hellingafwaarts tot 10 m hellingopwaarts en bestaat uit geremanieerde siltige mergels met variabel grind gehalte. Compacte blauwe mergels met soms een kalkinsluiting liggen onder deze twee lagen. Het grondwater is aangetroffen tussen de 3 en 6 m onder maaiveld. Verder heeft het veldonderzoek opgeleverd dat de onverzadigde zone uit een goed permeabele eerste 40 cm bestaat.

5 Evaluatie van de hydrologische tijdseries

Dit hoofdstuk analyseert de meteorologische en hydrologische gegevens die op en rond de Beline helling zijn verzameld, te weten neerslag, verdamping, bodemvocht en grondwater. Eerst is een kwaliteitscontrole op de tijdseries uitgevoerd. Daarna zijn de meteorologische en hydrologische tijdseries statistisch aan elkaar gerelateerd en is een

conceptueel model voor de hydrologische processen die in de Beline helling spelen, opgesteld.

De lokale neerslag gegevens zijn vergeleken met die van de dichtsbijzijnde klimaatstation van Météo France, in Arbois. Hieruit bleek dat de meteorologische gegevens van Arbois representatief zijn voor de situatie op de Beline helling, met uitzondering van sommige lokale zomerbuien. Verder komt uit de analyse dat over het algemeen de neerslag intensiteiten vrij laag zijn.

De bodemvocht gegevens zijn samengevat in twee tijdseries, één tot 50 cm diepte en één van 50 tot 100 cm diepte. Oktober bleek de droogste bodem te hebben en februari de natste. Dit sluit naadloos aan bij respectievelijk de afsluiting van de neerslagtekort periode van maart-oktober en de neerslagoverschot periode aan het eind van februari. De grondwater gegevens toonde een grondwaterstand aan tussen de 3 en 6 m onder maaiveld met een jaarlijkse fluctuatie van zo'n 30 cm.

Het relateren van de meteorologische en hydrologische tijdseries is gedaan met behulp van cross-associatie ("matching") en cross-correlaties. Door de tijdseries iedere keer één dag van elkaar te laten opschuiven kan de tijdsverschuiving tussen de twee tijdseries bepaald worden. Bodemvocht reageert na maximaal twee dagen en het grondwater reageert gemiddeld na vijf dagen op een periode van regen. Van de laatste is de statistische relatie echter zwak.

De bovenstaande analyse is bedoeld voor het kwantificeren van korte termijn reacties. Om de seizoenale relaties zichtbaar te maken zijn de effectieve neerslag, de bodemvocht en de grondwater tijdseries gestandardiseerd en met elkaar vergeleken. Hieruit bleek dat het systeem reageert op seizoenale overschotten of tekorten. Het grondwater stijgt als gevolg van een bovengemiddelde vochtgehalte dat op zijn beurt het gevolg is van een langdurig neerslagoverschot. Dit is een sterk bewijs voor het in evenwicht zijn van het hydrologische systeem van de Beline helling met de klimatologische omstandigheden.

De bovenbeschreven analyses zijn zeer bruikbaar gebleken voor het zorgvuldig analyseren van een lokaal hydrologisch systeem en leiden dan ook tot een conceptueel model van het hydrologische systeem. De grondwaterstanden reageren voornamelijk op seizoenale veranderingen en amper op individuele neerslaggebeurtenissen. De respons op neerslag is sterk vertraagd en gedempt door de onverzadigde zone. Snelle preferente stroming door de vier meter dikke onverzadigde zone bestaat wel maar zorgt niet voor grote hoeveelheden grondwater aanvulling.

6 De onverzadigde zone

De doelstellingen van dit hoofdstuk laten zich samenvatten met de vraag: "Is het mogelijk het hydrologische gedrag van de Beline onverzadigde zone met een deterministisch model te kwantificeren en wat is dan de voorspellende waarde?". Met een goed werkend deterministsich model is het vervolgens mogelijk om de effecten van landgebruik- of klimaatsverandering op de grondwater aanvulling te berekenen. Een set van empirische modellen was opgesteld. Ook is een fysisch model gemaakt met behulp van de Hydrus-1D software pakket. Één jaar aan gegevens is gebruikt voor calibratie en de rest van de gegevens is gebruikt voor validatie van de modellen.

Voor de empirische modellen zijn effectieve neerslag en gestandardiseerde bodemvocht tijdseries uit hoofdstuk 5 gebruikt als invoerserie om de grondwaterstandfluctuaties te beschrijven en voorspellen. Na validatie was de conclusie

dat niet één van de lineaire modellen in staat was de grondwaterstandfluctuaties betrouwbaar te voorspellen uit neerslag en bodemvocht gegevens. De empirische modellen bleken echter wel erg goed te gebruiken voor het analyseren van het hydrologische systeem. De resultaten bevestigden dan ook de bevindingen van hoofdstuk 5 dat neerslag slechts een zeer beperkte voorspellende waarde heeft voor grondwaterstandfluctuaties en dat bodemvocht conditie een veel betere voorspeller is.

Met Hydrus1D software is een computermodel van de onverzadigde zone gemaakt, waarbij de onverzadigde doorlatendheid beschreven wordt met het model van 'van Genuchten-Mualem'. De hydraulische parameters van het permeabiliteitsmodel zijn met behulp van een stapsgewijze inverse modellering gecalibreerd, waarbij het bodemvocht als objectieve reeks diende. Een gevoeligheidsanalyse op het inverse model maakte onder meer duidelijk dat de grondwaterstandfluctuaties (een ondergrensvoorwaarde van het model) geen merkbare invloed hadden op de parameter optimalisatie. De grondwaterstandsfluctuaties beïnvloeden echter wel het gedrag van de grondwateraanvulling (de onverzadigde zone flux) qua timing en amplitude.

De validaties toonde de robuustheid van het fysisch-mathematische model aan. Hierdoor konden er ook scenario studies doorgerekend worden waarin landgebruik of neerslag- en verdampingsinvoer veranderen. Een twee jaar durende vernatting van de Beline helling (10 % meer neerslag of 10 % minder potentiele verdamping) resulteerde in een verdubbeling van de grondwateraanvulling in die periode. De conclusie is dat in het algemeen (op de korte tijdschaal) een vernatting veel meer invloed heeft dan verdroging.

7 De verzadigde zone, het grondwater

Dit hoofdstuk beschrijft de 2D modellering van de grondwaterstandfluctuaties: de schematisatie, calibratie en validatie. De doelstelling van dit hoofdstuk zijn:

- het modelleren van de ruimtelijke verdeling van de poriedruk in de helling voor de berekeningen van de hellingsstabiliteit
- het modelleren van de grondwaterstandfluctuaties
- het kwantificeren van de invloed van veranderingen in landgebruik en klimaat op het hydrologische gedrag van de helling

De voorgestelde methodologie om grondwaterstandfluctuaties te bestuderen in kleihellingen bestaat uit het afzonderlijk modelleren van de onverzadigde en verzadigde zone. De resultaten van hoofdstuk 6 tonen aan dat deze twee systemen niet gekoppeld zijn en staan zo'n aanpak dus toe.

Het modelleren van de gemiddelde grondwaterstand bleek niet eenvoudig, aangezien de gemeten grondwaterstanden veel spreiding vertoonden. De eerste doelstelling van dit hoofdstuk kan daarom niet volledig vervuld worden. De noodzakelijke schematisatie van de ondergrond blijkt te eenvoudig te zijn om de ruimtelijke verdeling van het grondwater goed te kunnen modelleren.

Grondwaterstandfuctuaties worden gemodelleerd met als input de berekende dagelijkse onverzadigde zone flux (de grondwateraanvullingsreeks). Hiermee bleek het niet mogelijk de gemeten grondwaterstandfluctuaties te volgen. De gemodelleerde grondwaterstanden vertoonden een te vloeiend en vertraagd beeld. Maar ook met het gebruik van (een fractie van) de neerslagreeks als grondwateraanvulling bleek het niet mogelijk de gemeten grondwaterstandfluctuaties te modelleren. Deze resultaten gaven

wel een grilliger verloop van het grondwater maar niet de seizoenale variatie die in het veld was gemeten. De rol van de onverzadigde zone blijkt doorslaggevend voor de mate van grondwaterstandfluctuaties als reactie op de input. Daarom is een 'vochttoestand-afhankelijk' grondwateraanvullingsmodel voorgesteld dat de neerslag transformeert tot grondwateraanvulling door het te schalen naar de vochtcondities van de onverzadigde zone. Als maat voor de vochtcondities is hier de verhouding van de matrix onverzadigde zone flux en de jaarlijks gemiddelde onverzadigde zone flux genomen. Hiermee blijkt de grondwaterstandfluctuaties veel beter te beschrijven dan met andere grondwateraanvullingsreeksen. Als geen bodemvochtcondities bekend zijn, is een empirische sinusfunctie voorgesteld om de vochttoestand van de onverzadigde zone te benaderen. De vochttoestand-afhankelijke functie is een redelijk directe en bruikbare methode om de, voor grondwatermodellering zo belangrijke, grondwateraanvulling uit neerslagreeksen te halen.

De laatste doelstelling van dit hoofdstuk is om de invloed van landgebruik en klimaatsverandering op het grondwatersysteem te kwantificeren. De veranderde grondwateraanvullingsreeksen uit hoofdstuk 6 als gevolg van aldaar gedefinieerde scenarios zijn gebruikt. De resultaten tonen aan dat het hydrologische systeem bijna een jaar aan veranderingen van input kan bufferen. Na dit jaar reageert de grondwaterspiegel des te harder op de veranderingen. In het tweede jaar kan de grondwaterspiegel 20-30 cm meer stijgen dan in de onveranderde situatie op slechts 10 % toenamen van neerslag. De algemene trend van de model scenarios is dat veranderingen die leiden tot vernatting op de korte tijdschaal meer invloed hebben dan de veranderingen die leiden tot verdroging.

8 Stabiliteit en verplaatsing

Dit hoofdstuk heeft tot doel de bewegingen van de aardverschuiving te analyseren en de effecten van veranderingen van de grondwaterstand op de stabiliteit te bepalen. In het veld is de verplaatsing gemeten met een zogenaamde inclinometer. Hierbij wordt de verplaatsing niet alleen aan het aardoppervlak maar ook met de diepte gemeten. Een maximale verplaatsing van 14 mm is waargenomen in 2 jaar. Grondmonsters zijn genomen om de sterkte karakteristieken van het materiaal te bepalen met behulp van directe schuifproeven en triaxiaal testen. Daarnaast zijn ook kruiptesten voor de bepaling van de viscositeit gedaan met verschillende bovenbelastingen (normaal spanning). De resultaten van deze viscositeitstesten ondersteunen het theoretische kruipmodel van Yen. Dit model gaat uit van een normaalbelasting onhankelijke viscositeit en een kruipdrempel die een functie is van de residuele sterkte van het materiaal.

De bewegingsanalyse toont aan dat in de Beline helling sprake is van een kruipproces. De kruipzone is gedimensioneerd op zo'n 20-30 cm en is waarschijnlijk gelocaliseerd op zo'n 4,5-5 m diepte (ter plekke van de inclinometer buis). Veranderingen in de grondwatercondities hebben twee belangrijke consequenties voor de verplaatsing door kruip op de Beline helling. Er zal een grote versnelling van de kruipverplaatsing optreden bij grondwaterstandverhogingen. Maar waarschijnlijk nog belangrijker is dat door de lange duur van relatief hoog grondwater de cumulatieve verplaatsing flink zal toenemen. De impact die de verlengde periode van hoge grondwaterstanden heeft, is waarschijnlijk de meest kritische factor bij het optreden van katastrofaal bezwijken van een helling. Vanuit dit oogpunt heeft een lange termijn verandering van vegetatiepatroon meer invloed dan een korte termijn verandering in klimaatinput.

Synthese

Het centrale thema van dit proefschrift was om de hydrologische processen in onstabiele kleihelling te analyseren. Uit de analyses die beschreven staan in dit proefschrift is een conceptueel model van het hydrologische gedrag van de studie-helling gedestilleerd.

De grondwaterstand in de helling fluctueert voornamelijk op seizoenale tijdschaal. De onverzadigde zone dempt en vertraagt het neerslagsignaal. De seizoenaliteit van de grondwateraanvulling impliceert dat alleen in het geval van een erg natte onverzadigde zone grondwateraanvulling kan plaatsvinden. Hierdoor heeft neerslag een zeer beperkte voorspellende waarde op grondwaterstandfluctuaties. Echter, gecombineerd met bodemvocht ontstaat een redelijke goede voorspeller voor grondwaterstandfluctuaties.

Verder wordt er als hypothese gesteld dat grondwateraanvulling door een fijnkorrelige ondergrond met lage (matrix) permeablititeit plaatsvindt door preferente matrix stroming ("vingers"). Deze stroompaden in de onverzadigde zone onderscheiden zich niet door texturele verschillen van de omgeving maar door een verschil in vochttoestand. Hierdoor ontstaat een groot verschil in doorlatendheid.

Aanbevelingen voor verder onderzoek

- Verder ontwikkelen van geochemische onderzoekstechnieken ten behoeve van hydrologisch onderzoek
- Het verbeteren van hydrologische meetapparatuur die ook goed functioneren in kleiïge (fijnkorrelige) ondergrond
- Het ontwikkelen van flexibelere inclinometers die gedetaillerder inzicht geven in het verplaatsingspatroon van aardverschuivingen

REFERENCES

ANDERSON, M.G., M.J. KEMP & D.M. LLOYD (1988). Application of soil water finite difference models to slope stability problems. In: C. Bonnard (Ed.) Proceedings of fifth international symposium on landslides, Lausanne, 1, pp. 525-530.

ANDERSON, M.P. & W.W. WOESNER (1992). Applied groundwater modelling. Simulation of flow and advective transport. Academy press, Inc., San Diego.

ANGELI, M.-G., R.M. MENOTTI, A. PASUTO & S. SILVANO (1992). Landslide studies in the Eastern Dolomites Mountains, Italy. Proceedings, 6th International Symposium on Landslides, Christchurch, New Zealand, 1, pp. 275-282.

ANGELI, M.G., J. BUMA, P. GASPARETTO, & A. PASUTO (1998). A combined hillslope hydrology/stability model for low-gradient clay slopes in the Italian Dolomites. Engineering Geology, 49, pp. 1-13.

ANGELI, M.-G., A. PASUTO & S. SILVANO (1999). Towards the definition of slope instability behaviour in the Alverà mudslide (Cortina d'Ampezzo, Italy). Geomorphology, 30. pp. 201-211.

ANTOINE P., D. FABER, A. GIRAUD & M. AL HAYARI (1988). Properties geotechnique de quelques ensembles Geologique propices aux glissements de terrain. In: C. Bonnard (ed), Proceedings of the fifth international symposium on landslides, Lausanne, Switzerland, pp. 1301-1306.

APPELO, C.A.J. & D. POSTMA (1993). Geochemistry, groundwater and pollution. Balkema, Rotterdam.

ASTÉ, J-P. (1997). Hycosi project. Etude spécifique 3D de la stabilité du versant de la Béline à Salins-les-Bains (Jura). Rapport JPAc 12997.

BALTASSAT, J.M. & P.CHARBONNEYRE (1995). HYCOSI project: Reconnaissance par méthodes géoélectrrique et sismique réfraction du glissement de terrain des Près Moureaux à Salins-les-Bains (Jura). BRGM report R38571.

BATHURST, J.C. & P.E. O'CONNELL (1992). Future of distributed modelling. The Système Hydrologique Europeen. Hydrological Processes, 6, pp. 265-277.

BELMANS, C., J.G. WESSELING & R.A. FEDDES (1983). Simulation model of the water balans of a cropped soil: SWATRE. Journal of Hydrology, 63, pp. 271-286.

BEVEN, K. & P. GERMANN (1982). Macropores and water flow in soils. Water Resources Research, 18, pp. 1311-1325.

BIERKENS, M.F.P. (1998). Modeling water table fluctuations by means of a stochastic differential equation. Water resources research, 34, pp. 2485-2499.

BJERRUM, L. (1954). Geotechnical properties of Norwegian marine clays. Geotechnique, 4, pp. 49-69.

BOGAARD, T.A. & TH.W.J VAN ASCH (1996). Geophysical and hydrochemical investigation of a complex large-scale landslide in southern France. In: K. Senneset (ed.), Proceedings of the seventh International Symposium on Landslides, Trondheim, Norway, Balkema Rotterdam. pp. 643-647.

BOGAARD, T.A., TH.W.J. VAN ASCH & O. MONGE (1998). Study on the influence of 3D hydrological ground water flow on the stability of a landslide in Salins-les-Bains, eastern France. In: D.P Moore and O.Hungr (eds.), 8th International IAEG Congress, Vancouver, Canada. Balkema Rotterdam. 3, pp. 1765-1772.

BOGAARD, T.A., P. ANTOINE, P. DESVARREUX, A. GIRAUD,& TH.W.J. VAN ASCH (2000). The slope movements within the Mondorès graben (Drôme, France); the interaction between geology, hydrology and typology. Engineering Geology, 55, pp. 297-312.
BOEIJE, R.P. & J.A.M. TEUNISSEN (1997). HYCOSI project. Three dimensional stability 3DSTAB. Delft Geotechnics CO-351150/17.
BRAKENSIEK, D.L., H.B. OSBORN & W.J. RAWLS (eds) (1979). Field manual for research in agricultural hydrology. U.S. Department of Agriculture, Agriculture Handbook 224.
BRGM (1967). 1:50.000 Carte géologique Salins-les-Bains (Sheet XXXIII 25). BRGM Orléans.
BROOKS, R.H. & A.T. COREY(1964). Hydraulic properties of porous media. Hydrology Papers 3, Colorado State. University, Fort Collins.
BURGER, H.R. (1992). Exploration geophysics of the shallow subsurface. Prentice-Hall, New Jersey. pp. 18.
CARSON, M.A. & M.J. KIRKBY (1972). Hillslope Form and Process. Cambridge.
CHANDLER, R.J. (1986). Processes leading to landslides in clay slopes: a review. Chapter 16 in: A.D. Abrahams (ed.), Hillslope processes. Allen & Unwin Inc. Boston, pp. 343-360.
CHASSAGNEUX, D. & E. LEROI (1995). Synthèse des connaissances acquises sur le site Boulc-en-Diois. BRGM R38777.
CHAUVE, P. (ed.) (1975). Guides Géologiques Régionaux: Jura. Masson & Cie, Éditeurs, Paris.
CHIANG, W.-H. & W. KINZELBACH (1996). Manual for Processing Modflow for Windows. Scientific Software Group, Washington, USA.
CORDIER, J-P. (1985). Velocities in reflection seismology. D.Reidel Publishers, Dordrecht.
COROMINAS, J., J. MOYA, A. LEDESMA, J.A. GILI, A. LLORET & J. RIUS (1998). New technologies for landslide hazard assessment and management in Europe (Newtech). ENV-CT96-0248. Final report.
CROZIER, M.J. (1984). Field assessment of slope instability. In: D. Brunsden & D.B. Prior (eds.), Slope instability. John Wiley & Sons, New York. pp. 103-142.
CRAIG, R.F. (1992). Soil mechanics. Chapman & Hall, London.
CRUDEN, D.M. & D.J. VARNES (1996). Landslide types and processes. Chapter 3 in: A.K Turner & S.L. Schuster (eds.). Landslides, investigation and mitigation. Special Report 247, Transportation Research Board, National Research Council. National Academy Press, Washington, D.C.
DAVIS, J.C. (1986). Statistics and data analysis in Geology. 2nd Edition. John Wiley & Sons, New York.
DEGANUTTI, A.M. & P. GASPARETTO (1992). Some aspects of a mudslide in Cortina, Italy. In: D.H. Bell (ed.), Proceedings of the sixth International Symposium on Landslides, Christchurch, New Zealand. Balkema Rotterdam, 1, pp. 373-378.
DE JOODE, A., 2000. A sediment budget for a subcatchment of the Riou Bourdoux, France. Unpublished M.Sc. Thesis, Department of Physical Geography, Utrecht University, The Netherlands.
DEKKER, L.W. & C.J. RITSEMA (1996). Preferential flow paths in a water repellent clay soil with grass cover. Water Resources Research, 32, pp. 324-333.

DE ROOIJ, G.H. (2000). Modeling fingered flow of water in soils owing to wetting front instability: a review. Journal of Hydrology, 231-232, pp. 277-294.
DI MAIO, C. (1996). The influence of pore fluid composition on the residual shear strength of some natural clayey soils. In: K. Senneset (ed.), Proceedings of the seventh International Symposium on Landslides, Trondheim, Norway, Balkema Rotterdam. pp. 1189-1194.
DOHERTY, J., L. BREBBER & P. WHYTE (1994). PEST. Model-independent parameter estimation. User's manual. Watermark computing, Australia.
DUNNE, TH. (1983). Relation of field studies and modeling in the prediction of storm runoff. Journal of Hydrology, 65, pp. 25-48.
EWERT, F.K. (1990). Engineering geology related to groundwater flow: determination, impermeabilization, supply. In: Proceedings sixth international IAEG congress. Amsterdam, the Netherlands. Balkema, Rotterdam, pp. 1109-1142.
FEDDES, R.A., P. KABAT, P.J.T. VAN BAKEL, J.J.B. BRONSWIJK & J. HALBERTSMA (1988). Modelling soil water dynamics in the unsaturated zone – state of the art. Journal of Hydrology, 100, pp. 69-111.
FLURY, M., H. FLÜHLER, W.A. JURY & J. LEUENBERGER (1994). Susceptibility of soils to preferential flow of water: a field study. Water Resources Research, 30, pp. 1945-1954.
FORSTER, C. & L. SMITH (1988a). Groundwater flow systems in mountainous terrain. 1. Numerical modeling technique. Water Resources Research, 24, pp. 999-1010.
FORSTER, C. & L. SMITH (1988b). Groundwater flow systems in mountainous terrain. 2. Controlling factors. Water Resources Research, 24, pp. 1011-1023.
FREEZE, R.A. & P.A. WITHERSPOON (1967). Theoretical analysis of regional groundwater flow. 2. Effect of water-table configuration and subsurface permeability variation. Water Resources Research, 3, pp. 623-634.
FREEZE, R.A. (1969). The mechanism of natural ground-water recharge and discharge: 1. One-dimensional, vertical, unsteady, unsaturated flow above a recharging or discharging ground-water flow system. Water Resources Research, 5, pp. 153-171.
FREEZE, R.A. (1971). Three-dimensional, transient, saturated-unsaturated flow in a groundwater basin. Water Resources Research, 7, pp. 347-366.
GASPARETTO, P., M. PANIZZA, A. PASUTO, S. SILVANO & M. SOLDATI (1994). Research in the Cortina d'Ampezzo area. In: Casale, R., R. Fantechi & J.C. Flageollet (eds.). Temporal occurrence and forecasting of landslides in the European Community (Final Report). Science Research Development. European Commision, Bruxelles, pp. 741-768.
GASPARETTO, P., M. MOSSELMAN & TH.W.J. VAN ASCH (1996). The mobility of the Alverà landslide (Cortina d'Ampezzo, Italy). Geomorphology, 15, pp. 327-335.
GOSTELOW, T.P. (1996). Landslides. Chapter 8 in: V.P. Singh (ed.), Hydrology of disasters. Kluwer Publisher, Rotterdam.
GRIMM, R.E. (1962). Applied clay mineralogy. McGraw-Hill, New York.
HEMEL, R.B.J., I.C. KROON & H. LEUSHUIS (1997). HYCOSI Project. Karst hydrology in the French Jura near Salins-les-Bains. MSc thesis, Department of Physical Geography, Utrecht University, The Netherlands. Published in Leroi (1997).
HEWLETT, J.D. & A.R. HIBBERT (1967). Factors affecting the response of small watersheds to precipitation in humid areas. In: W.E. Sopper & H.W. Lull (eds.) International symposium on forest hydrology. Pergamon, Oxford, pp. 275-290.

HODGE, R.A.L. & R.A. FREEZE (1977). Groundwater flow systems and slope stability. Canadian Geotechnical Journal, 14, pp. 466-476.
HORTON, J.H. & R.H. HAWKINS (1965). Flow path of rain from the soil surface to the water table. Soil Science, 100, pp. 377-383.
HUTCHINSON, J.N. (1961). A landslide on a thin layer of quick clay at Furre, Central Norway. Geotechnique 11, pp. 69-94.
HUTCHINSON, J.N. (1988). General report: Morphological and geotechnical parameters of landslides in relation to geology and hydrogeology. In: C.Bonnard (ed.), Proceedings of the fifth International Symposium on Landslidse, Lausanne, Switzerland.Balkema, Rotterdam, 1, pp. 3-35.
IVERSON, R.M. & J.J. MAJOR (1987). Rainfall, ground-water flow, and seasonal movement at Minor Creek landslide, northwest California: Physical interpretation of empirical relations. Geological Society of America Bulletin, 99, pp. 579-594.
IVERSON, R.M. & M.E. REID (1992). Gravity-driven groundwater flow and slope failure potential. 1. Elastic effective-stress model. Water Resources Research, 28, pp. 925-938.
JACKSON, C.R. (1992a). Hillslope infiltration and lateral downslope unsaturated flow. Water Resources Research, 28, pp. 2533-2539.
JACKSON, C.R. (1992b). Reply on "Comment on "Hillslope infiltration and lateral downslope unsaturated flow."by J.R. Philip (1992)" Water Resources Research, 29, pp. 4169.
JIBSON, R.W., E.L. HARP & J.A. MICHAEL (1998). A method for producing digital propabilistic seismic hazards maps: An example from the Los Angeles, California, area. USGS, open-file report 98-113. http://geohazards.cr.usgs.gov/pubs/ofr/98-113/ofr98-113.html.
JOHNSON, K.A. & N. SITAR (1990). Hydrologic conditions leading to debris-flow initiation. Canadian Geotechnical Journal, 27, pp. 789-801.
KESSLER, J. & R. OOSTERBAAN (1974). Determinating hydraulic conductivities of soils. In: Drainage principles and applications. Publication 16, III, international Institute for Land Reclamation and Improvement (ILRI), Wageningen, The Netherlands, pp. 253-296.
KLEMES, V. (1990). The modelling of mountain hydrology. Hydrology in mountainous regions. Proceedings of the Strbské Pleso Workshop, Czechoslovakia. International association of hydrological science (IAHS) Publications 190, pp. 29-43.
KLEYN, A.H. (1983). Seismic reflection interpretation. Elsevier Science publishing, New York, pp. 1-4.
KILSBY, C.G., T.A. BUISHAND & P.D. JONES (1998). POPSICLE. Final report. EV5V-CT94-0510. Http://www.ncl.ac.uk/wrincle/reports.html.
KIRKBY, M.J. (1978). Hillslope hydrology. John Wiley & Sons, New York.
KLUTE, A. (ed.) (1986). Methods of soil analysis, Part 1. Physical and mineralogical methods. Agronomy Monograph no. 9 (2nd edition). American Society of Agronomy, Madison Wisconsin.
KUTILEK, M. & D.R. NIELSEN (1994). Soil Hydrology. Catena Verlag, Reiskirchen.
LAINÉ, C. (1989). Etude de l'influence de la zone non saturee sur l'equilibre des pentes instables. Ph.D. Thesis L'institute national des sciences appliquées de Lyon.
LE JEUNE, F.& A. BESSE (1996). HYCOSI Project. Étude par microgravimétrie en profils tests sur le site sw Salins-les-Bains (Jura). BRGM Report R39093.

LEROI, E. & O. MONGE (1996). HYCOSI Project. Reconnaissance et instrumentation du site de Salins-les-Bains: Compte-rendu d'intervention. BRGM Report R38890.
LEROI, E. (ed.) (1997). HYCOSI - Impact of hydrometeorologic changes on slope instability. Final report. BRGM Report 39794.
MANGIN, A. (1975). Contribution à l'étude hydrodynamique des aquifères karstiques. DES thesis, Université. Dijon, France.
MCCORD, J.T. & D.B. STEPHENS (1987). Lateral moisture movement on sandy hillslope in the apparent absence of an impeding layer. Journal of Hydrological Processes, 1, pp. 225-228.
MCCORD, J.T., D.B. STEPHENS & J.L. WILSON (1991). Hysteresis and state-dependent anisotropy in modeling unsaturated hillslope hydrologic processes. Water Resources Research, 27, pp. 1501-1518.
MCDONALD, M.G. & A.W. HARBAUGH (1988). A modular three dimensional finite difference groundwater flow model. Scientific Software Group, U.S. Government, Washington.
MICHAELIDES, K. (1995). Clay behaviour and the stability of the Tessina landslide, Italy: the effects of water chemistry and piezometry. B.Sc. Dissertation, King's College, London.
MIYAZAKI, T. (1988). Water flow in unsaturated soil in layered slopes. Journal of Hydrology, 102, pp. 201-214.
MONGE, O & E. LEROI (1997). HYCOSI Project. Instrumentation du site de Salins-les-Bains. Rapport d'avancement 3ème année. BRGM Report R39172.
MORSE, J.W. & F.T. MACKENZIE (1990). Geochemistry of sedimentary carbonates. Developments in sedimentology: 48. Elsevier science publishers B.V. Amsterdam, pp. 147-149.
MUALEM, Y. (1986). Hydraulic conductivity of unsaturated soils: prediction and formulas. Chapter 31 in A. Klute (ed.): Methods of soil analysis, Part 1. Physical and mineralogical methods. Agronomy Monograph no. 9 (2nd edition). American Society of Agronomy, Soil science society of America. pp. 799-823.
MULDER, H.F.H.M. (1991). Assessment of landslide hazard. Amsterdam/Utrecht, KNAG/Faculteit Ruimtelijke Wetenschappen, Utrecht University. (Doctoral Thesis, Netherlands Geographical Studies 124).
NEN5757 (1991). Determination of carbonate concentration in soils. Volumetric method (in Dutch). Nederlands Normalisatie Instituut, Delft.
NEUMAN, S.P. (1973). Saturated-unsaturated seepage by finite elements. ASCE Journal of the Hydraulic Division, 99, pp. 2233-2250.
NIEUWENHUIS, J.D. (1987). Deformation, creep and flow of soil masses, part 2. Lecture notes, Faculty of Geographical Sciences, Utrecht, The Netherlands.
OKUNISHI, K. & T. OKIMURA (1987). Groundwater models for mountain slopes. Chapter 8 in: M.G. Anderson & K.S. Richards (eds.), Slope Stability. John Wiley & Sons, New York.
PARASNIS, D.S. (1997). Principles of applied geophysics, Chapman & Hall, London. pp. 273-276.
PHAN THI SAN HA (1992). Propriétés physiques et caractéristiques géotechniques des 'Terres Noires' du sud-est de la France. Thèse Université Joseph Fourier, Grenoble.
PHILIP, J.R. (1991a). Hillslope infiltration: planar slopes. Water Resources Research, 27, pp. 109-117.

PHILIP, J.R. (1991b). Hillslope infiltration: divergent and convergent slopes. Water Resources Research, 27, pp. 1035-1040.
PHILIP, J.R. (1991c). Infiltration and downslope unsaturated flows in concave and convex topographies. Water Resources Research, 27, pp. 1041-1048.
PHILIP, J.R. (1992). Comment on "Hillslope infiltration and lateral downslope unsaturated flow" by C.R. Jackson. Water Resources Research, 29, pp. 4167.
REID, M.E. & R.M. IVERSON (1992). Gravity-driven groundwater flow and slope failure potential. 2. Effects of slope morphology, material properties and hydraulic heterogeneity. Water Resources Research, 28, pp. 939-950.
REID, M.E. (1994). A pore-pressure diffusion model for estimating landslides-inducing rainfall. Journal of Geology, 102, pp. 709-717.
RITSEMA, C.J. & L.W. DEKKER (1994). How water moves in a water repellent sandy soil; 2 Dynamics of fingered flow. Water Resources Research, 30, pp. 2519-2531.
RITSEMA, C.J. (1998). Flow and transport in water repellent sandy soils. Doctoral thesis, Wageningen Agricultural University, The Netherlands.
RITSEMA, C.J. & L.W. DEKKER (2000). Preferential flow in water repellent sandy soils: principles and modeling implications. Journal of Hydrology, 231-232, pp. 308-319.
ROELANDSE, A. & K. BLATTER (1996). HYCOSI project. Unpublished M.Sc. Thesis, Department of Physical Geography, Utrecht University, The Netherlands.
RULON, J.J., R. RODWAY & R.A. FREEZE (1985). The development of multiple seepage faces on layered slopes. Water Resources Research, 21, pp. 1625-1636.
SALVUCCI, G.D. & D. ENTEKHABI (1994a). Equivalent steady soil moisture profile and the time compression approximation in water balance modeling. Water Resources Research, 30, pp. 2737-2749.
SALVUCCI, G.D. & D. ENTEKHABI (1994b). Comparison of the Eagleson statistical-dynamical water balance model with numerical simulations. Water Resources Research, 30, pp. 2751-2757.
SENNESET, K. (ed.) (1996). Proceedings of the seventh International Symposium on Landslides, Trondheim, Norway, Balkema Rotterdam.
ŠIMŮNEK, J., T. VOGEL & M.TH. VAN GENUCHTEN (1994). The SWMS-2D Code for simulating water flow and solute transport in two-dimensional variably saturated media. Research Report No.132. U.S. Salinity Laboratory, Agricultural research service, U.S. Department of agriculture, Riverside, California.
ŠIMŮNEK, J., M. ŠEJNA & M.TH. VAN GENUCHTEN (1998). HYDRUS 1D, manual. Software package for simulating the 1D movement of water, heat and multiple solutes in variably saturated-media. Agricultural research service. IGWMC TPS70, Colorado School of Mines, Golden, Colorado, USA.
SOWERS, G.B. & G.F. SOWERS (1970). Introductory soil mechanics and foundations. Macmillan, New York, 3rd edition.
SUHAYDU, J.N. & D.B. PRIOR (1978). Explanation of submarine landslide morphology by stability analysis and rheological models. Off-shore Technology Conference, Houston, pp. 1075-1079.
TER-STEPANIAN, G. (1963). On the long-term stability of slopes. Norwegian Geotechnical Institue, 52, pp. 1-14.
TER-STEPANIAN, G. (1965). In-situ determination of the rheological characteristics of soils on slopes. Proceedings sixth international Conference on soil mechanics, Montreal, 2, pp. 575-577.

THOMAS, G.W. (1982). Exchangeable cations. Chapter 9 in: Page, (ed.). Methods of soil analysis, part 2: Chemical and Microbiological Properties. in serie: Agronomy (9) of American Society of Agronomy and Soil Science Society of America, Madison, Wisconsin, USA.

TÓTH, J. (1963). A theoretical analysis of groundwater flow in small drainage basins. Journal of Geophysical Research, 68, pp. 4795-4812.

VAN ASCH, TH.W.J. & P.M.B. VAN GENUCHTEN (1990). A comparison between theoretical and measured creep profiles of landslides. Geomorphology, 3, pp. 45-55.

VAN ASCH, TH.W.J., M.R. HENDRIKS, R. HESSEL, & F.E. RAPPANGE (1996). Hydrologic triggering conditions of landslides in varved clays in the French Alps. Engineering Geology, 42, pp. 239-251.

VAN ASCH, TH.W.J., S.J.E. VAN DIJCK & M.R. HENDRIKS (2001). The role of overland flow and subsurface flow on spatial distribution of soil moisture in the topsoil. Accepted by Hydrological processes.

VAN DEN EIJNDEN, A.J. (1998). Hydrological investigation of the Belin-slope, Salins-les-Bains, France. Unpublished M.Sc. Thesis, Department of Physical Geography, Utrecht University, The Netherlands.

VAN ESCH, J.M. (1995). Hycosi project. Groundwater flow modelling. Delft Geotechnics CO-351150/7.

VAN GENUCHTEN, M.TH. (1980). A closed-form equation for predicting the hydraulic conductivity of unsaturated soils. Soil Science Society America Journal, 44, pp. 892-898.

VAN GENUCHTEN, M.TH., F.J. LEIJ, S.R. YATES & J.R. WILLIAMS (1991). RETC manual: Code for quantifying the hydraulic functions of unsaturated soils. http://www.epa.gov/ada/kerrlab.html

VAN GENUCHTEN, P.M.B. (1989). Movement mechanisms and slide velocity variations of landslides in varved clays in the French Alps. Amsterdam/Utrecht, KNAG/Faculteit Ruimtelijke Wetenschappen, Utrecht University. (Doctoral Thesis, Netherlands Geographical Studies 98).

VARNES, D.J. (1978). Slope movements. Types and processes, Transportation Research Board Report 176. Landslides. Analysis and control, pp. 11-33.

WALLACH, R. & D. ZASLAVSKY (1991). Lateral flow in a layered profile of an infinite uniform slope. Water Resources Research, 27, pp. 1809-1818.

WARD, R.C. (1984). On the response to precipitation of headwater streams in humid areas. Journal of Hydrology, 74, pp. 171-189.

WIECZOREK, G.F. (1996). Lanslide triggering mechanisms. Chapter 4 in: A.K Turner & S.L. Schuster (eds.), Landslides, investigation and mitigation. Special Report 247, Transportation Research Board, National Research Council. National Academy Press, Washington, D.C.

WILSON, C.J. & W.E. DIETRICH (1987). The contribution of bedrock groundwater flow to storm runoff and high pore pressure development in hollows. Proceedings of the Corvallis Symposium: Erosion and Sedimentation in the Pacific Rim. IAHS Publications 165, pp. 49-59.

WILKINSON, P.L., S.M. BROOKS & M.G. ANDERSON (2000). Design and application of an automated non-circular slipsurface within a combined hydrology and stability model (CHASM). Hydrological Processes, 14, pp. 2003-2017.

WÖSTEN, J.H.M. & M.TH. VAN GENUCHTEN (1988). Using texture and other soil properties to predict the unsaturated soil hydraulic functions. Soil Science Society America Journal, 52, pp. 1762-1770.
YEN, B.C. (1969). Stability of slopes undergoing creep deformation. Journal of Soil Mechanics and Foundation Division SM 4, pp. 1075-1096.
ZASLAVSKY, D. & G. SINAI (1981a). Surface hydrology: 1-Explanation of phenomena. ASCE Journal of the Hydraulics Division, 107, pp. 1-16.
ZASLAVSKY, D. & G. SINAI (1981b). Surface hydrology: 2-Distribution of raindrops. ASCE Journal of the Hydraulics Division. 107, pp. 17-36.
ZASLAVSKY, D. & G. SINAI (1981c). Surface hydrology: 3-Causes of lateral flow. ASCE Journal of the Hydraulics Division. 107, pp. 37-52.
ZASLAVSKY, D. & G. SINAI (1981d). Surface hydrology: 4-Flow in sloping, layered soil. ASCE Journal of the Hydraulics Division. 107, pp. 53-64.
ZASLAVSKY, D. & G. SINAI (1981e). Surface hydrology: 5-In-surface transient flow. ASCE Journal of the Hydraulics Division. 107, pp. 65-93.
ZIMMERMAN, U., K.O. MONNICH, W. ROETHER, K. SCHUBACH & O. SIEGEL (1966). Tracers determine movement of soil moisture and evapotranspiration. Science 152, pp. 346-347.

CURRICULUM VITAE

Thom Bogaard is geboren op 13 november 1968 te Bussum. Op het Bisschoppelijk College St. Joseph te Sittard haalde hij zijn gymnasium diploma in 1987. In dat jaar begon hij de studie Fysische Geografie aan de Faculteit der Aardwetenschappen van de Vrije Universiteit Amsterdam. In 1993 studeerde hij af in de geografische hydrologie met een aanvullend examen in de micrometeorologie. Het afstudeeronderzoek betrof onderzoek naar de waterhuishouding en erosie op steile landbouwgronden in de Gunung Kidul, Java, Indonesië (1992-1993). Verdere onderzoeksprojecten die hij uitgevoerd heeft zijn: hydrochemische laboratorium doorstroomproeven (1991), micrometeorologisch onderzoek in Tomelloso, Spanje (1991) en hydrochemische karakterisatie van kwartair-geologische waarnemingen (1992).

In 1988 behaalde hij zijn motorrijbewijs.

Van september 1993 tot maart 1994 was hij verbonden als junior docent aan de Faculteit der Aardwetenschappen van de Vrije Universiteit waar hij het vak “Computergebruik en inleiding programmeren” begeleidde en daarna doceerde hij “Geofysische Prospectie Methoden” en “Geofysische Interpretatie”. In februari 1994 begon hij als assistent in opleiding bij de vakgroep Fysische Geografie van de Universiteit Utrecht aan het EU-project Hycosi. Dit vormde de basis voor het onderhavige promotie-onderzoek.

In 1997 beklom hij zijn eerste 4000-er.

Vanaf december 1996 werd hij aangesteld als universitair docent in de landdegradatie hydrologie. Hier is hij verantwoordelijk voor het vak ‘Oppervlaktewater hydrologie’, het veldpraktikum hydrologische meettechnieken en begeleidt hij studenten bij hun afstudeeronderzoek en stage. Tevens is hij als coördinator van het vervolgdoctoraal verantwoordelijk voor de studie Fysische Geografie in het 3^{e}, 4^{e} en 5^{e} jaar.

In 2000 kocht hij zijn eerste huis.

Naast het landdegradatie hydrologische onderzoek is hij recentelijk met zijn onderzoek teruggekeerd naar Java, Indonesië waar hij zich bezighoudt met onderzoek naar de hydrologische factoren van natuurlijke vulkanische verontreiniging van de Ijen vulkaan.

PUBLICATIONS OF THOM BOGAARD

Articles in international refereed journals

BOGAARD, T.A., P. ANTOINE, P. DESVARREUX, A. GIRAUD AND TH.W.J. VAN ASCH (2000). The slope movements within the Mondores graben (Drome, France), the interaction between geology, hydrology and typology. Engineering Geology, 55, pp. 297-312.

BOGAARD, T.A. AND TH.W.J. VAN ASCH (2001). The role of the soil moisture balance in the unsaturated zone on movement and stability of the Beline landslide, France. Earth Surface Processes and Landforms (submitted).

Refereed congress articles or proceedings

NIEUWENHUIS, J.D., T.A. BOGAARD, TH.W.J. VAN ASCH & J. VAN ESCH (1995). Effects of hydrometeorology on the stability of some landslides. Proceedings of XIth ECSMFE in Copenhagen, 6, pp.127-133.

BOGAARD, T.A. & TH.W.J. VAN ASCH (1996). Geophysical and hydrochemical investigation of a complex large-scale landslide in southern France. Proceedings 7th International Symposium on Landslide, Trondheim, Norway. Balkema Rotterdam. 2, pp.643-647.

BOGAARD, T.A., TH.W.J. VAN ASCH & O. MONGE (1998). Study on the influence of 3D hydrological ground water flow on the stability of a landslide in Salins-les-Bains, eastern France. 8th International IAEG Congress, Vancouver, Canada. Balkema Rotterdam. 3, pp.1765-1772.

VAN ASCH, TH.W.J. & T.A. BOGAARD (1998). A study on the displacement of a landslide near Salins-les-Bains (eastern France). 8th International IAEG Congress, Vancouver, Canada. Balkema Rotterdam. 3, pp.1641-1646.

BOGAARD, T.A. (2002). A state-dependent ground water recharge model for landslide research, which simulates preferential flow. 9th international IAEG congress, Durban, South Africa. [in prep.]

Abstracts

BOGAARD, T.A. (1999). Study of the role of the unsaturated zone in simulating ground water level fluctuations in a clayey slope. XXIV General Assembly of the EGS, The Hague, The Netherlands, 19-23 April 1999 [Solicited paper].

VAN BEEK, L.P.H., T.A. BOGAARD & TH.W.J. VAN ASCH (2000). Influence of changing evapotranspiration on sediment yield and surface run off in temperate and mediterranean environments. XXV General Assembly of the EGS, Nice, France, 25-29 April 2000.

Technical reports

BOGAARD, T.A. & M.R. HENDRIKS (2001). Hydrological pilot study of the Ijen caldera and Asembagus irrigation area. ICG Report 01/01.

EU reports

BOGAARD, T.A. (1996a). Hydrological, hydrochemical and geodetical study on the Boulc-Bonneval landslide, Boulc-en-Diois (Drome), France. Second year HYCOSI progress report. Department of Physical Geography, University Utrecht, the Netherlands.

BOGAARD, T.A., J.T. BUMA & C.J.M. KLAWER (1996). Use of geochemical techniques in identifying hydrological systems in weathering marls. HYCOSI / NEWTECH technical report no.2. Department of Physical Geography, University Utrecht, the Netherlands.

BOGAARD, T.A. (1996b). Determination of strength parameters of blue marls and red Oligocene marls from the Boulc-Bonneval landslide and remoulded marls from Salins-les-Bains. HYCOSI technical report no.3. Department of Physical Geography, University Utrecht, the Netherlands.

BOGAARD, T.A. (1996c). Determination of hydrological parameters of remoulded marls, Salins-les-Bains, France. HYCOSI technical report no.4. Department of Physical Geography, University Utrecht, the Netherlands.

BOGAARD, T.A. & O. MONGE (1997). Hydrological modelling of the 'La Beline' slope, Salins-les-Bains, France. HYCOSI technical report no.5. Department of Physical Geography, University Utrecht, The Netherlands and BRGM report R39513

MONGE, O & T.A. BOGAARD (1997). Hydrological and geotechnical investigation of the 'La Beline' slope, Salins-les-Bains, Jura, France. BRGM Report R39514.